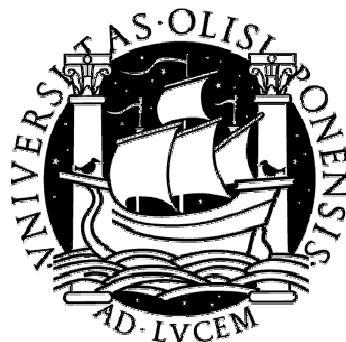


UNIVERSIDADE DE LISBOA, FACULDADE DE FARMÁCIA



**Potential Irreversible Inhibitors of Cysteine Proteases  
based on Sultam and Naphthoquinone Scaffolds**

Cláudia Sofia dos Santos Valente

DOUTORAMENTO EM FARMÁCIA (QUÍMICA FARMACÊUTICA)

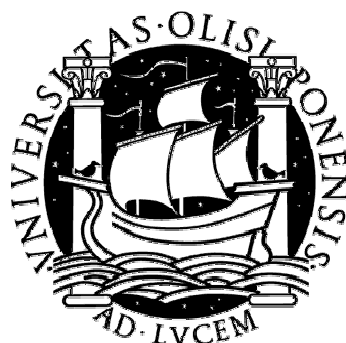
2007







UNIVERSIDADE DE LISBOA, FACULDADE DE FARMÁCIA



**Potential Irreversible Inhibitors of Cysteine Proteases  
based on Sultam and Naphthoquinone Scaffolds**

Cláudia Sofia dos Santos Valente

Tese orientada pelo Professor Doutor Rui Moreira

**Dissertação apresentada à Faculdade de Farmácia da Universidade de Lisboa, com vista  
à obtenção do grau de Doutor em Farmácia (Química Farmacêutica)**

**Lisboa 2007**



Este trabalho foi desenvolvido sob orientação científica do Professor Doutor Rui Moreira, no Centro de Estudos de Ciências Farmacêuticas da Faculdade de Farmácia da Universidade de Lisboa.

O trabalho foi apoiado financeiramente pela Fundação para a Ciência e a Tecnologia e pelo Fundo Social Europeu, no âmbito do III Quadro Comunitário de Apoio – Bolsa de Doutoramento (SFRH/BD/10815/2002).





## ACKNOWLEDGEMENTS

I respectfully acknowledge my supervisor, Professor Rui Moreira.

To Professor Jim Iley from The Open University, UK, I am grateful for the thoughtful suggestions throughout these studies and also for the NMR and ESI-MS analyses.

I wish to express my gratitude to Professor Maria José Umbelino Ferreira, who first believed in me and gave me the opportunity to do research.

I gratefully acknowledge Professor Kenneth Douglas for kindly receiving me at the University of Manchester, UK, and to the members of his lab for all the assistance, in particular to Tim and João Neres.

To Professor Philip J. Rosenthal from the University of California, San Francisco, I thank for the antimalarial testing of the compounds.

I want to thank Professor Rita C. Guedes for performing the Molecular Orbital Calculations and the Molecular Modelling work of this thesis.

To Dr. Célia Fernandes, from the ITN, for the elemental analyses, and to Eng. Ana Isabel Rodrigues, from the INETI, for making possible the access to the polarimeter and for all the assistance. I am also thankful to Professor Maria José Brito and Professor Paula Ferreira, both from Faculdade de Ciências, Universidade de Lisboa, for their support and advice in the handling of the NMR spectrometer.

I would like to express my gratitude to Professor José Nascimento, who helped me to understand some publications in German, which were very useful in the initial stage of this work. I am also thankful to Professor Ana Paula Leandro for her invaluable guidance during the dialysis assays, and to Professor Fátima Cabral, Professor Judite Costa, Dr. Isabel Joglar and Dr. Virginia Carvalho, for all the availability and technical help during some equipment problems in the last steps of my experimental work.

For those who gave me their support, sympathy and patience on a daily basis: research assistants and technical staff of my department (some of you saw me “growing up”!) and also my fellows. I will always keep you on my mind.

To the ones I have the privilege to call friends, especially Analisa, Catarina, Marina, Raquel, Rui and Zé. “*You raise me up...*”

Most of all, to my family, for whom a thousand words would not be enough. I will never be able to compensate my “absence”.



# GENERAL INDEX

INDEX OF FIGURES.....	iv
INDEX OF SCHEMES.....	vi
INDEX OF TABLES.....	viii
ABSTRACT .....	xi
KEYWORDS .....	xi
RESUMO .....	xiii
PALAVRAS CHAVE.....	xiii
ABBREVIATIONS AND SYMBOLOGY .....	xv
<b>1. INTRODUCTION.....</b>	<b>1</b>
<b>1.1 Cysteine proteases.....</b>	<b>1</b>
1.1.1 Update.....	1
1.1.2 Potential therapeutic targets.....	2
1.1.3 Structural differences.....	5
1.1.4 Catalytic mechanism .....	6
<b>1.2 Inhibitors of cysteine proteases.....</b>	<b>9</b>
1.2.1 Irreversible <i>versus</i> reversible action .....	9
1.2.2 Epoxysuccinyl derivatives.....	10
1.2.3 Vinyl sulfones and analogues.....	14
1.2.3.1 As inhibitors of cysteine proteases .....	14
1.2.3.2 Synthesis.....	18
<b>1.3 Introductory remarks on quinones .....</b>	<b>20</b>
<b>1.4 Aims of the thesis .....</b>	<b>25</b>
<b>2. DIPEPTIDE VINYL SULTAMS.....</b>	<b>29</b>
<b>2.1 Synthesis .....</b>	<b>29</b>
2.1.1 Overall strategy .....	29
2.1.2 Strategies for sultam scaffolds.....	30
2.1.2.1 $\beta$ -Sultams .....	30
2.1.2.2 $\gamma$ - and $\delta$ -Sultams .....	36
2.1.3 Synthesis of sultams core .....	37
2.1.3.1 $\beta$ -Sultams .....	38
<i>N</i> -Phenyl- $\beta$ -sultam .....	38
<i>N</i> -Benzyl- $\beta$ -sultam .....	44
2.1.3.2 $\gamma$ -Sultams .....	46
2.1.3.3 $\delta$ -Sultams.....	48
2.1.4 Synthesis of dipeptide vinyl sultams .....	50
2.1.4.1 Aminoacid and dipeptidyl aldehydes.....	50
2.1.4.2 Aldol-type reaction of sultam carbanions .....	53
2.1.4.3 Sultam phosphonates .....	54
2.1.4.4 Horner-Wadsworth-Emmons reaction .....	56
2.1.4.5 Dipeptide vinyl sultams.....	59
Deprotection (removal of Boc protecting group) .....	59
Coupling with aminoacids and endcapping of the dipeptide moiety.....	60

NMR Spectral characterisation .....	62
2.1.5 Synthesis of vinyl sulfonamides .....	70
2.2 Kinetic study of the reaction with cysteine .....	73
2.2.1 Introductory remarks .....	73
2.2.2 Results and Discussion.....	74
2.3 Inhibitory activity against papain, falcipain-2 and <i>Plasmodium falciparum</i> .....	77
<b>3. 1,4-NAPHTHOQUINONE DERIVATIVES.....</b>	<b>85</b>
3.1 Synthesis.....	85
3.1.1 Reaction of 1,4-naphthoquinones with nitrogen and oxygen nucleophiles.....	86
3.1.2 Aminomethyl derivatives .....	90
3.2 Kinetic study of the reaction with cysteine .....	92
3.2.1 Introductory remarks .....	92
3.2.2 Results and Discussion.....	93
Kinetic studies.....	93
Relationship between LUMO energies and the reactivity toward cysteine.....	98
3.3 Inhibitory activity against cysteine proteases .....	100
3.3.1 Papain inhibition studies .....	101
3.3.2 Bovine spleen cathepsin B inhibition studies.....	109
3.3.3 Falcipain-2 and <i>Plasmodium falciparum</i> inhibition studies.....	110
3.3.4 Porcine pancreatic elastase inhibition studies .....	110
<b>4. CONCLUSIONS AND FUTURE DIRECTIONS .....</b>	<b>113</b>
<b>5. EXPERIMENTAL SECTION.....</b>	<b>119</b>
5.1 Synthesis.....	119
5.1.1 Reagents and Solvents .....	119
5.1.2 Chromatography.....	119
5.1.3 Equipment .....	119
5.1.4 Experimental procedures and product characterisation .....	120
5.1.4.1 <i>N</i> -Phenyl- $\beta$ -sultam.....	120
5.1.4.2 <i>N</i> -Benzyl- $\beta$ -sultam .....	124
5.1.4.3 $\gamma$ -Sultams core .....	125
5.1.4.4 $\delta$ -Sultams core.....	127
5.1.4.5 Aminoacid and dipeptide aldehydes .....	129
5.1.4.6 Sultam phosphonates.....	135
5.1.4.7 Horner-Wadsworth-Emmons reaction.....	137
5.1.4.8 Deprotection (removal of Boc protecting group).....	140
5.1.4.9 Coupling with aminoacids and endcapping of the dipeptide moiety .....	143
5.1.4.10 Synthesis of vinyl sulfonamides .....	149
5.1.4.11 1,4-Naphthoquinone derivatives.....	151
5.2 Kinetic study of the reaction with cysteine .....	157
5.2.1 Reagents and Solvents .....	157
5.2.2 Equipment .....	158
5.2.3 Buffers and substrate solutions .....	158
5.2.4 Determination of free thiol content .....	158
5.2.5 UV Spectrophotometry.....	160
5.2.6 Determination of $k_{\text{obs}}$ .....	161
5.3 Molecular modelling .....	161

5.4 Molecular orbital calculations .....	162
<b>APPENDIX I. Protocols for enzymatic assays.....</b>	<b>165</b>
<b>AI.1 Papain.....</b>	<b>165</b>
<b>AI.1.1 Development of papain inhibition assay .....</b>	<b>165</b>
<b>AI.1.1.1 Introductory remarks.....</b>	<b>165</b>
<b>AI.1.1.2 Determination of the papain activity in the presence of Cbz-Gly-ONp.....</b>	<b>166</b>
<b>AI.1.1.3 Determination of the papain activity in the presence of BAPA.....</b>	<b>168</b>
<b>AI.1.2 Purification of papain by gel-filtration chromatography.....</b>	<b>174</b>
<b>AI.1.3 Dialysis experiment .....</b>	<b>177</b>
<b>AI.2 Bovine spleen cathepsin B.....</b>	<b>178</b>
<b>AI.2.1 Introductory remarks .....</b>	<b>178</b>
<b>AI.2.2 Development of cathepsin B inhibition assay .....</b>	<b>179</b>
<b>AI.3 Inhibition assay for porcine pancreatic elastase.....</b>	<b>181</b>
<b>AI.4 Experimental Section .....</b>	<b>182</b>
<b>AI.4.1 Reagents and Solvents .....</b>	<b>182</b>
<b>AI.4.2 Gel-filtration chromatography .....</b>	<b>182</b>
<b>AI.4.3 Dialysis experiments.....</b>	<b>182</b>
<b>AI.4.4 Equipment.....</b>	<b>183</b>
<b>AI.4.5 Procedures for papain.....</b>	<b>183</b>
<b>AI.4.6 Procedures for bovine spleen cathepsin B.....</b>	<b>188</b>
<b>AI.4.7 Inhibition assay for porcine pancreatic elastase.....</b>	<b>188</b>
<b>AI.4.8 Determination of <math>k_{obs}</math>, <math>k_2</math>, <math>K_I</math> and <math>k_{inact}</math> .....</b>	<b>189</b>
<b>APPENDIX II. Pseudo first-order rate constants for the cysteine-catalysed decomposition of vinyl sultams, vinyl sulfonamide and naphthoquinones .....</b>	<b>191</b>
<b>APPENDIX III. Spectral scanning for the reaction of a naphthoquinone with cysteine.....</b>	<b>195</b>
<b>APPENDIX IV. Kinetic equation for the reaction of 1,4-naphthoquinone with cysteine.....</b>	<b>197</b>
<b>APPENDIX V. Data for the graphical representation in Figure 3.11 .....</b>	<b>201</b>
<b>APPENDIX VI. Pseudo first-order rate constants for papain- and cathepsin B-catalysed decomposition of quinones.....</b>	<b>203</b>
<b>BIBLIOGRAPHY .....</b>	<b>207</b>

# INDEX OF FIGURES

<b>Figure 1.1</b> IDN-6556 ( <b>1.1</b> ), CRA-3316 ( <b>1.2a</b> ) and rupintrivir ( <b>1.3a</b> ).....	2
<b>Figure 1.2</b> Active-site of papain. ....	8
<b>Figure 1.3</b> Hanzlik <i>et al.</i> lead compounds for inhibition of papain.....	14
<b>Figure 1.4</b> Representative chemical structures of quinones.. ....	20
<b>Figure 1.5</b> Vitamin K <sub>2</sub> .....	20
<b>Figure 1.6</b> Structures of mitomycin C ( <b>1.16</b> ), daunorubicin ( <b>1.17a</b> ), doxorubicin ( <b>1.17b</b> ) and atovaquone ( <b>1.18</b> ). Generic structure of menadione derivatives ( <b>1.15b</b> ). ....	21
<b>Figure 1.7</b> Structures of Cpd 5 ( <b>1.25a</b> ) and NSC 95397 ( <b>1.25b</b> ). Generic structure of 2-(quinazolin-4-ylamino)-[1,4] benzoquinone derivatives ( <b>1.26</b> ). ....	24
<b>Figure 2.1</b> Generic structures of $\beta$ -aminothiols ( <b>2.13</b> ), $\beta$ -aminodisulfides ( <b>2.14</b> ) and 2-aminoethanesulfonic acids ( <b>2.15</b> ). ....	31
<b>Figure 2.2</b> Structure of 2-chloro- <i>N</i> -phenylethanesulfonamide. ....	39
<b>Figure 2.3</b> <i>N</i> -(2-Methanesulfonyloxyethyl)- <i>N</i> -benzylmethanesulfonamide mesylate <b>2.49c</b> . ....	46
<b>Figure 2.4</b> <i>N</i> -Benzyl-3-(benzylamino)propane-1-sulfonamide ( <b>2.52a</b> ) and <i>N</i> -phenyl-3-(phenylamino)propane-1-sulfonamide ( <b>2.52b</b> ). ....	47
<b>Figure 2.5</b> Structure of 3-(phenylamino)propanesulfonyl chloride <b>2.29a</b> . ....	47
<b>Figure 2.6</b> Diastereotopic groups and stereocentre in sultam phosphonates. ....	56
<b>Figure 2.7</b> Relevant NOE correlations observed for <b>2.70b</b> . ....	59
<b>Figure 2.8</b> Stereocentres in dipeptide sultams. ....	62
<b>Figure 2.9</b> Observed <sup>1</sup> H NMR <i>dddd</i> signal and splitting pattern diagram for one allylic methylene proton of compound <b>2.74a</b> . ....	63
<b>Figure 2.10</b> Observed <sup>1</sup> H NMR double triplet signal and splitting pattern diagram for the vinylic proton of compound <b>2.72b</b> . ....	64
<b>Figure 2.11</b> Observed <sup>1</sup> H NMR double quartet signal and splitting pattern diagram for the methylene protons OCH <sub>2</sub> CH <sub>3</sub> of compound <b>2.86</b> . ....	72
<b>Figure 2.12</b> Plot of the pseudo first-order rate constants, <i>k</i> <sub>obs</sub> , for the reaction of vinyl sultam <b>2.69b</b> with cysteine, against the total cysteine concentration at pH 6.93 ( $\alpha = 5.8 \times 10^{-2}$ ) at 25 °C and ionic strength 0.5 M.....	74
<b>Figure 2.13</b> Plot of the pseudo first-order rate constants, <i>k</i> <sub>obs</sub> , for the reaction of vinyl sultam <b>2.69b</b> with cysteine, against the cysteine thiolate concentration at pH 6.93, at 25 °C and ionic strength 0.5 M. ....	75
<b>Figure 2.14</b> Compounds assayed for inhibitory activity against cysteine proteases.....	77
<b>Figure 2.15</b> Gold-generated active site interaction of cruzain with <b>1.2d</b> (a), <b>2.4a</b> (b) and <b>2.4b</b> (c).....	80
<b>Figure 2.16</b> Gold-generated active site interaction of papain with <b>2.4a</b> (a) and <b>2.4b</b> (b).....	81
<b>Figure 3.1</b> Generic structures of <i>N</i> -(1,4-naphthoquinon-2-yl)amino derivatives ( <b>3.1-3.3</b> ) and of <i>N</i> -[(1,4-naphthoquinon-2-yl)methyl]amino derivatives ( <b>3.4a</b> ). Structure of 2-ethoxy-1,4-naphthoquinone ( <b>3.5</b> ). ....	85
<b>Figure 3.2</b> Structure of 6-bromo-2-methylquinoline-5,8-dione.....	87
<b>Figure 3.3</b> Observed <sup>1</sup> H NMR triple doublet signals and splitting pattern diagram for the aromatic protons H-6 and H-7 of compound <b>3.1c</b> . ....	89

<b>Figure 3.4</b> Observed $^1\text{H}$ NMR not well resolved <i>dd</i> signals for the aromatic protons H-5 and H-8 of compound <b>3.2c</b> .....	<b>90</b>
<b>Figure 3.5</b> Generic structures of aminoalkyl derivatives.....	<b>91</b>
<b>Figure 3.6</b> Plot of the pseudo first-order rate constants, $k_{\text{obs}}$ , for the reaction of compound <b>3.13</b> with cysteine, against the total cysteine concentration at pH 7.12 ( $\alpha = 8.8 \times 10^{-2}$ ) at 25 °C and ionic strength 0.5 M. ....	<b>94</b>
<b>Figure 3.7</b> Plot of the pseudo first-order rate constants, $k_{\text{obs}}$ , for the reaction of compound <b>3.13</b> with cysteine, against the cysteine thiolate concentration at pH 7.12, at 25 °C and ionic strength 0.5 M. ...	<b>95</b>
<b>Figure 3.8</b> Plot of the catalytic rate constants, $k_{\text{cat}}$ , for the reaction of <b>3.11</b> with cysteine, against the fraction of conjugate base, $\alpha$ , at 25 °C and ionic strength 0.5 M. ....	<b>95</b>
<b>Figure 3.9</b> (a) Plot of the pseudo first-order rate constants, $k_{\text{obs}}$ , for the reaction of naphthoquinone <b>3.8</b> with cysteine, against the total cysteine concentration at pH 7.08 ( $\alpha = 7.08 \times 10^{-2}$ ) at 25 °C and ionic strength 0.5 M; (b) Plot of the pseudo first-order rate constants, $k_{\text{obs}}$ , for the reaction of naphthoquinone <b>3.8</b> with cysteine, against the cysteine thiolate concentration at pH 7.08, at 25 °C and ionic strength 0.5 M. ....	<b>96</b>
<b>Figure 3.10</b> Possible adduct resulting from the reaction of cysteine thiolate with naphthoquinone <b>3.8</b> . ....	<b>97</b>
<b>Figure 3.11</b> Linear correlation between the LUMO energy of naphthoquinones and the Hammett $\sigma_{\text{p}}$ constants.....	<b>99</b>
<b>Figure 3.12</b> Linear correlation between the LUMO orbital energies and the second-order rate constants, $k_{\text{cys}^-}$ , for the reaction of naphthoquinones with the thiolate anion.....	<b>99</b>
<b>Figure 3.13</b> Frontier molecular orbitals of a low-energy conformation of the glycine derivative <b>3.1b</b> . ....	<b>100</b>
<b>Figure 3.14</b> Structure of the assayed indolequinones and kinetic data for inactivation of papain. ....	<b>103</b>
<b>Figure 3.15</b> (a) Plot of the pseudo first-order inactivation rate constants, $k_{\text{obs}}$ , against inhibitor concentration for the inactivation of papain by derivative <b>3.2b</b> , at pH 7.0 at 25 °C; (b) plot of the pseudo first-order inactivation rate constants, $k_{\text{obs}}$ , for the inactivation of papain by derivative <b>3.2c</b> against inhibitor concentration, at pH 7.0 at 25 °C.....	<b>104</b>
<b>Figure 3.16</b> Gold-generated active site interaction of papain with <b>3.1b</b> . ....	<b>106</b>
<b>Figure 3.17</b> Time course of papain inactivation by juglone <b>3.12</b> , at pH 7.0 at 25 °C.....	<b>107</b>
<b>Figure 4.1</b> Inhibitors <b>3.1b</b> , <b>3.21</b> and <b>3.22</b> . ....	<b>115</b>
<b>Figure 4.2</b> Proposed structure for inhibitor development.....	<b>115</b>
<b>Figure 5.1</b> Thiol titration curve for a cysteine solution using Ellman's reagent. ....	<b>159</b>
<b>Figure 5.2</b> Progress curve for the reaction of vinyl sultam <b>2.68a</b> with cysteine (895 $\mu\text{M}$ ), at pH 6.93 at 25 °C and ionic strength 0.5 M.....	<b>160</b>
<b>Figure AI.1</b> Progression curves for the papain-catalysed hydrolysis of Cbz-Gly-ONp.....	<b>168</b>
<b>Figure AI.2</b> Benzoyl-S-arginine-4-nitroanilide (BAPA).....	<b>169</b>
<b>Figure AI.3</b> Reaction rate, $v$ , plotted against the BAPA concentration, [BAPA], for the papain-catalysed hydrolysis of this compound, at pH 7.0 at 25 °C.....	<b>174</b>
<b>Figure AI.4</b> Elution profile (absorbance <i>versus</i> collected fractions) for papain purification by gel-filtration chromatography using a PD-10 desalting column.....	<b>175</b>
<b>Figure AI.5</b> Reaction rate, $v$ , plotted against the papain concentration, [papain], for the papain-catalysed hydrolysis of BAPA, at pH 7.0 at 25 °C.....	<b>176</b>

<b>Figure AI.6</b> Time course of papain inactivation by 2-bromo-1,4-naphthoquinone derivative <b>3.6</b> , at pH 7.0 at 25 °C. ....	177
<b>Figure AI.7</b> Reaction rate, $v$ , plotted against the Cbz-S-Lys-ONp concentration, [Cbz-S-Lys-ONp], for the bovine spleen cathepsin B-catalysed hydrolysis of this compound, at pH 5.0 at 25 °C. ....	181
<b>Figure AI.8</b> Structure of <b>I.5</b> , an inhibitor of porcine pancreatic elastase. ....	182
<b>Figure AI.9</b> Dependence of the absorption at 595 nm on the amount of papain inactivated by <b>3.1b</b> . ....	187
<b>Figure AI.10</b> Visible spectra depicting the dye-papain complex in the presence and absence of the inhibitor <b>3.1b</b> . ....	187
<b>Figure AI.11</b> Series of progression curves for the papain-catalysed hydrolysis of BAPA, at different times of the enzyme-inhibitor incubation. ....	189
<b>Figure AIII.1</b> UV-visible spectra depicting the reaction, at 25 °C, of <b>3.1b</b> (50 $\mu$ M) with cysteine <i>ca.</i> 5 mM in 50 mM K <sub>2</sub> HPO <sub>4</sub> /KH <sub>2</sub> PO <sub>4</sub> buffer, pH 7.14, containing KCl to maintain ionic strength at 0.5 M. ....	195

## INDEX OF SCHEMES

<b>Scheme 1.1</b> Currently accepted catalytic mechanism for papain-like cysteine proteases. ....	7
<b>Scheme 1.2</b> Mechanism of inhibition of cysteine proteases by epoxysuccinyl derivatives. ....	13
<b>Scheme 1.3</b> Schematic representation of the binding modes of epoxysuccinyl derivatives. ....	13
<b>Scheme 1.4</b> Mechanism of inhibition of cysteine proteases by vinyl sulfones. ....	14
<b>Scheme 1.5</b> Synthetic pathway to vinyl sulfones and their analogues. ....	19
<b>Scheme 1.6</b> Formation of reactive oxygen species by redox cycling of quinones. ....	22
<b>Scheme 1.7</b> Michael-type addition of thiols to quinones. ....	23
<b>Scheme 1.8</b> Approach to the design of potential irreversible inhibitors of cysteine proteases. ....	26
<b>Scheme 2.1</b> Strategic routes for the synthesis of dipeptide vinyl sultams <b>2.1-2.4</b> . ....	30
<b>Scheme 2.2</b> Main strategic routes for the preparation of the $\beta$ -sultam ring. ....	31
<b>Scheme 2.3</b> Representation of the $\beta$ -sultam synthesis carried out by Baganz <i>et al.</i> ....	32
<b>Scheme 2.4</b> Main precursors for the preparation of 2-aminoethanesulfonic acid derivatives. ....	33
<b>Scheme 2.5</b> Synthetic pathway to 2-aminoethanesulfonic acid derivatives from alkyl ethenesulfonates. ....	33
<b>Scheme 2.6</b> Synthesis of the $\beta$ -sultam ring by cyclisation of 1-fluorosulfonyl-2-aminoethane derivatives. ....	34
<b>Scheme 2.7</b> Products from the reaction of ethenesulfonyl chloride with amines. ....	34
<b>Scheme 2.8</b> Synthetic routes to ethenesulfonyl fluoride. ....	35
<b>Scheme 2.9</b> Synthetic pathway to $\beta$ -sultam ring from $\beta$ -hydroxysulfonamide mesylates. ....	35
<b>Scheme 2.10</b> Main strategic routes for the preparation of the $\gamma$ - and $\delta$ -sultam rings. ....	36
<b>Scheme 2.11</b> Synthesis of $\delta$ -sultam by C-C ring closure. ....	37



<b>Scheme 2.12</b> Synthesis of <i>N</i> -phenyl- $\beta$ -sultam by cyclisation of <i>N</i> -phenyl-2-hydroxyethanesulfonamide mesylate. ....	<b>39</b>
<b>Scheme 2.13</b> Mechanism of the formation of ethenesulfonamides. ....	<b>39</b>
<b>Scheme 2.14</b> Reaction products from <i>N</i> -phenyl-2-hydroxyethanesulfonamide mesylate. ....	<b>40</b>
<b>Scheme 2.15</b> Attempted synthesis of <i>N</i> -phenyl- $\beta$ -sultam by cyclisation of <i>N,N</i> -disubstituted-methanesulfonamides. ....	<b>41</b>
<b>Scheme 2.16</b> Attempted synthesis of <i>N</i> -phenyl- $\beta$ -sultam by cyclisation of 2-(phenylamino)ethanesulfonyl chloride hydrochloride. ....	<b>42</b>
<b>Scheme 2.17</b> Attempted synthesis of <i>N</i> -benzyl- $\beta$ -sultam. ....	<b>44</b>
<b>Scheme 2.18</b> Synthesis of <i>N</i> -phenyl- and <i>N</i> -benzyl- $\gamma$ -sultams. ....	<b>46</b>
<b>Scheme 2.19</b> Synthesis of <i>N</i> -phenyl- and <i>N</i> -benzyl- $\delta$ -sultams by cyclisation of the corresponding 1-chlorosulfonyl-4-aminobutane hydrochlorides. ....	<b>48</b>
<b>Scheme 2.20</b> Synthesis of the <i>N</i> -benzyl- $\delta$ -sultam by cyclisation of the 4-bromo- <i>N</i> -benzylbutanesulfonamide. ....	<b>49</b>
<b>Scheme 2.21</b> Synthesis of <i>N</i> -Boc- <i>S</i> -phenylalanylal from <i>N</i> -Boc- <i>S</i> -phenylalanine <i>via</i> hydroxamate... ..	<b>51</b>
<b>Scheme 2.22</b> Attempted synthesis of <i>N</i> -Boc- <i>S</i> -phenylalanylal from <i>N</i> -Boc- <i>S</i> -phenylalanine ethyl ester. ....	<b>52</b>
<b>Scheme 2.23</b> Synthesis of dipeptidyl aldehydes. ....	<b>53</b>
<b>Scheme 2.24</b> Synthesis of <i>E</i> - and <i>Z</i> -vinyl sultams <i>via</i> an aldol-like reaction. ....	<b>53</b>
<b>Scheme 2.25</b> Synthesis of <i>E</i> - and <i>Z</i> -vinyl sultams through Horner-Wadsworth-Emmons chemistry. .	<b>54</b>
<b>Scheme 2.26</b> Attempted synthesis of dipeptide vinyl sultams from dipeptidyl aldehydes. ....	<b>58</b>
<b>Scheme 2.27</b> Removal of the <i>N</i> -Boc protecting group of <i>E</i> - and <i>Z</i> -vinyl sultams. ....	<b>59</b>
<b>Scheme 2.28</b> Synthesis of dipeptide vinyl sultam <b>2.1</b> . ....	<b>60</b>
<b>Scheme 2.29</b> Synthesis of dipeptide vinyl sultams <b>2.2-2.4</b> . ....	<b>61</b>
<b>Scheme 2.30</b> Attempted synthesis of a dipeptide vinyl sultam from <i>N</i> -Mu- <i>S</i> -phenylalanine. ....	<b>61</b>
<b>Scheme 2.31</b> Synthesis of vinyl sulfonamides. ....	<b>70</b>
<b>Scheme 2.32</b> Adducts from the reaction of $\alpha$ -methylene- $\gamma$ -sultams with thiols. ....	<b>73</b>
<b>Scheme 3.1</b> Reaction of amines with the reduced form of 2-bromo-1,4-naphthoquinone. ....	<b>86</b>
<b>Scheme 3.2</b> Synthesis of <i>N</i> -(1,4-naphthoquinon-2-yl)amino derivatives and of 2-ethoxy-1,4-naphthoquinone. ....	<b>87</b>
<b>Scheme 3.3</b> Preparation of aminomethyl derivatives by Prezhdo <i>et al.</i> ....	<b>91</b>
<b>Scheme 3.4</b> Attempted synthesis of aminomethyl derivatives.. ....	<b>91</b>
<b>Scheme 3.5</b> The proposed reaction mechanism of cysteine with dopaminoquinone. ....	<b>96</b>
<b>Scheme 3.6</b> Proposed mechanism of glyceraldehyde-3-phosphate dehydrogenase by 9,10-phenanthrenequinone under aerobic conditions. ....	<b>101</b>
<b>Scheme 5.1</b> Reaction of Ellman's reagent with thiols. ....	<b>159</b>
<b>Scheme AI.1</b> Determination of the papain activity using Cbz-Gly-ONp as substrate. ....	<b>166</b>
<b>Scheme AI.2</b> Possible procedures to be used for the inhibition assay. ....	<b>172</b>

## INDEX OF TABLES

<b>Table 1.1</b> Pathologically relevant cysteine proteases.....	2
<b>Table 1.2</b> (a) Second-order rate constants for inactivation of cysteine proteases by epoxysuccinyl derivatives; (b) IC <sub>50</sub> values of epoxysuccinyl derivatives for cysteine proteases.....	11
<b>Table 1.3</b> Vinyl sulfones and analogues: second-order rate constants for inactivation of cruzain and results of <i>in vitro</i> assays against <i>Trypanosoma cruzi</i> . ....	16
<b>Table 1.4</b> Vinyl sulfones and analogues: (a) IC <sub>50</sub> values for falcipain-2 and cultured <i>Plasmodium falciparum</i> parasites; (b) second-order rate constants for inactivation of falcipains 2 and 3. ....	17
<b>Table 2.1</b> Conditions for the synthesis of <i>N</i> -phenyl-β-sultam from <b>2.49a</b> . ....	42
<b>Table 2.2</b> Conditions for the cyclisation of <i>N</i> -benzyl-2-hydroxyethanesulfonamide mesylate into <i>N</i> -benzyl-β-sultam. ....	44
<b>Table 2.3</b> Conditions for the synthesis of 3-chloro- <i>N</i> -phenylpropane-1-sulfonamide <b>2.39a</b> from <b>2.41a</b> . ....	47
<b>Table 2.4</b> Conditions for the synthesis of sultam phosphonates. ....	54
<b>Table 2.5</b> NMR data of <b>2.65a</b> [400 MHz ( <sup>1</sup> H), 100.61 MHz ( <sup>13</sup> C), CDCl <sub>3</sub> ]. ....	55
<b>Table 2.6</b> Yields and ratio of <i>E/Z</i> isomers. ....	57
<b>Table 2.7</b> Optical rotations, [α] <sub>D</sub> <sup>21</sup> , of <i>E/Z</i> isomers. ....	57
<b>Table 2.8</b> Chemical shifts δ and coupling constants <i>J</i> [400 MHz ( <sup>1</sup> H), CDCl <sub>3</sub> ] for vinyl and methine protons of <i>E/Z</i> isomers.....	58
<b>Table 2.9</b> NMR data of <b>2.1</b> [400 MHz ( <sup>1</sup> H), 100.61 MHz ( <sup>13</sup> C), CDCl <sub>3</sub> ]. ....	65
<b>Table 2.10</b> NMR data of <b>2.2</b> [400 MHz ( <sup>1</sup> H), 100.61 MHz ( <sup>13</sup> C), CDCl <sub>3</sub> ]. ....	66
<b>Table 2.11</b> NMR data of <b>2.3</b> [400 MHz ( <sup>1</sup> H), 100.61 MHz ( <sup>13</sup> C), CDCl <sub>3</sub> ]. ....	67
<b>Table 2.12</b> NMR data of <b>2.4a</b> [400 MHz ( <sup>1</sup> H), 100.61 MHz ( <sup>13</sup> C), CDCl <sub>3</sub> ]. ....	68
<b>Table 2.13</b> NMR data of <b>2.4b</b> [400 MHz ( <sup>1</sup> H), 100.61 MHz ( <sup>13</sup> C), CDCl <sub>3</sub> ]. ....	69
<b>Table 2.14</b> NMR data of <b>2.86</b> [400 MHz ( <sup>1</sup> H), 100.61 MHz ( <sup>13</sup> C), CDCl <sub>3</sub> ]. ....	71
<b>Table 2.15</b> Cysteine-catalysed second-order rate constants, <i>k</i> <sub>cys<sup>-</sup></sub> , for vinyl sultams and for an analogous vinyl sulfonamide. ....	76
<b>Table 2.16</b> IC <sub>50</sub> values of vinyl sultams for falcipain-2 and <i>Plasmodium falciparum</i> W2. ....	78
<b>Table 3.1</b> Conditions for the synthesis of aminomethyl derivatives. ....	92
<b>Table 3.2</b> LUMO energies and cysteine-catalysed second-order rate constants, <i>k</i> <sub>cys<sup>-</sup></sub> , for naphthoquinones. ....	98
<b>Table 3.3</b> LUMO energies and kinetic data for inactivation of papain by naphthoquinones. ....	102
<b>Table 3.4</b> LUMO energies and kinetic data for inactivation of bovine spleen cathepsin B by naphthoquinones. ....	109
<b>Table 5.1</b> Conditions for the synthesis of <i>N</i> -phenylmethanesulfonamide. ....	123
<b>Table AI.1</b> Papain activity in the presence of different DTT concentrations. ....	171
<b>Table AI.2</b> Papain activity for several activation time periods. ....	173

<b>Table AII.1</b> Pseudo first-order rate constants, $k_{\text{obs}}$ , for the reaction of vinyl sultams <b>2.67a</b> , <b>2.67b</b> , <b>2.68a</b> and <b>2.69b</b> with cysteine at pH 6.9, at 25 °C and ionic strength 0.5 M. ....	<b>191</b>
<b>Table AII.2</b> Pseudo first-order rate constants, $k_{\text{obs}}$ , for the reaction of vinyl sulfonamide <b>2.84a</b> with cysteine at pH 6.9, at 25 °C and ionic strength 0.5 M. ....	<b>191</b>
<b>Table AII.3</b> Pseudo first-order rate constants, $k_{\text{obs}}$ , for the reaction of naphthoquinones <b>3.1a</b> , <b>3.1b</b> , <b>3.1c</b> , <b>3.5</b> , <b>3.8</b> , <b>3.13</b> and <b>3.11</b> with cysteine at pH 7.1, at 25 °C and ionic strength 0.5 M.....	<b>192</b>
<b>Table AV.1</b> LUMO energies and Hammett $\sigma_p$ constants for naphthoquinones. ....	<b>201</b>
<b>Table AVI.1</b> Pseudo first-order rate constants, $k_{\text{obs}}$ , for inactivation of the papain by quinones <b>3.1b-d</b> , <b>3.2a-c</b> , <b>3.3a,b</b> , <b>3.5</b> , <b>3.6</b> , <b>3.9</b> , <b>3.11</b> , <b>3.13</b> , <b>3.20</b> , <b>3.21</b> and <b>3.22</b> , at pH 7.0 at 25 °C. ....	<b>203</b>
<b>Table AVI.2</b> Pseudo first-order rate constants, $k_{\text{obs}}$ , for inactivation of bovine spleen cathepsin B by quinones <b>3.1b</b> , <b>3.2b</b> , <b>3.5</b> and <b>3.6</b> at pH 5.0 at 25 °C.....	<b>205</b>



## ABSTRACT

Among the enzymes dependent on a thiol nucleophile (cysteine) at their active sites, the largest and best studied is the papain superfamily, which encompasses parasite enzymes (falcipain, cruzain and rhodesain) and mammalian enzymes (*e.g.* cathepsins and calpains). The first group is crucial in the metabolism and reproductive function of *Plasmodium falciparum* and *Trypanosoma* spp., while elevated levels of the second group of enzymes are evident in pathological processes, such as muscular dystrophy, osteoporosis, chronic inflammatory diseases and cancer. Therefore, papain-like cysteine proteases represent major therapeutic targets for protease inhibitor development. This work focused on the evaluation of the vinyl sultam and 1,4-naphthoquinone scaffolds as potential building blocks for the design of novel irreversible inactivators for these enzymes.

Five dipeptide vinyl sultams were synthesised through an initial Horner-Wadsworth-Emmons reaction between *N*-Boc-*S*-phenylalaninal and sultam phosphonates, followed by the attachment of the *E*- and *Z*- intermediates to *N*-protected amino acids, under standard peptide coupling conditions. These compounds were found to be inactive against papain at concentrations up to 50  $\mu\text{M}$  and weakly active toward recombinant falcipain-2 ( $\text{IC}_{50}$  between 13.7 and 48.4  $\mu\text{M}$ ) and *Plasmodium falciparum* W2 ( $\text{IC}_{50} > 7.8 \mu\text{M}$ ). Docking studies suggested that two different binding modes of vinyl sultams to cysteine proteases are available, neither of which is favourable for the conjugate addition of Cys25 to the vinyl sultam system.

A series of 1,4-naphthoquinone derivatives was prepared by reaction of methylamine, amino acid ethyl esters and EtOH with commercial 1,4-naphthoquinones. These compounds were found to be irreversible inhibitors of papain and bovine spleen cathepsin B, with second-order rate constants,  $k_2$ , ranging from 0.67 to 35.4  $\text{M}^{-1} \text{s}^{-1}$  for papain, and from 0.54 to 8.03  $\text{M}^{-1} \text{s}^{-1}$  for cathepsin B. Some compounds displayed saturation inhibition kinetics with respect to inhibitor concentration, with  $K_i$  values between 9.57 and 266  $\mu\text{M}$  for papain, and between 14.0 and 797  $\mu\text{M}$  for cathepsin B. The chemical reactivity of the compounds toward cysteine as a model thiol is dependent on the naphthoquinone LUMO energy, whereas papain inactivation is not.

The 1,4-naphthoquinone derivatives were unable to inhibit recombinant falcipain-2 and *Plasmodium falciparum* W2 at concentrations up to 10  $\mu\text{M}$ , and were also inactive against the serine protease, porcine pancreatic elastase.

## KEYWORDS

Vinyl sultams, Naphthoquinones, Irreversible Inhibitors, Cysteine Protease Inhibitors, Thiols, Reactivity.



## RESUMO

A superfamília a que pertence o enzima papaína é o maior grupo de proteases de cisteína e também o mais estudado. Entre os seus membros, incluem-se alguns dos enzimas presentes nos parasitas (falcipaína, cruzaina e rodesaina) e nos mamíferos (*e.g.* catepsinas e calpaínas). O primeiro grupo é crucial no metabolismo e na reprodução do *Plasmodium falciparum* e *Trypanosoma* spp. Relativamente às catepsinas e às calpaínas, o seu aumento está associado a patologias como a distrofia muscular, a osteoporose, as doenças inflamatórias crónicas e o cancro. Desta forma, a inactivação destas proteases é uma estratégia viável em terapêutica, através do desenvolvimento de inibidores apropriados. O trabalho aqui apresentado teve como objectivo a avaliação de um grupo de sultamas vinílicas e de 1,4-naftoquinonas como potenciais inibidores irreversíveis destes enzimas.

Foram preparadas cinco sultamas vinílicas, cuja estrutura inclui um segmento dipeptídico. A sua síntese envolveu duas etapas principais: (i) a síntese de sultamas vinílicas intermediárias *E*- e *Z*- com um só aminoácido, através da reacção de Horner-Wadsworth-Emmons entre o *N*-Boc-*S*-fenilalaninal e os diversos fosfonatos das sultamas e (ii) a reacção dessas sultamas com aminoácidos *N*-protegidos, em condições usadas habitualmente em síntese peptídica. Estes compostos não inibiram a papaína quando testados até uma concentração máxima de 50  $\mu\text{M}$  e mostraram uma fraca acção antimalária, através do estudo do seu efeito inibitório na actividade da falcipaína-2 recombinante (valores de  $\text{CI}_{50}$  compreendidos entre 13,7 e 48,4  $\mu\text{M}$ ) e no crescimento do *Plasmodium falciparum* W2 ( $\text{CI}_{50} > 7,8 \mu\text{M}$ ). Estudos de *docking* apresentaram dois modelos possíveis para a interacção entre as sultamas vinílicas e as proteases de cisteína, ambos desfavoráveis ao ataque da Cys25 aos compostos.

Os derivados da 1,4-naftoquinona foram preparados através da reacção de diversas 1,4-naftoquinonas comerciais com a metilamina, ésteres etílicos dos aminoácidos e com o etanol. Este grupo de compostos inibiu a papaína e a catepsina B bovina, de forma irreversível, com constantes cinéticas de segunda ordem,  $k_2$ , compreendidas entre 0,67 e 35,4  $\text{M}^{-1} \text{s}^{-1}$  para a papaína, e entre 0,54 e 8,03  $\text{M}^{-1} \text{s}^{-1}$  para a catepsina B. Alguns compostos exibiram uma cinética de saturação relativamente à concentração do inibidor, com valores de  $K_I$  entre 9,57 e 266  $\mu\text{M}$  para a papaína e entre 14,0 e 797  $\mu\text{M}$  para a catepsina B. Estudou-se a reactividade química de algumas 1,4-naftoquinonas na presença do aminoácido cisteína e verificou-se que este parâmetro é dependente da energia da LUMO da naftoquinona, enquanto a actividade como inibidores da papaína é independente. As 1,4-naftoquinonas não inibiram a falcipaína-2 recombinante nem o crescimento do *Plasmodium falciparum* W2 quando testadas até uma concentração máxima de 10  $\mu\text{M}$ . Foram também inactivas contra uma protease de serina, a elastase porcina pancreática.

## PALAVRAS CHAVE

Sultamas Vinílicas, Naftoquinonas, Inibidores Irreversíveis, Inibidores das Proteases de Cisteína, Tióis, Reactividade.





## ABBREVIATIONS AND SYMBOLOGY

Amino acids are written in the three-letter code. Other abbreviations are:

abs	absolute
Ac	acetyl
Anal. Calcd.	Analysis Calculated
Ar	aromatic group
AU	Absorbance Units
Boc	<i>tert</i> -Butoxycarbonyl
BOP	(benzotriazol-1-yloxy)tris(dimethylamino)phosphonium hexafluorophosphate
b.p.	boiling point
br	broad
brd	broad doublet
brdd	broad double doublet
brq	broad quartet
brs	broad singlet
brt	broad triplet
<i>n</i> -BuLi	<i>n</i> -butyllithium
Bz	benzyl
Cbz	benzyloxycarbonyl
CDCl <sub>3</sub>	deuterated chloroform
CD <sub>3</sub> CN	deuterated acetonitrile
<sup>13</sup> C NMR	carbon-13 Nuclear Magnetic Resonance
CNS	Central Nervous System
conc.	concentrated
d	doublet
DCC	<i>N,N'</i> -dicyclohexylcarbodiimide
DCM	dichloromethane
dd	double doublet
ddd	doublet of doublet of doublets
dddd	doublet of doublet of doublet of doublets
DEPT	Distortionless Enhancement by Polarization Transfer
DIBAL	diisobutylaluminum hydride
DMSO	dimethyl sulfoxide
d <sub>6</sub> -DMSO	deuterated dimethyl sulfoxide
D <sub>2</sub> O	deuterium oxide
dt	triple doublet
DTT	DL-dithiothreitol
EDTA	ethylenediaminetetraacetic acid
ESI-MS	Electrospray Ionization Mass Spectrometry
Et	ethyl
EtOAc	ethyl acetate
EtOH	ethanol
GC-MS	Gas Chromatography - Mass Spectrometry
GSH	glutathione
<sup>1</sup> H- <sup>1</sup> H COSY	Proton-Proton COrrrelation SpectroscopY

HMBC	Heteronuclear Multiple Bond Correlation
HMQC	Heteronuclear Multiple Quantum Correlation
<sup>1</sup> H NMR	Proton Nuclear Magnetic Resonance
HOBt	1-hydroxybenzotriazole
Hph	homophenylalanine
HPLC	High Performance Liquid Chromatography
HR-ESI-MS	High Resolution Electrospray Ionization Mass Spectrometry
HTyr	homotyrosine
<i>i</i> -Am	<i>iso</i> -amylamine
IC <sub>50</sub>	the concentration of a drug that is required for 50% of its maximal inhibitory effect
iPr	isopropyl
IR	infrared
<i>J</i>	proton-proton coupling constant
<sup>1</sup> <i>J</i>	one-bond coupling constant
<sup>2</sup> <i>J</i>	geminal coupling constant
<sup>3</sup> <i>J</i>	vicinal coupling constant
<i>J</i> <sub>HP</sub>	one-bond coupling constant for proton-phosphorus ( <sup>31</sup> P)
<i>J</i> <sub>CP</sub>	one-bond coupling constant for proton-carbon ( <sup>13</sup> C)
<sup>2</sup> <i>J</i> <sub>CH</sub>	geminal coupling constant for proton-carbon ( <sup>13</sup> C)
<i>J</i> <sub>ortho</sub>	ortho coupling constant
LDA	Lithium DiisopropylAmide
lit.	literature
LUMO	Lowest Unoccupied Molecular Orbital
m	multiplet
Me	methyl
MeOD	deuterated methanol
MeOH	methanol
mol eq	mole equivalent
m.p.	melting point
Ms	mesyl
Mu	4-morpholinecarbonyl
m/z	mass-to-charge ratio
NMR	Nuclear Magnetic Resonance
NOE	Nuclear Overhauser Effect
NOESY	Nuclear Overhauser Effect Spectroscopy
<i>n</i> -Pr	<i>n</i> -propyl
Ph	phenyl
q	quartet
qd	double quartet
rel. int.	relative intensity
R <sub>f</sub>	retardation factor
rt	room temperature
s	singlet
Suc	succinyl
t	triplet
TBTU	<i>N,N,N,N'</i> -tetramethyl- <i>O</i> -(benzotriazol-1-yl)uronium tetrafluoroborate
td	double triplet
TEA	triethylamine
TFA	trifluoroacetic acid
THF	tetrahydrofuran

TLC	Thin Layer Chromatography
TMEDA	<i>N,N,N',N'</i> -tetramethylethylenediamine
tt	triple triplet
UV	ultraviolet
w/v	weight/volume percentage solution
$A_x$	absorbance at $X$ nm
$N_2$	nitrogen atmosphere
$(M^+)$	molecular ion peak (in mass spectrometry)
$\nu_{\max}$	maximum wave number



# **CHAPTER 1**

## **INTRODUCTION**



# 1. INTRODUCTION

This chapter has three main purposes. Firstly, it will focus on the emergent role of cysteine proteases as attractive therapeutic targets for protease inhibitor development. Secondly, it will summarise the development of vinyl sulfones and analogues as a promising class of cysteine protease irreversible inhibitors. In connection, the synthetic pathway to these compounds is briefly described. Finally, it will focus on the chemical reactivity of the quinone scaffold and on its therapeutic usefulness, including the targeting of cysteine residues.

## 1.1 Cysteine proteases

### 1.1.1 Update

Cysteine proteases are one of the most ubiquitously distributed enzyme classes in nature. They have been found in mammals, virus, bacteria, protozoa, plants and fungi.<sup>1</sup>

This group of enzymes has been widely studied over the years. Nevertheless, until the past decade, they were considered to be of little if any therapeutic interest, because it was thought that they were restricted to housekeeping functions, through the non-specific degradation of proteins in lysosomes or equivalent cellular compartments.<sup>2</sup> However, the recent elucidation of their physiological roles has changed this view. At present, cysteine proteases are known to regulate key biological processes in humans and their overexpression, in particular, has been associated with very diverse pathological manifestations ranging from cardiovascular, inflammatory, neurological, respiratory, musculo-skeletal, immunological and CNS disorders to cancer.<sup>3</sup> On the other hand, they perform critical functions in disease-causing parasites and viruses.<sup>3,4</sup>

Therefore, there is an increasing interest in the effective inhibition of cysteine proteases for therapeutic intervention.<sup>2</sup> This situation is manifested in a fair number of recent reviews<sup>1-3,5-8</sup> and major efforts in protease inhibitor discovery, which has been improved by the availability of three-dimensional structural information for representative cysteine proteases.

At present, several inhibitors are already in clinical drug development (Figure 1.1).<sup>2</sup> For example, compound **1.1** is an available orphan drug for the treatment of patients undergoing organ transplantations (phase IIb); **1.2a** is being developed for the treatment of Chagas

disease (pre-clinical) and **1.3a** for the treatment of common cold (phase II/III).<sup>2,9</sup> Further, a search in a patents database<sup>10</sup> revealed more than 50 patents concerning cysteine protease inhibitors, for the period between 2002 and 2006.

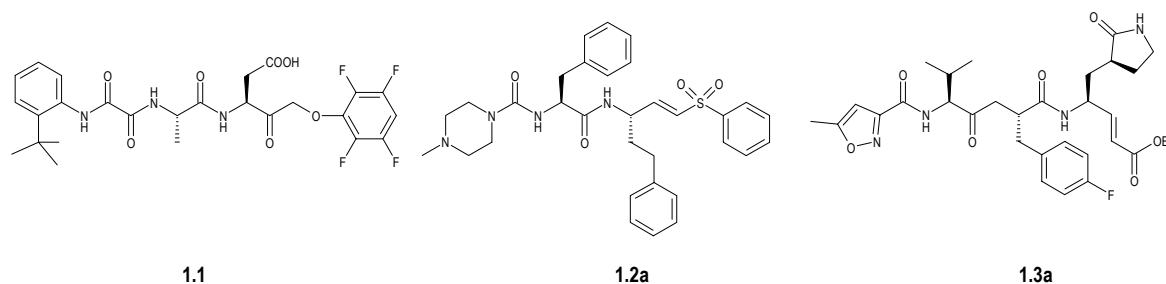


**Figure 1.1** IDN-6556 (1.1), CRA-3316 (1.2a) and ruprintrivir (1.3a).

### 1.1.2 Potential therapeutic targets

To date, the cysteine proteases of therapeutic importance have been categorised into three groups: papain-like (clan CA), ICE-like (clan CD) and picornain-like (clan PA(C)).<sup>8</sup> Table 1.1 lists the proteases with larger impact at the present time. For cathepsin K, caspases and rhinovirus 3C protease, inhibitor development is currently in clinical trials.<sup>2</sup> Inhibition of cathepsin S and of cruzain is under pre-clinical study.<sup>2</sup>

**Table 1.1** Pathologically relevant cysteine proteases.

Clan	Family	Protease
CA	C1 (mammalian)	Cathepsins B, K and S
	C1 (parasite)	Falcpains, cruzain and rhodesain
	C2 (mammalian)	Calpains
CD	C14 (mammalian)	Caspases
PA(C)	C3 (viral)	Rhinovirus 3C
	C30 (viral)	SARS-CoV 3CL <sup>pro</sup>

The largest and best studied is the papain-like group (clan CA), which encompasses papain (a plant protease), mammalian (cathepsins and calpains) and parasite (falcpain, cruzain and rhodesain) enzymes.<sup>8</sup>

Papain has been extensively investigated since the earlier twentieth century and it is a good study model for this group of enzymes.<sup>8</sup>



For mammalian proteases, major advances in drug discovery have been accomplished for cathepsins, mainly cathepsins K, S and B.<sup>2</sup> The first one is the major protease responsible for bone resorption and therefore is a novel therapeutic target for diseases characterised by excessive bone loss, such as osteoporosis and rheumatoid arthritis.<sup>2</sup> Cathepsin S plays a key role in processing antigens for presentation to the immune cells system. Thus, its inhibitors are being developed for the treatment of inflammation and immune system-related diseases (*e.g.* rheumatoid arthritis, inflammatory bowel disease, myasthenia gravis, asthma).<sup>2,3</sup> An elevated cathepsin B has been associated with the development of cancer. It has been demonstrated that this enzyme is involved in the degradation of the extracellular matrix allowing the invasive growth of malignant tumours and the formation of metastases. However, it is considered that more than 20 years of research did not provide sufficient preclinical data to establish the potential of cathepsin B inhibitors in cancer chemotherapy, which was demonstrated in *in vitro* studies.<sup>11</sup> In addition, the enzyme has been associated with other important pathological processes, *e.g.* inflammation, neurodegenerative disorders and ischemic neuronal death.<sup>2,11</sup>

Calpains have a calcium-dependent proteolytic activity. They have been implicated in ischaemia/reperfusion injuries (*e.g.* myocardial infarction), CNS diseases (*e.g.* Alzheimer's disease) and cataract formation.<sup>2,5</sup> Nevertheless, most of their physiological functions are still unknown and clinical investigations on the role of its inhibitors as effective drugs have yet to be reported.<sup>2</sup>

Cysteine proteases have proved to be essential in the life cycle of many species of parasites (*e.g.* replication or growth, cell differentiation, signalling, host invasion).<sup>3</sup> Cruzipain (also known as cruzain) is the enzyme with the highest proteolytic activity in *Trypanosoma cruzi*, which is the causative agent of Chagas disease.<sup>3</sup> *Trypanosoma brucei rhodesiense* (sleeping sickness) expresses rhodesain whereas *Plasmodium falciparum*, the most virulent malaria-causing parasite in humans, expresses a family of four papain-like proteases, named falcipains 1, 2, 3 and 2'.<sup>3,12</sup> Falcipain-2 is the most abundant and best-studied enzyme among the falcipains.<sup>13</sup> This enzyme and the related falcipain-3 play critical roles in the host haemoglobin proteolysis to provide free amino acids required for parasite survival, while function of falcipain-1 remains uncertain, although it has been demonstrated that it is not essential for normal development during erythrocytic stage.<sup>14</sup> Falcipain 2' has been recently described.<sup>15</sup> It is very similar in sequence to falcipain-2 and the studies suggest that it may

play an identical role. Investigations also suggest the possibility of generate effective inhibitors that target all falcipains 2, 3 and 2'.<sup>15,16</sup>

The mentioned vector-borne protozoan diseases are some of the major and increasing causes of morbidity and mortality in Africa, Asia, Central and South America.<sup>3</sup> Due to socioeconomic reasons, these infections have received limited attention from pharmaceutical companies.<sup>3</sup> At present, few drugs are available and the present chemotherapy is decades old and is not satisfactory in terms of drug resistance and also due to the toxicity associated to long-term treatments.<sup>12</sup> In addition, vector resistance to insecticides is other significant obstacle.<sup>12</sup> In this context, the development of new therapies is urgently required, a situation appreciated by the World Health Organization.<sup>17</sup> The studies with cysteine protease inhibitors have established these enzymes as molecular targets for an alternative to traditional antiparasitic chemotherapy.<sup>12</sup>

A second group of therapeutically relevant mammalian cysteine proteases is the one of caspases (clan CD, family C14). Caspase-1 (also known as ICE<sup>a</sup>) is the most studied and it is required for the activation of cytokines, which play essential roles in inflammatory diseases (*e.g.* asthma, rheumathoid arthritis, psoriasis, inflammatory bowel disease).<sup>2</sup> Currently, ICE inhibitors are in clinical development as anti-inflammatory agents.<sup>2</sup> The other caspases (2, 3, 6, 7, 8, 9, 10 and 14) are involved in cascades that lead to apoptosis, but the exact role of the individual caspases is not fully known to date.<sup>2</sup> Thus, broad-spectrum caspase inhibitors are being developed for the treatment and prevention of situations in which cell death contributes to organ damage (*e.g.* liver diseases, CNS diseases, organ transplantations).<sup>2</sup>

The third group is the picornain-like cysteine proteases, clan PA(C), which play key roles in viral life cycles. They are required to the cleavage of a polyprotein into mature viral proteins. Inhibition of this process disables the replication of the virus.<sup>5</sup> HRV-3C protease is essential for human rhinoviruses, which may well be responsible for more than 50% of common cold in adults and children.<sup>2</sup> The protease SARS-CoV 3CL<sup>pro</sup> is equally important to SARS coronavirus, identified as the causative agent of the severe acute respiratory syndrome. This illness was the first severe and readily transmissible disease of the 21st century (from November 2002 to July 2003).<sup>18</sup> Due to its rapid transmission (it was reported in 26 countries) and high mortality rate, SARS is a potential global threat and there is no effective drug available for its treatment.<sup>2,18</sup>

---

<sup>a</sup> Interleukin-1 $\beta$  Converting Enzyme.

Protease-inhibitor X-ray crystal structures are available from the PDB database<sup>9</sup> for the majority of the above-mentioned cysteine proteases. Exceptions are found in the calpain and caspase families, along with rhodesain and falcipains 1, 3 and 2<sup>7</sup>.

During the time course of this thesis, two crystal structures of falcipain-2 in complex to iodoacetamide<sup>19</sup> and cystatin<sup>13</sup> have been reported. This provides an opportunity to the rational discovery of effective inhibitors against malaria, which is already being exploited by GlaxoSmithKline (Spain).<sup>13</sup> It is noteworthy that the three-dimensional structure of falcipain-2 was compared to those in the PDB database.<sup>19,20</sup> Cruzain was identified as the most similar structural homologue.<sup>19</sup> Thus, it is considered that the inhibitors designed against cruzain, *e.g.* vinyl sulfones (Section 1.2.3), provide starting compounds for the rational design of novel antimalarials.<sup>19</sup>

### 1.1.3 Structural differences

Enzymes of the same family show evidence of their evolutionary relationship by their similar tertiary structures, by the order of catalytic residues in their sequences or by common sequence motifs around the catalytic residues. Related families are grouped into a clan.<sup>7</sup> Structural differences between clans are important in the design of specific inhibitors.

The picornain-like cysteine proteases, clan PA(C), have no homology to papain (clan CA) and caspase families (clan CD). The sequence and fold of clan PA(C) cysteine proteases is most similar to the one of the serine protease chymotrypsin and although an active site cysteine exist instead of a serine nucleophile, the catalytic mechanism resembles more the one of a serine protease than that of a classical cysteine protease (Section 1.1.4).<sup>1,5</sup>

The papain-like proteases (clan CA) and caspases (clan CD) are also unrelated. A useful difference concerns the primary specificity site.<sup>b</sup> Caspases show selectivity for substrates with an aspartate at the P1 position.<sup>7</sup> Papain-like cysteine proteases do not have a well-defined S1 subsite and the most important element of substrate specificity is the hydrophobic S2 subsite, which is highly selective for bulky *S*-amino acids such as Phe or Leu.<sup>1</sup>

---

<sup>b</sup> In describing the binding of substrates and inhibitors to the active site of proteases, it is considered that enzymatic binding pockets (subsites) from the scissile peptide bond toward the *N*-terminus (non-prime side) are termed S1, S2, etc. and those toward the *C*-terminus (prime side) S1', S2', etc. The corresponding substrate or inhibitor amino acids associated with each subsite are termed P1, P2, etc.<sup>6</sup>

A major challenge in inhibitor design is selectivity within the same family or within the same clan. For example, members of the papain clan, *i.e.* papain superfamily, have similar non-primed substrate binding pockets and as mentioned above they share a P2-selectivity for hydrophobic residues. Larger differences exist within the prime side.<sup>5</sup>

A unique feature of cathepsin B, which distinguishes it from other papain-like proteases, is the presence of an 18-residue-long insertion known as the occluding loop. This structure is characterised by two adjacent histidine residues (His110 and His111, cathepsin B numbering) in the S2' region, which bind to the C-terminal carboxylic group of the substrate allowing the carboxypeptidase activity of this enzyme.<sup>2,11</sup> This insight was applied in inhibitor design. Thus, the dipeptidyl sequences Ile(or Leu)-Pro-OH were used to interact with the S1' and S2' subsites. Selective and highly potent inhibitors of cathepsin B were achieved, from which CA-074 (Section 1.2.2) is a representative member.<sup>2,11</sup>

In addition, the S2 subsite of cathepsin B lacks a residue equivalent to Val157 of papain, which means that the S2 pocket is larger.<sup>1</sup> Cathepsin B and cruzain also possess an extra Glu residue in the mentioned subsite, which explains the dual specificity of both enzymes for substrates containing either a hydrophobic (*e.g.* Phe) or basic residue (*e.g.* Arg) at the P2 position.<sup>21</sup>

Thus, by exploiting the prime side and the subtle differences at the P2 pocket it should be possible to selectively inhibit individual papain-like proteases.<sup>5</sup>

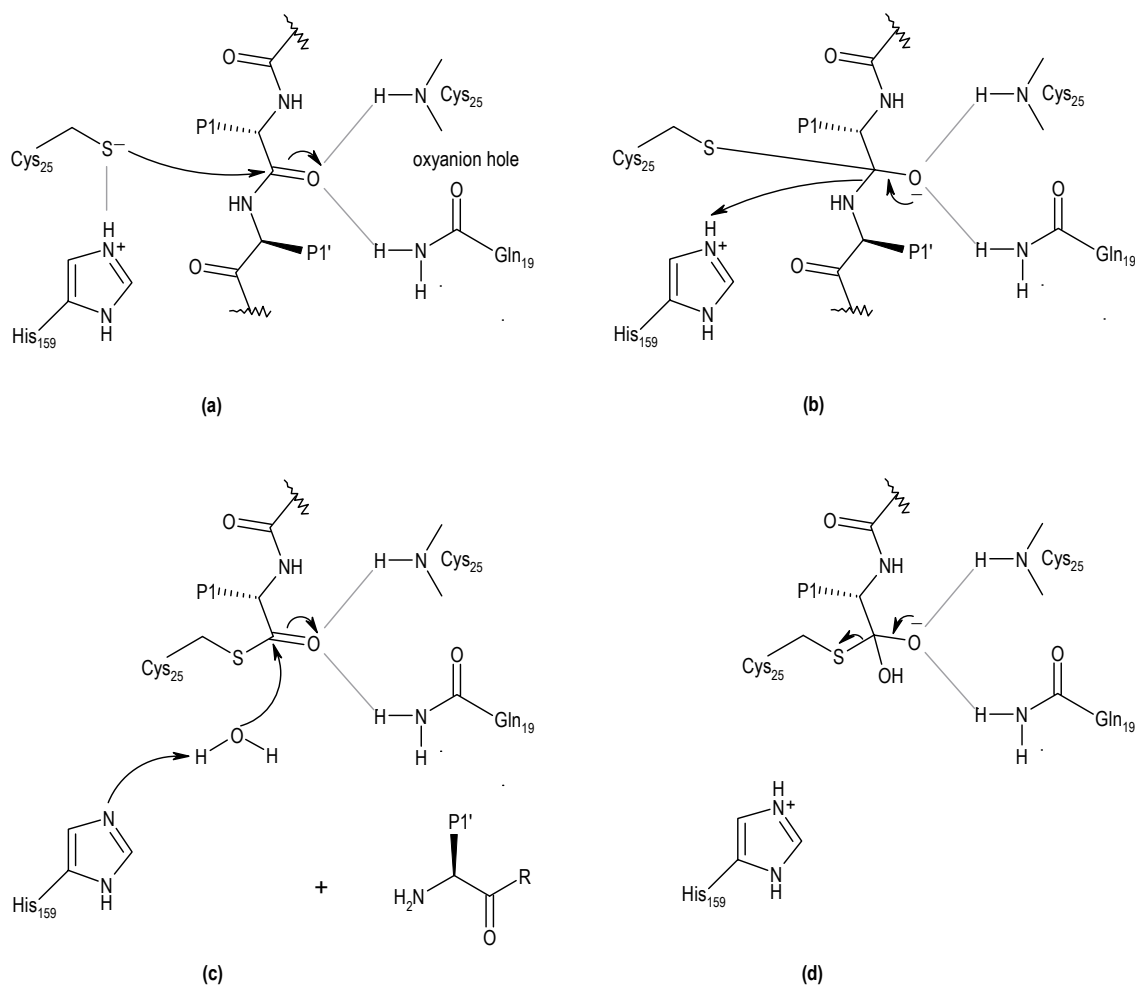
On the other hand, this similarity is regarded as an opportunity to target several disease-related enzymes, when broad-spectrum drugs might be an advantage, *e.g.* antiprotozoal agents.<sup>22</sup>

### 1.1.4 Catalytic mechanism

The catalytic mechanism herein described is the one of a classical cysteine protease, which means a papain-like (Scheme 1.1).

The activity of these enzymes depends on the nucleophilicity of the cysteine thiolate group which, after the formation of the non-covalent Michaelis complex (Scheme 1.1a), attacks the carbonyl carbon of the scissile amide bond leading to a tetrahedral intermediate (Scheme 1.1b). This situation is favoured by the stabilization of the produced tetrahedral intermediate anion through hydrogen bonding to the side chain of Gln19 and to the amide group of Cys25, which are commonly referred to as the oxyanion hole. In the next step

(Scheme 1.1b), the imidazolium ion protonates the nitrogen of a leaving amine to form an acyl-enzyme. Subsequently (Scheme 1.1c), the imidazole nitrogen polarizes a water molecule which attacks the acyl-enzyme and a second tetrahedral intermediate is produced (Scheme 1.1d). Finally, the acid is released and the free enzyme is regenerated.<sup>1,4,7</sup>



**Scheme 1.1** Currently accepted catalytic mechanism for papain-like cysteine proteases. Amino acid residues are in papain numbering. Hydrogen bonds are in grey.

The main feature in the active site of papain-like cysteine proteases is the close proximity of the residues Cys25 and His159, which are spatially orientated to form a catalytic ion pair (Figure 1.2). The histidine imidazole group polarizes the cysteine thiol, allowing deprotonation even at physiological conditions.<sup>4</sup> Therefore, the reactive species is a thiolate

anion, which explains the unusually high reactivity of cysteine proteases in comparison with simple thiols. In fact, the thiol moiety of cysteine proteases has a  $pK_a$  of 2.5, in contrast with the  $pK_a$  of free cysteine thiol, which is 8.3.<sup>2</sup>

It has been proposed that the thiolate/imidazolium ion pair is significantly stabilised by the residues Asp158, Trp177 and Asn175. The latter amino acid forms with Cys25 and His159 the referred “catalytic triad of the papain superfamily” and it may be also responsible to direct the histidine imidazole’s position through the different steps of the catalytic mechanism.<sup>23,24</sup> However, the exact role of these residues, *i.e.* Asp158, Trp177 and Asn175, remains under discussion.<sup>25</sup>

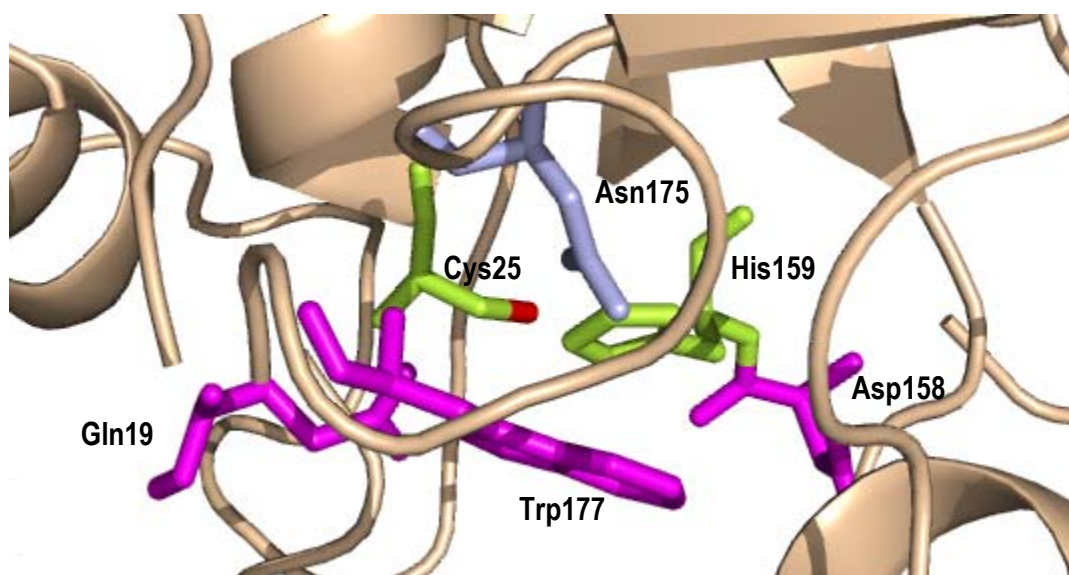


**Figure 1.2 Active-site of papain.** Cys25 and His159 are in green. The sulphur atom of Cys25 is highlighted in red. Asn175 is in blue. Gln19, Asp158 and Trp177 are in magenta. This figure was prepared from 1PPN<sup>20</sup> using Pymol software.<sup>26</sup>

## 1.2 Inhibitors of cysteine proteases

### 1.2.1 Irreversible *versus* reversible action

In general, the ideal protease inhibitor would be highly selective for its target enzyme and it would bind with such high affinity that the dissociation, although possible, would be very slow (tight binding).<sup>1,27</sup>

To achieve a tight binding interaction, efforts have been directed to inhibitors with an electrophilic moiety capable of forming a reversible covalent bond.<sup>4</sup> For cysteine proteases, this goal has been pursued through the design of inhibitors employing aldehyde and ketone “warheads”.<sup>4</sup> This strategy was based on the mechanism of the catalytic process. Thus, bearing in mind that the transition state involves a tetrahedral intermediate (Scheme 1.1b), it was rationalised that aldehydes/ketones would react with the enzyme with production of an analogous product, *i.e.* a tetrahedral hemithioacetal/hemithiocetal.<sup>1</sup> However, because cysteine and serine proteases have a similar proteolytic mechanism, the incorporation of these functional groups (aldehyde in particular) afforded inhibitors for both classes of enzymes, with concomitant pharmacological problems.<sup>1,4</sup> Furthermore, aldehydes are easily oxidized to the corresponding carboxylic acids and are prone to racemisation, displaying poor bioavailability.<sup>4</sup>

On the other hand, a great number of compounds capable of react irreversibly with the active site cysteine have been reported.<sup>7</sup> These inhibitors usually possess a peptide segment corresponding to the sequence of a good substrate, which is important in the formation and stability of the non-covalent enzyme-inhibitor complex. This moiety is attached to an intrinsically reactive functional group (*e.g.* fluoromethyl ketones, epoxides, Michael acceptors), whose electrophilicity determines the rate of the inhibition irreversible step.<sup>1</sup> Because the active site cysteine has a greater nucleophilicity compared to the serine group, these inhibitors are generally quite selective for cysteine *versus* serine proteases.<sup>1</sup>

However, the therapeutical usefulness of irreversible inhibitors is always subject of discussion. A major concern is their potential for developing immunological disorders *in vivo*.<sup>7,8</sup> This biological response might occur when the proteases are cleaved to fragments which are presented to the immune system cells. Reversible inhibitors will dissociate from the protease as the recognition sites of the protein are destroyed, but the irreversible ones may remain attached leading to covalently derivatized peptides, which may be recognised as

foreign.<sup>8</sup> While theoretically a problem, evidence exists that this issue is probably less important in acute conditions (*i.e.* infectious diseases) than it would be in chronic diseases (*e.g.* cancer, osteoporosis), where therapy might have to be continuously administered for years.<sup>7,8</sup> A strong argument in support of this view is the application of  $\beta$ -lactam antibiotics which although irreversible are among the most successful antimicrobials available.<sup>8</sup>

Therefore, irreversible inhibitors have been exploited for short-term therapies, *e.g.* bacterial, viral and parasite infections.<sup>7,8</sup> In this connection, it should be noted that the three mentioned inhibitors in clinical development (Figure 1.1) act in an irreversible manner.

Another concern that has severely limited the applicability of protease irreversible inhibitors, under biological conditions, is their capacity to react in an unspecific manner with many nucleophiles *en route* to the intended target.<sup>4</sup>

Vinyl sulfones and their analogues are a promising class among cysteine protease irreversible inhibitors. These compounds were found to be highly potent, selective over serine proteases and effectively inert in the absence of an enzyme's catalytic machinery. The latter means that they do not react significantly with irrelevant nucleophiles, such as low molecular weight thiols.<sup>1,5,7</sup> The design of this group of inhibitors has followed the discovery of another interesting class, the epoxysuccinyl derivatives.<sup>1,5,7</sup> Both are briefly described in the following sections.

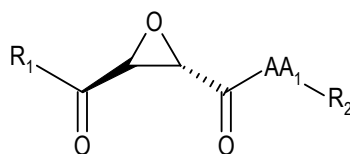
### 1.2.2 Epoxysuccinyl derivatives

The first epoxysuccinyl peptide discovered was E-64 **1.4a** (Table 1.2), isolated from culture extract of *Aspergillus japonicus* in 1978.<sup>1</sup> Once recognised its potent and irreversible inhibitory action against papain and a large number of other cysteine proteases (Table 1.2), a new generation of epoxysuccinyl derivatives has been designed and synthesised.<sup>7</sup>

In addition to their potency as cysteine protease inhibitors, these compounds showed little or no activity against serine, metallo and aspartic proteases.<sup>2</sup> They also revealed specificity for papain superfamily proteases, *i.e.* the clan CA. Neither the caspase family enzymes (clan CD) nor viral clan PA enzymes are inhibited.<sup>5</sup> Another advantage is their stability under physiological conditions toward simple thiols.<sup>1,7</sup> Prominent examples of this class are the mentioned natural lead E-64 **1.4a** and its synthetic analogues E-64c **1.4b**, E-64d **1.4c**, CA-030 **1.4d**, CA-074 **1.4e** and CA-074Me **1.4f** (Table 1.2).<sup>2,7</sup>



**Table 1.2 (a) Second-order rate constants for inactivation of cysteine proteases by epoxysuccinyl derivatives; (b) IC<sub>50</sub> values of epoxysuccinyl derivatives for cysteine proteases.**



**a**

Inhibitor	R <sub>1</sub>	AA <sub>1</sub>	R <sub>2</sub>	k <sub>2</sub> (M <sup>-1</sup> s <sup>-1</sup> ) <sup>a</sup>			
				Papain	CatB <sup>b</sup>	CatL <sup>c</sup>	Cruzain
<b>1.4a</b> , E-64	HO	Leu	Agm <sup>d</sup>	638000	89400	96300	—
<b>1.4b</b> , E-64c	HO	Leu	NH(CH <sub>2</sub> ) <sub>2</sub> CH(CH <sub>3</sub> ) <sub>2</sub>	357000	298000	206000	—
<b>1.4c</b> , E-64d	EtO	Leu	NH(CH <sub>2</sub> ) <sub>2</sub> CH(CH <sub>3</sub> ) <sub>2</sub>	—	—	—	—
<b>1.4h</b>	BzONH	D-HTyr	NH(CH <sub>2</sub> ) <sub>2</sub> CH(CH <sub>3</sub> ) <sub>2</sub>	1450	—	—	441600
<b>1.4i</b>	BzONH	D-Hph	Ph	—	—	—	179700

<sup>a</sup> These values are from a most cited review.<sup>7</sup> They are herein presented to illustrate the potency of E-64 derivatives. However, it is noteworthy that the values may be different in other papers, according to the employed conditions. <sup>b</sup> Cathepsin B; <sup>c</sup> Cathepsin L; <sup>d</sup> Agmatine.

**b**

Inhibitor	R <sub>1</sub>	AA <sub>1</sub>	AA <sub>2</sub>	R <sub>2</sub>	IC <sub>50</sub> (nM) <sup>a</sup>		
					Papain	CatB	CatL
<b>1.4d</b> , CA-030	EtO	Ile	Pro	OH	16000	2.3	32000
<b>1.4e</b> , CA-074	<i>n</i> -Pr-NH	Ile	Pro	OH	57400	2.2	172000
<b>1.4f</b> , CA-074Me	<i>n</i> -Pr-NH	Ile	Pro	OMe	—	—	—
<b>1.4g</b> , CA-028	HO	Ile	Pro	OH	—	30.4	530

<sup>a</sup> These values are from a most cited review.<sup>1</sup> They are herein presented to illustrate the potency and selectivity of compound CA-074 and of its analogues. However, it is noteworthy that the values may be different in other papers, according to the employed conditions.

Since its discovery, E-64 has been used as an active site tritrant and a diagnostic tool for the identification of cysteine proteases.<sup>7</sup> Its derivatives have been labelled with biotin, radiolabeled iodine and fluorescent dyes, such as rhodamine B, to be used as affinity labels in studies of the biological function and histochemical mapping of cysteine proteases.<sup>7</sup>

The replacement of the guanidine function of E-64 by an uncharged substituent was expected to improve cell permeability.<sup>1</sup> The resultant compound, E-64c, maintained the inhibitory activity and showed to be effective in animal models of muscular dystrophy when it was administered by subcutaneous and intraperitoneally injection.<sup>7</sup> Unfortunately, it was inactive when given orally due to poor absorption in the gastrointestinal tract.<sup>7</sup>

Thus, esterification of the acid group at C-3 led to the prodrug E-64d (also known as aloxistatin and loxistatin).<sup>1</sup> The ester moiety of this compound is hydrolysed during permeation through the intestinal membrane, giving E-64c.<sup>7</sup>

E-64d was tested in clinical trials in Japan for the treatment of muscular dystrophy, but the development was stopped in 1992 in phase III due to its low efficacy and toxicity, such as hepatic injury and teratogenic effects on rat embryogenesis.<sup>1,7</sup> This inhibitor in the form of eyes drops has also been shown to be effective in the prevention and treatment of cataracts probably by inhibition of calpain.<sup>1</sup>

Compounds CA-030 and CA-074 are part of a group developed to selectively target cathepsin B.<sup>7,11</sup> As mentioned earlier (Section 1.1.3), the Ile(or Leu)-Pro-OH sequence is complementary to the unique prime site of this enzyme. This dipeptide was therefore attached to the epoxide ring, along with different amide and ester substituents at C-2 position.<sup>11</sup> While CA-074 is specific for cathepsin B within living cells, the derivative CA-030 is not, because the ethyl ester of the epoxysuccinyl moiety is hydrolysed by esterases to produce the non-specific inhibitor CA-028 (**1.4g**, Table 1.2b).<sup>7</sup>

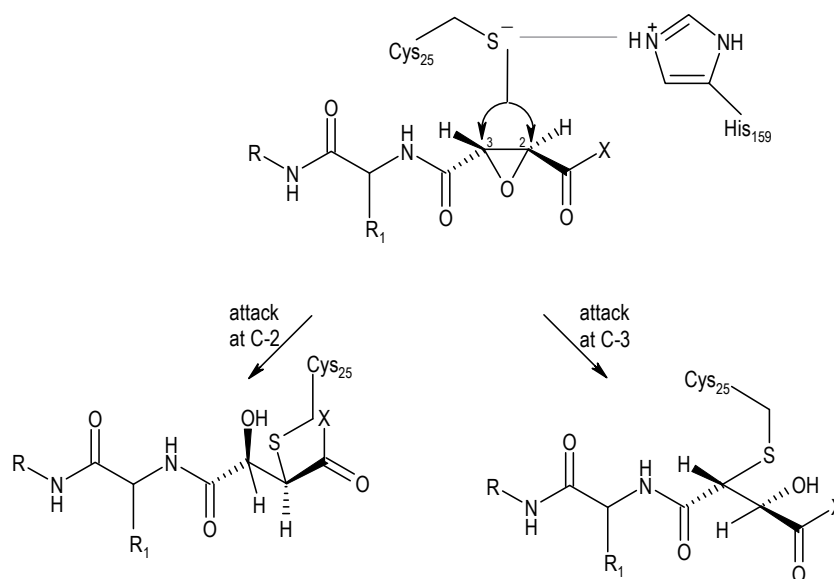
The derivative CA-074Me is a prodrug of CA-074, which requires intracellular deesterification for activity.<sup>2</sup> It is membrane-permeable, but is a comparatively weak and non-selective inhibitor for cathepsins.<sup>2</sup>

This class of inhibitors has also provided avenues to targeting parasitic cysteine proteases, particularly cruzain.<sup>22</sup> Although potent (**1.4h** and **1.4i**, Table 1.2a), most of the compounds show little or no activity *in vitro* when tested against *Trypanosoma cruzi* infected-cells.<sup>7</sup>

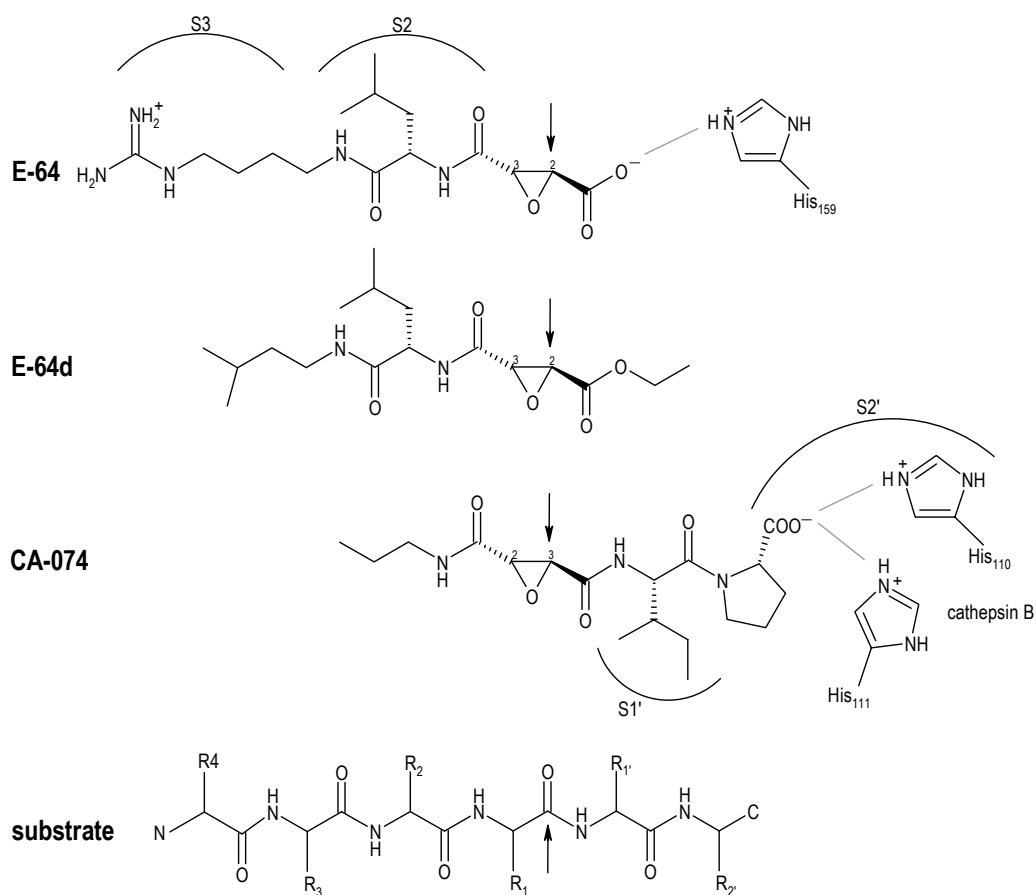
Epoxysuccinyl derivatives inhibit cysteine proteases by alkylating the active site cysteine, which results in the opening of the epoxide ring (Scheme 1.2).<sup>7</sup> The nucleophilic attack occurs at either C-2 or C-3 positions depending on the orientation of the inhibitor in the active site.<sup>7</sup>

A great number of X-ray structures of these inhibitors complexed to cysteine proteases have been reported, explaining in detail the binding modes (Scheme 1.3) as well as answering the question which carbon is attacked.<sup>5,20</sup> Thus, binding in the S subsites (*e.g.* E-64, E-64d) leads to C-2 attack, whereas binding in the S' subsites leads to C-3 attack.<sup>7</sup> The latter is associated with cathepsin B, *i.e.* CA-074 and analogues.<sup>7</sup> Interestingly, the peptide chain direction of E-64 is reversed to that of a substrate.<sup>7</sup>

Once the epoxide ring was discovered to be the reactive group essential for inhibition, it was replaced by a Michael system, which may also undergo nucleophilic attack.<sup>1</sup> These investigations generated a new class of inhibitors, which is described in the following section.



**Scheme 1.2 Mechanism of inhibition of cysteine proteases by epoxysuccinyl derivatives.** Hydrogen bonds are in grey.



**Scheme 1.3 Schematic representation of the binding modes of epoxysuccinyl derivatives.** The arrow indicates the carbon atom that is attacked by Cys25. Hydrogen bonds are in grey.

### 1.2.3 Vinyl sulfones and analogues

#### 1.2.3.1 As inhibitors of cysteine proteases

In the middle 1980's, Hanzlik *et al.* designed a series of dipeptidyl derived Michael acceptors and demonstrated their inhibitory activity toward papain (second-order rate constants ranging from 0.05 to 26.1 M<sup>-1</sup> s<sup>-1</sup>).<sup>28-30</sup> The most reactive derivatives were the unsaturated ester **1.3b** and the simple vinyl sulfone **1.2b** (Figure 1.3).<sup>30</sup>

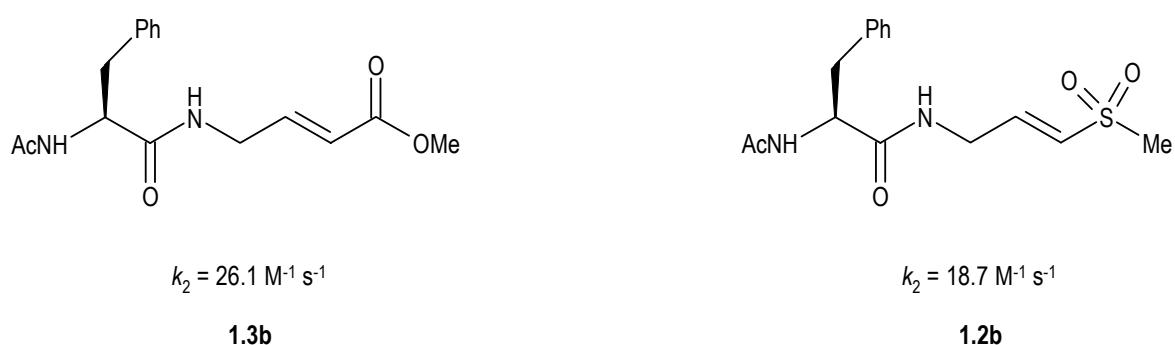
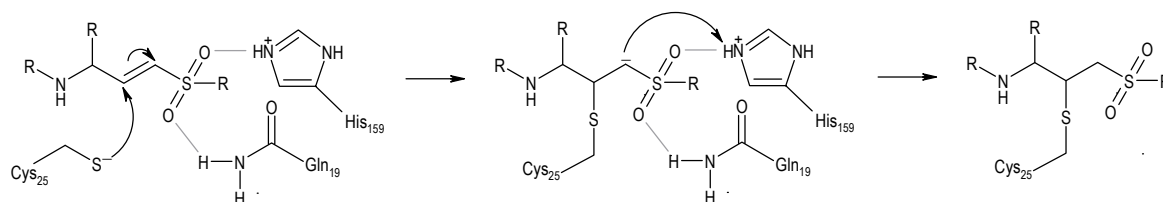


**Figure 1.3** Hanzlik *et al.* lead compounds for inhibition of papain.

In connection with efforts to develop selective inhibitors of cysteine proteases, Palmer *et al.*<sup>31</sup> became interested in the vinyl sulfone scaffold for two reasons. Firstly, this functionality appeared as sufficiently chemical stable.<sup>31</sup> Secondly, it was reasoned and validated by molecular modelling studies that the sulfonyl unit would be capable of hydrogen-bond formation with the enzymatic residues Gln19 and His159 (Scheme 1.4). This recognition process would serve to direct the vinyl sulfone in the active site in proximity to the sulphur atom of Cys25, leading to Michael addition chemistry.<sup>31,32</sup>



**Scheme 1.4** Mechanism of inhibition of cysteine proteases by vinyl sulfones. Hydrogen bonds are in grey.

With this background, Palmer *et al.*<sup>31</sup> developed dipeptidyl vinyl sulfones as a new class of irreversible inhibitors for a variety of disease-associated papain-like cysteine proteases. These first-generation compounds displayed second-order rate constants higher than  $10^7 \text{ M}^{-1} \text{ s}^{-1}$ , but they had broad activity.<sup>7</sup> Cathepsin S was the most easily inactivated enzyme followed by cathepsin L, cruzain, cathepsin K and cathepsin B, whereas the calpains were resistant to most vinyl sulfone inhibitors.<sup>7</sup>

The reaction of a vinyl sulfone inhibitor with GSH showed a second-order rate constant smaller by seven orders of magnitude than that found against cysteine proteases. On the basis of this experiment, vinyl sulfones were considered to be stable toward circulating thiols.<sup>31</sup>

To investigate selectivity over serine proteases, Palmer *et al.*<sup>31</sup> targeted the serine protease human leukocyte elastase (HLE), using a vinyl sulfone bearing a peptide sequence complementary to this enzyme. The compound failed the inhibition.

The specificity of vinyl sulfones for cysteine proteases has been rationalised in terms of the mechanism in Scheme 1.4. Protease-inhibitor X-ray crystal structures have uncovered the suggested hydrogen bonding interactions, and it has been proposed that the protonated histidine polarizes the vinyl group, giving the  $\beta$ -vinyl carbon a partial positive charge and promoting nucleophilic attack by the active site thiolate. Histidine also acts as a general acid by protonating the emerging negative charge at the  $\alpha$ -carbon, forcing the reaction into irreversibility. In serine proteases, the active site histidine plays an opposite role, *i.e.* is unprotonated and acts as a general base. This situation is seen as the determining factor in the selectivity over serine proteases.<sup>5,7</sup>

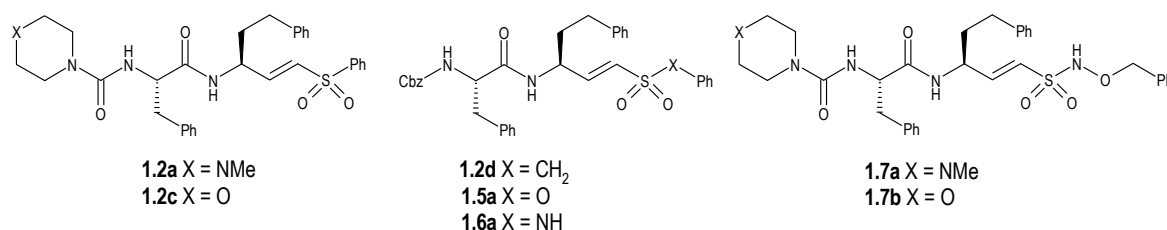
In view of these promising results, several vinyl sulfone analogues have been optimized for *in vivo* use against specifically enzymes. Prominent examples were accomplished in the targeting of the parasitic cysteine proteases (Table 1.3).

Therefore, **1.2a** is in pre-clinical studies for the treatment of Chagas disease.<sup>2</sup> This compound rescued mice from this infection.<sup>7</sup> On the basis of these data, extensive rat and dog toxicology tests have been conducted, along with pharmacokinetic analysis.<sup>2</sup> It is expected that it will enter human clinical trials in a foreseeable future.<sup>2</sup>

Taking this lead compound and its analogue **1.2c**, Roush *et al.*<sup>33</sup> reasoned that spanning the inhibitor structure into the prime site region (S1', S2') could result in additional potency and selectivity against cruzain. The resultant compounds (**1.2d**, **1.5a** and **1.6a**) were characterised by a spacer unit between the sulfonyl group and the phenyl substituent. The function of this linker was to direct the phenyl ring into the prime site residue Trp177, probing their potential interaction.<sup>7,33</sup>

With this strategy, Roush *et al.*<sup>33</sup> introduced vinyl sulfonate (e.g. **1.5a**) and vinyl sulfonamide scaffolds (e.g. **1.6a**) as inhibitors of cysteine proteases. These compounds (sulfonates in particular) revealed improved potency against cruzain comparatively to vinyl sulfones **1.2a,c**.<sup>34</sup> Unfortunately, they were inactive against *Trypanosoma cruzi* in tissue culture assays.<sup>34</sup> To overcome this situation, the inhibitor structures were further manipulated on both prime and non-prime site. Thus, *N*-sulfonyl hydroxylamine vinyl sulfonamides **1.7** were designed to combine the Michael acceptor reactivity of a sulfonate with the hydrogen bond capacity of a sulfonamide.<sup>34</sup> The latter aspect contributes to the formation of the non-covalent enzyme-inhibitor complex. These compounds were also expected to have improved aqueous solubility due to the incorporation of the P3 morpholinyl and *N*-methylpiperazinyl urea in addition to the possibility that the hydroxylamine unit might be partially ionized at physiological pH.<sup>34</sup> This new generation of compounds found to be highly effective inhibitors of cruzain, with significant activity in tissue culture experiments.<sup>34</sup>

**Table 1.3 Vinyl sulfones and analogues: second-order rate constants for inactivation of cruzain and results of *in vitro* assays against *Trypanosoma cruzi*.**



Inhibitor	$k_2$ (M <sup>-1</sup> s <sup>-1</sup> ) <sup>a</sup>	Survival of <i>Trypanosoma cruzi</i> treated J744 macrophage <sup>a</sup>
None	—	6 (control)
<b>1.2a</b>	419,500	> 24
<b>1.2c</b>	181,000	> 24
<b>1.2d</b>	1,400,000	6
<b>1.5a</b>	16,800,000	Toxic
<b>1.6a</b>	242,000	6
<b>1.7a</b>	6,480,000	> 24
<b>1.7b</b>	2,270,000	> 24

<sup>a</sup> These values are from Roush *et al.*<sup>34</sup>

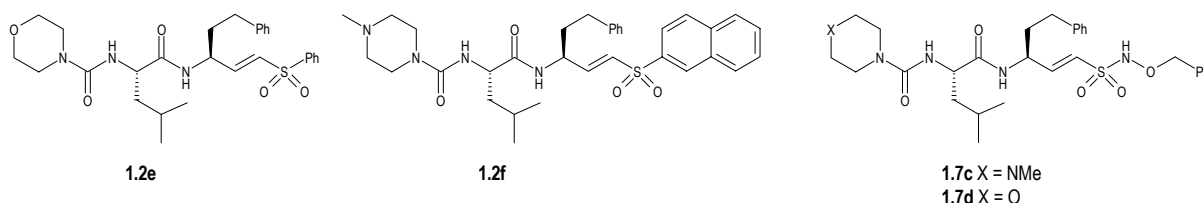
Vinyl sulfones were also evaluated as antimalarial agents (Table 1.4). In general, the presence of phenylalanine at the P2 position appears to be less effective for the malarial cysteine proteases.<sup>6</sup>

Rosenthal *et al.*<sup>35</sup> identified **1.2e** as the compound that most effectively inhibited falcipain and also most effectively blocked parasite haemoglobin degradation, metabolic activity and development. Subsequently, the morpholine urea group of **1.2e** was replaced with *N*-methyl piperazine urea to improve aqueous solubility and presumably bioavailability.<sup>36</sup> One of the resultant analogues, **1.2f**, cured about 40% of mice from malaria (*Plasmodium vinckei*).<sup>36</sup>

Further studies afforded several related compounds, which included two potent *N*-sulfonyl hydroxylamine vinyl sulfonamides (**1.7c,d**).<sup>16,34</sup>

It is noteworthy that the differences between the second-order rate constants for inhibition of falcipains 2 and 3 are fairly small (Table 1.4b).<sup>16</sup> Findings like this argue that drug discovery against these two enzymes will likely not be complicated by the need to develop separate inhibitors.<sup>16</sup>

**Table 1.4 Vinyl sulfones and analogues: (a) IC<sub>50</sub> values for falcipain-2 and cultured *Plasmodium falciparum* parasites; (b) second-order rate constants for inactivation of falcipains 2 and 3.**



**a**

Inhibitor	IC <sub>50</sub> (nM) <sup>a</sup>	
	rec-FP-2 <sup>b</sup>	<i>Plasmodium falciparum</i> W2
<b>1.2e</b>	3.5/10 <sup>c</sup>	22
<b>1.2f</b>	2 <sup>c</sup>	—
<b>1.7c</b>	2.3	4.4
<b>1.7d</b>	2.2	46

<sup>a</sup> These values are from Shenai *et al.*<sup>16</sup> <sup>b</sup> Recombinant falcipain-2. <sup>c</sup> The value of 10 nM (compound **1.2e**) is from non-recombinant falcipain.<sup>36</sup> It is herein included for comparison purposes with the value of **1.2f**, which is also from non-recombinant falcipain.<sup>36</sup>

**b**

Inhibitor	<i>k</i> <sub>2</sub> (M <sup>-1</sup> s <sup>-1</sup> ) <sup>a</sup>	
	Falcipain-2	Falcipain-3
<b>1.2e</b>	78,600	57,100
<b>1.7c</b>	74,700	147,000
<b>1.7d</b>	411,000	407,000

<sup>a</sup> These values are from Shenai *et al.*<sup>16</sup>

In summary, vinyl sulfones and their analogues have demonstrated marked potency against parasitic cysteine proteases. The reported efficacy of orally administered compounds in animal models, without undue toxicity to the host,<sup>36,37</sup> has provided an important “proof of concept” for its use *in vivo*. As illustrated by the above representative compounds, major efforts exist to further improvement of the current leads.

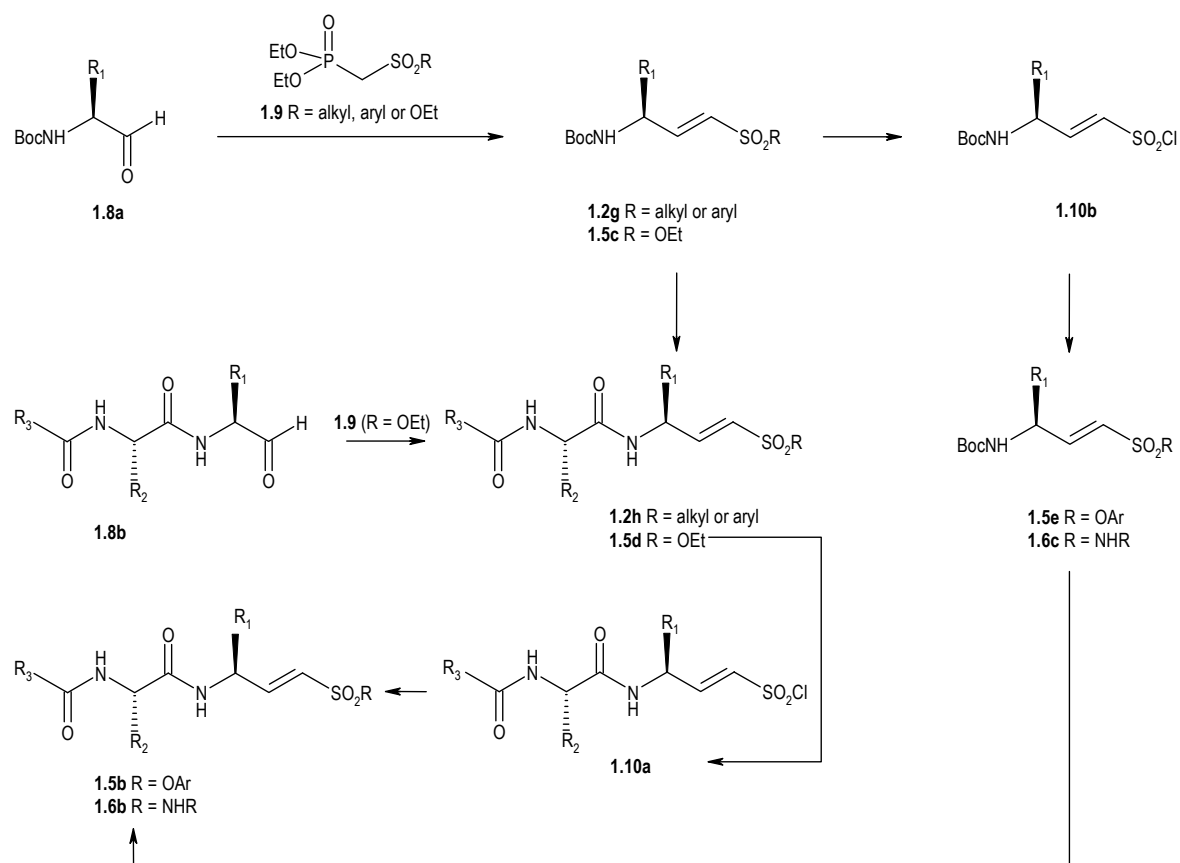
### 1.2.3.2 Synthesis

Peptidyl vinyl sulfones **1.2g** (Scheme 1.5) have been provided by Horner-Wadsworth-Emmons reaction of *N*-Boc amino acid aldehydes **1.8a** with phosphonates **1.9**.<sup>31</sup> Although small amounts of the vinyl sulfone *Z*-isomer cannot be excluded,<sup>38,39</sup> *E*-vinyl derivatives have been the only to be characterised and evaluated against cysteine proteases.<sup>16,29,31,33,34</sup>

Removal of the Boc group and subsequent coupling with *N*-protected amino acids give dipeptidyl derivatives **1.2h**.<sup>16,31,33,34</sup>

Dipeptidyl vinyl sulfonates **1.5b** and vinyl sulfonamides **1.6b** are usually achieved by following the above mentioned strategy, starting from the preparation of the mono-peptidyl vinyl sulfonate **1.5c**, which is converted into **1.5d** to obtain the sulfonyl chloride **1.10a**. This last intermediate is then reacted with the appropriate amine or phenol.<sup>16,33,34</sup> Small variations to this general scheme have been reported, but the reasons for that were not given. Thus, intermediate **1.5d** was also synthesised by the Horner-Wadsworth-Emmons reaction of the dipeptidyl aldehyde **1.8b** with phosphonate **1.9** (R = OEt).<sup>33</sup> Another variation concerns the incorporation of amino acid at the P2 position, which can be carried out after the substitution at the sulfonyl centre (**1.5b/1.6b via 1.10b**).<sup>16,34</sup>





Scheme 1.5 Synthetic pathway to vinyl sulfones and their analogues.

### 1.3 Introductory remarks on quinones

Quinones present in their molecular skeleton a characteristic conjugated dione ring, which is incorporated in an aromatic system, *e.g.* a naphthalenyl ring (Figure 1.4).<sup>40</sup>

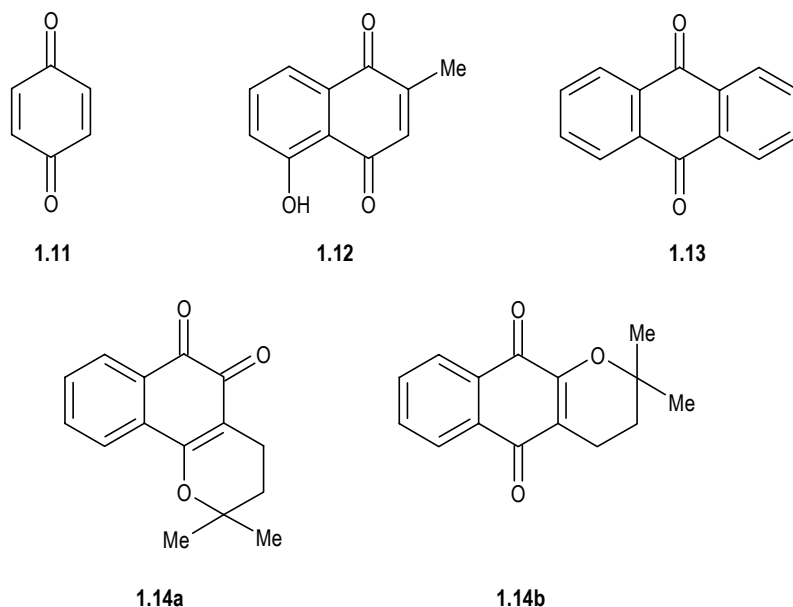


**Figure 1.4 Representative chemical structures of quinones.** Quinones occurring as benzo- (*e.g.* **1.11**), naphtho- (*e.g.* **1.12**) and anthraquinones (*e.g.* **1.13**) represent the largest class of quinoid compounds.<sup>41</sup> Isomeric forms exist due to the different positions of the carbonyl groups in the quinoid ring (*e.g.* **1.14a** and **1.14b**).

This class of compounds is probably found in all living cells, where they, *i.e.* ubiquinones, function primarily as components of the electron transport chains involved in cellular respiration and photosynthesis. In addition, vitamin K<sub>2</sub> (**1.15a**, Figure 1.5) is required to blood coagulation. Quinones also play a role in cellular defence (in animals and plants), because they effectively inhibit the growth of bacteria, fungi and parasites.<sup>40,42</sup>

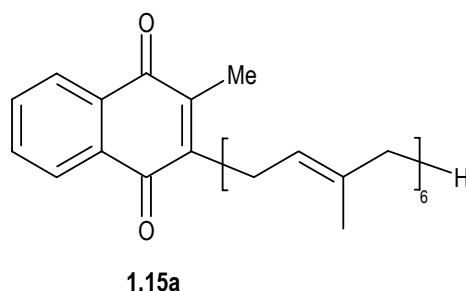


**Figure 1.5 Vitamin K<sub>2</sub>.**

Many of these substances are used in folk medicine and they have become the subject of intense research due to their interesting pharmacological, *e.g.* antitumour, trypanocidal, leishmanicidal, anti-inflammatory, antiviral, molluscicidal and antifungal properties.<sup>43,44</sup>

Some have reached clinical use, such as mitomycin C **1.16**, daunorubicin **1.17a** and doxorubicin **1.17b** (Figure 1.6), which are used as antineoplastic drugs.<sup>42</sup> Among naphthoquinones, atovaquone (**1.18**, Figure 1.6) is an effective broad-spectrum antiprotozoal drug used against *Plasmodium* spp., *Pneumocystis carinii*, *Babesia* spp. and *Toxoplasma gondii*.<sup>45</sup> Vitamin K analogues (**1.15b**, Figure 1.6) have found clinical use as haemostatics and radiosensitizers.<sup>42</sup>

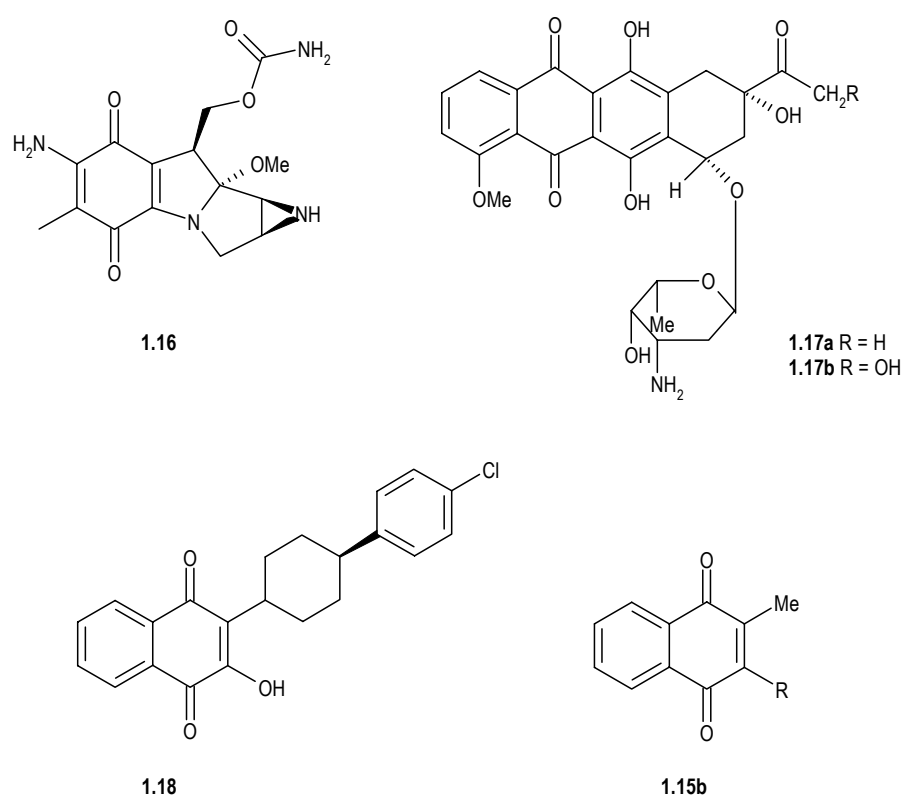


**Figure 1.6** Structures of mitomycin C (**1.16**), daunorubicin (**1.17a**), doxorubicin (**1.17b**) and atovaquone (**1.18**). Generic structure of menadione derivatives (**1.15b**).

Unfortunately, the potential usefulness of quinones is limited by their toxicity, associated with effects such as myelosuppression, cardiomyopathy and haemolytic anaemia.<sup>42</sup>

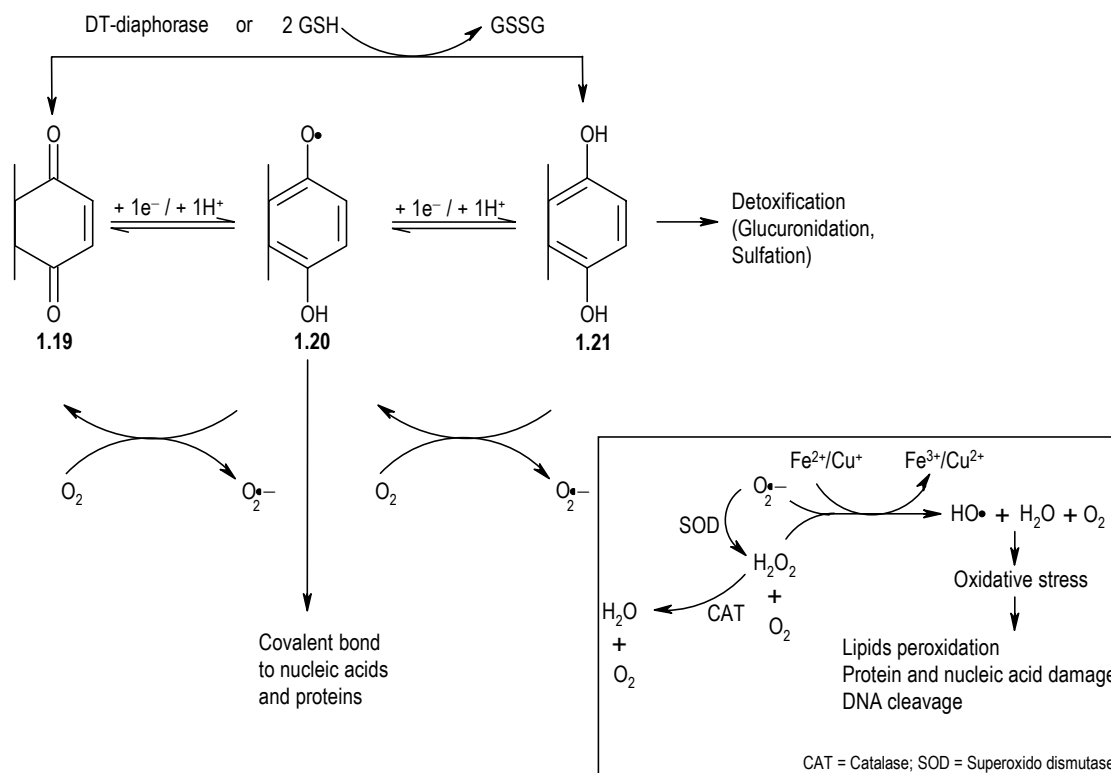
Their actions and toxicity are still difficult to understand, although at least two competing mechanisms have been identified: (i) their capacity to undergo redox cycling and (ii) their capacity to act as electrophiles.<sup>42</sup>

The redox cycle mechanism is complex and is still largely unknown (Scheme 1.6).<sup>40</sup> Briefly, quinones **1.19** are able to accept electrons through a process mediated by some reductases, *e.g.* NADPH-cytochrome P450 reductase. The first one-electron reduction leads to a semiquinone radical **1.20** that can be subsequently converted to a hydroquinone **1.21**. Alternatively, hydroquinones **1.21** may be produced by reaction of quinones **1.19** with GSH or through a direct two-electron reduction mediated by the enzyme DT-diaphorase.<sup>42</sup>

Hydroquinones **1.21** may lead to the production of reactive oxygen species or to a detoxification process, depending on their properties, *i.e.* redox potential.<sup>43</sup>

Semiquinone radicals **1.20** are very unstable substances, toxic by themselves, which may be re-oxidized to the parent quinone **1.19**, with the concomitant reduction of oxygen to superoxide anion radical.<sup>42,43</sup>

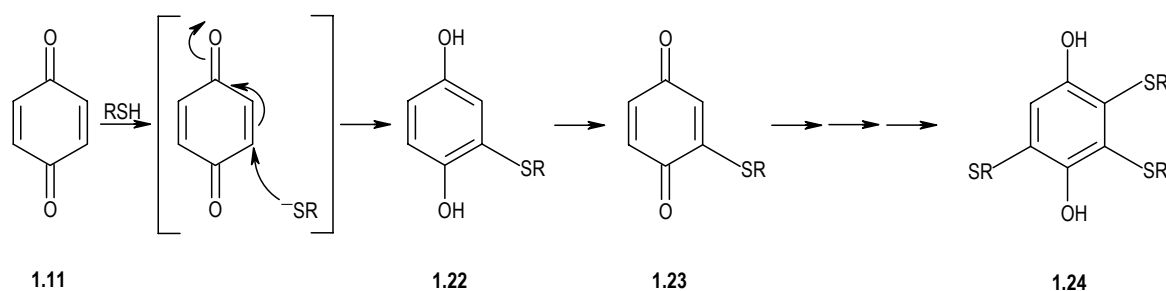
Thus, quinones are involved in a cyclic process (a futile redox cycling) which leads to cytotoxic levels of hydrogen peroxide.<sup>42</sup> In addition, they promote the depletion of GSH, compromising one of the cellular defences against oxidative stress.<sup>42</sup> Disruption of the cellular environment might lead, in extreme situations, to the induction of apoptosis.<sup>40</sup>



**Scheme 1.6 Formation of reactive oxygen species by redox cycling of quinones.** Adapted from dos Santos *et al.*<sup>44</sup> and O'Brien *et al.*<sup>42</sup>

Regarding the capacity of quinones to act as electrophiles, some compounds unsubstituted at one or several positions of the quinone ring can lead to the covalent modification of thiols or other vital physiological components, *i.e.* proteins, DNA and RNA.<sup>42,43</sup>

The reactions of quinones with sulphur nucleophiles, including GSH, can be characterised as Michael-type additions, yielding as primary product the mono-substituted hydroquinone (*e.g.* **1.22**, Scheme 1.7).<sup>41,42</sup>



**Scheme 1.7** Michael-type addition of thiols to quinones. Exemplified for 1,4-benzoquinone **1.11**.

The site of attack by nucleophiles is largely influenced by the nature, *i.e.* electron-donating or electron-withdrawing character, of the quinone substituents.<sup>41</sup> Usually, the addition occurs at the position having the largest LUMO coefficient.<sup>46</sup>

The substituents also determine the rate of the reaction, which is generally decreased by electron-donor groups (*e.g.*  $-\text{Me}$  and  $-\text{OMe}$ ) and increased by electron-withdrawal ones (*e.g.*  $-\text{Br}$ ).<sup>42</sup>

The resultant adducts are not redox inert and may be re-oxidized, for example, by a second molecule of quinone or by oxygen. When a thiol-derived quinone, such as **1.23**, possesses available sites for nucleophilic addition, it may react with an excess of thiol producing poly-substituted conjugates **1.24**.<sup>41,42</sup>

Most of the mechanistic schemes presented for quinones have been originated from studies under anaerobic conditions.<sup>41,42</sup> Thus, they might be an oversimplification of the reactions occurring in aerobic systems, because, as mentioned above, the resultant adducts can be re-oxidized, causing oxidative stress as readily as or even more readily than the quinone.<sup>41</sup> The application of the mentioned mechanisms to biological systems requires even more caution, because the intracellular situation also involves the enzymatic catalysed reduction, which might greatly enhance the redox cycle.<sup>42</sup>

Whether a quinone acts as an electrophile, a redox cyler or as both is closely associated with its reduction potential.

To undergo redox cycling, the quinone must have a reduction potential sufficiently high to allow efficient reduction by cellular reductases but not so high that it prevents the re-oxidation of hydro- and semiquinones.<sup>47</sup> Thus, high reduction potentials have been related to quinones acting mainly by Michael addition.<sup>48</sup> For example, 1,4-benzoquinone (reduction potential is +99 mV) is known to be cytotoxic only due to its electrophilic action, whereas 2,3-dimethoxy-1,4-naphthoquinone, with a much lower reduction potential (-240 mV), was reported as a pure redox cyler.<sup>48</sup>

Until recently, most of the drug investigations involving quinones, *e.g.* as antineoplastic drugs, have focused on the production of oxygen reactive species. However, the electrophilicity of this class is now being exploited in inhibitor design against enzymes/receptors containing a thiol residue at or near the active site, in order to achieve more selective cytotoxic compounds.<sup>49-51</sup> In this context, compounds **1.25a,b** (Figure 1.7) have been proposed as inhibitors of CDC25 phosphatases and a series of derivatives **1.26** has been developed to target vascular endothelial growth factor receptor-2 (VEGFR-2).<sup>51,52</sup>

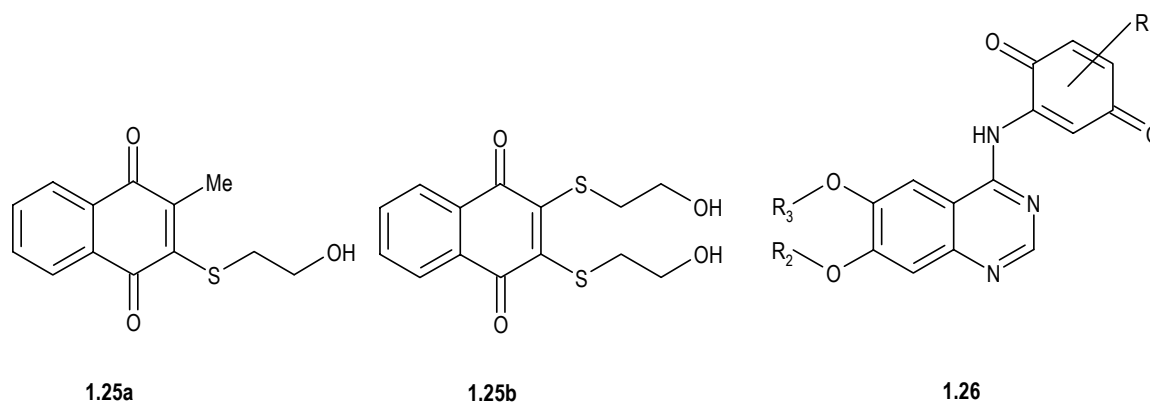


**Figure 1.7** Structures of Cpd 5 (**1.25a**) and NSC 95397 (**1.25b**). Generic structure of 2-(quinazolin-4-ylamino)-[1,4] benzoquinone derivatives (**1.26**).

An important issue in the design of inhibitors targeting cysteine enzymes is the selectivity over serine proteases. Studies involving 2-chloro-3-substituted-1,4-naphthoquinones have corroborated the possibility of achieving specificity, because these compounds showed to be potent inactivators of Human Cytomegalovirus Protease, a serine protease, but due to the covalent modification of a cysteine residue instead. In connection, the same compounds were tested against the prototypical serine proteases thrombin and human neutrophil elastase

(HNE). They failed the inhibition of the former and only one revealed moderate inhibition against HNE.<sup>53</sup>

In spite of the potential toxicity associated with quinones, evidence exists that it should be possible to modulate this property by the appropriate choice of substituents. A strong argument in support of this view is the already mentioned atovaquone **1.18**, which is considered to have an excellent safety profile and is tolerated by infants and small children.<sup>45,54</sup> Interestingly and in clear contrast, its analogues (2-hydroxy-3-alkyl-1,4-naphthoquinones) were reported as causing haemolytic anaemia and renal damage in rats.<sup>55</sup>

In addition, atovaquone is orally effective. Its bioavailability is still considered far from satisfactory, but progresses have been made by reformulating it as a micronized suspension (the drug was originally released as a tablet).<sup>45</sup>

## 1.4 Aims of the thesis

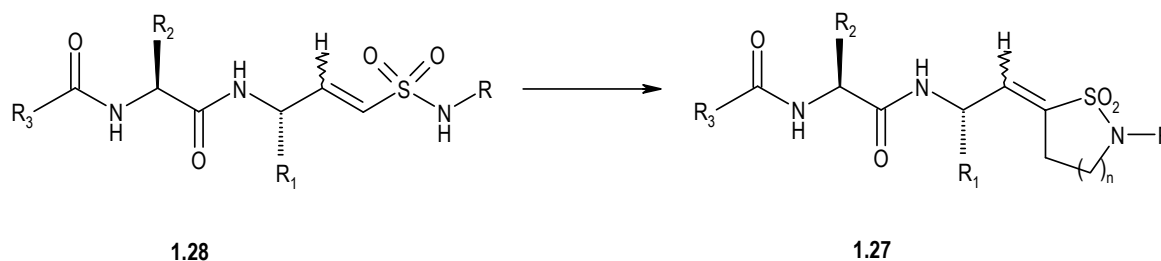
The main aim of this project was to contribute to the ongoing research in the development of irreversible inhibitors of papain-like cysteine proteases.

Initially, the work focused on the inactivation of falcipain-2, a cysteine protease which plays a crucial role in the life cycle of *Plasmodium falciparum* and is, therefore, an attractive antimalarial target. To achieve this goal, a series of vinyl sultam derivatives was designed and synthesised as potential inhibitors (Chapter 2).

Vinyl sultam scaffold (**1.27**, Scheme 1.8) was chosen for three main reasons. Firstly, it is a cyclic isostere of vinyl sulfonamides **1.28**, which inactivate cysteine proteases by irreversible alkylation of the active site Cys25 *via* Michael addition chemistry. Vinyl sulfonamides are particularly successful against cruzain and, as such, provide an interesting starting point for the rational design of inhibitors toward falcipain-2, due to the similarity between both enzymes. Secondly, vinyl sultams are structurally similar to  $\alpha$ -methylene lactones, which are known acceptors for thiols.<sup>56,57</sup> Finally, vinyl sultams appeared to be resistant to the blood pH, because previous investigations found that  $\beta$ -sultams, including vinyl derivatives, are sufficiently stable at neutral pH to be used as potential enzyme inhibitors.<sup>58,59</sup>

In this context, it was reasoned that vinyl sultams would be able to reach the action site, *i.e.* the erythrocyte infected with the malaria parasite, and inactivate falcipain-2 by a mechanism identical to that of vinyl sulfonamides.

It should be noted that the vinyl sultam scaffold has been incorporated in the design of potent inhibitors against both cyclooxygenase-2 (COX-2) and 5-lipoxygenase (5-LO), but the inactivation process does not involve nucleophilic addition to the vinylic moiety.<sup>60</sup>



**Scheme 1.8** Approach to the design of potential irreversible inhibitors of cysteine proteases.

In a second phase of this PhD project, commercial 1,4-naphthoquinone derivatives were screened for papain-inhibitory activity, on the basis of the known reactivity of quinones toward thiol nucleophiles and enzymes with thiol residues at or near the active site. These compounds revealed interesting results, and the 1,4-naphthoquinone moiety was further employed as an alternative building block for the design of novel inhibitors (Chapter 3). To the best of author's knowledge, this thesis presents the first evaluation of this scaffold in the targeting of papain-like cysteine proteases.

The potential inactivators were tested against falcipain-2, *Plasmodium falciparum* W2, papain and bovine spleen cathepsin B. For the two latter enzymes, the assessment of the inhibitory activity required the development of a methodology through the adjustment and validation of reported inhibition assays (Appendix I).

The intrinsic chemical reactivity of the compounds was investigated by carrying out reactivity studies toward the simple thiol cysteine.



## **CHAPTER 2**

### **DIPEPTIDE VINYL SULTAMS**



## 2. DIPEPTIDE VINYL SULTAMS

This chapter is divided in three main parts: firstly, the synthesis of dipeptide vinyl sultams and of analogous vinyl sulfonamides; secondly, reactivity studies of those compounds toward cysteine; finally, the evaluation of vinyl sultams against papain, falcipain-2 and *Plasmodium falciparum* W2, in conjunction with molecular docking studies involving cruzain and papain.

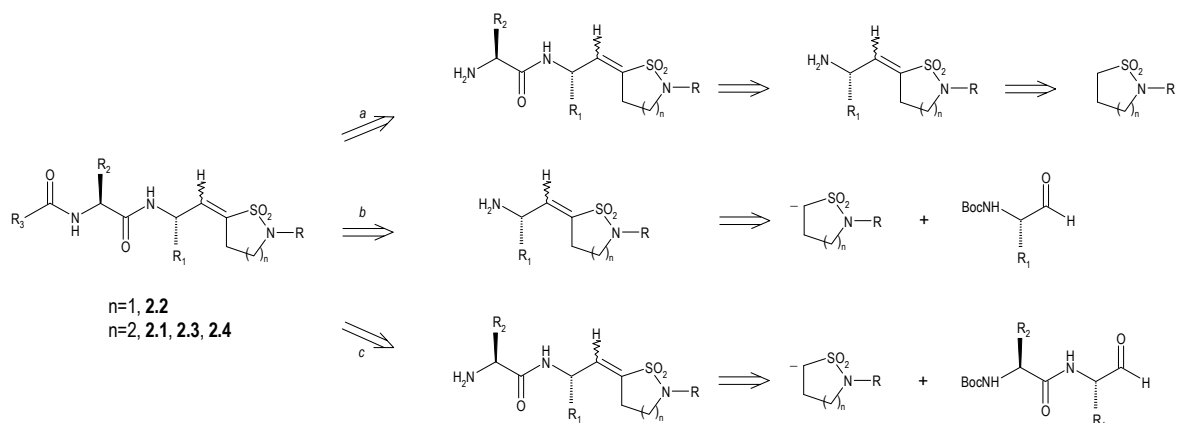
### 2.1 Synthesis

#### 2.1.1 Overall strategy

With the aim of designing effective inhibitors for falcipain-2, the vinyl sultam scaffold was attached to a peptide moiety, Mu-Leu-Phe. The choice of this sequence was based on prior studies involving vinyl sulfones (Section 1.2.3.1), which identified the analogous segment Mu-Leu-Hph as the optimal sequence for this enzyme. A vinyl sultam with the Ac-Phe-Phe moiety was also prepared according to the success of Cbz-Phe-Hph-VS-R vinyl sulfones against the homologous enzyme cruzain. Finally, on the basis of the representative vinyl sulfone inhibitors for falcipain/cruzain, the nitrogen atom of the sultam ring was connected either a benzyl or phenyl group. It was expected that this substituent could interact with the hydrophobic prime site (S1', S2') of the enzyme.

The synthesis of the compounds began with the preparation of the sultam cores, which were subsequently linked to the peptide moiety according to the pathways illustrated in Scheme 2.1.

Reported investigations provided vinyl sultams through: (i) intramolecular Heck reaction,<sup>61</sup> (ii) cyclisation of chlorobutenesulfonamide in the presence of a base,<sup>62</sup> (iii) direct coupling by an aldol-like reaction, followed by dehydration,<sup>60,63</sup> and (iv) reaction of sultam ring with benzonitrile.<sup>64</sup> In the present investigation, preparation of these compounds involved two approaches, an aldol-like reaction and Horner-Wadsworth-Emmons chemistry. Both strategies lay in the acidity of the hydrogens at the  $\alpha$ -position to sulfonamide group, which can be removed to afford anions that react with electrophiles (an aldehyde in this case).



**Scheme 2.1** Strategic routes for the synthesis of dipeptide vinyl sultams **2.1-2.4**. These pathways were based on the ones reported for the analogous vinyl sulfones, which were described in Section 1.2.3.2.

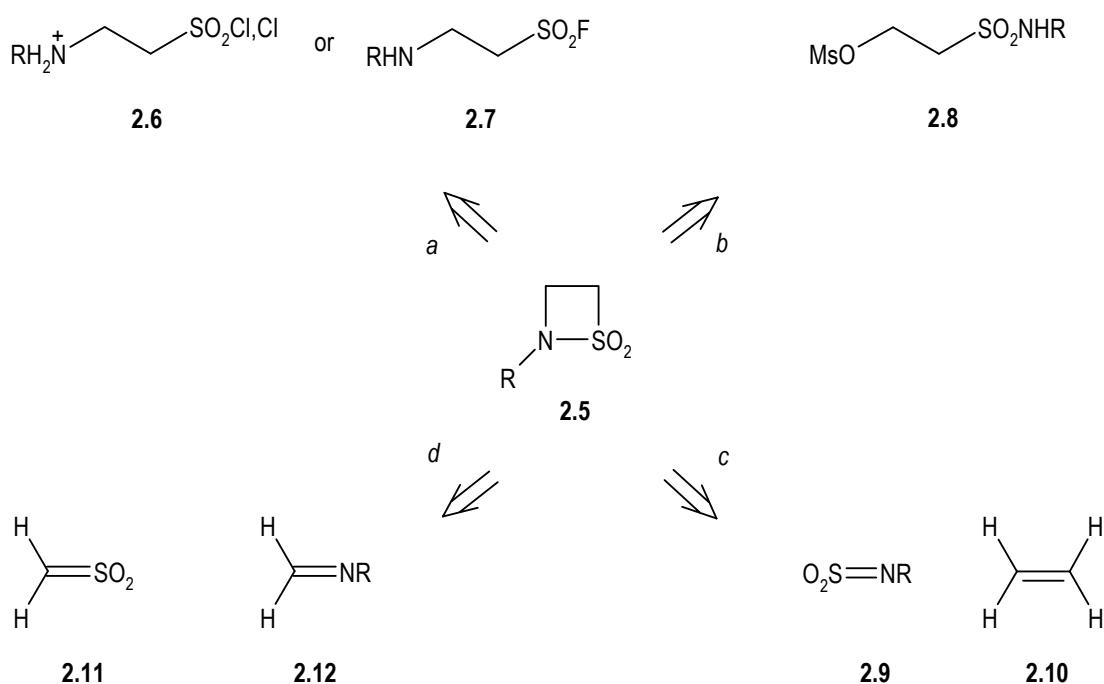
## 2.1.2 Strategies for sultam scaffolds

### 2.1.2.1 $\beta$ -Sultams

Four main strategic routes exist for the preparation of the  $\beta$ -sultam ring **2.5** (Scheme 2.2):<sup>58,59</sup>

- N-S bond formation (corresponding to retrosynthetic analysis *a*), by cyclisation of hydrochlorides **2.6** and of derivatives **2.7**;
- N-C bond formation (retrosynthetic analysis *b*), by cyclisation of mesylates **2.8**;
- cycloadditions of sulfonylamines **2.9** with alkenes **2.10** (retrosynthetic analysis *c*);
- cycloadditions of sulfenes **2.11** with imines **2.12** (retrosynthetic analysis *d*).

Methods involving cycloadditions have been employed in the preparation of *C*-substituted- $\beta$ -sultams.<sup>58,59</sup> However, their potential usefulness is considered limited by the difficulty in preparing the extremely reactive sulfonylamines **2.9** and sulfenes **2.11**.<sup>65</sup>



Scheme 2.2 Main strategic routes for the preparation of the  $\beta$ -sultam ring.

**By N-S ring closure.** Cyclisation of hydrochlorides **2.6** is usually carried out in anhydrous EtOAc, at rt. A base (aqueous ammonia or sodium carbonate) is required to remove the extra proton of the hydrochloride salt, allowing the attack of the nitrogen nucleophile to the sulfonyl centre with displacement of the chloride anion.<sup>65-67</sup> The main variation in this method is on the route to compounds **2.6**, which can be prepared (Figure 2.1): (i) from the oxidative chlorination of  $\beta$ -aminothiols **2.13**<sup>65,66</sup> or  $\beta$ -aminodisulfides **2.14**,<sup>68</sup> and (ii) from the chlorination of sulfonic acids **2.15** with  $\text{POCl}_3/\text{PCl}_5$  mixtures either in tetrachloromethane or under solventless conditions.<sup>65-67,69</sup>

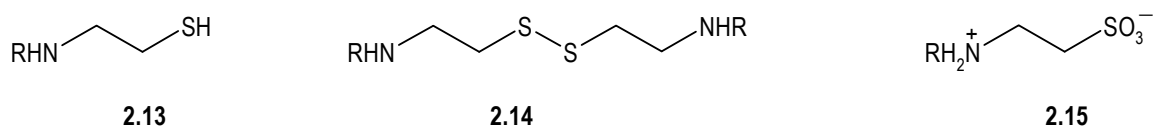
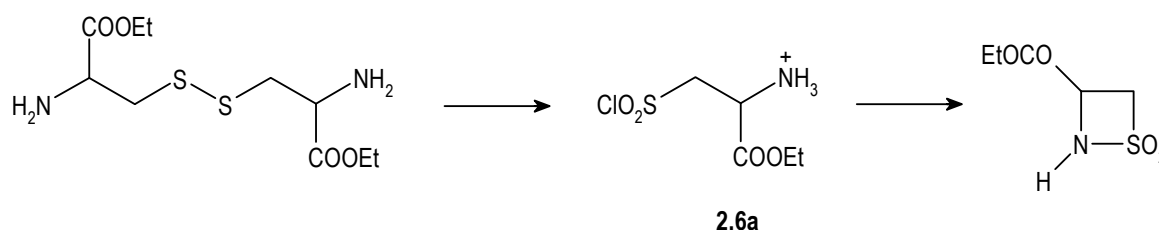


Figure 2.1 Generic structures of  $\beta$ -aminothiols (**2.13**),  $\beta$ -aminodisulfides (**2.14**) and 2-aminoethanesulfonic acids (**2.15**).

To the best of author's knowledge, Baganz *et al.*<sup>68</sup> were the first to synthesise a  $\beta$ -sultam from a hydrochloride (**2.6a**, Scheme 2.3), followed by Le Berre *et al.*,<sup>66</sup> who obtained the unsubstituted  $\beta$ -sultam using taurine (**2.15**, R = H, Scheme 2.4) as starting material. Thereafter, this approach was employed in the synthesis of several *N*-alkyl- $\beta$ -sultams (45-95% yield).<sup>58,65,69</sup> The method also allowed the preparation of two *N*-aryl- $\beta$ -sultams (phenyl and 1-naphthyl),<sup>65,69</sup> although more recent investigations<sup>58</sup> were unable to reproduce the yields described for *N*-phenyl- $\beta$ -sultam (50 and 82%) due to problems concerning the synthesis of *N*-phenyltaurine (**2.15**, R = Ph), its chlorination and cyclisation.



**Scheme 2.3** Representation of the  $\beta$ -sultam synthesis carried out by Baganz *et al.*

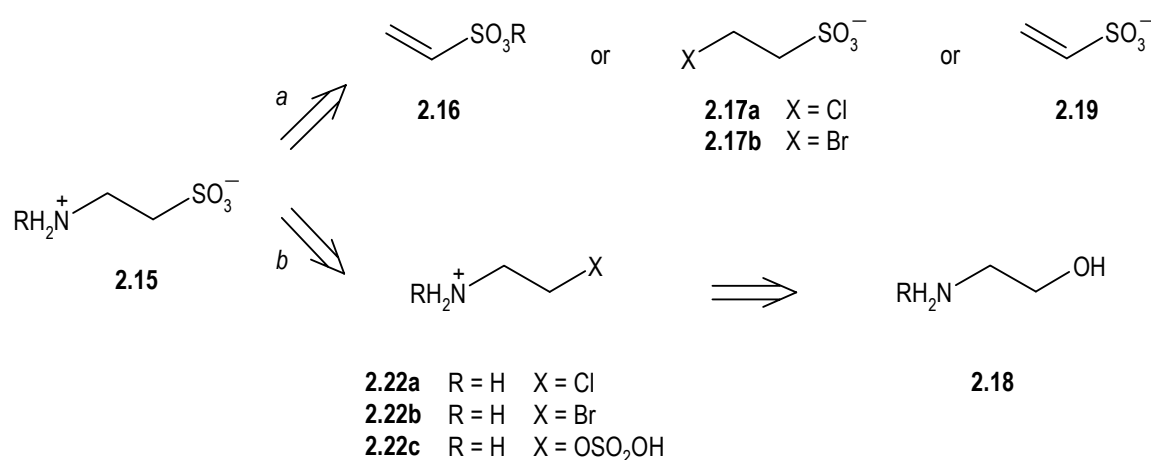
Taurine is commercially available, but most of its *N*-substituted analogues are not. These intermediates have been synthesised by several procedures, some of them characterised by their complexity and difficult work-up.<sup>70</sup> Four main precursors have been used (Scheme 2.4): ethenesulfonates **2.16**, 2-chloroethanesulfonate **2.17a**, 2-bromoethanesulfonate **2.17b** and ethanolamine (**2.18**, R = H). Moreover, a German patent discloses the preparation of *N*-methyltaurine (**2.15**, R = Me) from the sodium salt of vinylsulfonic acid **2.19**.<sup>71</sup>

Ethanesulfonates **2.16** are usually prepared by reaction of sulfonyl chloride **2.20a** with an alcohol in the presence of pyridine (Scheme 2.5).<sup>72,73</sup> Reaction between **2.16** and amines, *i.e.* aliphatic, primary or secondary, occurs preferentially *via* Michael addition instead of involving the attack to the sulfonyl centre. The resultant sulfonates **2.21** need not to be isolated and the process proceeds with the hydrolysis of the ester group to afford the taurines **2.15**.<sup>72</sup> Isopropyl ethanesulfonate (**2.16**, R = *i*Pr) has been employed in the synthesis of several *N*-alkyl taurine analogues (31-88% yield).<sup>65,67</sup> It also allowed the preparation of the *N*-Ph taurine (**2.15**, R = Ph) in 98% yield,<sup>65</sup> although more recent investigations resulted in a yield of 19%, which was ascribed to the poor nucleophilicity of the aniline amino group.<sup>58</sup>

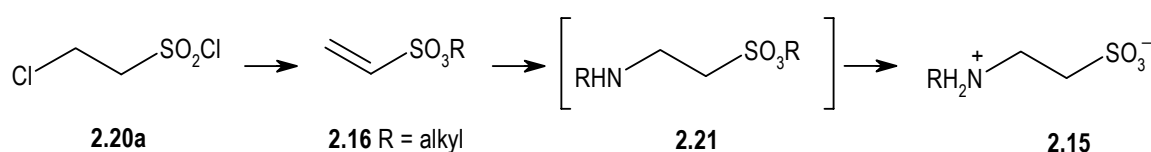
2-Chloroethanesulfonate **2.17a** and 2-bromoethanesulfonate **2.17b** allowed the preparation of taurine through the reaction with aqueous ammonia, in yields of 90% and 51%, respectively.<sup>70,71</sup> The best outcome was accomplished by the study of different temperatures,

catalysts and reaction times. This study was also applied to *N*-methyltaurine, which was prepared in 80% yield from sodium 2-chloroethanesulfonate and anhydrous methylamine.<sup>71</sup> Both sodium chloro- and bromoethanesulfonates were used as starting materials in the synthesis of *N*-phenyltaurine, by reaction with aniline (60-80% yield).<sup>74</sup>

Finally, the synthesis of taurine from ethanolamine involved the initial preparation of an intermediate (Scheme 2.4); *e.g.* hydrochlorides **2.22a,b**,<sup>71,75,76</sup> or hydrogen sulfate **2.22c**,<sup>77</sup> through the reaction of ethanolamine with thionyl chloride, hydrobromic acid or fuming sulfuric acid, respectively. These intermediates were subsequently converted to taurine in the presence of sodium sulfite or bisulfite,<sup>71,76,77</sup> with yields ranging from 50 to 80%.



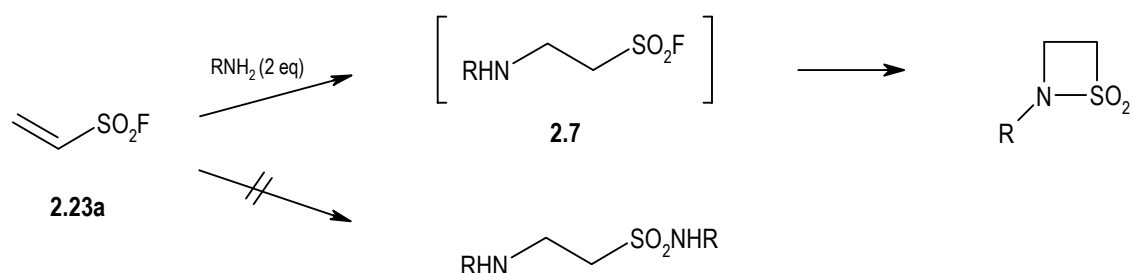
**Scheme 2.4** Main precursors for the preparation of 2-aminoethanesulfonic acid derivatives.



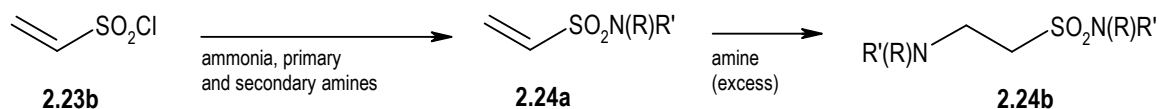
**Scheme 2.5** Synthetic pathway to 2-aminoethanesulfonic acid derivatives from alkyl ethenesulfonates.

The second approach to the N-S ring closure employs derivatives **2.7** (Scheme 2.6) and has been used in the preparation of *N*-alkyl- $\beta$ -sultams either brominated at the  $\alpha$  position (11-80% yield) or not (42-74% yield).<sup>58,65</sup> This process was first described by Le Berre *et al.*<sup>65</sup> and proceeds from the initial formation of ethenesulfonyl fluoride **2.23a**, which cyclises spontaneously in the presence of two equivalents of a primary amine. The reaction is thought

to occur *via* an initial Michael addition followed by the attack of the amino nucleophile to the sulfonyl group with the departure of the hydrofluoric acid (HF), which is trapped by the second equivalent of amine.<sup>58,65</sup> This strategy is based on the finding that for **2.23a** the Michael type addition is a more favourable process than attack at the sulfonyl group, due to the poor ability of the fluoride anion to act as a leaving group. Its displacement only occurs when the amino group is part of the molecule and the entropic advantage allows the intramolecular ring closure to occur.<sup>58</sup> Thus, the behaviour of ethenesulfonyl fluoride **2.23a** contrasts with that of its chloro analogue **2.23b** (Scheme 2.7) which, in the presence of an amine, affords acyclic sulfonamides **2.24a,b**.<sup>78</sup> For this reason, in the approach involving hydrochlorides **2.6**, the amino group must be introduced before sulfonyl group activation.



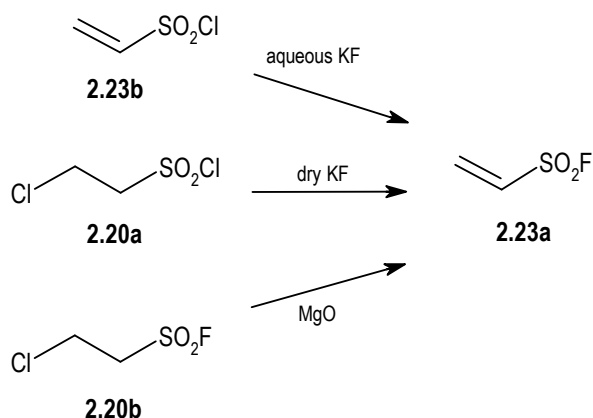
Scheme 2.6 Synthesis of the  $\beta$ -sultam ring by cyclisation of 1-fluorosulfonyl-2-aminoethane derivatives.



Scheme 2.7 Products from the reaction of ethenesulfonyl chloride with amines.

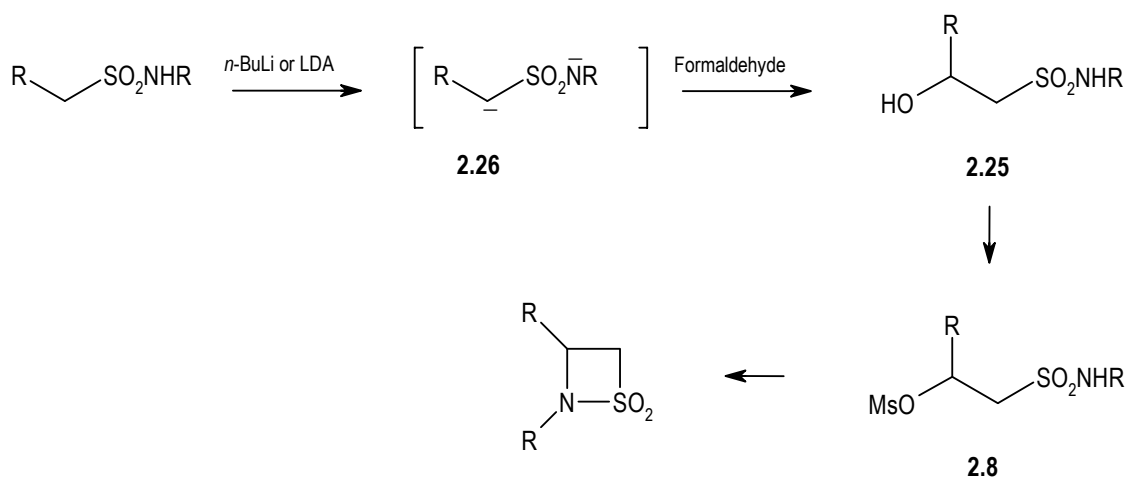
Ethenesulfonyl fluoride (**2.23a**, Scheme 2.8) may be prepared from ethenesulfonyl chloride **2.23b**, from 2-chloroethanesulfonyl chloride **2.20a** and from 2-chloroethanesulfonyl fluoride **2.20b**. The route involving **2.20b** and magnesium oxide was considered the most efficient.<sup>79</sup>





**Scheme 2.8** Synthetic routes to ethenesulfonyl fluoride.

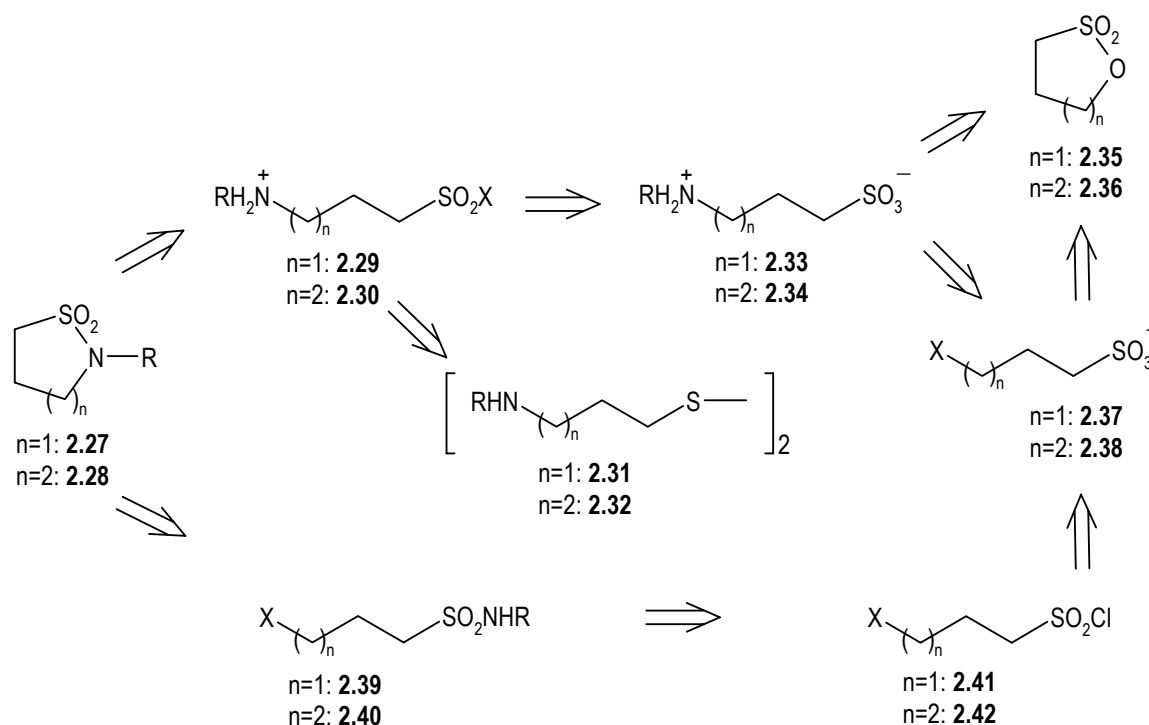
**By N-C ring closure.** Synthesis of the  $\beta$ -sultam ring through N-C bond formation uses  $\beta$ -hydroxysulfonamides **2.25** as key intermediates (Scheme 2.9), usually obtained from the addition of formaldehyde to a sulfonamide dianion **2.26**. Hydroxysulfonamides **2.25** are converted to the more reactive mesylate esters **2.8** before the cyclisation step. The ring closure is achieved in the presence of a base, by the attack of the nitrogen nucleophile to the carbon bearing the mesylate leaving group. This strategy was first described by Thompson<sup>80</sup> and was most recently adapted as an alternative synthetic approach for the preparation of *N*-aryl- $\beta$ -sultams (23-94% cyclisation step yield) to overcome problems concerning the method involving ethenesulfonates.<sup>58,67</sup>



**Scheme 2.9** Synthetic pathway to  $\beta$ -sultam ring from  $\beta$ -hydroxysulfonamide mesylates.

2.1.2.2  $\gamma$ - and  $\delta$ -Sultams

The preparation of  $\gamma$ - and  $\delta$ -sultams is mainly achieved by similar approaches to those described for  $\beta$ -sultams, *i.e.* N-S bond formation and N-C bond formation (Scheme 2.10), although processes involving a C-C bond formation are also known (Scheme 2.11).



Scheme 2.10 Main strategic routes for the preparation of the  $\gamma$ - and  $\delta$ -sultam rings.

**By N-S ring closure.** A good general route to a wide variety of  $\gamma$ - and  $\delta$ -sultams (**2.27** and **2.28**, Scheme 2.10) is provided by the cyclisation of the corresponding hydrochlorides **2.29** and **2.30**.

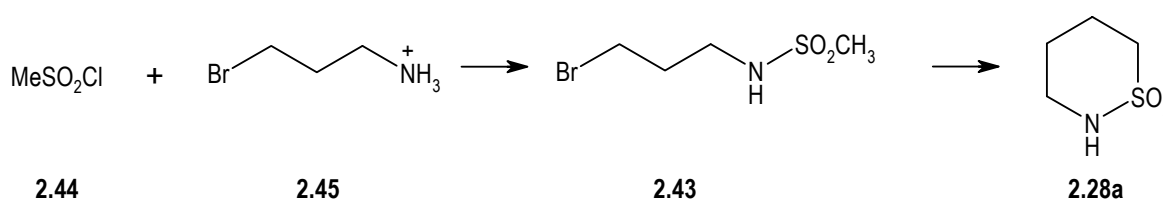
The unsubstituted  $\delta$ -sultam (**2.28**, R = H) was obtained from both sulfonyl chloride (**2.30**, R = H, X = Cl) and bromide (**2.30**, R = H, X = Br) which were respectively prepared by chlorination and bromination of **2.32** (R = H).<sup>81,82</sup>

When applied to *N*-substituted sultams, this approach requires the synthesis of the appropriate aminoalkanesulfonic acid **2.33/2.34** from the reaction of a primary amine with a sultone **2.35/2.36**<sup>83-85</sup> or with a haloalkanesulfonic acid **2.37/2.38**.<sup>83</sup> The latter can be prepared by reaction of a sultone **2.35/2.36** with a potassium halide.<sup>85,86</sup> Chlorination of

**2.33/2.34** is achieved in the presence of phosphorus pentachloride, phosphorus oxychloride, a mixture of both, or phosphorus trichloride.<sup>81,83,85,87</sup>

**By N-C ring closure.** This synthetic approach involves the cyclisation of the sulfonamides **2.39/2.40** (Scheme 2.10) in the presence of a base. These intermediates are usually prepared by reaction of amines with chloroalkanesulfonyl chlorides **2.41/2.42**.<sup>60,83-85,87-89</sup>

**By C-C ring closure.** Preparation of the  $\gamma$ - and  $\delta$ -sultam rings by C-C bond formation is illustrated with the synthesis of the unsubstituted  $\delta$ -sultam **2.28a** (Scheme 2.11). The method employs *N*-(haloalkyl)alkanesulfonamides such as **2.43**, which result from the reaction of an alkanesulfonyl halide **2.44** with an haloalkylamine hydrochloride **2.45**.<sup>88,90</sup> Due to the acidity of the  $\alpha$ -hydrogens in **2.43**, cyclisation proceeds in the presence of a strong base, *i.e.* LDA or *n*-BuLi.



**Scheme 2.11** Synthesis of  $\delta$ -sultam by C-C ring closure.

### 2.1.3 Synthesis of sultams core

The preparation of *N*-substituted- $\beta$ -,  $\gamma$ - and  $\delta$ -sultams can be accomplished by two possible modes, one involving the modification at the nitrogen atom prior to cyclisation<sup>60,67,84</sup> and another involving the derivatisation of an unsubstituted sultam. The latter process has been used in the synthesis of *N*-alkyl-, acyl- and phosphoro-sultams.<sup>60,84,91,92</sup> Previous in-house work regarding the preparation of the unsubstituted  $\beta$ -sultam presented difficulties and the project was dropped. Thus, the present study focused exclusively on the cyclisation of *N*-substituted intermediates.

### 2.1.3.1 $\beta$ -Sultams

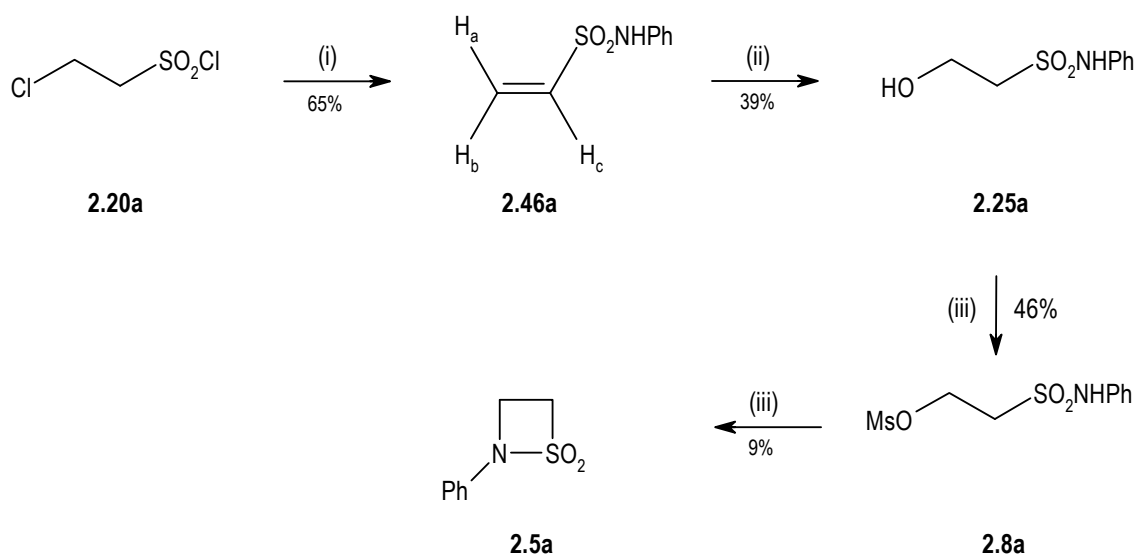
#### *N*-Phenyl- $\beta$ -sultam

Synthesis of *N*-phenyl- $\beta$ -sultam **2.5a** (Scheme 2.12) was achieved by cyclisation of the mesylate **2.8a**, as described by Page *et al.*,<sup>67</sup> although with a different route to the hydroxysulfonamide intermediate **2.25a**. Thus, Page *et al.* prepared this compound by reaction of formaldehyde with a sulfonamide dianion (Scheme 2.9). In the present investigation, it was synthesised in comparable yield (39% *versus* 53%<sup>67</sup>) from ethenesulfonamide **2.46a**.

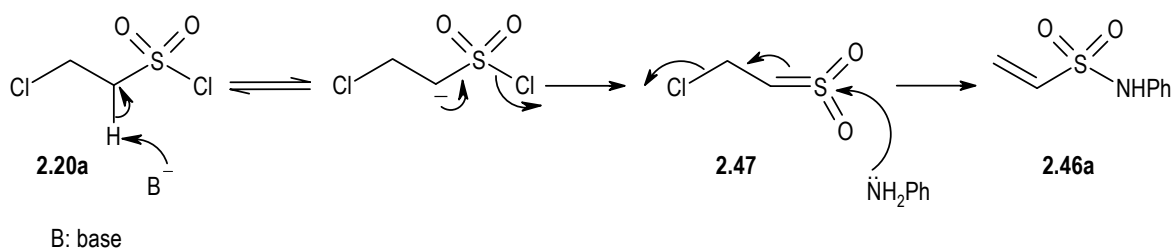
It is known that ethenesulfonamides, as **2.46a**, may be provided in substantial yield from the reaction of 2-chloroethanesulfonyl chloride **2.20a** with arylamines, which is rationalised in terms of an elimination-addition mechanism (E1cB) involving a sulfene intermediate **2.47** (Scheme 2.13).<sup>93,94</sup>

Thus, ethenesulfonamide **2.46a** was prepared using a modified reported procedure, in comparable yield (65% *versus* 72%<sup>93</sup>). Aniline was not used in excess and the temperature was kept at  $-10\text{ }^{\circ}\text{C}$  to prevent conjugate addition of the amine to the newly formed double bond of the ethenesulfonamide. The hydrochloric acid from the reaction was trapped by TEA. The presence of a mono-substituted double bond was confirmed by the NMR signals for three olefinic protons ( $\delta = 5.94$ , dd,  $J = 0.4$  and  $9.7$  Hz;  $\delta = 6.27$ , dd,  $J = 0.4$  and  $16.5$  Hz;  $\delta = 6.54$ , dd,  $J = 9.7$  and  $16.5$  Hz).

Synthesis of ethenesulfonamide **2.46a** was initially attempted in toluene<sup>67</sup> using 2 mol eq of aniline and stirring for 24 h at rt. Two products were afforded; firstly, the unusual<sup>93</sup> sulfonamide **2.48** (3% yield, Figure 2.2) and secondly, **2.46a** (37% yield). The procedure was repeated under reflux (2 h) leading to **2.46a** in a similar yield (31%), but no **2.48** could be detected.



**Scheme 2.12** Synthesis of *N*-phenyl- $\beta$ -sultam by cyclisation of *N*-phenyl-2-hydroxyethanesulfonamide mesylate. Reagents and conditions: (i)  $\text{NH}_2\text{Ph}$ , TEA, DCM,  $-10^\circ\text{C}$ , 20 min; (ii)  $\text{NaOH}$  (aqueous solution), reflux, 3 days; (iii)  $\text{MeSO}_2\text{Cl}$ , TEA, dry DCM,  $0^\circ\text{C}$ ,  $\text{N}_2$ , 30 min; (iv)  $\text{Na}_2\text{CO}_3$ , dry DMSO,  $60^\circ\text{C}$ ,  $\text{N}_2$ , 1 h.



**Scheme 2.13** Mechanism of the formation of ethenesulfonamides.

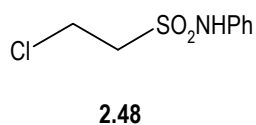
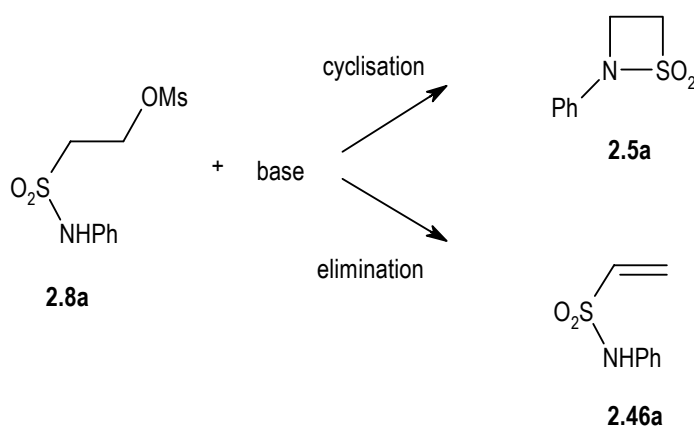


**Figure 2.2** Structure of 2-chloro-*N*-phenylethanesulfonamide.

The next step, *i.e.* the hydroxylation of ethenesulfonamide **2.46a**, was carried out in the presence of an aqueous solution of sodium hydroxide to obtain **2.25a** as a sodium salt that was subsequently neutralized by the addition of conc. hydrochloric acid. The subsequently conversion of **2.25a** into its mesylate ester **2.8a** was initially carried out with 1 mol eq of mesyl chloride and 1 mol eq of TEA, in dry DCM.<sup>67</sup> Unfortunately, it was impossible to reproduce the yield of the literature (21% *versus* 62%<sup>67</sup>). Employing 1.5 mol eq of both mesyl chloride and TEA improved the outcome of the reaction from 21 to 46%. Purification of **2.8a** by trituration from ether was previously described.<sup>67</sup> In the present work, better results were found by washing crude product with cold chloroform.

Finally, cyclisation was achieved as described, although in a poor yield (9% *versus* 42%<sup>58,67</sup>). As expected,<sup>58</sup> the <sup>1</sup>H NMR spectrum of the reaction medium showed the presence of two compounds (Scheme 2.14); (i) the major product *N*-phenyl- $\beta$ -sultam **2.5a**, which was purified by crystallization from a mixture of EtOH/water<sup>69</sup> and (ii) the elimination product **2.46a**, which was not isolated.

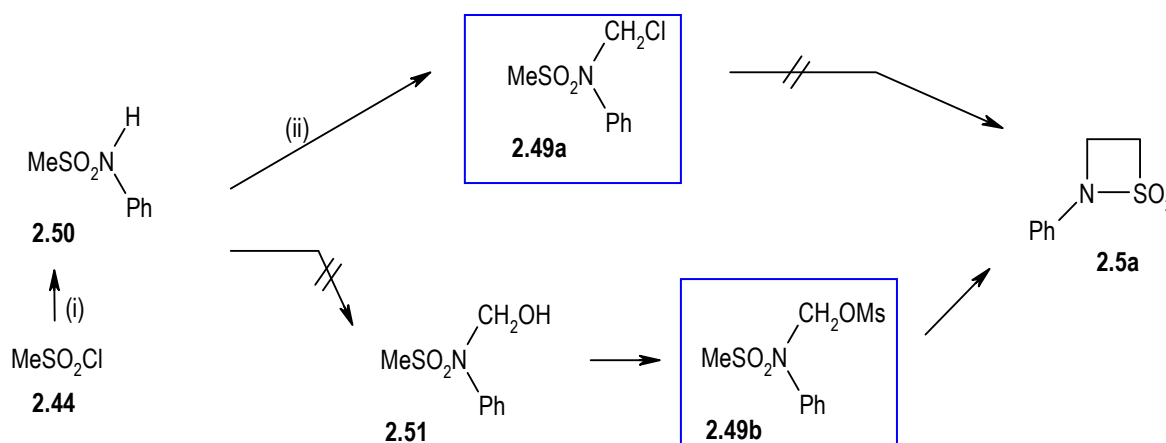


Scheme 2.14 Reaction products from *N*-phenyl-2-hydroxyethanesulfonamide mesylate.

To overcome the low yield obtained for *N*-phenyl- $\beta$ -sultam **2.5a**, two further synthetic routes were attempted: (i) C-C bond formation by cyclisation of compounds **2.49** (Scheme 2.15) and (ii) N-S bond formation by cyclisation of hydrochloride **2.6b** (Scheme 2.16).

To the best of author's knowledge,  $\beta$ -sultams have never been achieved by C-C ring closure. This approach was exploited by two possible routes, one involving intermediate **2.49a** and another involving mesylate **2.49b**. In both modes, cyclisation was expected to

occur in the presence of a deprotonating agent, *i.e.* LDA or *n*-BuLi, due to the attack of the  $\alpha$ -methanesulfonamide anion to the carbon bearing the leaving group, *i.e.* chloro or mesylate group.



**Scheme 2.15** Attempted synthesis of *N*-phenyl- $\beta$ -sultam by cyclisation of *N,N*-disubstituted-methanesulfonamides. Key intermediates are highlighted by a blue box. Reagents and conditions: (i)  $\text{NH}_2\text{Ph}$ , toluene, reflux, 2 h; (ii) paraformaldehyde, chlorotrimethylsilane, DCM, reflux, 21 h.

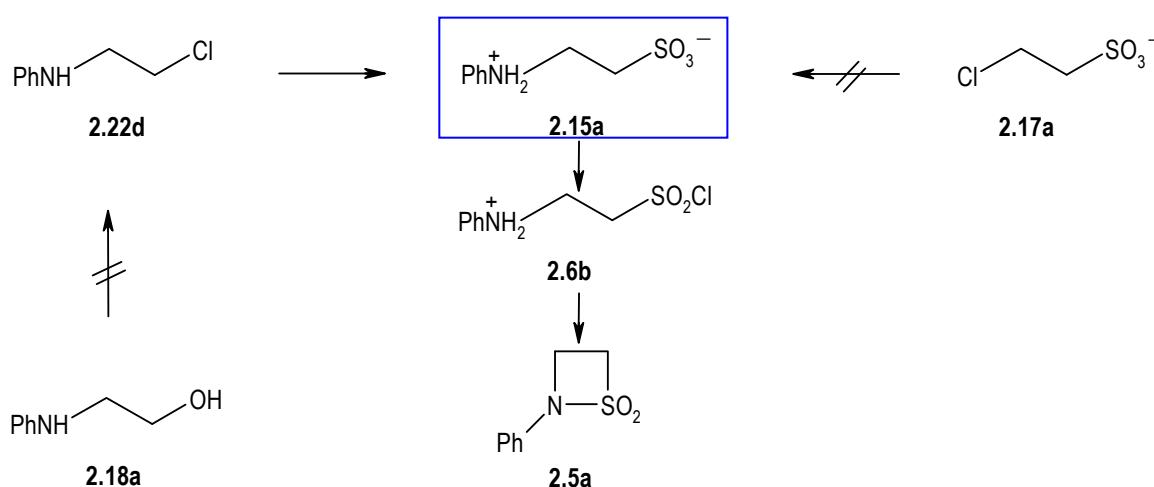
Preparation of the intermediate **2.49a** required the initial synthesis of sulfonamide **2.50**, which was then reacted in the presence of paraformaldehyde and chlorotrimethylsilane.<sup>95</sup> The reaction was monitored by  $^1\text{H}$  NMR spectroscopy until the signal integral ratio  $\text{CH}_2\text{Cl} : \text{CH}_3\text{S} : \text{Ph}$  became 2:3:5. The reported reaction time is 24 h (94% yield).<sup>95</sup> In the present study, the reaction did not proceed further between 5 h (81% yield) and 21 h (86% yield). Attempts to carry out the cyclisation of **2.49a** into the *N*-phenyl- $\beta$ -sultam **2.5a** failed (Table 2.1).

The route to mesylate **2.49b** also started from sulfonamide **2.50**, which was treated with an aqueous formaldehyde solution 37% (5.6 mol eq) and potassium carbonate (1.0 mol eq) in THF,<sup>96</sup> in order to obtain the *N*-hydroxymethylsulfonamide **2.51**. However, after refluxing for 6 h and stirring for 3 days at rt, only starting material was recovered. This is a rather similar result from that observed in the synthesis of the carbonyl analogues, acyclic tertiary *N*-hydroxymethylamides, which are hardly prepared from the corresponding amides.<sup>95</sup>

**Table 2.1** Conditions for the synthesis of *N*-phenyl- $\beta$ -sultam from **2.49a**.

Base/mol eq	Solvent/Temperature/Reaction time	TLC	<sup>1</sup> H NMR
<i>n</i> -BuLi /1.2	dry THF/−78 °C/N <sub>2</sub> /20 min	complex mixture	—
<i>n</i> -Buli/2.6	dry THF/−78 °C/N <sub>2</sub> /30 min	complex mixture	—
LDA/2.6	dry THF/−78 °C/N <sub>2</sub> /30 min	complex mixture	—
NaH/2.0	(a) dry THF /0 °C/N <sub>2</sub> , (b) rt/N <sub>2</sub> /3 h, (c) reflux/4 h, (d) rt/2 days	—	starting material <b>2.49a</b>

The second mentioned approach to *N*-phenyl- $\beta$ -sultam **2.5a** (Scheme 2.16), began with the attempt to prepare derivative **2.15a** from two possible starting materials, sodium 2-chloroethanesulfonate **2.17a** and *N*-phenyl-2-aminoethanol **2.18a**.



**Scheme 2.16** Attempted synthesis of *N*-phenyl- $\beta$ -sultam by cyclisation of 2-(phenylamino)ethanesulfonyl chloride hydrochloride. The key intermediate is highlighted by a blue box.

The preparation of **2.15a** from **2.17a** has been previously investigated.<sup>74</sup> Based on the reported procedure, **2.17a** and aniline (4.0 mol eq) were heated at 165 °C for 8 h, under agitation, during which time the mixture turned brown. Upon work-up, this afforded a brown



solid.  $^1\text{H}$  NMR (60 MHz,  $\text{D}_2\text{O}/\text{d}_6\text{-DMSO}$ ) spectrum showed no signals related to **2.15a** or another identifiable structure.

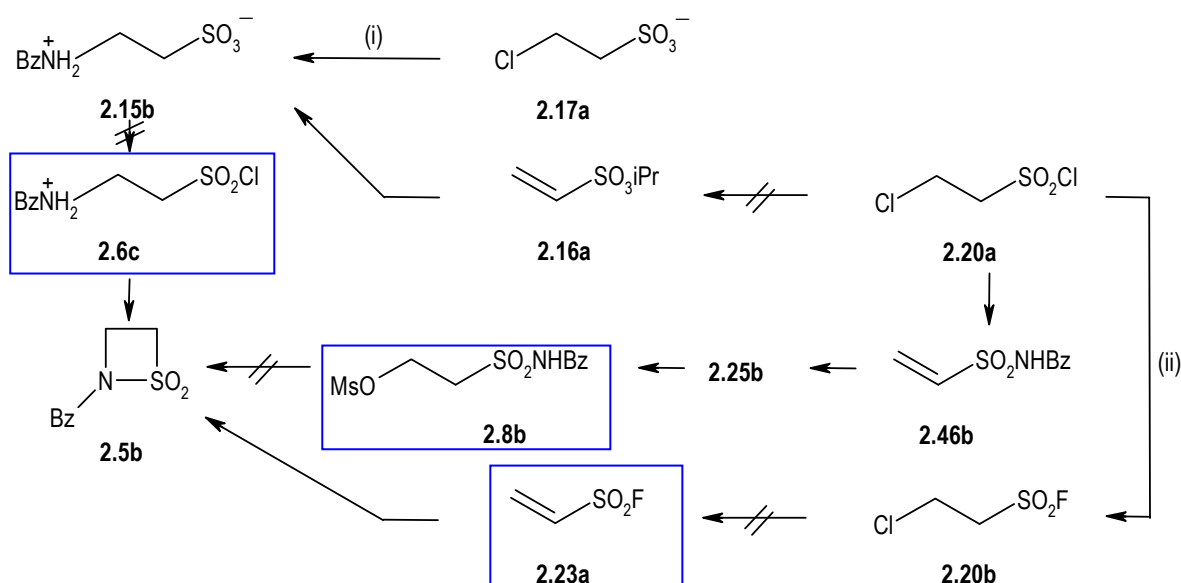
This procedure used aniline in a small volume, and thus to improve the contact between the starting materials another experiment was performed, in which **2.17a** was suspended in toluene. This solvent was chosen due to the employment of aromatic solvents in the preparation of 4-aminobutanesulfonic acids (**2.34**, Scheme 2.10).<sup>83</sup> The reaction mixture was refluxed for 24 h, after which a precipitate still remained; work-up afforded a solid that gave a complex spectrum lacking any signals for **2.15a**.

Alternatively, preparation of **2.15a** was tried from **2.18a**. This approach involved the initial attempt to prepare intermediate **2.22d**, as reported for 2-chloroethylamine (**2.22a**, Scheme 2.4).<sup>75</sup> Thus, thionyl chloride (9.7 mmol) was added dropwise to a solution of **2.18a** (7.3 mmol) in DCM (5 mL). On mixing the reactants, the medium turned from yellow to brown with evolution of hydrogen chloride. TLC (EtOAc) indicated the formation of a new compound with a higher  $R_f$  value and that no **2.18a** remained. The solvent was evaporated to give a brown solid, whose complex  $^1\text{H}$  NMR (300 MHz,  $\text{CDCl}_3$ ) spectrum was inconsistent with the desired product and could not be assigned to another structure.

Previous studies were also unsuccessful in this approach.<sup>74</sup> Although no details of the reaction were given, the result was ascribed to the complete polymerisation of **2.22d** through the attack of the nitrogen nucleophile to the carbon bearing the chloro leaving group. On the other hand, it was found that the chlorination of ethanolamine is better achieved starting from the hydrochloride than from the free base, which was related to the formation of thionylamine in the latter case.<sup>75</sup> Thus, it may be that prior neutralization of **2.18a** with conc. hydrochloric acid could lead to a different result, but due to time limitations, no further attempts were made.

***N*-Benzyl- $\beta$ -sultam**

Initially, preparation of *N*-benzyl- $\beta$ -sultam **2.5b** (Scheme 2.17) involved the attempted cyclisation of the mesylate **2.8b**, but the process failed. Usually, this method leads to the formation of the ethenesulfonamides **2.46** as by-products, in minor amounts.<sup>58</sup> However, when applied to mesylate **2.8b**, it afforded the ethenesulfonamide **2.46b** as the only product (24% yield). Other experimental attempts involving variation of the base, solvent and temperature, remained unsuccessful (Table 2.2).



**Scheme 2.17** Attempted synthesis of *N*-benzyl- $\beta$ -sultam. Key intermediates are highlighted by a blue box. Reagents and conditions: (i)  $\text{NH}_2\text{Bz}$ , 100 °C, 2 h; (ii)  $\text{KF}$ , dioxane/water, rt, 2 h.

**Table 2.2** Conditions for the cyclisation of *N*-benzyl-2-hydroxyethanesulfonamide mesylate into *N*-benzyl- $\beta$ -sultam.

Base	Solvent/Temperature/Reaction time	$^1\text{H}$ NMR
$\text{Na}_2\text{CO}_3$ (1 mol eq)	dry DMSO/60 °C/ $\text{N}_2$ /30 min	<b>2.46b</b>
	dry THF/reflux/2 h	<b>2.8b</b>
$\text{Na}_2\text{CO}_3$ (3 mol eq)	dry DMSO/60 °C/ $\text{N}_2$ /1 h	<b>2.46b</b>
	dry THF/reflux/10 h	<b>2.8b</b>
TEA (1 mol eq)	dry DMSO/60 °C/ $\text{N}_2$ /30 min	<b>2.46b</b>
	dry THF/reflux/45 min	<b>2.8b</b>
TEA (3 mol eq)	dry THF/reflux/22 h	complex mixture

Two further synthetic routes were attempted (Scheme 2.17), one involving hydrochloride **2.6c** and another involving ethenesulfonyl fluoride **2.23a**.

The route involving **2.6c** began with the attempted preparation of **2.15b**. This compound has been previously prepared from isopropyl ethenesulfonate **2.16a**, which is usually achieved by adding dry isopropanol to sulfonyl chloride **2.20a**, in the presence of pyridine.<sup>65,67</sup> Following the described procedure for **2.16a**, a yellow liquid was afforded that upon attempted purification by distillation, under reduced pressure (39 mmHg), turned the mixture dark brown and led to no distilled products. Decomposition of **2.16a** by distillation at pressures greater than 5 mmHg has been previously observed.<sup>73</sup>

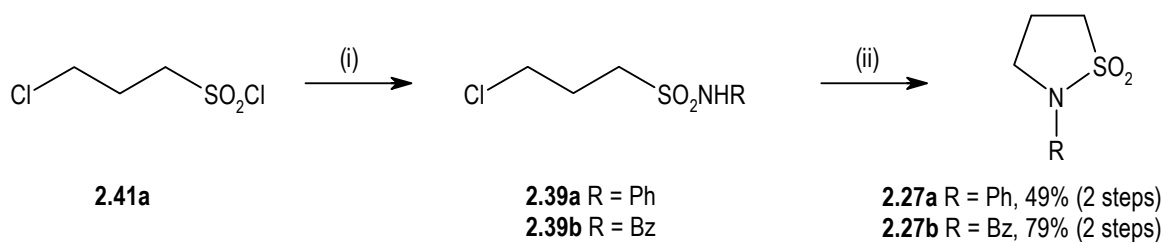
Thereafter, **2.15b** was achieved from **2.17a** by following a similar procedure to the one described for its phenyl analogue **2.15a**. However, attempted conversion of **2.15b** into **2.6c** by refluxing it with phosphorus oxychloride (18 eq) until complete dissolution (*ca.* 15 min) failed; both <sup>1</sup>H NMR (300 MHz, CDCl<sub>3</sub>) and ESI-MS analyses of the product after work-up were inconsistent with **2.6c** and could not be assigned to another structure.

The route involving ethenesulfonyl fluoride **2.23a**, began with the synthesis of **2.20b**,<sup>79</sup> the identity of which was confirmed by the comparison of its boiling point and spectroscopic data with those in the literature.<sup>58,79</sup> Although <sup>1</sup>H and <sup>13</sup>C NMR spectra of **2.20b** are known, the compound is basically characterised by its boiling point, mass or elemental analysis, and by its IR spectrum.<sup>58,79</sup> The latter showed an increase in the frequencies of sulfonyl stretching vibrations in comparison with the IR spectrum of its precursor **2.20a**.

The next step, *i.e.*, preparation of **2.23a**, was attempted by treating **2.20b** with TEA or magnesium oxide.<sup>58,79</sup> Both methods afforded yellow oils that gave NMR spectra (60 MHz, CDCl<sub>3</sub>) inconsistent with the desired product and impossible to assign.

2.1.3.2  $\gamma$ -Sultams

The synthesis of *N*-phenyl- and *N*-benzyl- $\gamma$ -sultams **2.27a,b** (Scheme 2.18) was accomplished by cyclisation of the corresponding sulfonamides **2.39a,b** in the presence of a base.



**Scheme 2.18** Synthesis of *N*-phenyl- and *N*-benzyl- $\gamma$ -sultams. Reagents and conditions: (i)  $\text{NH}_2\text{Ph}$ , TEA, DCM, reflux, 1 h or  $\text{NH}_2\text{Bz}$ , DCM,  $-10^\circ\text{C}$ , 1 h; (ii) NaOH, TEA, MeOH, reflux.

The literature reports the preparation of *N*-benzyl- $\gamma$ -sultam **2.27b** by C-C bond formation through *n*-BuLi mediated cyclisation of the mesylate **2.49c** (Figure 2.3) but, to the best of author's knowledge, this sultam has not been formed from the sulfonamide **2.39b**, which was obtained from the reaction of benzylamine with sulfonyl chloride **2.41a**. To prevent the formation of **2.52a** (Figure 2.4), reaction was carried out at  $-10^\circ\text{C}$  and benzylamine was employed in a 2:1 molar ratio to sulfonyl chloride **2.41a**.<sup>85</sup> The second equivalent of amine was used to trap hydrochloric acid from the reaction.

After the cyclisation step,<sup>85</sup> purification of *N*-benzyl- $\gamma$ -sultam **2.27b** from the remaining TEA and sulfonamide **2.39b**, was achieved by washing the crude product with hydrochloric acid 5% (w/v) and 2M-sodium hydroxide.

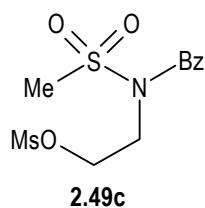
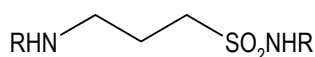


**Figure 2.3** *N*-(2-Methanesulfonyloxyethyl)-*N*-benzylmethanesulfonamide mesylate **2.49c**. Its cyclisation to *N*-benzyl- $\gamma$ -sultam was reported in 74% yield.<sup>97</sup>

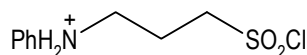


**2.52a** R = Bz

**2.52b** R = Ph

**Figure 2.4** *N*-Benzyl-3-(benzylamino)propane-1-sulfonamide (**2.52a**) and *N*-phenyl-3-(phenylamino)propane-1-sulfonamide (**2.52b**).

The synthesis of *N*-phenyl- $\gamma$ -sultam **2.27a** was reported by two possible routes, one involving the cyclisation of sulfonyl chloride **2.29a**<sup>85</sup> (Figure 2.5) and another *via* the formation of sulfonamide **2.39a**.<sup>83,84</sup> As already mentioned, the present investigation followed this latter route (Scheme 2.18). Thus, *N*-phenyl- $\gamma$ -sultam was achieved as described for the *N*-benzyl analogue, except that after several unsuccessful attempts the preparation of the sulfonamide **2.39a** required reflux conditions (Table 2.3). Even so, no formation of **2.52b** (Figure 2.4) could be detected, which probably reflects the poor nucleophilicity of aniline.



**2.29a**

**Figure 2.5** Structure of 3-(phenylamino)propanesulfonyl chloride **2.29a**.

**Table 2.3** Conditions for the synthesis of 3-chloro-*N*-phenylpropane-1-sulfonamide **2.39a** from **2.41a**.

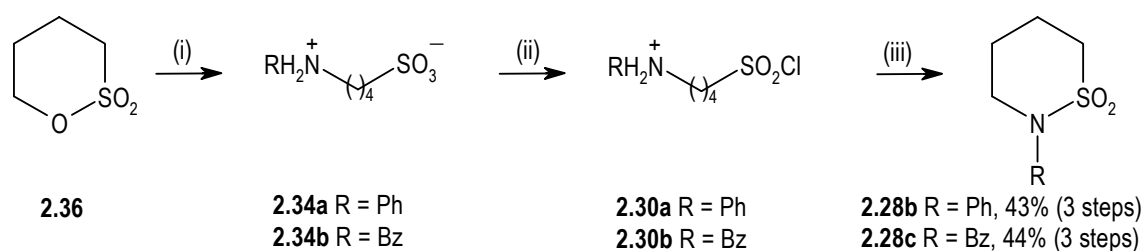
Base <sup>a</sup> /1 mol eq	Solvent/Temperature/Reaction time <sup>b</sup>	TLC	<sup>1</sup> H NMR
NH <sub>2</sub> Ph	DCM/−10 °C/1 h	starting material	—
TEA	DCM/−10 °C/8 h	new compound	impure <b>2.39a</b> (40% crude yield) <b>2.39a</b> (2% yield after chromatography)
TMP <sup>c</sup>	DCM/−10 °C/9 h	new compound	impure <b>2.39a</b> (55% crude yield)

<sup>a</sup> These bases were employed to trap hydrochloric acid from the reaction. In all cases, aniline (1 mol eq) was used to react with 3-chloropropanesulfonyl chloride **2.41a**. <sup>b</sup> Work-up: reaction medium was washed with hydrochloric acid 5% (w/v) and saturated sodium chloride solution, dried with anhydrous magnesium sulfate and evaporated. <sup>c</sup> 2,2,6,6-Tetramethylpiperidine.

2.1.3.3  $\delta$ -Sultams

Previous investigations have prepared *N*-phenyl- and *N*-benzyl- $\delta$ -sultams **2.28b,c** according to two approaches: (i) N-S bond formation by cyclisation of hydrochlorides **2.30a,b**<sup>83,90</sup> (Scheme 2.19) and (ii) N-C bond formation by cyclisation of sulfonamides such as **2.40a** (Scheme 2.20).<sup>83,89</sup> The present work exploited both routes, starting from sultone **2.36**.

In the first approach (Scheme 2.19), the sultone **2.36** was reacted with the appropriate amine to afford the sulfonic acids **2.34a,b**. This step followed the procedure reported for aniline, under solventless conditions.<sup>98</sup> The medium solidified as the reaction proceeds and, at the end, it gives a glassy solid.



**Scheme 2.19** Synthesis of *N*-phenyl- and *N*-benzyl- $\delta$ -sultams by cyclisation of the corresponding 1-chlorosulfonyl-4-aminobutane hydrochlorides. Reagents and conditions: (i)  $\text{NH}_2\text{Ph}$ , 100 °C; (ii)  $\text{POCl}_3$ , reflux, 90 min; (iii)  $\text{Na}_2\text{CO}_3$ , EtOAc, rt.

Concerning the following step, previous investigations chlorinated **2.34a** with phosphorus trichloride,<sup>83</sup> whereas chlorination of **2.34b** was achieved with phosphorus oxychloride.<sup>90</sup> In the present study, phosphorus oxychloride was preferred, only because it was available. The process was carried out using the procedure reported for the 2-*o*-toluidine analogue,<sup>83</sup> that uses phosphorus oxychloride as solvent. TLC and  $^1\text{H}$  NMR analyses were ineffective in monitoring the reaction, thus it was kept during the time reported (90 min),<sup>83</sup> and then the excess phosphorus oxychloride was evaporated to afford hydrochlorides **2.30a,b**.

This latter type of intermediates is, according to the literature,<sup>83</sup> converted into  $\delta$ -sultams by treatment with cold water, followed or not by the addition of a sodium hydroxide solution to render the medium alkaline. Under these conditions, sultams separate in a crystalline

form.<sup>83</sup> However, in the present work, mixing the crude compound **2.30a** with a 2M-sodium hydroxide solution did not afford the desired sultam, even after several days at 4 °C. Thus, cyclisation was attempted by following the procedure used for  $\gamma$ -sultams (Section 2.1.3.2), *i.e.* by refluxing a 1:1:1 molar mixture of sodium hydroxide : TEA : **2.30a** in MeOH, but the process failed. TLC analysis (ethyl ether) of the reaction mixture showed the disappearance of the starting material, but no product could be detected. In addition, <sup>1</sup>H NMR spectrum (300 MHz, CDCl<sub>3</sub>) was inconsistent with both *N*-phenyl- $\delta$ -sultam **2.28b** and starting material **2.30a** structures. Finally,  $\delta$ -sultams were achieved by employing the conditions commonly used in the cyclisation of 1-chlorosulfonyl-2-aminoethane hydrochlorides **2.6** to  $\beta$ -sultams, *i.e.* by stirring the appropriate hydrochloride with sodium carbonate in EtOAc.<sup>67</sup>

The main difficulties arising from this first route to  $\delta$ -sultams were in purifying the intermediates and in monitoring the reaction progress. Thus, attempted crystallization of sulfonic acid **2.34a** from a mixture of EtOH/water<sup>98</sup> was unsuccessful. <sup>1</sup>H NMR spectra (60 MHz, d<sub>6</sub>-DMSO) of this compound and of its chloro derivative **2.30a** appeared as mixtures and the mass analyses were inconsistent with the required structures.

Overall, the process is mainly controlled by the solidification of the contents, in the first step (solventless conditions), and by the dissolution of the resultant material in phosphorus oxychloride, which occurs in the second step.

It is noteworthy that in the literature,<sup>83,90</sup> this route usually proceeds from the sultone **2.36** into the  $\delta$ -sultam without isolation of the intermediates.

The second mentioned approach, *i.e.* cyclisation of 4-halobutanesulfonamides, was employed in an alternative preparation of *N*-benzyl- $\delta$ -sultam **2.28c** (Scheme 2.20).



**Scheme 2.20** Synthesis of the *N*-benzyl- $\delta$ -sultam by cyclisation of the 4-bromo-*N*-benzylbutanesulfonamide. Reagents and conditions: (i) KBr, MeOH, reflux, 48 h; (ii) PCl<sub>5</sub>; (iii) NH<sub>2</sub>Bz, DCM, -10 °C, 1 h; (iv) NaOH, TEA, MeOH, reflux.

The first step consisted in the preparation of sulfonate **2.38a** from the known reaction of sultone **2.36** with potassium bromide.<sup>98</sup> TLC analysis (DCM, iodine chamber) indicated that production of a more polar compound had occurred and that no sultone **2.36** remained, but the <sup>1</sup>H NMR (300 MHz, d<sub>6</sub>-DMSO) spectrum was inconclusive and the mass spectrum was inconsistent with the desired structure. On the other hand, IR analysis supported the formation of **2.38a**, through the exhibition of characteristic sulphur-oxygen stretching vibrations for sulfonate salts (1351, 1198, 1172, 1058 cm<sup>-1</sup>). Based on this observation, the product was allowed to proceed into the chlorination step, which was carried out using phosphorus pentachloride at rt, as described for the chlorination of the analogous 3-bromopropane-1-sulfonate.<sup>85</sup>

The formation of sulfonyl chloride **2.42a** was suggested: (i) by TLC analysis (DCM, iodine chamber), which revealed the formation of a compound with a higher R<sub>f</sub> value, (ii) by the exhibition in the IR spectrum of sulfonyl stretching vibrations (1380, 1170 cm<sup>-1</sup>) at higher frequencies than those of the precursor **2.38a** and (iii) by three multiplets in the <sup>1</sup>H NMR spectrum (60 MHz, CDCl<sub>3</sub>). Although this latter also revealed the presence of impurities, **2.42a** was immediately used in the preparation of the sulfonamide **2.40a**, which was subsequently cyclised.

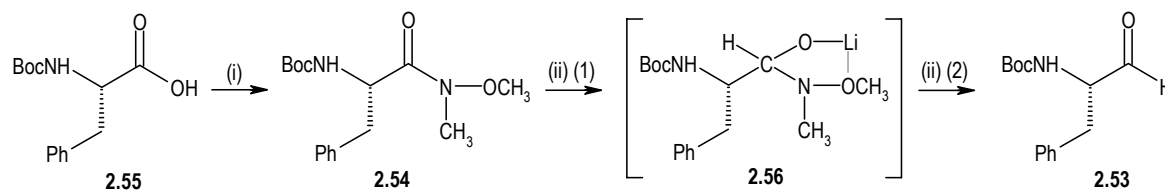
The <sup>1</sup>H NMR spectrum of the final product was consistent with the structure of *N*-benzyl- $\delta$ -sultam **2.28c** but also revealed the presence of impurities. This route led to a lower yield (18%, crude yield, 4 steps) than the mentioned cyclisation of hydrochlorides **2.30a,b** (Scheme 2.19). Thus, no purification was performed and this route was no further exploited.

### 2.1.4 Synthesis of dipeptide vinyl sultams

#### 2.1.4.1 Aminoacid and dipeptidyl aldehydes

***N*-Boc-*S*-Phenylalaninal.** The preparation of *N*-Boc-*S*-phenylalaninal **2.53** consisted in the reduction by lithium aluminium hydride of the corresponding hydroxamate **2.54** derived from *N*-Boc-*S*-phenylalanine **2.55** (Scheme 2.21).<sup>99</sup>





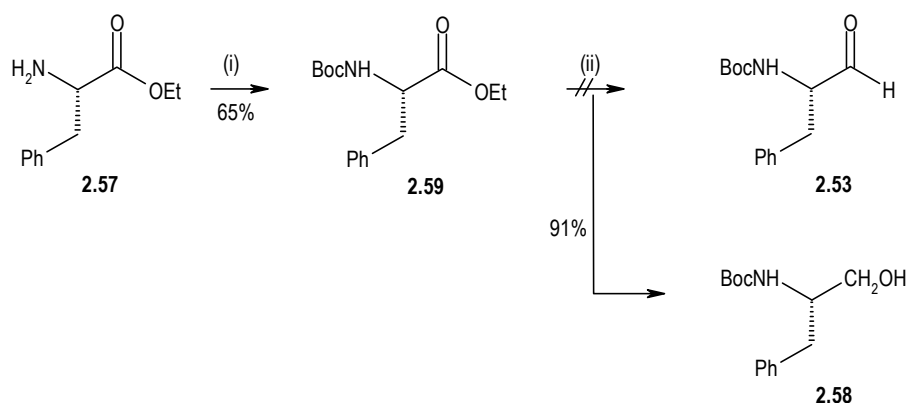
**Scheme 2.21** Synthesis of *N*-Boc-*S*-phenylalinal from *N*-Boc-*S*-phenylalanine via hydroxamate. Reagents and conditions: (i) (1) isobutyl chloroformate, TEA, DCM, -10 °C, 30 min, (2) *O*, *N*-dimethylhydroxylamine hydrochloride, rt, overnight; (ii) (1) LiAlH<sub>4</sub>, dry THF, 0 °C, 30 min, (2) KHSO<sub>4</sub> (aqueous solution), 83% yield. Hydrogen bonds are in grey.

The main difficulty arising from the synthesis of aldehydes is in the further reduction of these products to alcohols. The method mentioned above allows the reaction to be stopped at the aldehyde state due to intramolecular complexation of lithium salts **2.56**, which provide the aldehydes by hydrolysis.<sup>99</sup> The method also affords crude aldehydes in high yield (86-96%) and sufficiently pure to avoid further purification, *e.g.* silica gel chromatography, which may lead to racemisation.<sup>99</sup>

The synthesis of hydroxamate **2.54** was initially performed with BOP<sup>99</sup> and TBTU as coupling reagents, but isobutyl chloroformate<sup>33</sup> became a suitable alternative due to its availability and lower price. DCC was also employed following the BOP procedure (reaction time: 5 to 15 h), but TLC analysis (*n*-hexane/EtOAc 1:1) revealed several products. Nevertheless, the formation of **2.54** was supported by the <sup>1</sup>H NMR spectrum (60 MHz, CDCl<sub>3</sub>) through the observation of two singlets at  $\delta$  3.17 and  $\delta$  3.67, consistent with the methyl groups of the hydroxamate function.

Subsequent conversion of **2.54** to aldehyde **2.53** proceeded according to Fehrentz *et al.*, in comparable yield (83% versus 86%<sup>99</sup>).

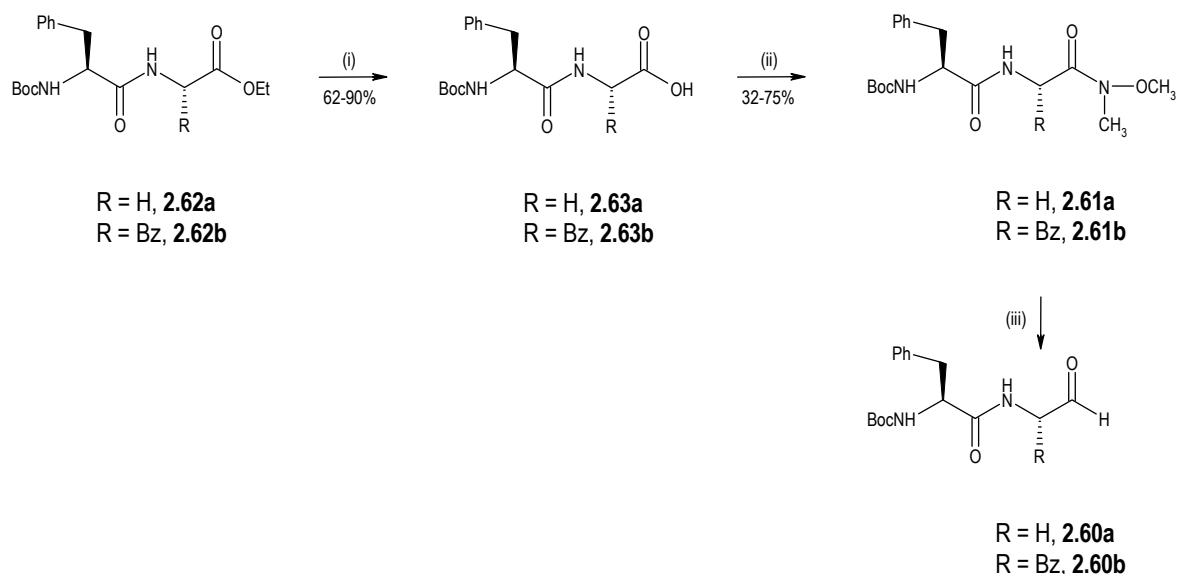
Previous investigations also achieved **2.53** from *N*-Boc-*S*-phenylalanine methyl ester using DIBAL as reducing agent.<sup>29</sup> In the present work, this route was also exploited through the *N*-Boc protection<sup>100</sup> of ethyl ester **2.57** (Scheme 2.22) and its subsequent reduction with DIBAL (3.3 mol eq). Instead of the aldehyde, the process afforded the alcohol **2.58**. Then, the reaction was carried out under the same conditions, but varying DIBAL equivalents. When 1 mol eq was used, a mixture of the *N*-protected ester **2.59** and a trace amount of aldehyde **2.53** was observed, whereas 2 mol eq yielded a mixture of alcohol **2.58**, aldehyde **2.53** and ester **2.59**.



**Scheme 2.22** Attempted synthesis of  $N$ -Boc- $S$ -phenylalaninal from  $N$ -Boc- $S$ -phenylalanine ethyl ester. Reagents and conditions: (i) Boc anhydride, TEA, THF, 0 °C to rt, 2.5 h; (ii) (1) DIBAL, dry THF, -78 °C, N<sub>2</sub>, 1 h, (2) MeOH, potassium sodium (+) tartrate (aqueous solution), rt, 1.5 h.

**Dipeptidyl aldehydes.** Reported investigations achieved the preparation of dipeptidyl aldehydes by the strategy described for  $N$ -Boc- $S$ -phenylalaninal **2.53**.<sup>33</sup> In the present study, the synthesis of aldehydes **2.60a,b** was also tried, although with a different route to the hydroxamate intermediates **2.61** (Scheme 2.23). Thus, in the literature<sup>33</sup> the dipeptidyl hydroxamates were prepared by coupling an  $\alpha$ -amino hydroxamate with  $N$ -protected amino acids, whereas in the syntheses of **2.61** the hydroxamate function was introduced after the dipeptide formation.

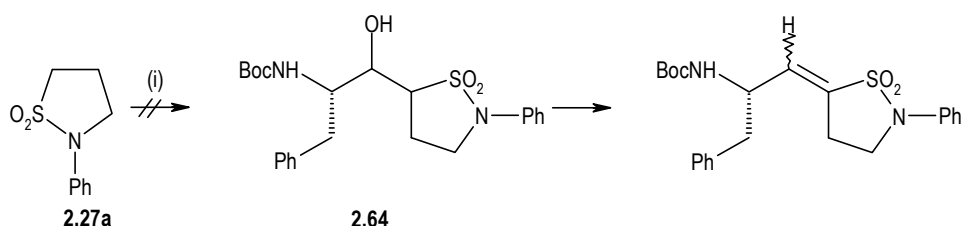
The process began with the preparation of dipeptidyl esters **2.62** which were hydrolyzed to the corresponding acids **2.63**.<sup>101</sup> These latter compounds were converted into hydroxamates **2.61**, which were tentatively reduced to aldehydes **2.60**. After 2.5 h, the reaction involving hydroxamate **2.61a** was quenched to afford a 2:1 mixture of aldehyde **2.60a** and starting material **2.61a** (showed by the signal integral ratio in the <sup>1</sup>H NMR spectrum). For hydroxamate **2.61b**, a 30 min reaction yielded a 1:1 mixture of **2.60b** and **2.61b** (showed by the signal integral ratio in the <sup>1</sup>H NMR spectrum). Nevertheless, crude aldehyde **2.60b** was employed in a Horner-Wadsworth-Emmons reaction described in Section 2.1.4.4.



**Scheme 2.23 Synthesis of dipeptidyl aldehydes.** Reagents and conditions: (i) 1M-NaOH, THF, reflux, 25 min; (ii) (1) TBTU, TEA, DCM, rt, 30 min, (2) *O*, *N*-dimethylhydroxylamine hydrochloride, TEA, rt, 13 h; (iii) (1)  $\text{LiAlH}_4$ , dry THF, 0 °C, 30 min; (2)  $\text{KHSO}_4$  (aqueous solution).

#### 2.1.4.2 Aldol-type reaction of sultam carbanions

The aldol-like reaction involved a direct coupling between *N*-Boc-*S*-phenylalaninal **2.53** and the anion of *N*-phenyl- $\gamma$ -sultam **2.27a** (Scheme 2.24). The reactants were employed at the same molar ratio of Horner-Wadsworth-Emmons reaction and the process followed the same procedure. The medium was fractionated by column chromatography on silica gel (*n*-hexane/EtOAc 1:1), affording aromatic impurities and the starting sultam (64% recovered), instead of the desired hydroxylated product **2.64**. This route was no further investigated.

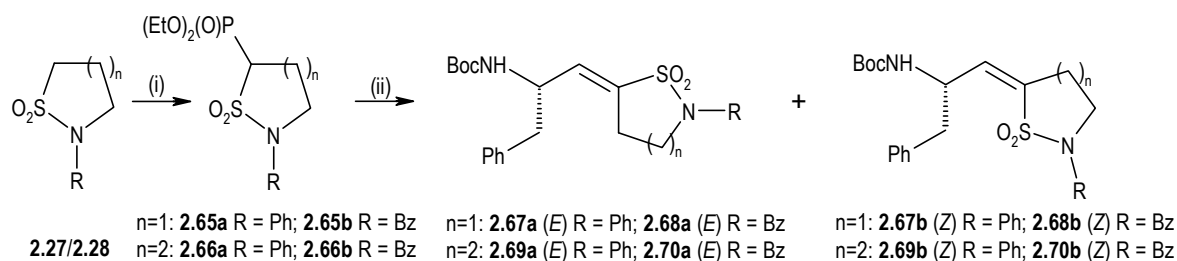


**Scheme 2.24 Synthesis of *E*- and *Z*-vinyl sultams via an aldol-like reaction.** Reagents and conditions: (i) *n*-BuLi, dry THF, *N*-Boc-*S*-phenylalaninal **2.53**, -78 °C to rt,  $\text{N}_2$ , 1 h.

## 2.1.4.3 Sultam phosphonates

The first approach to sultam phosphonates **2.65** and **2.66** (Scheme 2.25) consisted in the preparation of **2.66a** from sultam **2.28b**, in a two step reaction: (i) formation of **2.28b** anion by deprotonation with *n*-BuLi, and (ii) reaction of this anion with diethyl chlorophosphate. The reaction was performed under method A conditions<sup>38,64</sup> (Table 2.4), employing 1 mol eq of diethyl chlorophosphate, 2 mol eq of *n*-BuLi and 2 mol eq of **2.28b**. These two latter reactants must be used in excess because the  $\alpha$ -hydrogen of sultam phosphonates is more acidic than those of sultams. Thus, the sultam anion deprotonates the newly formed sultam phosphonate, regenerating the sultam which is the first compound to be eluted from the column during the chromatographic purification process.

When method A conditions were applied to the other sultams it furnished either decomposition or poor yields. For these reasons, conditions B and C were investigated. In general, LDA at  $-78$  °C afforded higher yields of the sultam phosphonates than *n*-BuLi either at  $-78$  °C or rt.



**Scheme 2.25** Synthesis of *E*- and *Z*-vinyl sultams through Horner-Wadsworth-Emmons chemistry.

Reagents and conditions: (i) (1) LDA, dry THF,  $-78$  °C, N<sub>2</sub>, 10 min, (2) (EtO)<sub>2</sub>POCl,  $-78$  °C, N<sub>2</sub>, 1 h; (ii) *n*-BuLi, dry THF, *N*-Boc-*S*-phenylalaninal **2.53**,  $-78$  °C to rt, N<sub>2</sub>, 20 min.

**Table 2.4** Conditions for the synthesis of sultam phosphonates.

Phosphonate	Yield (%)		
	Method A	Method B	Method C
<b>2.65a</b>	27	56	65
<b>2.65b</b>	0	—	43
<b>2.66a</b>	48	—	45
<b>2.66b</b>	15	—	34

Method A: *n*-BuLi, dry THF, rt, N<sub>2</sub>; Method B: *n*-BuLi, dry THF,  $-78$  °C, N<sub>2</sub>; Method C: LDA, dry THF,  $-78$  °C, N<sub>2</sub>.

**NMR spectral characterisation.** NMR signal assignments for sultam phosphonates were effected using DEPT and 2D NMR techniques ( $^1\text{H}$ - $^1\text{H}$  COSY and HMQC). Table 2.5 lists the data for **2.65a** as a typical example. The main features in the spectra are (i) the complexity of the  $^1\text{H}$  NMR signals comparatively to the ones showed by the sultam precursors, and (ii) the splitting of the carbon signals due to the  $^{13}\text{C}$ - $^{31}\text{P}$  couplings.

Sultam phosphonates were isolated as a mixture of the two possible enantiomers because the molecules have an asymmetrical carbon atom (shown by an asterisk in Figure 2.6). Due to the existence of a stereocentre, the two protons of each methylene group are diastereotopic to one another. Thus, each gives separate  $^1\text{H}$  NMR signals except in cases when the resonance frequencies are accidentally the same. Another consequence of the sultam phosphonates chirality is that pentavalent phosphorus atom became a prochiral centre. Therefore, the methylene and methyl groups from each ethyl component are non-equivalent giving an  $\text{ABX}_3$  spin system.<sup>102</sup> This situation cannot be easily deduced from the complex proton signals, but it is rather clear in the  $^{13}\text{C}$  NMR spectrum, which exhibited two separate signals for methylene groups 1 and 1' whereas the similar resonances of methyl groups 2 and 2' led to an obscure signal classified as a multiplet. The  $^{13}\text{C}$  NMR spectrum also showed the characteristic doublet splittings with  $J_{\text{CP}}$  of 143.6, 4.8 and 9.0 Hz (average values), consistent with  $^1J$ ,  $^2J$  and  $^3J$  couplings of the  $^{31}\text{P}$  and  $^{13}\text{C}$  nucleus.<sup>103</sup>

**Table 2.5 NMR data of 2.65a [400 MHz ( $^1\text{H}$ ), 100.61 MHz ( $^{13}\text{C}$ ),  $\text{CDCl}_3$ ].**

Position	$^1\text{H}$	$^{13}\text{C}$ (HMQC)
$\text{CH}_2\text{N}$	3.82 m <sup>a</sup>	45.8 d (10.1)
$\text{CHCH}_2$	2.70-2.83 m	21.9 d (3.0)
CH	3.80 m <sup>a</sup>	55.9 d (149.9)
$[\text{OCH}_2]_{\text{a}}$	4.28 m <sup>b</sup>	63.7 d (6.0)
$[\text{OCH}_2]_{\text{b}}$	4.34 m <sup>b</sup>	64.4 d (6.0)
$[\text{CH}_3]_{\text{a}}$	1.37–1.40 m <sup>c</sup>	16.4–16.5 m <sup>d</sup>
$[\text{CH}_3]_{\text{b}}$	1.37–1.40 m <sup>c</sup>	16.4–16.5 m <sup>d</sup>
Ph	7.16-7.20 m (1H)	125.2
	7.26-7.29 m (2H)	120.5
	7.34-7.38 m (2H)	129.4
		137.3

<sup>a</sup> Overlapped signals.  $\delta$  Values from HMQC spectrum; <sup>b</sup> Overlapped signals.  $\delta$  Values from HMQC spectrum; <sup>c</sup> Overlapped signals; <sup>d</sup> Overlapped signals.

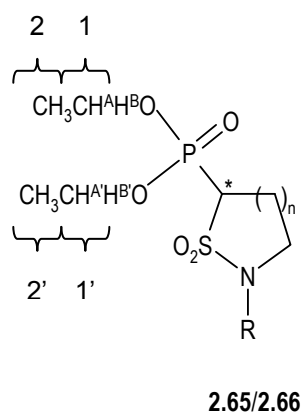


**Figure 2.6** Diastereotopic groups and stereocentre in sultam phosphonates.

#### 2.1.4.4 Horner-Wadsworth-Emmons reaction

To the best of author's knowledge, this thesis presents the first application of the Horner-Wadsworth-Emmons reaction to sultams. This method has been widely applied to the synthesis of vinyl sulfones and their analogues. In such cases, it is performed using sodium hydride,<sup>31,34,104</sup> *n*-BuLi,<sup>33</sup> or more rarely, sodium methoxide.<sup>39</sup> Although no details of the reaction were given, it was reported that sodium hydride improved the reaction outcome over *n*-BuLi.<sup>34</sup>

Thus, sodium hydride was used as deprotonating agent in the attempted Horner-Wadsworth-Emmons reaction of phosphonate **2.65a** and *N*-Boc-*S*-phenylalaninal **2.53**, following a procedure described for  $\alpha,\beta$ -unsaturated sulfonate and carboxyl derivatives.<sup>29</sup> The process afforded three products, whose <sup>1</sup>H NMR spectra were consistent with: (i) a mixture of vinyl sultam **2.67a** and aldehyde **2.53**, (ii) vinyl sultam **2.67b** and (iii) the regenerated *N*-phenyl- $\gamma$ -sultam **2.27a**.

Then, adopting a procedure with *n*-BuLi<sup>38</sup> provided *E*- and *Z*-vinyl sultams **2.67-2.70** (Scheme 2.25 and Table 2.6) with a short reaction time (after 20 min, sultam phosphonates were completely transformed). The *E/Z* ratio is consistent with the general observation that phosphonates with alkyl groups give mostly the thermodynamically more stable *E*-olefins.<sup>39,105</sup>

Table 2.6 Yields and ratio of *E/Z* isomers.

Phosphonate	Product	<i>E/Z</i>	Yield (%)	<i>E/Z</i> ratio
2.65a	2.67a	<i>E</i>	60	79:21
	2.67b	<i>Z</i>	16	
2.65b	2.68a	<i>E</i>	58	67:33
	2.68b	<i>Z</i>	29	
2.66a	2.69a	<i>E</i>	65	90:10
	2.69b	<i>Z</i>	7	
2.66b	2.70a	<i>E</i>	54	86:14
	2.70b	<i>Z</i>	9	

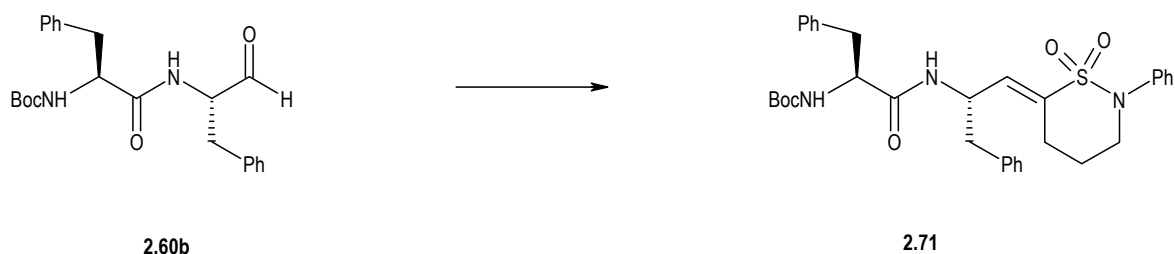
Despite being recognised that the strongly basic conditions of the Horner-Wadsworth-Emmons reaction might lead to the aldehyde's racemisation,<sup>29</sup> optical rotations of the resultant *E/Z* vinyl sulfones are rarely given. When this property is reported, it refers almost always to the coupled processed products, *i.e.* dipeptide vinyl sulfones and their analogues. Nevertheless, in the pioneering work of Hanzlik *et al.*,<sup>29</sup> it was stressed the substantial optical activity of the obtained Horner-Wadsworth-Emmons reaction products. No attempt was made to determine the enantiomeric purity of those compounds, because it was considered that there was no reason to expect substantial racemisation. Similarly, the vinyl sultams herein described showed a significant optical activity (Table 2.7).

Table 2.7 Optical rotations,  $[\alpha]_D^{21}$ , of *E/Z* isomers.

Compound	<i>E/Z</i>	Optical rotation	<i>c</i>
2.67a	<i>E</i>	+29	0.14
2.67b	<i>Z</i>	+57	0.93
2.68a	<i>E</i>	+31	0.10
2.69a	<i>E</i>	+13	0.13
2.70a	<i>E</i>	+24	0.13

**Condensation of sultam phosphonates with peptidyl aldehydes.** Another approach to dipeptide vinyl sultams involved the Horner-Wadsworth-Emmons reaction between sultam phosphonate **2.66a** and crude aldehyde **2.60b** (Scheme 2.26). After chromatography, the <sup>1</sup>H NMR spectrum of the reaction product showed a mixture of two olefinic compounds, which

cannot be separated. Mass spectra measurements supported the existence of the expected structure **2.71** through the observation of the ions at  $m/z$  608 ( $\text{MNH}_4^+$ ) and 613 ( $\text{MNa}^+$ ) (rel. int. 52 and 100, respectively).



**Scheme 2.26** Attempted synthesis of dipeptide vinyl sultams from dipeptidyl aldehydes. Reagents and conditions: **2.66a**, *n*-BuLi, dry THF,  $-78$  °C to rt,  $\text{N}_2$ , 20 min.

**NMR spectral characterisation.** Stereochemistry of vinyl sultams came from the examination of the chemical shifts of vinyl and methine protons (Table 2.8). This process was reported as a reliable criterion for stereochemical assignment of vinyl sulfonates:<sup>38</sup> as a result of the deshielding effect of the sulfonyl group, the vinyl proton resonance is generally found downfield in the *E*-isomer compared to the *Z*-isomer, whereas the methine proton signal appears upfield. Stereochemistry was further supported by means of NOESY spectrum, on the basis of a NOE cross-peak between the vinyl and  $=\text{CCH}_2$  protons in the *Z*-isomer **2.70b** (Figure 2.7).

**Table 2.8** Chemical shifts  $\delta$  and coupling constants  $J$  [400 MHz ( $^1\text{H}$ ),  $\text{CDCl}_3$ ] for vinyl and methine protons of *E/Z* isomers.

Compound	<i>E/Z</i>	$\delta_{\text{CH=}}$	$\delta_{\text{CHCH}_2\text{Ph}}$
<b>2.67a</b>	<i>E</i>	6.31 brd (8.8)	4.53 brs
<b>2.67b</b>	<i>Z</i>	6.35 brs	4.91 m
<b>2.68a</b>	<i>E</i>	6.29 brd (9.2)	4.48 m
<b>2.68b</b>	<i>Z</i>	6.26 brs	4.96 m
<b>2.69a</b>	<i>E</i>	6.24 brd (8.8)	4.71 m
<b>2.69b</b>	<i>Z</i>	6.12 brs	5.10 brs
<b>2.70a</b>	<i>E</i>	6.21 d (9.6)	4.68-4.74 m
<b>2.70b</b>	<i>Z</i>	5.98 brs	5.17 brs



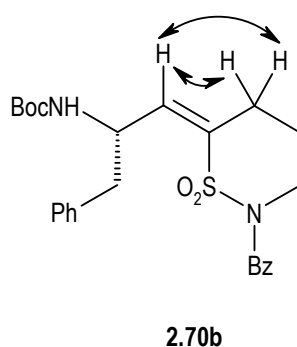
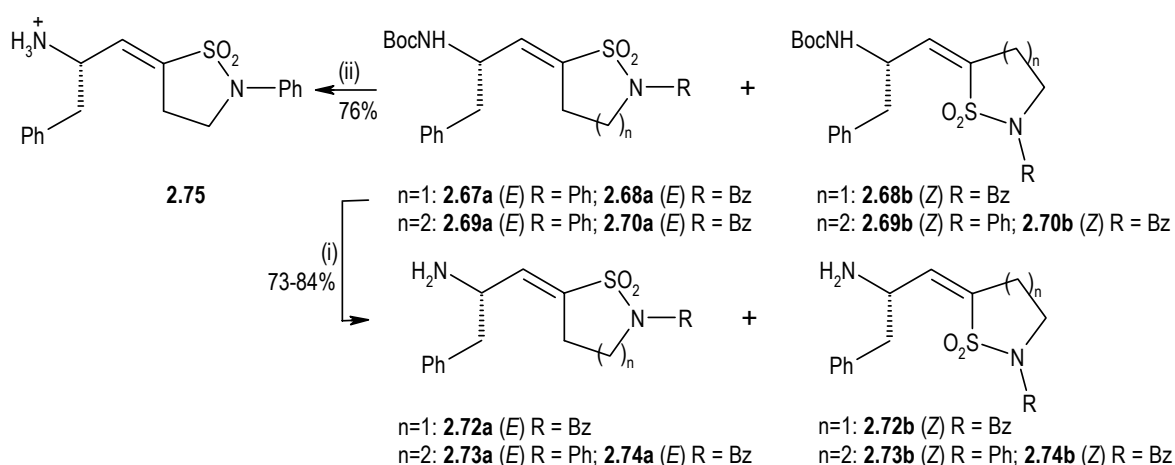


**Figure 2.7** Relevant NOE correlations observed for **2.70b**.

### 2.1.4.5 Dipeptide vinyl sultams

#### Deprotection (removal of Boc protecting group)

The *N*-Boc group of diastereomers **2.67-2.70** was easily cleaved with TFA<sup>100,106</sup> to afford either free amines **2.72-2.74** or hydrochloride **2.75** (Scheme 2.27), which were further processed to provide dipeptide vinyl sultams.

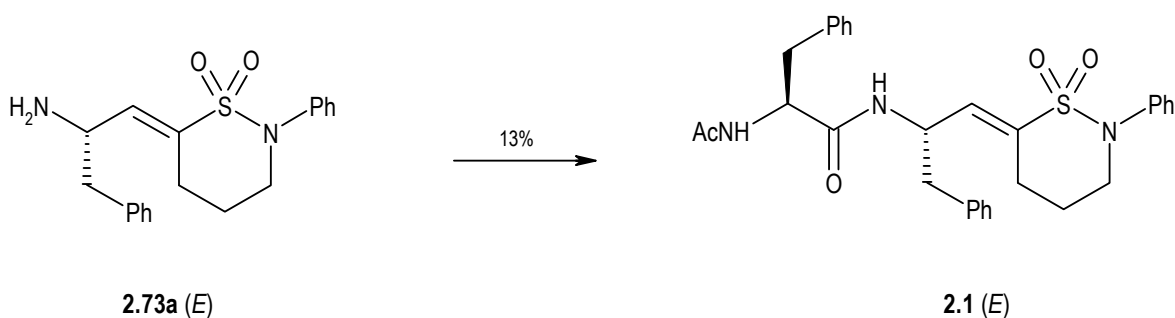


**Scheme 2.27** Removal of the *N*-Boc protecting group of *E*- and *Z*-vinyl sultams. Reagents and conditions: (i) (1) TFA 50% (w/v DCM solution), rt, 20 min, (2) K<sub>2</sub>CO<sub>3</sub> 30% (w/v aqueous solution); (ii) **2.67a**, TFA 50% (w/v DCM solution), rt, 20 min.

### Coupling with aminoacids and endcapping of the dipeptide moiety

The first attempt to the synthesis of dipeptide vinyl sultam **2.1** (Scheme 2.28) used TBTU as coupling reagent (see experimental for **2.54** in Section 5.1.4.5). After the usual work-up and fractionation on preparative TLC plates (DCM/EtOAc 1:1 as eluent), the mass spectrum of the product (30 mg) was consistent with the structure **2.1** [ $m/z$  (rel. int.) 550 ( $MNH_4^+$ ) (72)], but  $^1H$  NMR spectrum (400 MHz,  $CDCl_3$ ) revealed significant impurities.

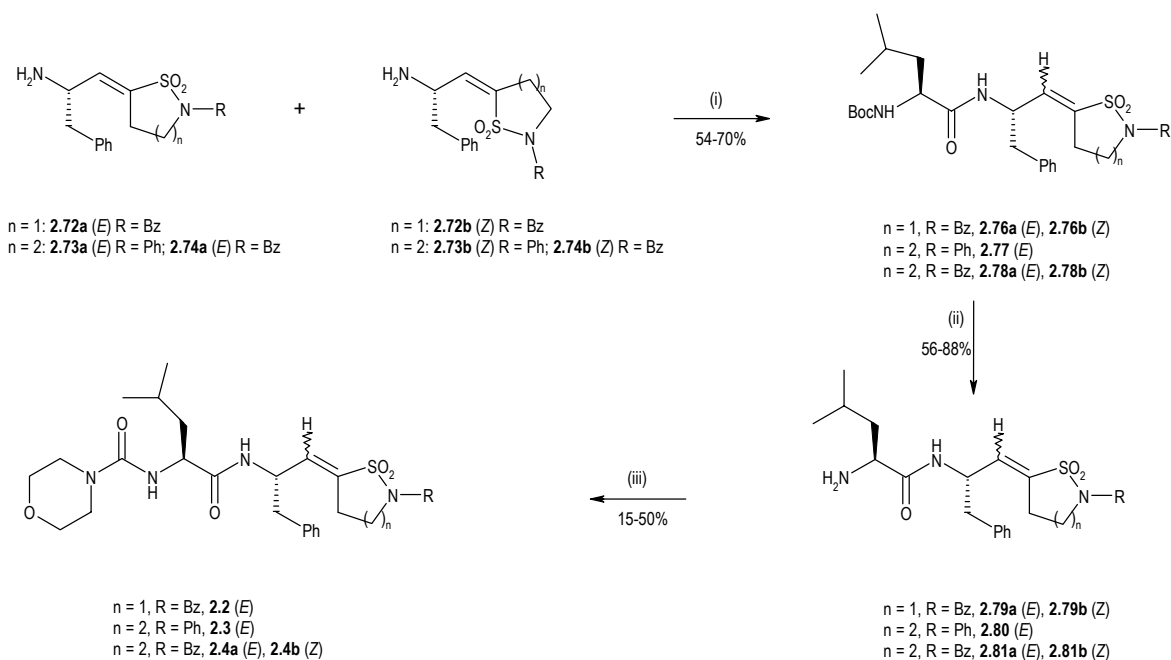
TBTU was used in the preparation of hydroxamates along this investigation. Although successful, products from regular syntheses occasionally presented the impurity pattern mentioned above. For this reason, the synthesis of **2.1** was tried with another coupling reagent, the DCC/HOBt method,<sup>106</sup> which afforded the desired vinyl sultam, although in a poor yield.



**Scheme 2.28** Synthesis of dipeptide vinyl sultam **2.1**. Reagents and conditions: *N*-Ac-*S*-phenylalanine, TEA, HOBt, DCC, DCM, rt, 3 days.

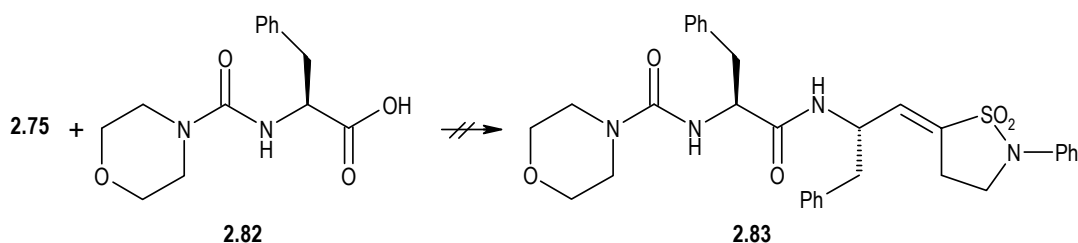
The synthesis of dipeptide vinyl sultams **2.2-2.4** from free amines **2.72-2.74** proceeded according two approaches: (i) step-wise introduction of leucinylyl and morpholinylcarbonyl substituents (Scheme 2.29) and (ii) direct attachment to *N*-Mu-*S*-phenylalanine (Scheme 2.30).

The strategy in Scheme 2.29 began with the condensation of free amines **2.72-2.74** with *N*-Boc-*S*-leucine-*N*-hydroxysuccinimide ester under standard peptide coupling conditions.<sup>101</sup> The resultant dipeptide vinyl sultams **2.76-2.78** were *N*-Boc deprotected and allowed to react with 4-morpholinecarbonyl chloride. Because some intermediates were not achieved in sufficient quantity to follow into the next step, the overall process gave four of the possible eight dipeptide vinyl sultams.



**Scheme 2.29** Synthesis of dipeptide vinyl sultams **2.2-2.4**. Reagents and conditions: (i) *N*-Boc-*S*-leucine-*N*-hydroxysuccinimide ester, TEA, dry THF, rt, 14-48 h, (ii) (1) TFA 50% (w/v DCM solution), rt, 20 min, (2)  $K_2CO_3$  30% (w/v aqueous solution); (iii) 4-morpholinecarbonyl chloride, TEA, dry THF, rt, 14-16 h.

The strategy in Scheme 2.30 required the initial synthesis of *N*-Mu-*S*-phenylalanine **2.82** and its attempted condensation with hydrochloride **2.75**, through BOP-mediated coupling<sup>99</sup> (see experimental for **2.54** in Section 5.1.4.5). The usual work-up and fractionation on preparative TLC plates (EtOAc as eluent) afforded two products, whose  $^1H$  NMR spectra (400 MHz,  $CDCl_3$ ) lacked the signals for **2.83** and could not be assigned to another structure.



**Scheme 2.30** Attempted synthesis of a dipeptide vinyl sultam from *N*-Mu-*S*-phenylalanine. Reagents and conditions: (1) BOP, TEA, DCM, rt, 5 min, (2) *O*, *N*-dimethylhydroxylamine hydrochloride, TEA, rt, 2 h.

## NMR Spectral characterisation

Due to the peptidyl moiety, dipeptide vinyl sultams contain two stereocentres (shown by asterisks in Figure 2.8) and several prochiral carbon atoms. Methylene protons are therefore diastereotopic to one another. Because these geminal protons couple with each other and with the neighbours, inspection of the  $^1\text{H}$  NMR spectra frequently revealed *dd* and *ddd* signals, along with more complex patterns rationalised by diagrams (Figures 2.9 and 2.10 and Tables 2.9-2.13). Very often, the signals lack some of the theoretic lines due to co-incident peaks. In such cases, the remaining parameters were deduced by manual calculation.

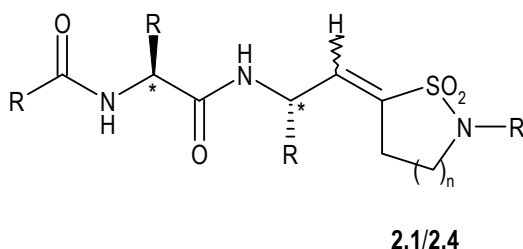
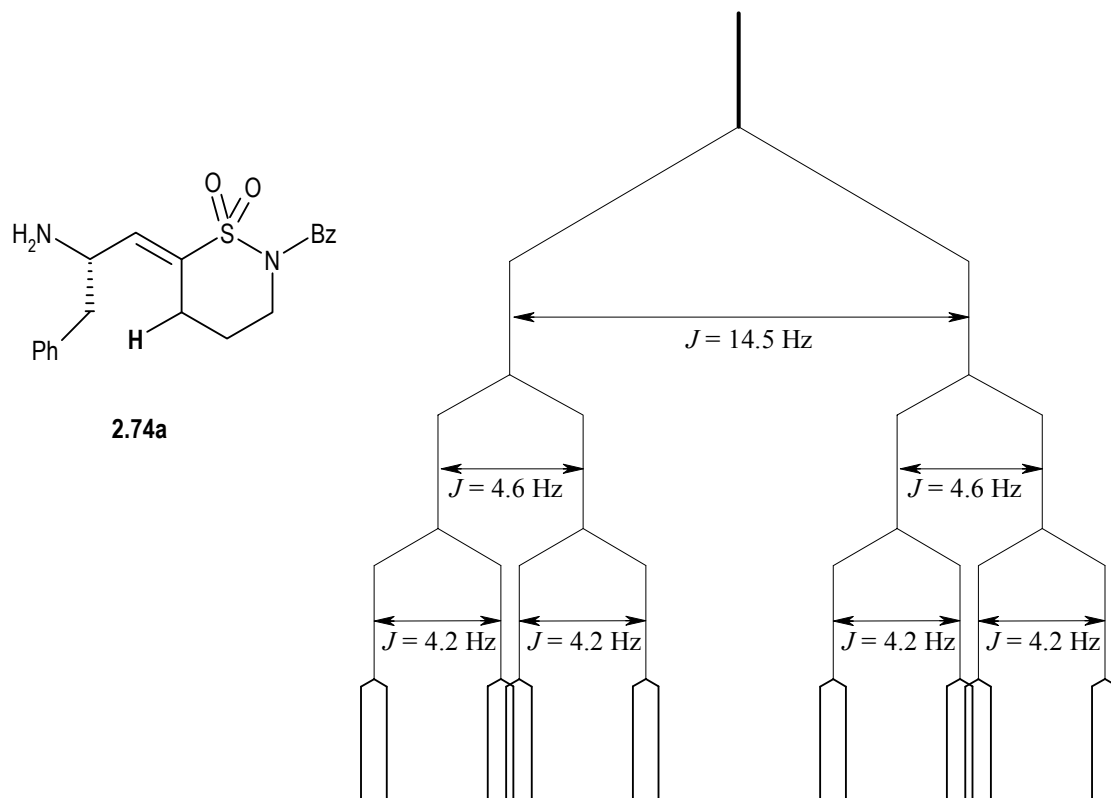


Figure 2.8 Stereocentres in dipeptide sultams.

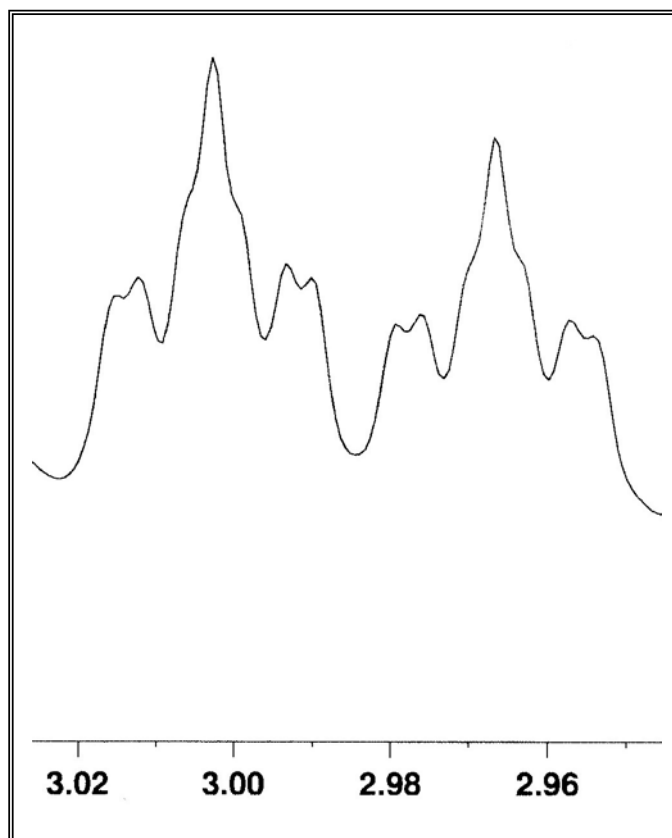
The signal at  $\delta$  2.98 *dddd* for compound **2.74a** (Figure 2.9) was assigned to one of the allylic methylene protons on the basis of the small constant of *ca.* 1 Hz, consistent with an allylic coupling.<sup>107</sup>

For leucine derivatives, the isopropyl methyl groups  $\text{CH}(\text{CH}_3)_2$  exhibited a doublet for each methyl group protons, except when accidental overlap occurred leading to a broad doublet or to a not well resolved multiplet. In the  $^{13}\text{C}$  NMR spectrum, two separate signals were also found for each methyl carbon. These observations are explained by the fact that these two methyl groups are attached to a prochiral carbon atom and are therefore diastereotopic.



**Figure 2.9** Observed <sup>1</sup>H NMR *dddd* signal and splitting pattern diagram for one allylic methylene proton of compound 2.74a.

Constant not shown is 1.2 Hz (allylic coupling).



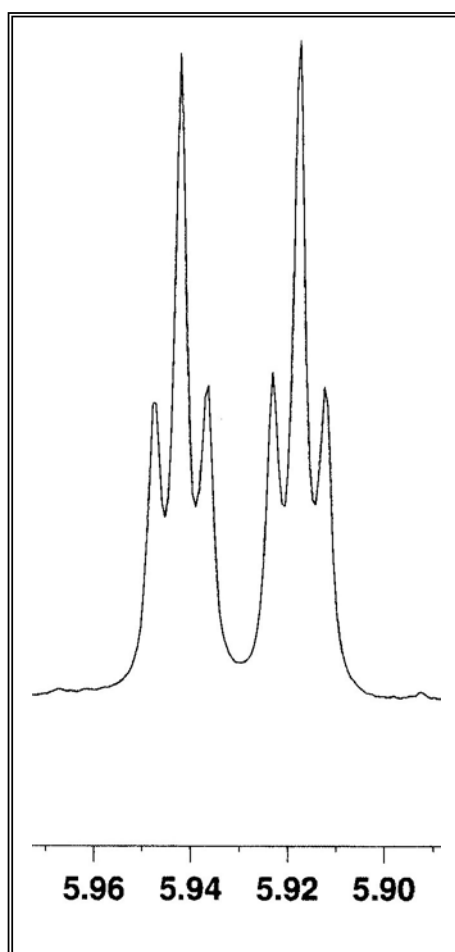
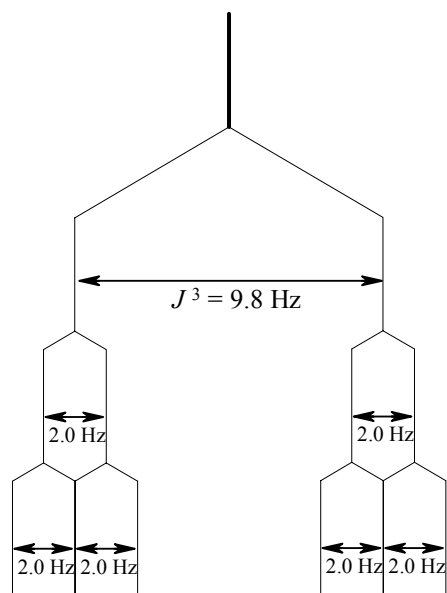
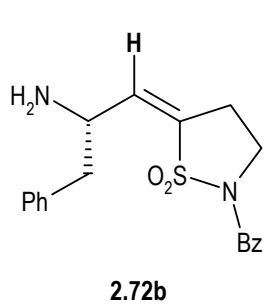


Figure 2.10 Observed  $^1\text{H}$  NMR double triplet signal and splitting pattern diagram for the vinylic proton of compound 2.72b.

The 2.0 Hz constant corresponds to the allylic coupling.

Table 2.9 NMR data of 2.1 [400 MHz ( $^1\text{H}$ ), 100.61 MHz ( $^{13}\text{C}$ ),  $\text{CDCl}_3$ ].

Position	$^1\text{H}$	$^{13}\text{C}$ (HMQC)	DEPT	$^1\text{H}$ - $^1\text{H}$ COSY
<i>N-Ac-Phe</i>				
CHHPh	2.99 brd (6.8)	38.7	CH <sub>2</sub>	CHCH <sub>2</sub> , Ph (7.07-7.32 m)
CHHPh			CH <sub>2</sub>	CHCH <sub>2</sub> , Ph (7.07-7.32 m)
CHCH <sub>2</sub>	4.65-4.70 m	54.3	CH	NH ( <i>N</i> -Ac-Phe), CH <sub>2</sub> Ph
NH	6.25 d (8.0)	—	—	CHCH <sub>2</sub>
CH <sub>3</sub>	1.94 s	23.3	CH <sub>3</sub>	—
CH <sub>3</sub> CO	—	170.0 <sup>c</sup>	C	—
COCH	—	170.2 <sup>c</sup>	C	—
<i>Phe</i>				
CHHPh	2.73-2.82 m <sup>a</sup>	40.6	CH <sub>2</sub>	CHCH <sub>2</sub> , CHHPh
CHHPh	2.53 dd (8.9; 13.4)			CHCH <sub>2</sub> , CHHPh
CHCH <sub>2</sub>	4.82 ddd (5.6; 8.9; 18.0)	48.0	CH	NH (Phe), CH=, CH <sub>2</sub> Ph
CH=	6.17 d (10.0)	130.5	CH	CHCH <sub>2</sub> , =CCH <sub>2</sub>
NH	6.88 brd (8.0) <sup>b</sup>	—	—	CHCH <sub>2</sub>
<i>sultam core</i>				
=C	—	141.0 <sup>d</sup>	C	—
=CCHH	2.73-2.82 m <sup>a</sup>	27.2	CH <sub>2</sub>	CH=, CH <sub>2</sub> CH <sub>2</sub> CH <sub>2</sub>
=CCHH	2.56-2.65 m			CH=, CH <sub>2</sub> CH <sub>2</sub> CH <sub>2</sub>
CH <sub>2</sub> CHHCH <sub>2</sub>	1.81 m	26.2	CH <sub>2</sub>	CH <sub>2</sub> N, =CCH <sub>2</sub> , CH <sub>2</sub> CHHCH <sub>2</sub>
CH <sub>2</sub> CHHCH <sub>2</sub>	1.34 m			CH <sub>2</sub> N, =CCH <sub>2</sub> , CH <sub>2</sub> CHHCH <sub>2</sub>
CH <sub>2</sub> N	3.63-3.78 m	53.3	CH <sub>2</sub>	CH <sub>2</sub> CH <sub>2</sub> CH <sub>2</sub>
<i>aromatic</i>				
	7.07-7.32 m	127.0	CH	CH <sub>2</sub> Ph ( <i>N</i> -Ac-Phe)
		127.0	CH	—
		127.1	CH	—
		127.3	CH	—
		128.6	CH	—
		128.7	CH	—
		129.1	CH	—
		129.4	CH	—
		129.6	CH	—
		136.2 <sup>d</sup>	C	—
		136.4 <sup>d</sup>	C	—
		140.2 <sup>d</sup>	C	—

<sup>a</sup> Overlapped signals; <sup>b</sup> Not well resolved signal; <sup>c</sup>  $\delta$  Values are interchangeable; <sup>d</sup>  $\delta$  Values are interchangeable.

Table 2.10 NMR data of 2.2 [400 MHz ( $^1\text{H}$ ), 100.61 MHz ( $^{13}\text{C}$ ),  $\text{CDCl}_3$ ].

Position	$^1\text{H}$	$^{13}\text{C}$ (HMQC)	DEPT	$^1\text{H}$ - $^1\text{H}$ COSY
<i>Mu</i>				
$\text{CH}_2\text{O}$	3.69 m	66.4	$\text{CH}_2$	$\text{CH}_2\text{N}$
$\text{CH}_2\text{N}$	3.27-3.39 m	44.0	$\text{CH}_2$	$\text{CH}_2\text{O}$
CO	—	157.5	C	—
<i>Leu</i>				
$\text{CH}_3$	0.90-0.93 m <sup>a</sup>	22.1	$\text{CH}_3$	$\text{CH}(\text{CH}_3)_2$
$\text{CH}_3$	0.90-0.93 m <sup>a</sup>	23.0	$\text{CH}_3$	$\text{CH}(\text{CH}_3)_2$
$\text{CH}(\text{CH}_3)_2$	1.61 m <sup>b</sup>	24.8	CH	$\text{CH}(\text{CH}_3)_2$
$\text{CH}_2$	1.54 m <sup>b</sup>	40.8 <sup>e</sup>	$\text{CH}_2$	$\text{CHNH}$
$\text{CHNH}$	4.22–4.29 m	52.7	CH	NH (Leu), $\text{CH}_2$
NH	4.55 m <sup>c</sup>	—	—	$\text{CHNH}$
CO	—	172.7	C	—
<i>Phe</i>				
$\text{CH}_2\text{Ph}$	2.76-3.01 m <sup>d</sup>	40.5 <sup>e</sup>	$\text{CH}_2$	$\text{CHCH}_2$
$\text{CHCH}_2$	4.52 m <sup>c</sup>	49.6	CH	NH (Phe), $\text{CH}=\text{}$ , $\text{CH}_2\text{Ph}$
$\text{CH}=\text{}$	6.28 td (2.6; 9.2)	130.1	CH	$\text{CHCH}_2$ , $=\text{CCH}_2$
NH	6.94 d (8.0)	—	—	$\text{CHCH}_2$
<i>sultam core</i>				
$=\text{C}$	—	138.8 <sup>f</sup>	C	—
$=\text{CCHH}$	2.76-3.01 m <sup>d</sup>	21.8	$\text{CH}_2$	$\text{CH}=\text{}$ , $=\text{CCHH}$
$=\text{CCHH}$	2.11-2.19 m	—	—	$\text{CH}=\text{}$ , $=\text{CCHH}$
$\text{CH}_2\text{N}$	2.76-3.01 m <sup>d</sup>	43.2	$\text{CH}_2$	—
$\text{CHHPH}$	4.09 d (14.0)	47.9	$\text{CH}_2$	<i>Ph</i> (7.17-7.36 m)
$\text{CHHPH}$	4.14 d (14.0)	—	—	<i>Ph</i> (7.17-7.36 m)
<i>aromatic</i>				
	7.17-7.36 m	127.0	CH	$\text{CH}_2\text{Ph}$ (sultam core)
		128.1	CH	—
		128.6	CH	—
		128.7	CH	—
		128.7	CH	—
		129.6	CH	—
		134.9 <sup>g</sup>	C	—
		136.1 <sup>f</sup>	C	—

<sup>a</sup> Overlapped signals; <sup>b</sup> Overlapped signals,  $\delta$  values from HMQC spectrum; <sup>c</sup> Overlapped signals,  $\delta$  values from  $^1\text{H}$ - $^1\text{H}$  COSY spectrum; <sup>d</sup> Overlapped signals; <sup>e</sup>  $\delta$  Values are interchangeable; <sup>f</sup>  $\delta$  Values are interchangeable; <sup>g</sup> This carbon was assigned to the aromatic ring of sultam core, on the basis of observed HMBC  $^2J_{\text{CH}}$  coupling between its resonance and the methylene protons  $\text{NCH}_2\text{Ph}$ .



Table 2.11 NMR data of 2.3 [400 MHz ( $^1\text{H}$ ), 100.61 MHz ( $^{13}\text{C}$ ),  $\text{CDCl}_3$ ].

Position	$^1\text{H}$	$^{13}\text{C}$ (HMQC)	DEPT	$^1\text{H}$ - $^1\text{H}$ COSY
<i>Mu</i>				
$\text{CH}_2\text{O}$	3.68 m	66.4	$\text{CH}_2$	$\text{CH}_2\text{N}$
$\text{CH}_2\text{N}$	3.28-3.41 m	44.0	$\text{CH}_2$	$\text{CH}_2\text{O}$
CO	—	157.4	C	—
<i>Leu</i>				
$\text{CH}_3$	0.90-0.93 m <sup>a</sup>	22.2	$\text{CH}_3$	$\text{CH}(\text{CH}_3)_2$
$\text{CH}_3$	0.90-0.93 m <sup>a</sup>	23.0	$\text{CH}_3$	$\text{CH}(\text{CH}_3)_2$
$\text{CH}(\text{CH}_3)_2$	1.62 m <sup>b</sup>	24.8	CH	$\text{CH}(\text{CH}_3)_2$
$\text{CH}_2$	1.55 m <sup>b</sup>	41.3	$\text{CH}_2$	$\text{CHNH}$
$\text{CHNH}$	4.28-4.34 m	52.9	CH	$\text{NH}$ (Leu), $\text{CH}_2$
NH	4.90 m <sup>c</sup>	—	—	$\text{CHNH}$
CO	—	172.8	C	—
<i>Phe</i>				
$\text{CHHPH}$	3.02 dd (5.8; 13.4)	40.9	$\text{CH}_2$	$\text{CHCH}_2$ , $\text{CHHPH}$
$\text{CHHPH}$	2.75 m <sup>d</sup>	—	—	$\text{CHCH}_2$ , $\text{CHHPH}$
$\text{CHCH}_2$	4.92 m <sup>c</sup>	47.8	CH	$\text{NH}$ (Phe), $\text{CH=}$ , $\text{CH}_2\text{Ph}$
$\text{CH=}$	6.26 d (9.6)	130.6	CH	$\text{CHCH}_2$
NH	7.07 d (8.0)	—	—	$\text{CHCH}_2$
<i>sultam core</i>				
=C	—	136.3 <sup>e</sup>	C	—
=C $\text{CHH}$	2.85 m <sup>d</sup>	27.2	$\text{CH}_2$	$\text{CH}_2\text{CH}_2\text{CH}_2$
=C $\text{CHH}$	2.62 ddd (4.0; 8.0; 14.4)	—	—	$\text{CH}_2\text{CH}_2\text{CH}_2$
$\text{CH}_2\text{CHHCH}_2$	1.79-1.88 m	26.2	$\text{CH}_2$	$\text{CH}_2\text{N}$ , =C $\text{CH}_2$ , $\text{CH}_2\text{CHHCH}_2$
$\text{CH}_2\text{CHHCH}_2$	1.43 m <sup>b</sup>	—	—	$\text{CH}_2\text{N}$ , =C $\text{CH}_2$ , $\text{CH}_2\text{CHHCH}_2$
$\text{CH}_2\text{N}$	3.71-3.75 m	53.4	$\text{CH}_2$	$\text{CH}_2\text{CH}_2\text{CH}_2$
<i>aromatic</i>				
	7.16-7.34 m	126.9	CH	—
		126.9	CH	—
		127.2	CH	—
		128.7	CH	—
		129.1	CH	—
		129.5	CH	—
		140.5 <sup>e</sup>	C	—
		141.1 <sup>f</sup>	C	—

<sup>a</sup> Overlapped signals; <sup>b</sup> Overlapped signals,  $\delta$  values from HMQC spectrum; <sup>c</sup> Overlapped signals,  $\delta$  values from  $^1\text{H}$ - $^1\text{H}$  COSY spectrum; <sup>d</sup> Overlapped signals,  $\delta$  values from  $^1\text{H}$ - $^1\text{H}$  COSY spectrum; <sup>e</sup>  $\delta$  Values are interchangeable; <sup>f</sup> This carbon was assigned to an aromatic ring on the basis of observed HMBC  $^2J_{\text{CH}}$  coupling with aromatic protons.

Table 2.12 NMR data of 2.4a [400 MHz ( $^1\text{H}$ ), 100.61 MHz ( $^{13}\text{C}$ ),  $\text{CDCl}_3$ ].

Position	$^1\text{H}$	$^{13}\text{C}$ (HMQC)	DEPT	$^1\text{H}$ - $^1\text{H}$ COSY
<i>Mu</i>				
$\text{CH}_2\text{O}$	3.67-3.71 m <sup>a</sup>	66.4	$\text{CH}_2$	$\text{CH}_2\text{N}$
$\text{CH}_2\text{N}$	3.37 m <sup>b</sup>	44.0	$\text{CH}_2$	$\text{CH}_2\text{O}$
$\text{CO}$	—	157.5	$\text{C}$	—
<i>Leu</i>				
$\text{CH}_3$	0.92-0.94 m <sup>c</sup>	22.2	$\text{CH}_3$	$\text{CH}(\text{CH}_3)_2$
$\text{CH}_3$	0.92-0.94 m <sup>c</sup>	23.0	$\text{CH}_3$	$\text{CH}(\text{CH}_3)_2$
$\text{CH}(\text{CH}_3)_2$	1.60 m <sup>d</sup>	24.9	$\text{CH}$	$\text{CH}_2$ , $\text{CH}(\text{CH}_3)_2$
$\text{CH}_2$	1.56 m <sup>d</sup>	41.4	$\text{CH}_2$	$\text{CH}(\text{CH}_3)_2$
$\text{CHNH}$	4.31-4.36 m	53.0	$\text{CH}$	$\text{NH}$ (Leu)
$\text{NH}$	4.90-4.98 m <sup>e</sup>	—	—	$\text{CHNH}$
$\text{CO}$	—	172.8	$\text{C}$	—
<i>Phe</i>				
$\text{CHHPH}$	3.12 m <sup>f</sup>	41.0	$\text{CH}_2$	$\text{CHCH}_2$ , $\text{CHHPH}$ , $\text{Ph}$ (7.21-7.36 m)
$\text{CHHPH}$	2.75 dd (10.0; 13.2)	—	—	$\text{CHCH}_2$ , $\text{CHHPH}$
$\text{CHCH}_2$	4.90-4.98 m <sup>e</sup>	47.9	$\text{CH}$	$\text{NH}$ (Phe), $\text{CH=}$ , $\text{CH}_2\text{Ph}$
$\text{CH=}$	6.24 d (10.0)	131.7	$\text{CH}$	$\text{CHCH}_2$ , $=\text{CCH}_2$
$\text{NH}$	7.16 d (7.6)	—	—	$\text{CHCH}_2$
<i>sultam core</i>				
$=\text{C}$	—	138.9 <sup>g</sup>	$\text{C}$	—
$=\text{CCH}_2$	2.60 m	27.0	$\text{CH}_2$	$\text{CH=}$ , $\text{CH}_2\text{CH}_2\text{CH}_2$
$\text{CH}_2\text{CHHCH}_2$	1.10 m	23.0	$\text{CH}_2$	$\text{CH}_2\text{CHHCH}_2$ , $=\text{CCH}_2$ , $\text{CH}_2\text{N}$
$\text{CH}_2\text{CHHCH}_2$	1.56 m <sup>d</sup>	—	—	$\text{CH}_2\text{CHHCH}_2$ , $=\text{CCH}_2$ , $\text{CH}_2\text{N}$
$\text{CHHN}$	3.30 m <sup>b</sup>	47.4	$\text{CH}_2$	$\text{CHHN}$ , $\text{CH}_2\text{CH}_2\text{CH}_2$
$\text{CHHN}$	3.07 m <sup>f</sup>	—	—	$\text{CHHN}$ , $\text{CH}_2\text{CH}_2\text{CH}_2$
$\text{CHHPH}$	4.03 d (14.0)	50.2	$\text{CH}_2$	$\text{CHHPH}$
$\text{CHHPH}$	3.67-3.71 m <sup>a</sup>	—	—	$\text{CHHPH}$
<i>aromatic</i>				
	7.21-7.36 m	127.0	$\text{CH}$	$\text{CHHPH}$
		127.8	$\text{CH}$	—
		128.4	$\text{CH}$	—
		128.6	$\text{CH}$	—
		128.8	$\text{CH}$	—
		129.5	$\text{CH}$	—
		136.0 <sup>h</sup>	$\text{C}$	—
		136.6 <sup>g</sup>	$\text{C}$	—

<sup>a</sup> Overlapped signals; <sup>b</sup> Overlapped signals,  $\delta$  values from HMQC and  $^1\text{H}$ - $^1\text{H}$  COSY spectra; <sup>c</sup> Overlapped signals; <sup>d</sup> Overlapped signals,  $\delta$  values from HMQC and  $^1\text{H}$ - $^1\text{H}$  COSY spectra; <sup>e</sup> Overlapped signals; <sup>f</sup> Overlapped signals,  $\delta$  values from HMQC and  $^1\text{H}$ - $^1\text{H}$  COSY spectra; <sup>g</sup>  $\delta$  Values are interchangeable; <sup>h</sup> This carbon was assigned to the aromatic ring of sultam core, on the basis of observed HMBC  $^2J_{\text{CH}}$  coupling between its resonance and the methylene protons  $\text{NCH}_2\text{Ph}$ .

Table 2.13 NMR data of 2.4b [400 MHz ( $^1\text{H}$ ), 100.61 MHz ( $^{13}\text{C}$ ),  $\text{CDCl}_3$ ].

Position	$^1\text{H}$	$^{13}\text{C}$ (HMQC)	DEPT	$^1\text{H}$ - $^1\text{H}$ COSY
<i>Mu</i>				
$\text{CH}_2\text{O}$	3.66 m	66.4	$\text{CH}_2$	$\text{CH}_2\text{N}$
$\text{CH}_2\text{N}$	3.30 m <sup>a</sup>	43.9	$\text{CH}_2$	$\text{CH}_2\text{O}$
CO	—	157.4	C	—
<i>Leu</i>				
$\text{CH}_3$	0.87-0.90 m <sup>b</sup>	22.1	$\text{CH}_3$	$\text{CH}(\text{CH}_3)_2$
$\text{CH}_3$	0.87-0.90 m <sup>b</sup>	23.0	$\text{CH}_3$	$\text{CH}(\text{CH}_3)_2$
$\text{CH}(\text{CH}_3)_2$	1.55 m <sup>c</sup>	24.8	CH	$\text{CH}(\text{CH}_3)_2$ , $\text{CH}_2$
$\text{CH}_2$	1.43 m <sup>c</sup>	40.9 <sup>d</sup>	$\text{CH}_2$	$\text{CHNH}$ , $\text{CH}(\text{CH}_3)_2$
$\text{CHNH}$	4.24-4.29 m	52.6	CH	$\text{NH}$ (Leu), $\text{CH}_2$
NH	4.87 d (8.0)	—	—	$\text{CHNH}$
CO	—	172.8	C	—
<i>Phe</i>				
$\text{CHHPH}$	3.00 brd (13.4)	41.0 <sup>d</sup>	$\text{CH}_2$	$\text{CHCH}_2$ , $\text{Ph}$ (7.22-7.43 m)
$\text{CHHPH}$	3.06 brd (13.4)	—	—	$\text{CHCH}_2$ , $\text{Ph}$ (7.22-7.43 m)
$\text{CHCH}_2$	5.46-5.54 m	49.0	CH	$\text{CH=}$ , $\text{CH}_2\text{Ph}$ , $\text{NH}$ (Phe)
$\text{CH=}$	5.96 d (8.8)	136.1	CH	$\text{CHCH}_2$ , $=\text{CCH}_2$
NH	6.74 d (6.8)	—	—	$\text{CHCH}_2$
<i>sultam core</i>				
$=\text{C}$	—	135.9 <sup>e</sup>	C	—
$=\text{CCH}_2$	2.65-2.79 m	34.8	$\text{CH}_2$	$\text{CH=}$ , $\text{CH}_2\text{CH}_2\text{CH}_2$
$\text{CH}_2\text{CH}_2\text{CH}_2$	1.75 m <sup>c</sup>	23.4	$\text{CH}_2$	$=\text{CCH}_2$ , $\text{CH}_2\text{N}$
$\text{CH}_2\text{N}$	3.45 m <sup>a</sup>	47.5	$\text{CH}_2$	$\text{CH}_2\text{CH}_2\text{CH}_2$
$\text{CHHPH}$	4.11 d (14.6)	50.4	$\text{CH}_2$	—
$\text{CHHPH}$	4.18 d (14.6)	—	—	—
<i>aromatic</i>				
	7.22-7.34 m	126.8	CH	$\text{CH}_2\text{Ph}$ (Phe)
		127.8	CH	—
		128.5	CH	—
		128.5	CH	—
		128.6	CH	—
		129.6	CH	—
		136.1 <sup>e</sup>	C	—
		137.1 <sup>f</sup>	C	—

<sup>a</sup> Overlapped signals,  $\delta$  values from  $^1\text{H}$ - $^1\text{H}$  COSY spectrum; <sup>b</sup> Overlapped signals, <sup>c</sup> Overlapped signals,  $\delta$  values from  $^1\text{H}$ - $^1\text{H}$  COSY spectrum; <sup>d</sup>  $\delta$  Values are interchangeable; <sup>e</sup>  $\delta$  Values are interchangeable; <sup>f</sup> This carbon was assigned to the aromatic ring of phenylalanine, on the basis of observed HMBC  $^2J_{\text{CH}}$  coupling between its resonance and the methylene protons  $\text{CH}_2\text{Ph}$  (Phe).

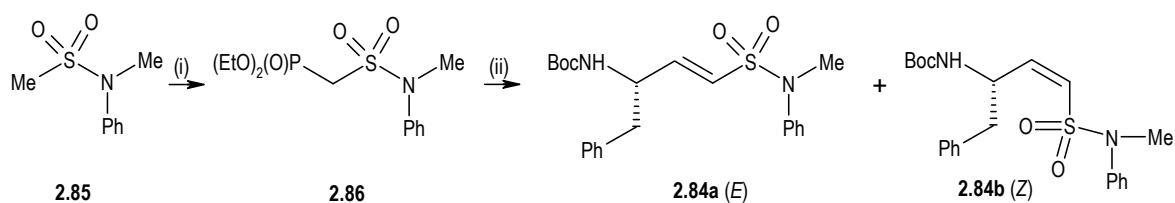
### 2.1.5 Synthesis of vinyl sulfonamides

Vinyl sulfonamides **2.84** (Scheme 2.31) were synthesised for comparison studies on chemical reactivity. Beyond the *N*-Ph substituent, the nitrogen atom was attached to a methyl group to better mimic the substitution pattern of the sulfonamide function in sultams.

The process required the initial preparation of sulfonamide **2.85** by a commonly procedure involving mesyl chloride and *N*-methylaniline. Alternatively, the compound was obtained through the recycling of *N*-phenylmethanesulfonamide **2.50** (Scheme 2.15, Section 2.1.3.1), using a Williamson ether synthesis adapted procedure.<sup>108</sup>

The following step involved the conversion of sulfonamide **2.85** to phosphonate **2.86**. The main variation in this synthesis comparatively to the one of sultam phosphonates is the employment of TMEDA. This agent was used in reactions involving methanesulfonamides and *n*-BuLi with the purpose of increase reactivity and solubility of the sulfonamide anion.<sup>58,67</sup> Phosphonate **2.86** was only partially purified by column chromatography. However, it can be concluded that the yield was poor (about 11%). This result may be due to the rt conditions, but the process was not optimized.

Horner-Wadsworth-Emmons afforded the expected *E*-vinyl derivative along with small amounts of the *Z*-isomer.<sup>29,33,38,39</sup> The latter compound was impure and in insufficient quantity for further purification (14 mg).



**Scheme 2.31 Synthesis of vinyl sulfonamides.** Reagents and conditions: (i) (1) *n*-BuLi, TMEDA, dry THF, rt,  $\text{N}_2$ , 10 min, (2)  $(\text{EtO})_2\text{POCl}$ , rt,  $\text{N}_2$ , 1 h; (ii) *n*-BuLi, dry THF, *N*-Boc-S-phenylalaninal **2.53**,  $-78^\circ\text{C}$  to rt,  $\text{N}_2$ , 20 min.

**NMR spectral characterisation of the sulfonamide phosphonate.** Similarly to sultam phosphonates, the NMR spectra of sulfonamide phosphonate **2.86** reflected the coupling of the  $^{31}\text{P}$  with  $^1\text{H}$  and  $^{13}\text{C}$  nuclei (Table 2.14). However, because **2.86** lack a stereocentre, it showed a much simpler  $^1\text{H}$  NMR spectrum. Thus, the methylene group  $\text{CH}_2\text{SO}_2$  showed a doublet splitting pattern with the one-bond coupling constant  $^{31}\text{P}$ - $^1\text{H}$  of 16.8 Hz and the methylene groups of the ethyl substituents exhibited a double quartet (Figure 2.11).<sup>38,107</sup> For the methyl groups  $\text{CH}_3\text{CH}_2\text{O}$ -, the  $^{31}\text{P}$ - $^1\text{H}$  coupling is not resolved but it is revealed by the broadening of the characteristic triplet.

**Table 2.14** NMR data of **2.86** [400 MHz ( $^1\text{H}$ ), 100.61 MHz ( $^{13}\text{C}$ ),  $\text{CDCl}_3$ ].

Position	$^1\text{H}$	$^{13}\text{C}$ (HMQC)
$\text{OCH}_2\text{CH}_3$	1.37 brt (7.1)	16.3 d (6.0)
$\text{OCH}_2\text{CH}_3$	4.24 qd (7.1; 8.0)	63.5 d (7.0)
$\text{CH}_3$	3.44 s	39.2
$\text{CH}_2\text{SO}_2$	3.56 d (16.8)	46.1 d (139.9)
Ph	7.31-7.35 m (1H)	127.8
	7.42 t (8.0) (2H)	129.5
	7.49 d (8.0) (2H)	126.9
		140.8

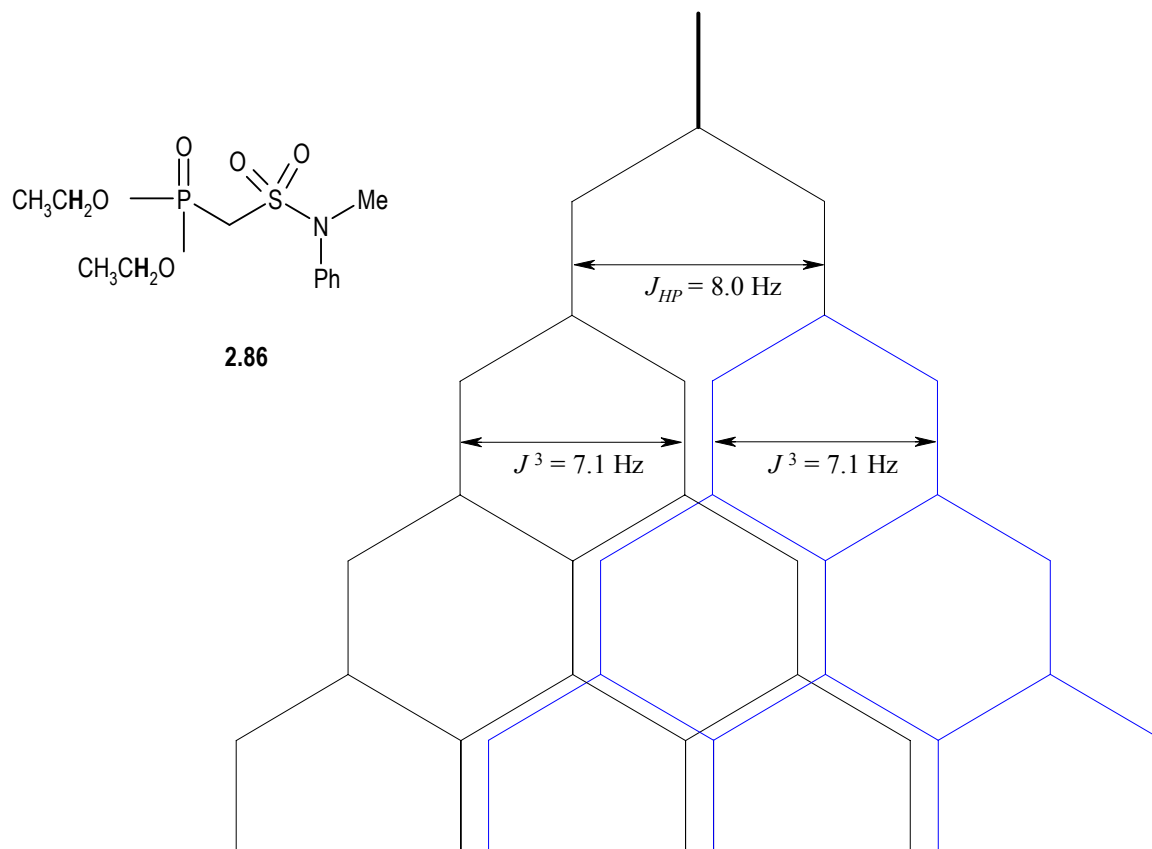
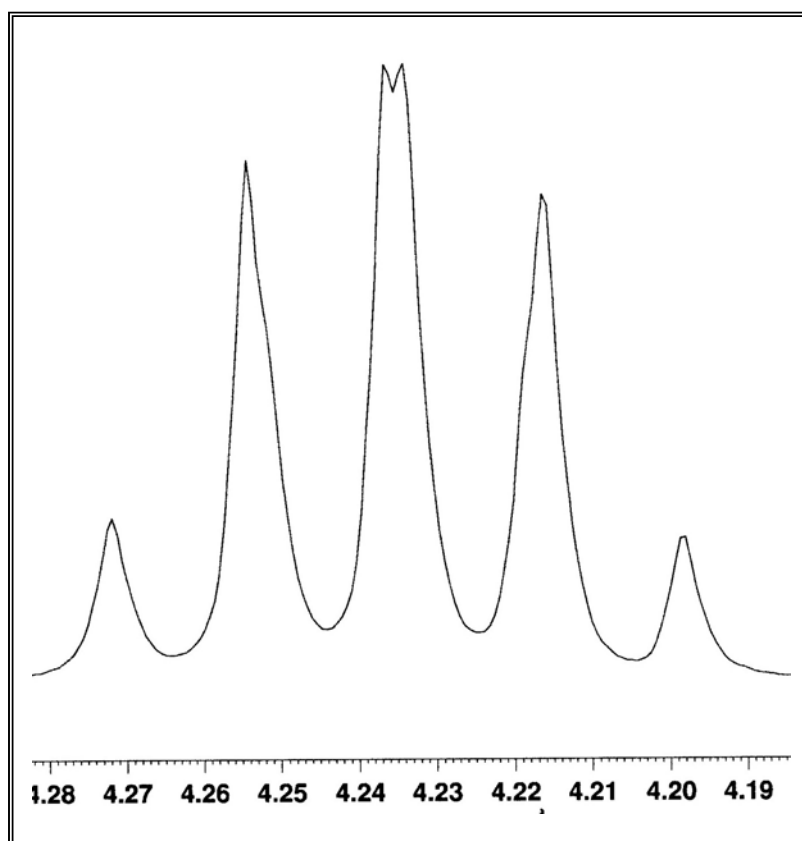


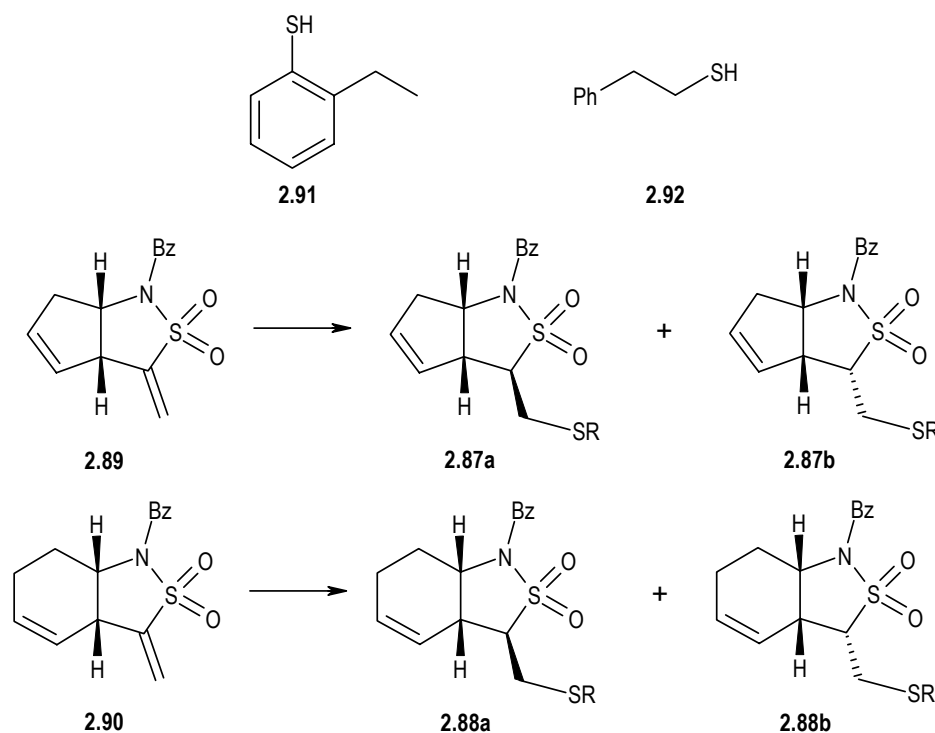
**Figure 2.11** Observed  $^1\text{H}$  NMR double quartet signal and splitting pattern diagram for the methylene protons  $\text{OCH}_2\text{CH}_3$  of compound 2.86.



## 2.2 Kinetic study of the reaction with cysteine

### 2.2.1 Introductory remarks

As stated earlier (Section 1.4), the development of vinyl sultams as inhibitors of cysteine proteases was based on the hypothesis that this scaffold would be a Michael acceptor for thiols. This situation was confirmed during the time course of the present investigation, by Merten *et al.*,<sup>61</sup> who afforded the adducts **2.87-2.88** of the reaction between bicyclic  $\alpha$ -methylene- $\gamma$ -sultams **2.89-2.90** and thiols **2.91** and **2.92** (Scheme 2.32). Nevertheless, a search of the literature indicated that no kinetic evaluation existed for such reactions.



Scheme 2.32 Adducts from the reaction of  $\alpha$ -methylene- $\gamma$ -sultams with thiols.<sup>61</sup>

The present work assessed the reactivity of vinyl sultams and compared it with the one of an analogous vinyl sulfonamide. The analysis was carried out by UV spectrophotometry at pH 6.9, at 25 °C, using cysteine as a model thiol. Cysteine was employed in large excess to ensure pseudo-first-order kinetics.

### 2.2.2 Results and Discussion

The reactivity studies began with the selection of the wavelength to be used in the kinetic measurements. With this goal, the reaction of cysteine with each of the vinyl sultams/vinyl sulfonamide was followed by repeated spectral scanning over the wavelength range of 350 to 200 nm. The first recorded spectrum showed to be similar to the one of the compound in buffer lacking cysteine. This situation is indicative that no reaction had occurred during the initial period of mixing of the reactants.

The kinetic measurements were performed at the wavelength which showed a maximum absorbance variation during the reaction progression.

Then, the pseudo first-order rate constants,  $k_{\text{obs}}$ , were determined by following the variation of absorbance until a plateau region had been reached. Plotting  $k_{\text{obs}}$  values (Appendix II) *versus* the total cysteine concentration,  $[\text{cys}]_t$ , resulted in a linear correlation (Figure 2.12) with an intercept at  $[\text{cys}]_t = 0$  indistinguishable from zero (Equation 2.1). This is consistent with the absence of spontaneous reaction by solvent or catalysis by  $\text{HO}^-$  or  $\text{H}^+$ .

In addition, the second-order rate constants,  $k_{\text{cat}}$ , were estimated from the slope of the least-squares regression lines.

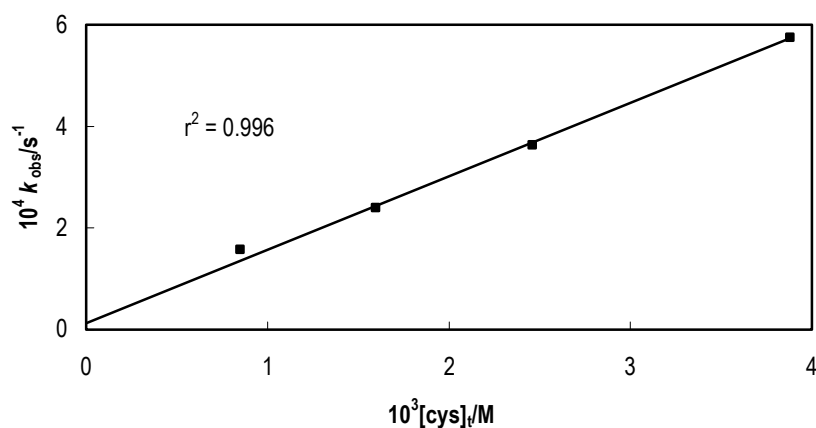


**Figure 2.12** Plot of the pseudo first-order rate constants,  $k_{\text{obs}}$ , for the reaction of vinyl sultam 2.69b with cysteine, against the total cysteine concentration at pH 6.93 ( $\alpha = 5.8 \times 10^{-2}$ ) at 25 °C and ionic strength 0.5 M. Points are experimental and line is theoretical for  $k_{\text{cat}} 0.14 \text{ M}^{-1} \text{ s}^{-1}$ .

$$k_{\text{obs}} = k_{\text{cat}}[\text{cys}]_t \quad (2.1)$$



The second-order rate constant,  $k_{\text{cat}}$ , is given by Equation 2.2, where  $k_{\text{cys}}(1 - \alpha)$  and  $k_{\text{cys}^-}\alpha$  are respectively the contribution of undissociated cysteine and of its thiolate to the overall reaction. The parameter  $\alpha$  is the fraction of cysteine present as conjugate base,  $\alpha = [\text{cys}^-]/[\text{cys}]_{\text{t}}$ , which is dependent on the reaction pH value.

$$k_{\text{cat}} = k_{\text{cys}}(1 - \alpha) + k_{\text{cys}^-}\alpha \quad (2.2)$$

A plot of the pseudo first-order rate constants,  $k_{\text{obs}}$ , against the concentration of the thiolate anion of cysteine,  $[\text{cys}^-]$ , (Figure 2.13) gave, according to Equation 2.3, a slope corresponding to the second-order rate constant for the reaction with the thiolate anion,  $k_{\text{cys}^-}$ .

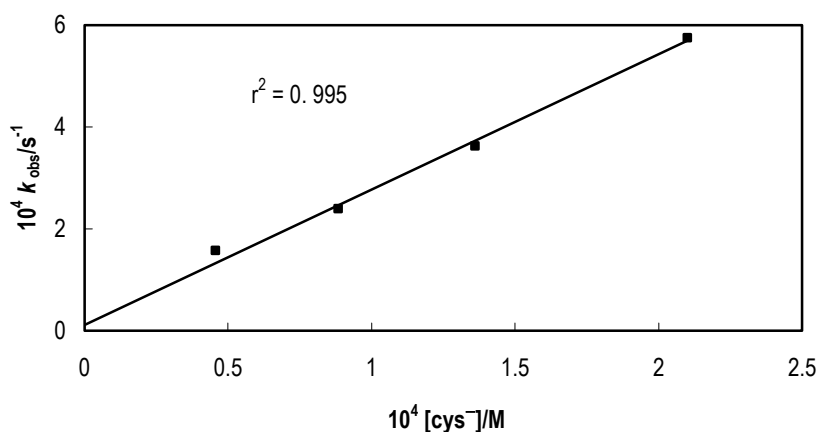


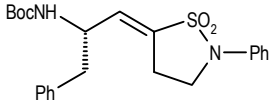
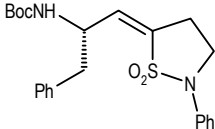
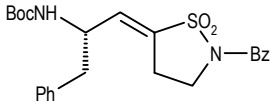
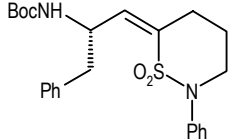
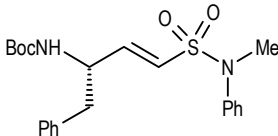
**Figure 2.13** Plot of the pseudo first-order rate constants,  $k_{\text{obs}}$ , for the reaction of vinyl sultam 2.69b with cysteine, against the cysteine thiolate concentration at pH 6.93, at 25 °C and ionic strength 0.5 M. Points are experimental and line is theoretical for  $k_{\text{cys}^-} 2.66 \text{ M}^{-1} \text{ s}^{-1}$ .

$$k_{\text{obs}} = k_{\text{cys}^-}[\text{cys}^-] \quad (2.3)$$

In addition, the intercept at  $[\text{cys}^-] = 0$  is indistinguishable from zero, indicating that there is no detectable reaction for the undissociated thiol. Thus, Equation 2.2 is simplified to Equation 2.4, and  $k_{\text{cys}^-}$  values could be alternatively determined by  $k_{\text{cys}^-} = k_{\text{cat}}/\alpha$ . The values obtained by both methods are in good agreement and are listed in Table 2.15.

$$k_{\text{cat}} = k_{\text{cys}^-}\alpha \quad (2.4)$$

**Table 2.15** Cysteine-catalysed second-order rate constants,  $k_{\text{cys}^-}$ , for vinyl sultams and for an analogous vinyl sulfonamide.

Compound	$k_{\text{cys}^-}$ ( $\text{M}^{-1} \text{s}^{-1}$ )		
	Method A <sup>a</sup>	Method B <sup>b</sup>	
	2.67a	1.93	1.94
	2.67b	2.11	2.15
	2.68a	2.42	2.41
	2.69b	2.66	2.65
	2.84a	2.49	2.44

<sup>a</sup> From the slope of  $k_{\text{obs}}$  versus  $[\text{cys}^-]$ . <sup>b</sup> From  $k_{\text{cys}^-} = k_{\text{cat}}/\alpha$ .

Overall, it is immediately clear that the studied vinyl sultams are similarly reactive toward cysteine, independently of the ring size (**2.67b** versus **2.69b**), geometry of the double bond (**2.67a** versus **2.67b**) or nitrogen substituent (**2.67a** versus **2.68a**).

These compounds also showed to be as reactive as the analogous vinyl sulfonamide **2.84a**. This result suggested a similarity in the inhibitory action on cysteine proteases. Bearing in mind that vinyl sulfonamides are established inhibitors of cruzain, this result corroborated the initial hypothesis (Section 1.4) that vinyl sultams scaffold would be a potential structure for the design of inhibitors against cruzain-related cysteine proteases, such as falcipain.

### 2.3 Inhibitory activity against papain, falcipain-2 and *Plasmodium falciparum*

This work afforded five dipeptide vinyl sultams **2.1-2.4**, along with eight mono-substituted precursors **2.67-2.70**, whose structures are conveniently repeated in this section (Figure 2.14).

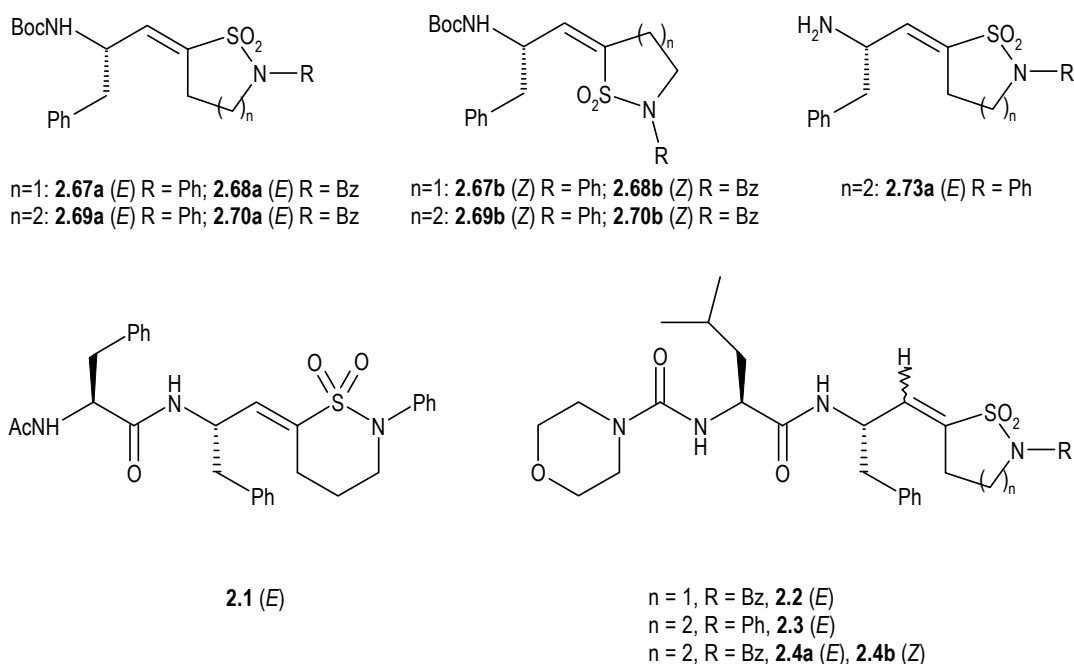


**Figure 2.14** Compounds assayed for inhibitory activity against cysteine proteases.

These compounds were screened for effectiveness against papain, using the procedure described in Appendix I. Their solubility in the assay buffer limited testing at 50  $\mu\text{M}$ , what could not be overcome by adding an extra volume of DMSO (in the enzyme-inhibitor incubation medium, the concentration of this solvent is usually 5%; in this case it was employed up to 10%). No inhibition could be detected after 30 min of incubation. In addition, the free amine **2.73a**, which did not reveal solubility problems, failed the inhibition up to 500  $\mu\text{M}$ .

The lack of papain-inhibitory activity of compounds bearing a Phe residue directly attached to the “warhead” was already reported, in a study involving vinylogous amino acid esters. The situation was ascribed to a binding mode where the Michael acceptor is far from

the reach of the sulphur of Cys25 due to the interaction between Phe and the S2 hydrophobic subsite of papain.<sup>28</sup>

Only dipeptide derivatives **2.1-2.4** were evaluated against falcipain-2 (the main target of this project) and *Plasmodium falciparum* W2. These studies were carried out by Dr. Philip J. Rosenthal's group (University of California), following a reported protocol.<sup>16</sup>

The compounds showed some activity against falcipain-2, albeit modest (Table 2.16).

**Table 2.16** IC<sub>50</sub> values of vinyl sultams for falcipain-2 and *Plasmodium falciparum* W2.

Inhibitor	IC <sub>50</sub> (μM)	
	rec-FP-2 <sup>a</sup>	<i>Plasmodium falciparum</i> W2
<b>2.1</b>	26.5	>10
<b>2.2</b>	48.4	>10
<b>2.3</b>	31.4	>10
<b>2.4a</b>	13.7	7.8
<b>2.4b</b>	23.6	>10
<b>1.2e<sup>b</sup></b>	0.0035	0.022

<sup>a</sup> Recombinant falcipain-2. <sup>b</sup> Mu-Leu-Hph-VS-Ph (from Table 1.4a in Section 1.2.3.1).

The derivative **2.4a** exhibited the best IC<sub>50</sub> value (13.7 μM), which was consistently accompanied by the most favourable activity against *Plasmodium falciparum* W2. Though the range of compounds is limited, the data presented suggested that the ring size (**2.2 versus 2.4a**), the geometry of the double bond (**2.4a versus 2.4b**) and the nitrogen substituent (**2.3 versus 2.4a**) may have some impact on activity. As shown by the data for compounds **2.1** and **2.3**, substitution of the Ac-Phe by the Mu-Leu moiety has little effect on activity.

Overall, what is immediately clear from these results is that dipeptide vinyl sultams are significantly less active ( $\approx 10^{-4}$ -fold) than their acyclic analogues, vinyl sulfones (see data for **1.2e**).

Developing conformationally restricted analogues, *i.e.* incorporation of ring moieties, is a commonly used approach to probe the binding site of receptors and to further improve activity.<sup>109</sup> It may, however, result in the opposite effect, by interfering with target binding, leading to a substantial reduction in the activity when compared to their acyclic counterparts. A situation like this was found in the development of cyclic peptide aldehydes as cysteine protease inhibitors.<sup>110</sup> The hypothesis that a similar explanation could be applied to vinyl sultams **2.1-2.4** was investigated by performing molecular modelling studies with the more

potent inhibitors **2.4a,b**. At that time, the crystal structure of falcipain-2 had not been released, but the similarity between this enzyme and cruzain was already recognised on the basis of 40% homology in the mature domain and about 90% for the binding site residues.<sup>111,112</sup>

Molecular modelling was therefore carried out on the 1F2A crystal structure,<sup>20,24</sup> a complex between cruzain and the vinyl sulfone Cbz-Phe-Hph-VS-Bz (**1.2d** in Section 1.2.3.1). The calculations were performed by Dr. Rita C. Guedes (from the Faculty of Pharmacy, University of Lisbon).

The top 10 solutions (*i.e.* those with the highest fitness score) were visually analysed for: (i) the hydrophobic and hydrophilic interactions between the ligand and enzyme surfaces and (ii) the distance between the  $\beta$ -carbon atom of the Michael acceptor system and the catalytic cysteine residue.

As mentioned earlier (Section 1.2.3.1), **1.2d** is a fairly good inhibitor for cruzain. When the compound was docked into the active site of cruzain (Figure 2.15a), it bound as reported,<sup>24</sup> *i.e.*, seven conformations presented hydrogen bonding interactions between the sulfonyl oxygen atoms and the imidazole NH of His159, indole NH of Trp177 and one of the NH of Gln19, while all 10 inspected conformations present the Phe side chain sitting in the S2 pocket of the enzyme, which is lined with hydrophobic residues Leu67, Ala133 and Leu157. Additional hydrogen bonding to the carbonyl oxygen atom of Gly66 enables further stabilization of the non-covalent complex. This conformation presents the  $\beta$ -carbon atom of the vinyl sulfone system in proximity (3.6-3.8 Å) to the sulphur atom of Cys25, as would be expected for Michael addition chemistry.

Interestingly, modelling the interaction of *E*-isomer **2.4a** with cruzain revealed that the top ranking conformation sits in the active site with an inverted orientation when compared to **1.2d**, the *N*-benzyl- $\delta$ -sultam moiety being accommodated in the S2 subsite through stabilizing van der Waals interactions with Leu67, Ala133 and Leu157 (Figure 2.15b). The most striking observation was that the sulphur atom of Cys25 is in the vicinity (3.4 Å) of the  $\beta$ -carbon and positioned 20° out of the plane defined by the carbon-carbon double bond, thereby disfavoured Michael addition of cysteine to the  $\beta$ -carbon atom of the vinyl sultam system. This type of reaction requires the sulphur nucleophile to approach the carbon atom almost perpendicularly to the double bond plane in order to achieve optimal orbital overlap.

In contrast, the preferred conformation of the *Z*-isomer **2.4b** is positioned in the active site of cruzain similarly to **1.2d**, that is, with the Leu side chain occupying the S2 pocket (Figure

2.15c). However, the Cys25(S)-C $\beta$  distance is probably too long (*ca.* 4.0 Å) for nucleophilic attack of cysteine to take place.

Taken together, these docking results suggest that the  $\delta$ -sultam ring increases the degrees of freedom of ligand binding to cruzain when compared with the acyclic vinyl sulfone analogue, leading to enzyme-inhibitor complexes that do not favour Michael addition chemistry.

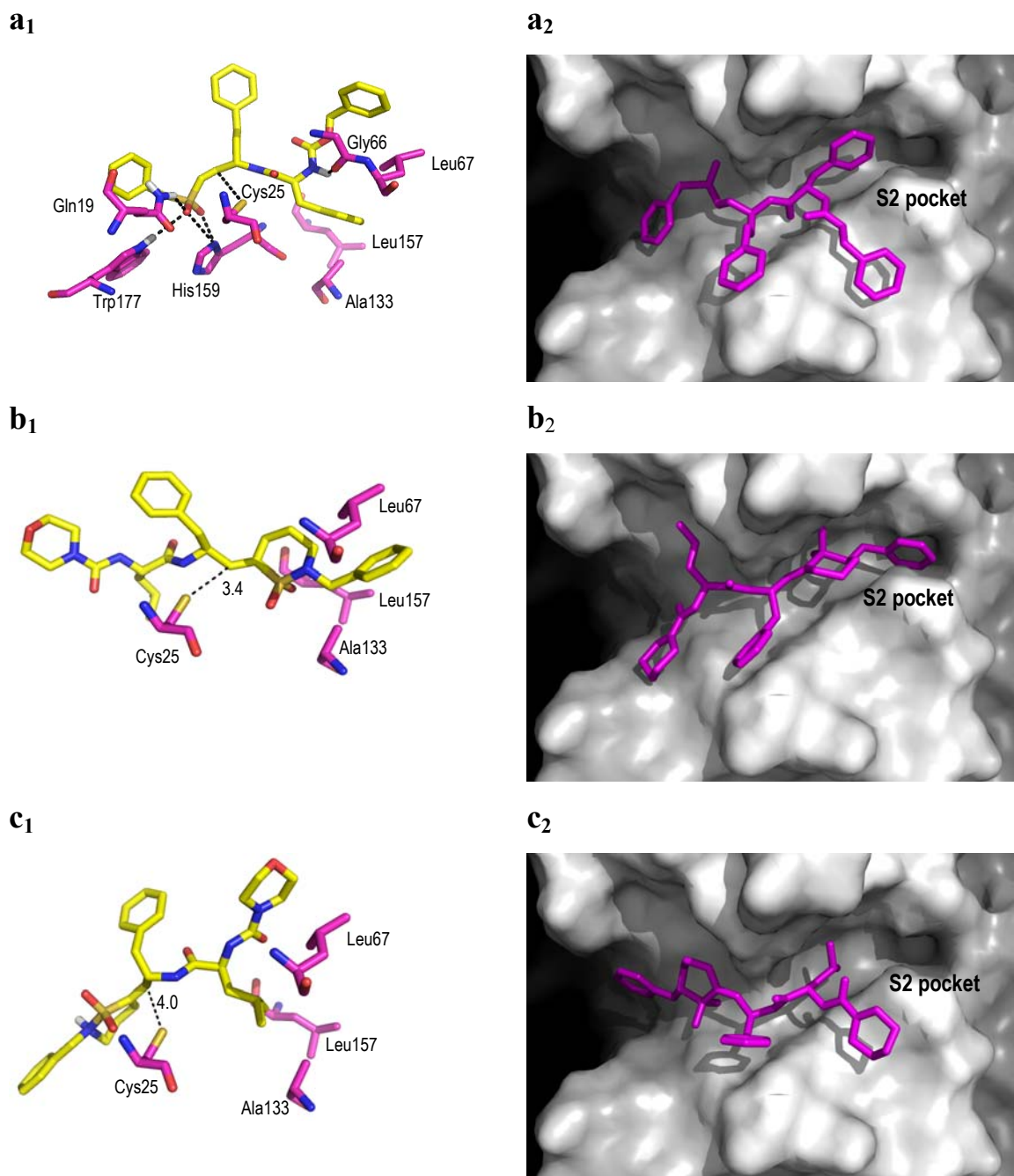


**Figure 2.15** Gold-generated active site interaction of cruzain with 1.2d (a), 2.4a (b) and 2.4b (c). Figure generated using Pymol software.<sup>26</sup>

Vinyl sultams **2.4a,b** were also docked into the active site of papain (PDB code: 1PPN)<sup>20,113</sup> as outlined in Figure 2.16.

For **2.4a**, seven of the top 10 solutions presented the *N*-benzyl- $\delta$ -sultam moiety being incorporated in the S2 subsite defined by Pro68, Val133 and Val157, and a Cys25(*S*)-C $\beta$  distance ranging from 4.6 to 4.9 Å. All docked conformations of **2.4b** showed the *N*-benzyl- $\delta$ -sultam in the S2 pocket.

Clearly, these results suggest that molecular recognition of **2.4a,b** by papain leads to enzyme-inhibitor complexes that are conformationally unfavourable to conjugate addition of Cys25 to the vinyl sultam, as required for enzyme inactivation.

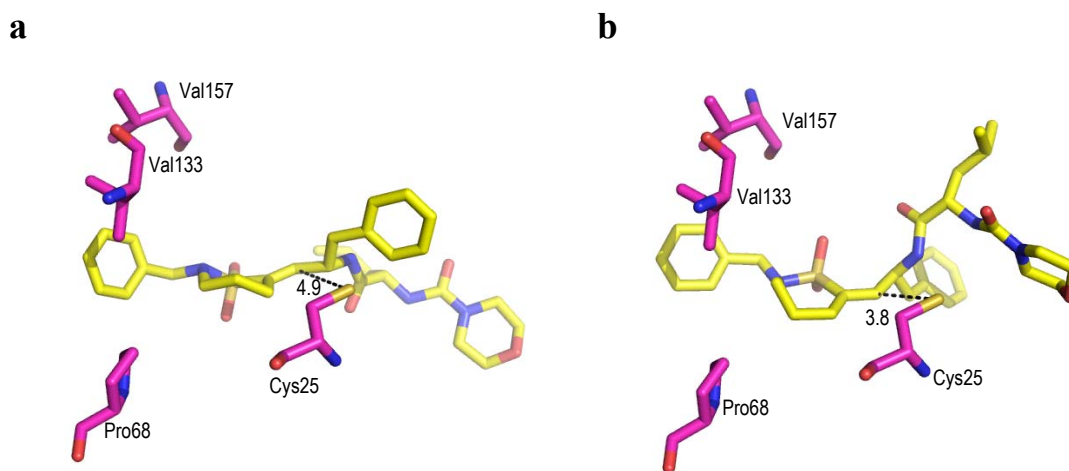


**Figure 2.16** Gold-generated active site interaction of papain with **2.4a** (a) and **2.4b** (b). Figure generated using Pymol software.<sup>26</sup>





## **CHAPTER 3**

### **1,4-NAPHTHOQUINONE DERIVATIVES**



### 3. 1,4-NAPHTHOQUINONE DERIVATIVES

The present chapter focuses on the inhibition kinetics of papain and bovine spleen cathepsin B by naphthoquinones, including commercially available compounds and some new derivatives, for which the synthesis is described. These compounds were also evaluated against falcipain-2, *Plasmodium falciparum* W2 and porcine pancreatic elastase. Investigations on reactivity toward cysteine were carried out to explore the relationship between the intrinsic chemical reactivity and the enzyme inhibitory activity.

#### 3.1 Synthesis

Earlier (Section 1.1.3), it was mentioned the preference of papain for bulky *S*-amino acids such as Phe. It is also known that papain favours ligands based on the *N*-Ac-*S*-Phe-Gly motif,<sup>30</sup> and on the Leu-*i*-Am sequence (side chain of the successful inactivator E-64c, in Section 1.2.2).

Thus, to probe the potential interaction between this enzyme and 1,4-naphthoquinone derivatives, the naphthoquinone core was attached to the Phe, Leu-*i*-Am and Gly moieties. This strategy involved the preparation of compounds **3.1-3.3** and the attempted synthesis of derivatives **3.4a** (Figure 3.1). The non-specific methylamino (**3.1** and **3.2**, R = Me) and ethoxy (**3.5**) derivatives were also synthesised for comparison on enzyme inhibitory activity.

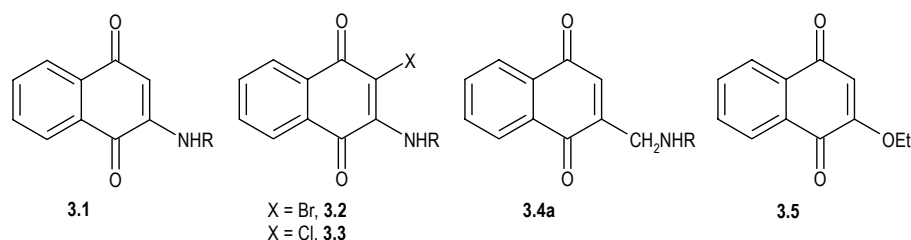
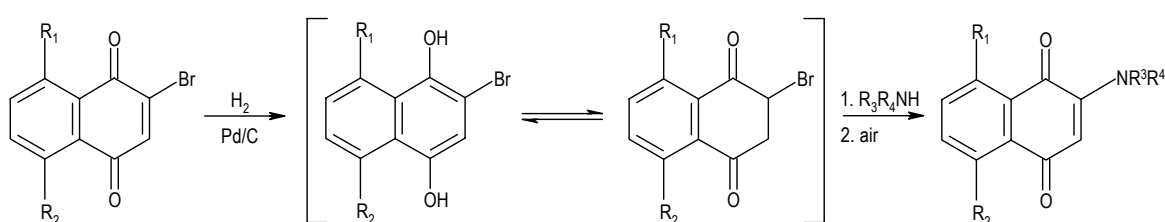


**Figure 3.1** Generic structures of *N*-(1,4-naphthoquinon-2-yl)amino derivatives (**3.1-3.3**) and of *N*-[(1,4-naphthoquinon-2-yl)methyl]amino derivatives (**3.4a**). Structure of 2-ethoxy-1,4-naphthoquinone (**3.5**).

The introduction of a methylene bridge in the **3.4a** series was planned to tentatively find the best binding interaction of the inhibitors with papain. It was also expected that these derivatives could be more reactive toward thiols than **3.1** due to the presence of an inductively electron withdrawing methyleneamino group instead of an electron donating amino substituent.

### 3.1.1 Reaction of 1,4-naphthoquinones with nitrogen and oxygen nucleophiles

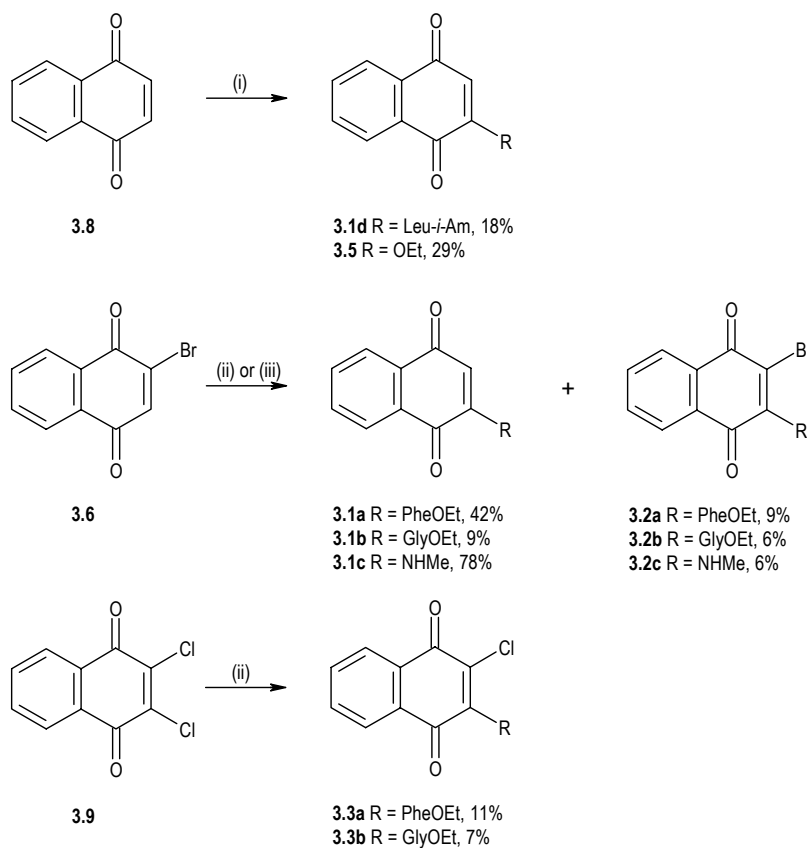
Previous investigations accomplished the synthesis of naphthoquinones through a Michael-type addition of amines to the quinone moiety.<sup>52,114-120</sup> Alternatively, the amine may be reacted with the reduced form of 2-bromo-1,4-naphthoquinones (Scheme 3.1).<sup>121</sup>



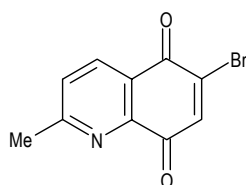
Scheme 3.1 Reaction of amines with the reduced form of 2-bromo-1,4-naphthoquinone.

In the present work, the first approach to the synthesis of **3.1-3.3** (Scheme 3.2) consisted in the reaction of 2-bromo-1,4-naphthoquinone **3.6** with *S*-phenylalanine ethyl ester hydrochloride (1 mol eq) and TEA (2 mol eq) in DCM, but after stirring for 3 h at rt, only starting material was recovered. Changing the solvent to abs ethanol, as previously described,<sup>115,119</sup> allowed the reaction to proceed smoothly through conjugate addition chemistry.<sup>122</sup> The process led to the formation, in a one-pot procedure, of two compounds: **3.1a**, obtained as the major product, and the bromo analogue **3.2a** as a minor product. Thereafter, employing glycine ethyl ester hydrochloride and methylamine under the same conditions afforded the compounds **3.1b**, **3.2b** and **3.1c**, **3.2c**, respectively. These results are consistent to the one involving coupling between quinone **3.7** (Figure 3.2) and amines, which also gave the bromo derivative in low yield,<sup>123</sup> but contrast with that recently described for

the reaction of 2-bromo-1,4-naphthoquinone **3.6** with *S*-amino acid methyl esters, in which the mono-substituted 1,4-naphthoquinones **3.1** were the only products isolated.<sup>117</sup>



**Scheme 3.2** Synthesis of *N*-(1,4-naphthoquinon-2-yl)amino derivatives and of 2-ethoxy-1,4-naphthoquinone. Reagents and conditions: (i) TEA, abs ethanol for **3.5** and TEA, Leu-*i*-Am, abs ethanol for **3.1d**; (ii) PheOEt or GlyOEt hydrochlorides, TEA, abs ethanol for **3.1a,b**, **3.2a,b** and **3.3a,b**; (iii) R = NH<sub>2</sub>Me, abs ethanol for **3.1c** and **3.2c**.



**3.7**

**Figure 3.2** Structure of 6-bromo-2-methylquinoline-5,8-dione.

This method was also applied to 1,4-naphthoquinone **3.8** and to 2,3-dichloro-1,4-naphthoquinone **3.9** to afford compounds **3.1d**, **3.5** and **3.3a,b**. The side-chain Leu-*i*-Am of

**3.1d** was prepared under standard peptide coupling conditions from *N*-Boc-*S*-leucine-*N*-hydroxysuccinimide ester and *iso*-amylamine, followed by the removal of the *N*-Boc group with TFA.<sup>101,106</sup>

During the time course of this work, Tandon *et al.*,<sup>114,117</sup> afforded derivative **3.3b** and the methyl esters analogues of compounds **3.1a,b**. The followed procedure is rather similar to the one mentioned above, but the employment of reflux conditions during a short time (3-5 h) led to yields ranging from 60% to 96% and all products were obtained as crystalline solids.

**NMR spectral characterisation.** All compounds gave NMR, ESI-MS and elemental analyses consistent with their structures. However, it is noteworthy that NMR analyses of derivatives **3.2/3.3** lacked the signals for carbons bearing the halo substituent, and in the case of **3.3a** also for the carbon at C-2.

The common feature in the <sup>1</sup>H NMR spectra is the characteristic triple doublet splitting of protons H-6 and H-7 (Figure 3.3), consistent with two *ortho* and one *meta* couplings. Each of the remaining aromatic protons (H-5 and H-8) was expected to give a *ddd* signal due to the split with the *ortho*, *meta* and *para* neighbouring protons. Instead, the spectra generally exhibited two not well resolved *brdd* (Figure 3.4) or *brd* signals. Generally, these signals present a  $J_{ortho}$  of 7.6 Hz, which reflects the H-5/H-6 and H-8/H-7 couplings and, for the *brdd* case, an additional small value constant which was ascribed to both *meta* and *para* split.

In phenylalanine derivatives, the methylene protons CHCH<sub>2</sub>Ph are diastereotopic to one another, due to the stereocentre of *S*-phenylalanine ethyl ester. Excluding the cases where accidental overlap might occur, each of these protons consists of a *dd* signal due to the coupling with each other and with the methine proton CHCH<sub>2</sub>Ph. An analogous situation was found for the methylene protons of the ester moiety OCH<sub>2</sub>CH<sub>3</sub>, whose resonance frequencies coincided in an obscure signal classified as a multiplet. The non-equivalence of these two protons also provides a convenient explanation for the complex signal, *i.e.* a multiplet, showed by the neighbouring methyl protons OCH<sub>2</sub>CH<sub>3</sub>. In contrast, glycine derivatives, which lack a stereocentre, exhibited the characteristic quartet and triplet splitting patterns for the ethyl component.

The *S*-Leu-*i*-Am derivative **3.1d** has also a stereocentre. Thus, the isopropyl methyl groups CH(CH<sub>3</sub>)<sub>2</sub> of the leucine and *iso*-amylamine components are diastereotopic. This situation is easily deduced for the leucine component, which exhibited a doublet for each methyl group protons and two separate carbon signals. In contrast, for *iso*-amylamine, the two

methyl groups appear to be equivalent, by showing a single doublet in the  $^1\text{H}$  NMR spectrum and one carbon signal. This situation was ascribed to an accidental coincidence in the chemical shift.

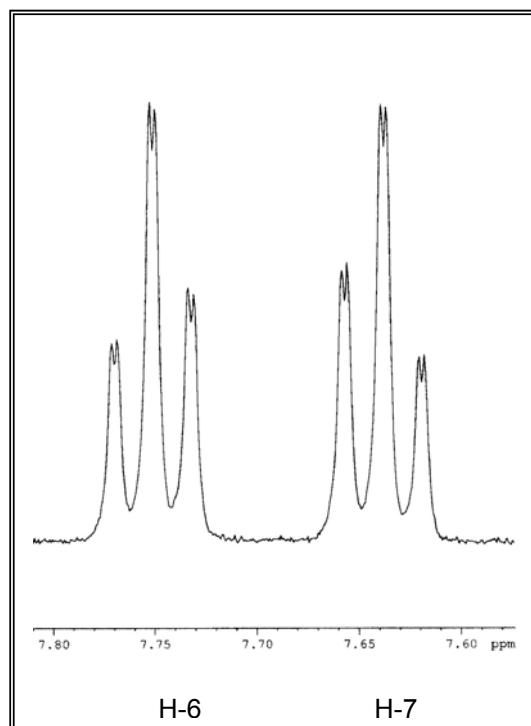
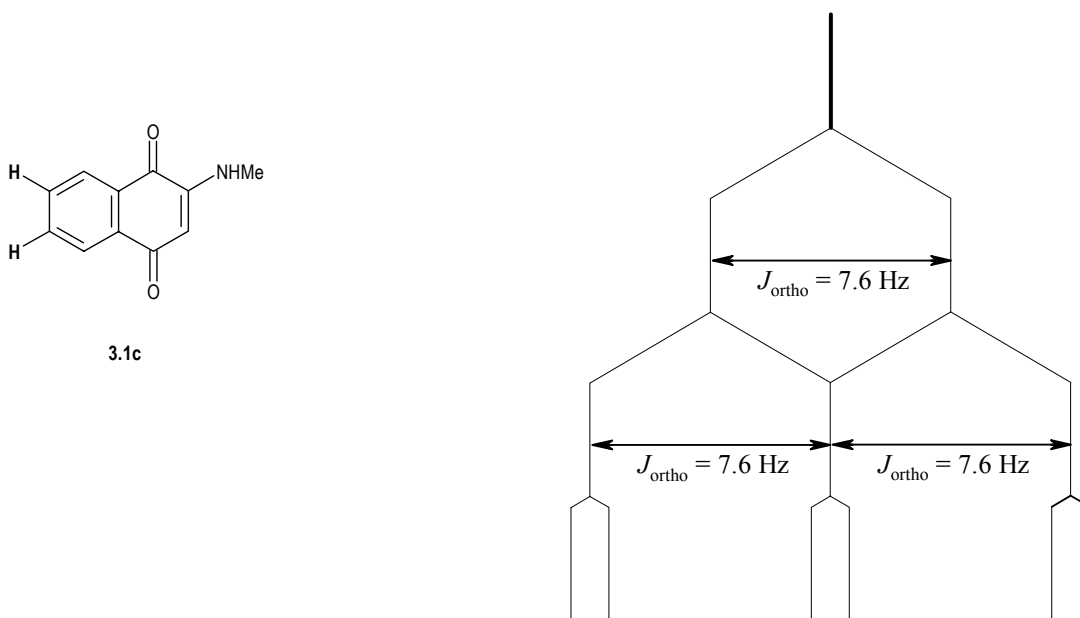


**Figure 3.3** Observed  $^1\text{H}$  NMR triple doublet signals and splitting pattern diagram for the aromatic protons H-6 and H-7 of compound 3.1c.

Constant not shown is 1.2 Hz (*meta* coupling).

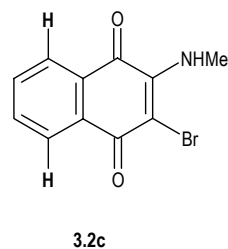
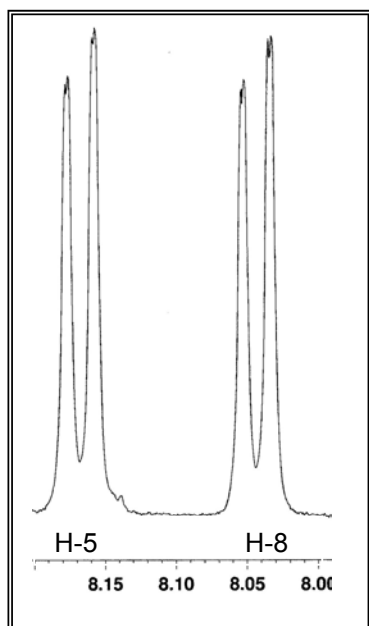


Figure 3.4 Observed  $^1\text{H}$  NMR not well resolved *dd* signals for the aromatic protons H-5 and H-8 of compound 3.2c.

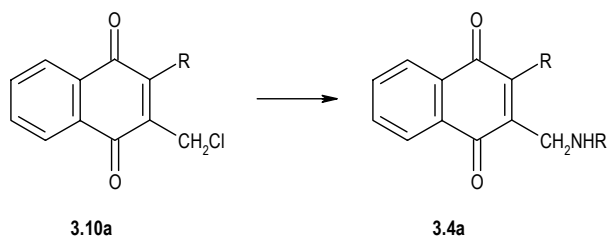
**Mass spectrum.** The ESI-MS of derivatives **3.2/3.3** showed the readily identifiable patterns indicative of the presence of bromine or chlorine in the molecule. Therefore, bromo derivatives exhibited a doublet at  $(\text{MH}^+)$  and  $(\text{MH}^++2)$ , the two peaks showing nearly equal intensity. Similarly, chloro derivatives presented  $(\text{MH}^+)$  ions two mass units apart, but in a 3:1 intensity ratio.

### 3.1.2 Aminomethyl derivatives

A search of the literature has not revealed much information concerning derivatives **3.4a** (Scheme 3.3). All reported compounds are substituted at the 3-position with electron donating or withdrawing groups ( $\text{R} = \text{Me}, \text{Cl}, \text{Br}, \text{OH}, \text{OMe}, \text{OCOMe}$ ).<sup>124-127</sup> Although no details of the reaction were given, Prezhdo *et al.*<sup>126</sup> claim the preparation of these derivatives from the appropriate 2-chloroalkyl naphthoquinone **3.10a**, and secondary aromatic amines in yields of 50-85%. Other investigations afforded the 3-hydroxyl derivatives through a Mannich reaction.<sup>124,125</sup>

The literature also reports derivatives **3.4b,c** (Figure 3.5),<sup>128,129</sup> along with the failure of the attempts to synthesise **3.4d** from the corresponding chloroalkyl naphthoquinones.<sup>126,127</sup>





Scheme 3.3 Preparation of aminomethyl derivatives by Prezhdo *et al.*<sup>126</sup>

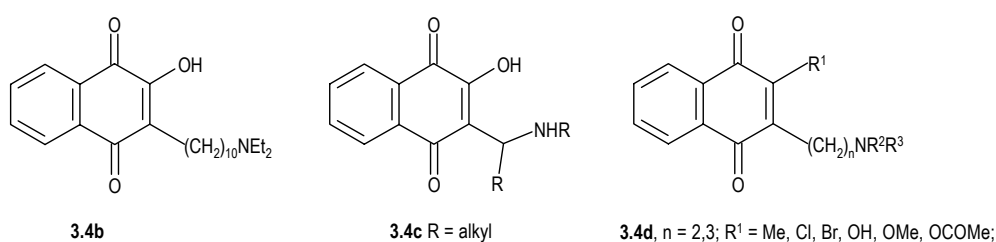
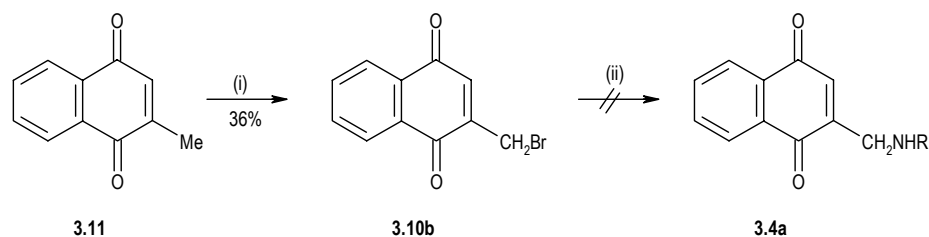


Figure 3.5 Generic structures of aminoalkyl derivatives.

In the present investigation, attempted preparation of derivatives **3.4a** (Scheme 3.4) proceeded *via* the bromination of 2-methyl-1,4-naphthoquinone **3.11**,<sup>130</sup> to afford **3.10b**, whose structure was confirmed by its <sup>1</sup>H NMR spectrum.

The next step consisted in the reaction of **3.10b** with methylamine or amino acid ethyl ester hydrochlorides, under several conditions (Table 3.1). In all cases dark brown mixtures were obtained, the TLC analyses of which showed intractable mixtures.



Scheme 3.4 Attempted synthesis of aminomethyl derivatives. Reagents and conditions: (i) *N*-Bromo-succinimide, benzoyl peroxide, CCl<sub>4</sub>, reflux, 24 h; (ii) see Table 3.1.

**Table 3.1 Conditions for the synthesis of aminomethyl derivatives.**

Amine or S-amino acid ethyl ester/1 mol eq	Solvent/Base <sup>a</sup> /Temperature/Reaction time
S-phenylalanine ethyl ester hydrochloride	DCM/TEA/reflux/2.5 h
	DCM/pyridine/reflux/1.5 h
	EtOH/TEA/rt/immediate
glycine ethyl ester hydrochloride	toluene/TEA/rt/14 h
NH <sub>2</sub> Me <sup>b</sup>	EtOH/NH <sub>2</sub> Me/rt/immediate
	acetone/NH <sub>2</sub> Me/rt/5 h
	DMF <sup>c</sup> /NH <sub>2</sub> Me/rt/immediate
	toluene/NH <sub>2</sub> Me/rt/14 h

<sup>a</sup> TEA and pyridine were used in a 2 mol eq molar ratio. <sup>b</sup> An excess of amine was used (1 mol eq) as indicated in the right column. <sup>c</sup> *N,N*-Dimethylformamide.

## 3.2 Kinetic study of the reaction with cysteine

### 3.2.1 Introductory remarks

As stated earlier (Section 1.4), the choice of the 1,4-naphthoquinone scaffold as a potential lead structure for the design of irreversible cysteine protease inhibitors laid in the known reactivity of thiols to quinones.

In an attempt to get insight into the factors that could affect the chemical reactivity of such compounds, this work exploited the relationship between the LUMO energies and the reactivity of some derivatives toward cysteine. This thiol was chosen because it showed to be highly reactive with 2- and 6-methyl-1,4-naphthoquinone derivatives, comparatively to GSH and DTT.<sup>131</sup> The reaction was followed spectrophotometrically at pH 7.1, at 25 °C, under pseudo-first-order conditions.

### 3.2.2 Results and Discussion

#### Kinetic studies

The reactivity studies began with the selection of the wavelength to be used in the kinetic measurements. With this goal, the reaction of cysteine with each of the naphthoquinones (Table 3.2) was followed by repeated spectral scanning over the wavelength range of 700 to 200 nm.

An attempt to study the reactivity of 2-bromo-1,4-naphthoquinone **3.6** and 5-hydroxy-1,4-naphthoquinone **3.12** was made, but, for each one, the first recorded scanning was not similar to the compounds spectra in buffer lacking cysteine. This situation is indicative that, due to their high reactivity, the compounds had reacted with cysteine during the initial period of mixing of the reactants.

For the remaining compounds, the main difficulty in the selection of the wavelength arose from the complexity of the spectra (see Appendix III for an example). In general, on mixing the reactants, there was a progressive change in the absorbance, followed by a region with a minimal variation in this property (plateau). Subsequently, the reaction was characterised by continuous spectral changes. Some of the spectra did not present an isosbestic point.

These observations are similar to previous reports regarding the reactivity of quinones,<sup>132</sup> which related this pattern to the occurrence of complex secondary reactions involving the hydroquinone product that results from the initial Michael addition (outlined in Scheme 1.7, Chapter 1). Because the present kinetic studies were performed without protection from air, the mentioned complexity may arise from the aerobic oxidation of those products.<sup>51,131</sup>

In order to simplify the kinetic interpretation of the overall process, some of the reported investigations were performed with exclusion of oxygen. To the best of author's knowledge, spectrophotometry has been used only once to investigate naphthoquinones, and then under anaerobic conditions.<sup>131</sup> Nevertheless, it has been recognised that these conditions may compromise any application of the results to biological systems.<sup>131</sup>

In the present investigation, the kinetic measurements were performed at the wavelength that showed a much well defined plateau region, along with a maximum absorbance variation during the reaction progress.

Then, the  $k_{\text{obs}}$  values (Appendix II) were determined by following the absorbance decrease or increase until the plateau region, and before any significant secondary reaction was observed.

For 1,4-naphthoquinone **3.8**, the UV-visible spectrum was recorded in the presence of buffer lacking cysteine during 19 h. The similarity between scans excluded any background reaction. As this compound revealed to be the most reactive during the above-mentioned selection of the wavelength, stability in the phosphate buffer was assumed for the other derivatives. Later, this situation was confirmed when the plot of the pseudo first-order rate constants,  $k_{\text{obs}}$ , versus the total cysteine concentration,  $[\text{cys}]_{\text{t}}$ , showed an intercept at  $[\text{cys}]_{\text{t}} = 0$  indistinguishable from zero (Figure 3.6). In addition, the second-order rate constants,  $k_{\text{cat}}$ , were given by the slope of this graph.

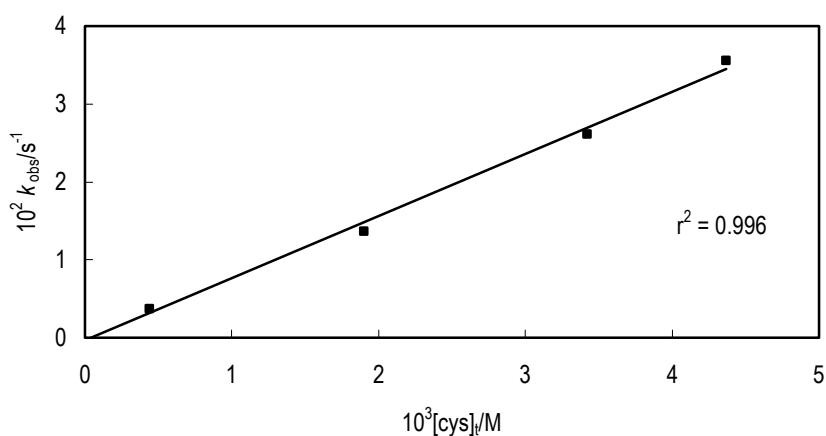


**Figure 3.6** Plot of the pseudo first-order rate constants,  $k_{\text{obs}}$ , for the reaction of compound **3.13** with cysteine, against the total cysteine concentration at pH 7.12 ( $\alpha = 8.8 \times 10^{-2}$ ) at 25 °C and ionic strength 0.5 M. Points are experimental and line is theoretical for  $k_{\text{cat}} 7.98 \text{ M}^{-1} \text{ s}^{-1}$ .

The pseudo first-order rate constants,  $k_{\text{obs}}$ , also showed a linear increase with the thiolate concentration,  $[\text{cys}^-]$ , (Figure 3.7) giving a slope corresponding to the second-order rate constants for the reaction with the thiolate anion,  $k_{\text{cys}^-}$ , (Table 3.2). This correlation resulted in an intercept at  $[\text{cys}^-] = 0$  indistinguishable from zero, indicating that there is no detectable reaction for the undissociated thiol. This result is consistent with previous studies with quinones which claim thiolate anion as the reactive species.<sup>131,132</sup>

Under these conditions, the second-order rate constants,  $k_{\text{cat}}$ , are strictly dependent on the fraction of cysteine present as conjugate base,  $\alpha$  (Equation 2.4, conveniently repeated in this section). This dependence was showed for compound **3.11** (Figure 3.8).

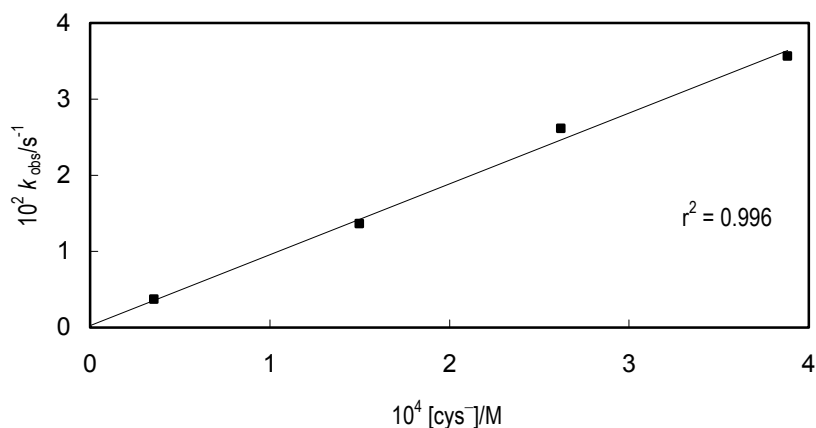


**Figure 3.7** Plot of the pseudo first-order rate constants,  $k_{\text{obs}}$ , for the reaction of compound 3.13 with cysteine, against the cysteine thiolate concentration at pH 7.12, at 25 °C and ionic strength 0.5 M. Points are experimental and line is theoretical for  $k_{\text{cys}^-} = 93.1 \text{ M}^{-1} \text{ s}^{-1}$ .

$$k_{\text{cat}} = k_{\text{cys}^-} \alpha \quad (2.4)$$

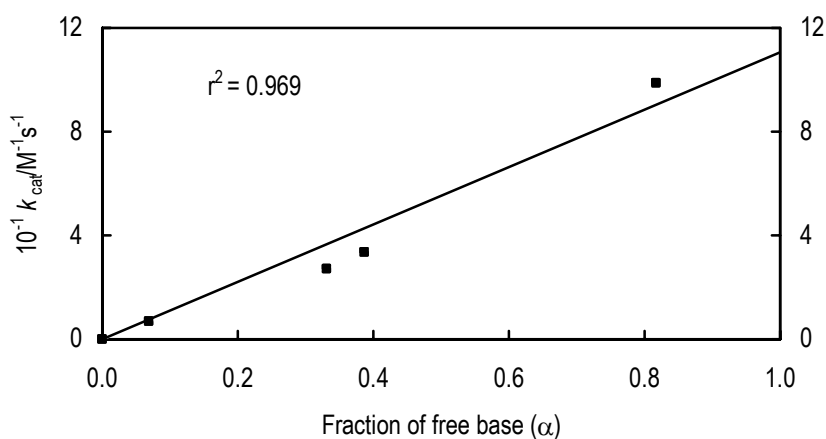


**Figure 3.8** Plot of the catalytic rate constants,  $k_{\text{cat}}$ , for the reaction of 3.11 with cysteine, against the fraction of conjugate base,  $\alpha$ , at 25 °C and ionic strength 0.5 M. The  $k_{\text{cat}}$  values were determined at four different pH values (7.1, 7.9, 8.0 and 8.8). Points are experimental and line is from linear regression analysis of the data.

According to Equation 2.4, the second-order rate constant,  $k_{\text{cys}^-}$ , could be determined from the intercept at  $\alpha = 1$ . For the remaining compounds,  $k_{\text{cys}^-}$  values were given by  $k_{\text{cys}^-} = k_{\text{cat}} / \alpha$

and showed to be in good agreement with the ones given by the slopes of  $k_{\text{obs}}$  versus the thiolate concentration,  $[\text{cys}^-]$ .

1,4-Naphthoquinone **3.8**, however, revealed a hyperbolic dependence of  $k_{\text{obs}}$  on the total cysteine concentration (Figure 3.9). Such a dependence has been reported for the reaction of dopaminoquinone **3.14** with cysteine (Scheme 3.5) and has been ascribed to an initial formation of the reversible tetrahedral intermediate **3.15**, resulting from cysteine conjugate addition to C-6 (dopaminoquinone numbering), which is then followed by the decomposition into the final product.<sup>133</sup>

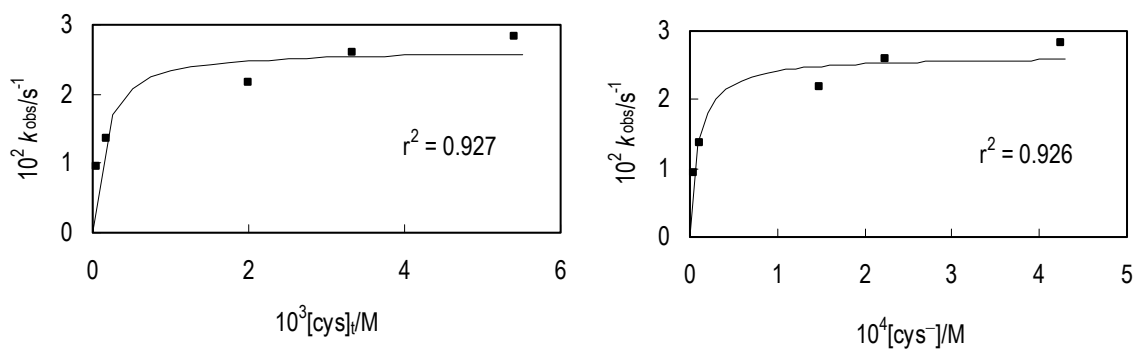
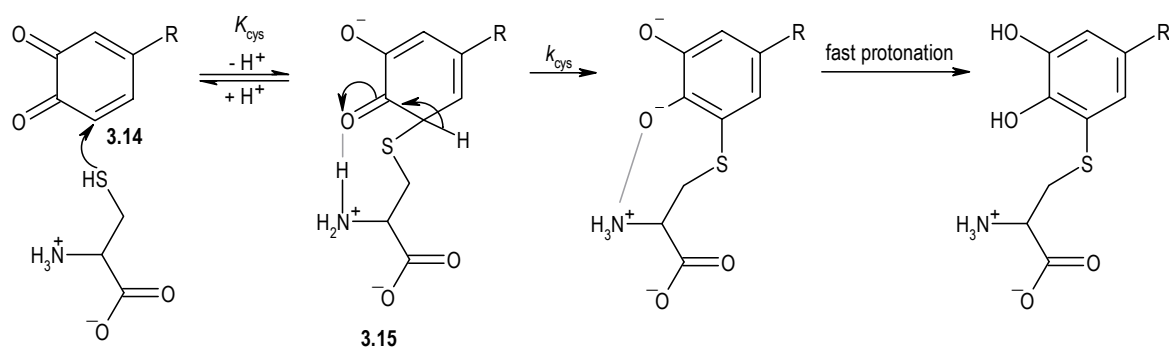
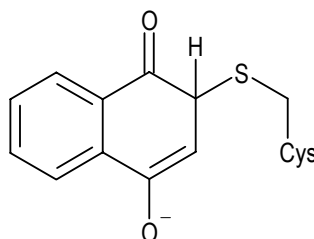


**Figure 3.9 (a)** Plot of the pseudo first-order rate constants,  $k_{\text{obs}}$ , for the reaction of naphthoquinone **3.8** with cysteine, against the total cysteine concentration at pH 7.08 ( $\alpha = 7.08 \times 10^{-2}$ ) at 25 °C and ionic strength 0.5 M. Points are experimental and line is theoretical for  $1/K_{\text{cys}} 9.26 \times 10^{-6} \pm 3.16 \times 10^{-6}$  M and  $k_{\text{cys}} 2.64 \times 10^{-2} \pm 0.17 \times 10^{-2}$  s<sup>-1</sup>; **(b)** Plot of the pseudo first-order rate constants,  $k_{\text{obs}}$ , for the reaction of naphthoquinone **3.8** with cysteine, against the cysteine thiolate concentration at pH 7.08, at 25 °C and ionic strength 0.5 M.



**Scheme 3.5** The proposed reaction mechanism of cysteine with dopaminoquinone. Hydrogen bonds are in grey.

Assuming that reaction of **3.8** with cysteine *thiolate* also involves initial reversible formation of an adduct (e.g. **3.16**, Figure 3.10), then  $k_{\text{obs}}$  dependence on  $[\text{cys}]_{\text{t}}$  follows Equation 3.1,



3.16

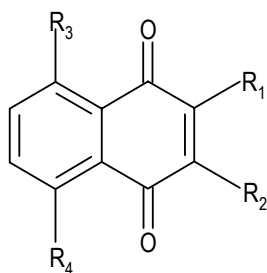
Figure 3.10 Possible adduct resulting from the reaction of cysteine thiolate with naphthoquinone **3.8**.

$$k_{\text{obs}} = \frac{k_{\text{cys}}[\text{cys}]_{\text{t}}}{\left\{ \left( \frac{1}{K_{\text{cys}}} \right) \left( K_{\text{a}} + [\text{H}^+] \right) / K_{\text{a}} \right\} + [\text{cys}]_{\text{t}}} \quad (3.1)$$

where  $K_{\text{cys}}$  is the stability constant for the formation of the adduct,  $k_{\text{cys}}$  is the first-order rate constant for the decomposition of the adduct and  $(K_{\text{a}} + [\text{H}^+])/K_{\text{a}}$  is  $1/\alpha$  (this equation was solved in Appendix IV).

Kinetic data were computer-fitted (Sigma Plot<sup>®</sup> software) to Equation 3.1 allowing the determination of  $K_{\text{cys}}$  ( $1.08 \times 10^5 \text{ M}^{-1}$ ), of  $k_{\text{cys}}$  ( $2.64 \times 10^{-2} \text{ s}^{-1}$ ) and thus of the second-order rate-constant for the reaction with the thiolate anion  $k_{\text{cys}^-}$  ( $= k_{\text{cys}}K_{\text{cys}}$ ).

Overall, the  $k_{\text{cys}^-}$  values varied by up to four orders of magnitude, with 1,4-naphthoquinone **3.8** as the most effective acceptor for cysteine.

**Table 3.2** LUMO energies and cysteine-catalysed second-order rate constants,  $k_{\text{cys}^-}$ , for naphthoquinones.

Compound	R <sup>1</sup>	R <sup>2</sup>	R <sup>3</sup>	R <sup>4</sup>	E <sub>LUMO</sub> /Hartree	$k_{\text{cys}^-}$ (M <sup>-1</sup> s <sup>-1</sup> )	
						Method A <sup>a</sup>	Method B <sup>b</sup>
3.1a	PheOEt	H	H	H	-0.1146	25.2	25.9
3.1b	GlyOEt	H	H	H	-0.1097	0.55	0.49
3.1c	NHMe	H	H	H	-0.1070	0.24	0.24
3.5	OEt	H	H	H	-0.1114	11.1	10.9
3.6	Br	H	H	H	—	—	—
3.8	H	H	H	H	-0.1245	2851.2 <sup>c</sup>	
3.11	Me	H	H	H	-0.1193	—	114.3
3.12	H	H	OH	H	—	—	—
3.13	Morpholinyl	Cl	H	H	-0.1161	93.1	93.1

<sup>a</sup> From the slope of  $k_{\text{obs}}$  versus  $[\text{cys}^-]$ . <sup>b</sup> From  $k_{\text{cys}^-} = k_{\text{cat}}/\alpha$ . <sup>c</sup> From Equation 3.1.

### Relationship between LUMO energies and the reactivity toward cysteine

Molecular orbital calculations were performed by Dr. Rita C. Guedes (from the Faculty of Pharmacy, University of Lisbon).

The interest in LUMO energies arose from two reported correlations; first, between the reactivity of quinones and their LUMO energy,<sup>46,48,51</sup> and second, between LUMO energies and electronic descriptors<sup>134</sup> thereby providing an alternative approach to QSAR studies.<sup>132,134-136</sup> In the context of this latter observation, the present study found a correlation between the LUMO energy of naphthoquinones and the corresponding Hammett  $\sigma_p$  constants for C-2 and C-3 substituents (Figure 3.11).



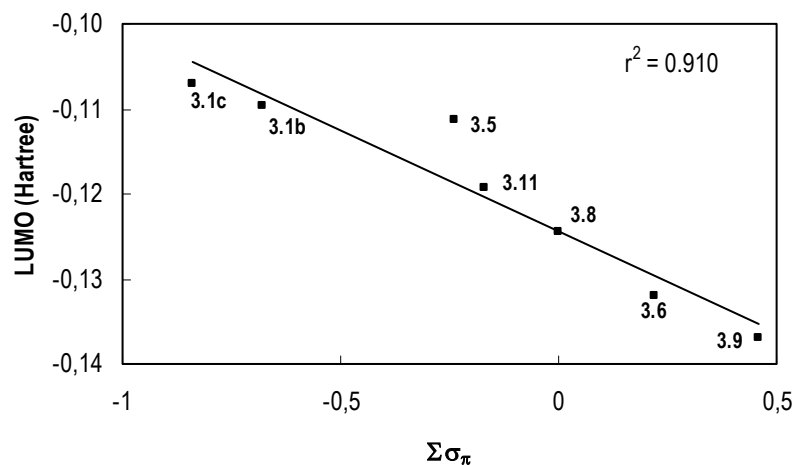


**Figure 3.11** Linear correlation between the LUMO energy of naphthoquinones and the Hammett  $\sigma_p$  constants. For data see Appendix V. Line is from linear regression analysis of the data.

Plotting  $\log k_{\text{cys}^-}$  against the corresponding LUMO energies resulted in a linear correlation (Figure 3.12), which shows that the lower the LUMO energy the more reactive the molecule.

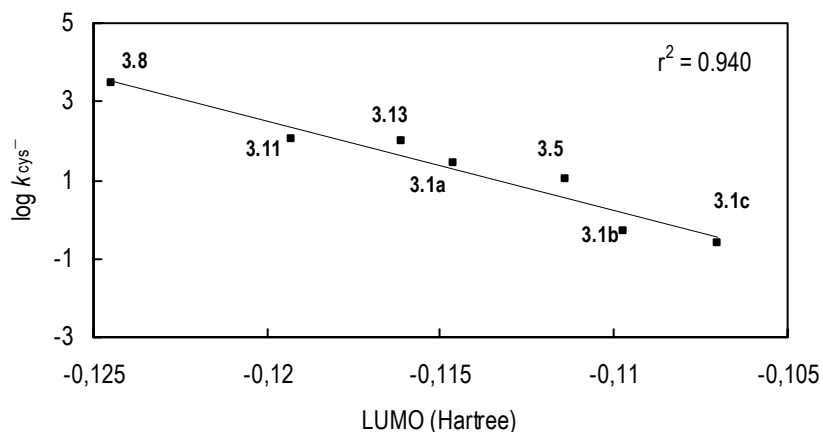


**Figure 3.12** Linear correlation between the LUMO orbital energies and the second-order rate constants,  $k_{\text{cys}^-}$ , for the reaction of naphthoquinones with the thiolate anion. Line is from linear regression analysis of the data.

Calculations of the LUMO density for the glycine derivative **3.1b** (Figure 3.13), as well for other aminoacid derivatives, showed that for these compounds this orbital is largely centred on the double bond of the quinone ring.

Overall, these observations are consistent with the occurrence of a Michael-type addition, which is dependent on the electrophilicity of the naphthoquinone.

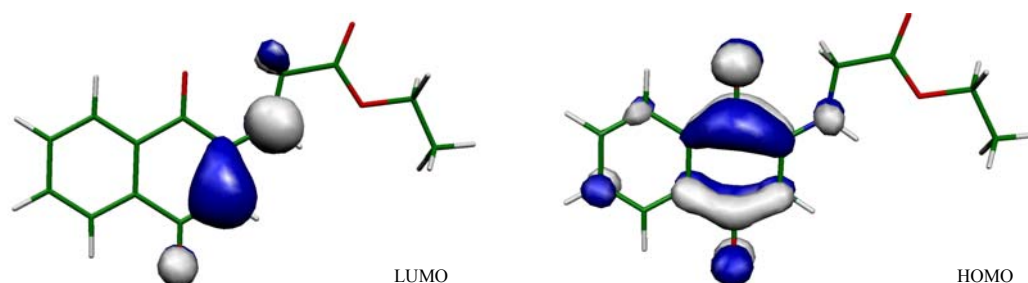


Figure 3.13 Frontier molecular orbitals of a low-energy conformation of the glycine derivative 3.1b.

### 3.3 Inhibitory activity against cysteine proteases

This section presents the results obtained for naphthoquinones in the inactivation studies on papain, bovine spleen cathepsin B, falcipain-2 and *Plasmodium falciparum* W2. To investigate the selectivity of the compounds for cysteine proteases, they were also evaluated against porcine pancreatic elastase, a serine protease. In addition, the papain-inhibitory activity of two indolequinones is described. These compounds contain an isosteric replacement of the fused benzene moiety and thus can provide structural information for structure-activity relationships.

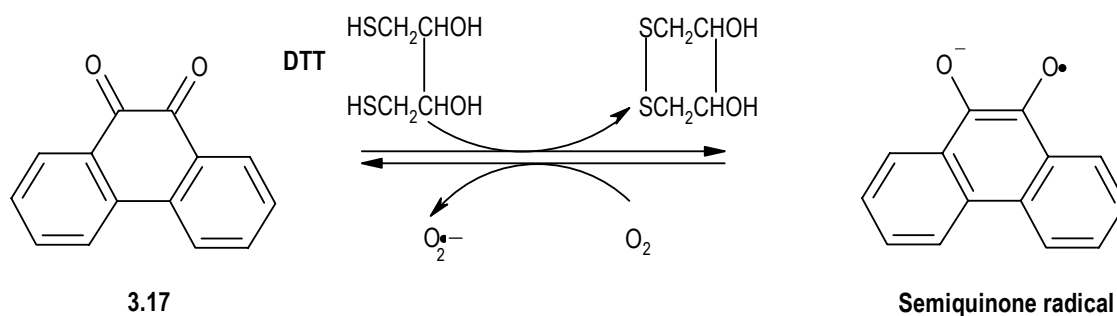
All kinetic inhibition assays were performed by Kitz and Wilson's pre-incubation method,<sup>137</sup> following the protocols described in Appendix I.

The inhibitory activity of the compounds is analysed in conjunction with the data from reactivity studies.

### 3.3.1 Papain inhibition studies

Earlier (Section 1.3), it was mentioned that quinones can interact with biological molecules by two mechanisms: (i) their capacity to undergo redox cycling, generating reactive oxygen species and (ii) their capacity to act as electrophiles leading to covalent modifications. Whether a quinone acts as an electrophile, a redox cycler or as both is mainly dependent on its reduction potential.

The redox cycle was illustrated in Scheme 1.6 (Chapter 1), which shows that the start of this mechanism requires the action of a reducing agent over quinones. Most of the inhibition assays for cysteine proteases, including the one used in this thesis, carry out the enzyme-inhibitor incubation in the presence of a reducing agent, *e.g.* DTT, which may, therefore, trigger the redox process, leading to the enzyme inactivation through oxidation of thiol groups. This mechanism was found in the inhibition of glyceraldehyde-3-phosphate dehydrogenase by **3.17**, which, under aerobic conditions, is able to transfer electrons from DTT to oxygen (Scheme 3.6). The inactivation process revealed to be more affected by the concentration of the thiol than by the quinone concentration, because the latter operates as a catalyst.<sup>138</sup>



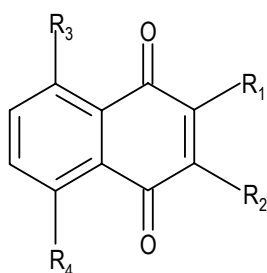
**Scheme 3.6** Proposed mechanism of glyceraldehyde-3-phosphate dehydrogenase by 9,10-phenanthrenequinone under aerobic conditions. Adapted from Rodriguez *et al.*<sup>138</sup>

Conversely, naphthoquinones (Table 3.3) and indolequinones (Figure 3.14) inactivated papain at a rate dependent on the concentration of the inhibitor as well as on the incubation time. This type of kinetic profile has been related recently to the quinone behaving as an electrophile.<sup>138</sup> In addition, performing an inhibition assay with compound **3.5** (58 μM) under

N<sub>2</sub> led to an inactivation degree similar to the one observed under aerobic conditions, excluding the existence of significant redox mechanism;  $k_{\text{obs}}$   $(3.13 \pm 0.16) \times 10^{-4} \text{ s}^{-1}$  versus  $(3.49 \pm 0.33) \times 10^{-4} \text{ s}^{-1}$ , respectively.

Therefore, the present results are consistent with covalent modification of papain.

**Table 3.3** LUMO energies and kinetic data for inactivation of papain by naphthoquinones.



Compound	R <sup>1</sup>	R <sup>2</sup>	R <sup>3</sup>	R <sup>4</sup>	E <sub>LUMO</sub> /Hartree	Papain		
						$k_2$ (M <sup>-1</sup> s <sup>-1</sup> )	$k_{\text{inact}}$ (10 <sup>-3</sup> s <sup>-1</sup> )	$K_i$ (μM)
3.1a <sup>*a</sup>	PheOEt	H	H	H	-0.1146	NI <sup>b</sup>	—	—
3.2a	PheOEt	Br	H	H	-0.1214	1.92	—	—
3.3a <sup>*</sup>	PheOEt	Cl	H	H	-0.1216	0.67	—	—
3.1b <sup>*</sup>	GlyOEt	H	H	H	-0.1097	35.4	0.34 ± 0.05	9.57 ± 4.18
3.2b <sup>*</sup>	GlyOEt	Br	H	H	-0.1172	14.7	1.32 ± 0.03	89.6 ± 7.08
3.3b <sup>*</sup>	GlyOEt	Cl	H	H	-0.1174	5.35	1.42 ± 0.16	266 ± 68.4
3.1c <sup>*</sup>	NHMe	H	H	H	-0.1070	0.76	—	—
3.2c <sup>*</sup>	NHMe	Br	H	H	-0.1149	1.03	—	—
3.1d <sup>*</sup>	Leu- <i>i</i> -Am	H	H	H	—	1.35	0.30 ± 0.04	222 ± 39.4
3.5 <sup>*</sup>	OEt	H	H	H	-0.1114	11.6	1.34 ± 0.18	115 ± 43.7
3.6 <sup>*</sup>	Br	H	H	H	-0.1320	33.3	2.20 ± 0.31	66.0 ± 20.0
3.8	H	H	H	H	-0.1245	(49.5 ± 4.2) <sup>c</sup>	—	—
3.9	Cl	Cl	H	H	-0.1370	6.39	—	—
3.11 <sup>*</sup>	Me	H	H	H	-0.1193	4.90	—	—
3.12	H	H	OH	H	—	(60.4 ± 4.1) <sup>c</sup>	—	—
3.13 <sup>*</sup>	Morpholinyl	Cl	H	H	-0.1161	9.29	—	—
3.18	Me	H	Me	Me	-0.1133	NI <sup>b</sup>	—	—
3.19	OH	H	H	H	-0.1170	(82.0 ± 4.4) <sup>d</sup>	—	—
3.20	H	H	OAc	H	-0.1335	14.6	—	—

<sup>a</sup> The derivatives with an asterisk were assayed for antimalarial activity (Section 3.3.3). Compounds **3.6**, **3.8**, **3.9**, **3.11**, **3.12**, **3.13** and **3.19** were commercially available. Derivatives **3.18** and **3.20** were kindly provided by Dr. Mohammed Jaffar (University of Manchester). <sup>b</sup> No inhibition when tested up to their solubility limit (50 μM for **3.1a** and 150 μM for **3.18**). <sup>c</sup> Inhibition % at 65 μM after 30-min incubation; <sup>d</sup> Inhibition % at 1.3 mM after 20-min incubation.

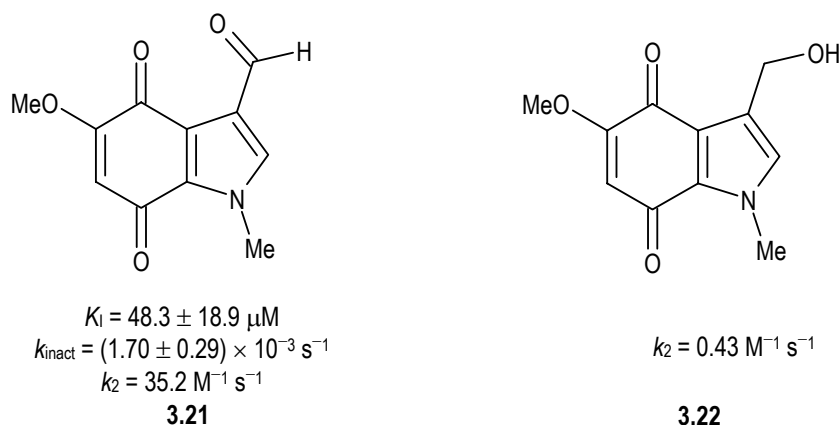


**Figure 3.14 Structure of the assayed indolequinones and kinetic data for inactivation of papain.** These compounds were kindly provided by Dr. Mohammed Jaffar, from the University of Manchester.

The time dependency of inhibition also suggested an irreversible process, which was confirmed by dialyses carried out after reaction of glycine derivative **3.1b** with papain, from which no enzymatic activity could be recovered after 24 h. Independently, no loss of activity was found for the control enzyme.

The simple reaction of an enzyme,  $E$ , with an irreversible inhibitor,  $I$ , (active-site directed) follows a model analogous to that of the Michaelis-Menten mechanism, *i.e.* there is an initial formation of a non-covalent enzyme-inhibitor complex,  $E \cdot I$ , followed by covalent modification,  $E \sim I$ , and hence irreversible inhibition (Equation 3.2).<sup>139</sup>



Overall, the process is described by Equation 3.3, where  $K_1$  represents the dissociation constant of the  $E \cdot I$  complex and  $k_{\text{inact}}$  is the first-order rate constant for the chemical inactivation step. According to this kinetic expression, the pseudo first-order inactivation rate constants,  $k_{\text{obs}}$ , should display a hyperbolic dependence with inhibitor concentration,  $[I]$ , indicative of saturation inhibition kinetics ( $k_{\text{obs}}$  values are listed in Appendix VI).

$$k_{\text{obs}} = \frac{k_{\text{inact}} [I]}{K_1 + [I]} \quad (3.3)$$

This behaviour was observed for compounds **3.1b**, **3.1d**, **3.2b**, **3.3b**, **3.5**, **3.6** and **3.21**, (Figure 3.15A), which suggests that the inactivation step is preceded by a specific non-covalent interaction between enzyme and inhibitor in a Michaelis-type complex.

In the case of derivatives **3.1c**, **3.2a,c**, **3.3a**, **3.9**, **3.11**, **3.13**, **3.20** and **3.22**,  $k_{\text{obs}}$  varied linearly with inhibitor concentration (Figure 3.15B), suggesting that  $K_I \gg [I]$ . In these conditions, Equation 3.3 simplifies to Equation 3.4, whose slope is the apparent second-order rate constant,  $k_2 (=k_{\text{inact}}/K_I)$ , for the enzyme inactivation process.

$$k_{\text{obs}} = \frac{k_{\text{inact}} [I]}{K_I} \quad (3.4)$$

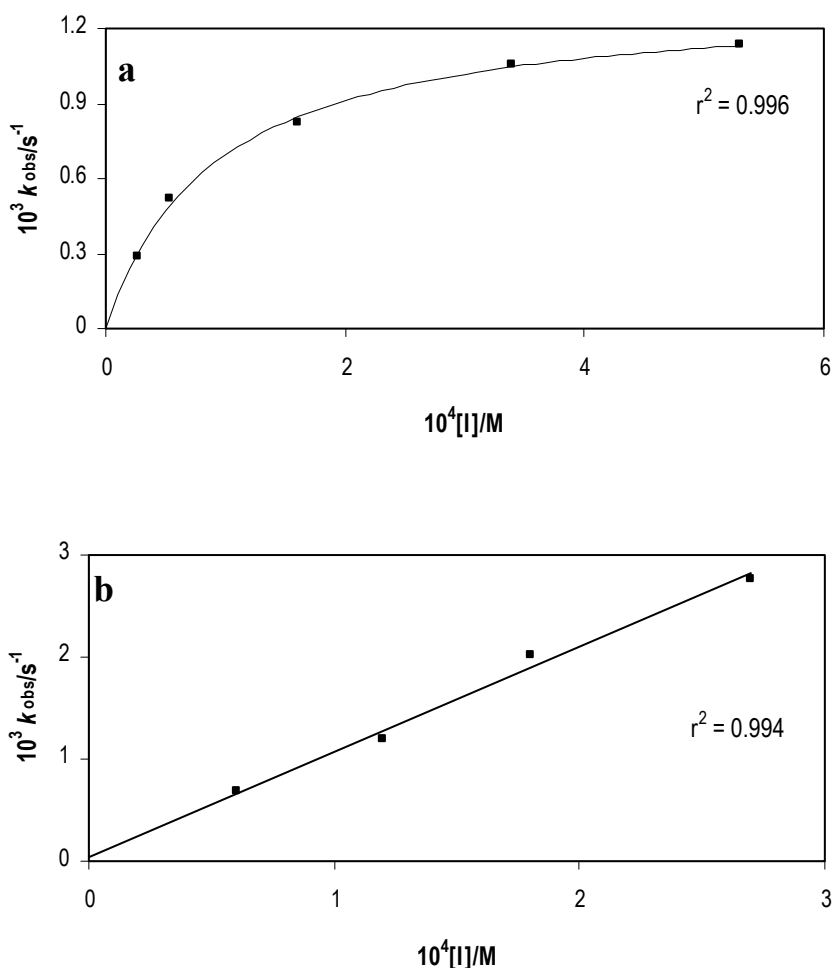


**Figure 3.15 (a)** Plot of the pseudo first-order inactivation rate constants,  $k_{\text{obs}}$ , against inhibitor concentration for the inactivation of papain by derivative 3.2b, at pH 7.0 at 25 °C; **(b)** plot of the pseudo first-order inactivation rate constants,  $k_{\text{obs}}$ , for the inactivation of papain by derivative 3.2c against inhibitor concentration, at pH 7.0 at 25 °C.

Naphthoquinone **3.8**, juglone **3.12** and lawsone **3.19** showed a departure from the two above-mentioned patterns and their inhibitory activity is discussed in the following section.

Overall, the compounds inhibited papain with the second-order rate constants for the inactivation process,  $k_2$ , ranging from 0.67 to 35.4 M<sup>-1</sup> s<sup>-1</sup>, which represents ~50-fold variation in their inhibitory activity.

Unfortunately, the Phe and Leu-*i*-Am fragments did not improve inhibitory potency as initially reasoned, although the observation of a hyperbolic dependence for the Leu-*i*-Am derivative **3.1d** supports a specific inhibition process. The phenylalanine derivative **3.1a** did not inactivate papain. The lack of papain-inhibitory activity of compounds bearing a Phe residue directly attached to the “warhead”, was already found by Hanzlik *et al.*<sup>28</sup> (as mentioned in Section 2.3) and it was further observed for the synthesised vinyl sultams.

The most potent inhibitors were the indolequinone **3.21**, the glycine derivative **3.1b** ( $k_2 = 35.4$  M<sup>-1</sup> s<sup>-1</sup>) and 2-bromo-1,4-naphthoquinone **3.6** ( $k_2 = 33.3$  M<sup>-1</sup> s<sup>-1</sup>). The action of **3.21** may, however, be due to the nucleophilic attack of Cys25 to aldehyde function, instead of involving Michael addition.

Comparing the kinetic parameters of **3.1b** and **3.6**, it is clear that the first-order rate constant for the chemical inactivation step,  $k_{\text{inact}}$ , plays an important role in the inhibitory activity of **3.6**. In fact, this compound showed the highest  $k_{\text{inact}}$  of all, consistent with the propensity of halo-quinones to undergo nucleophilic substitution, ascribed to the increased electron affinity provided by the substituent.<sup>122</sup> The expected contribution of an electron-withdrawing group to the increase of the activity is also clear in the Phe and NHMe series, particularly in the case of the brominated phenylalanine derivative **3.2a** (1.92 M<sup>-1</sup> s<sup>-1</sup>) compared to its inactive non-halo counterpart **3.1a**.

In contrast, the potency of the glycine derivative **3.1b** is connected with its  $K_I$  (9.57 μM), which is the lowest in the series. This suggests that the Gly residue is able to promote stabilization of the non-covalent enzyme-inhibitor complex, directing the naphthoquinone moiety to the active cysteine residue thereby enhancing the inhibitory potency, even at low alkylation rate constants. Modelling the interaction of this compound with papain revealed that all top 10 conformations presented hydrogen bonding interactions between the carbonyl oxygen atom at C-4 and NH of Gln19 (Figure 3.16). This orientation presents C-3 close (2.8-2.9 Å) to the sulphur atom of Cys25, as would be expected for Michael addition chemistry. The ethyl glycinate moiety is pointing toward the S2 pocket, although it does not reach this binding site.

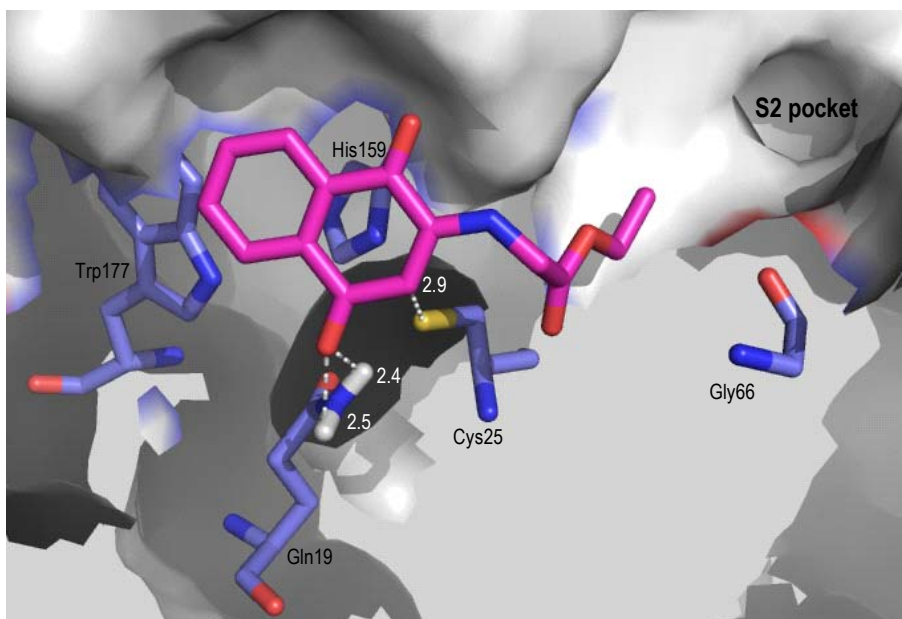


**Figure 3.16 Gold-generated active site interaction of papain with 3.1b (magenta).** Figure generated using Pymol software.<sup>26</sup> The molecular modelling calculations were performed by Dr. Rita C. Guedes (from the Faculty of Pharmacy, University of Lisbon).

The suggestion that the ability of the inhibitor to fit in the active site of papain may be much more important than the intrinsic electrophilicity of the naphthoquinone is further supported by the comparison of the kinetic parameters for the glycine derivatives, for which the halo compounds **3.2b** and **3.3b** are weaker inhibitors than the non-halo counterpart **3.1b** (largely, though not exclusively, due to an increase in the  $K_I$  value). These observations also suggest that substitution both at C-2 and C-3 positions of the naphthoquinone core may be detrimental to inhibitory activity. In fact, a similar situation seems to occur in the case of the methylamino bromo derivative **3.2c** which, in contrast to 2-bromo-1,4-naphthoquinone **3.6**, did not exhibit saturation kinetics.

Analysing both inhibition kinetic parameters and LUMO energy values (Table 3.3) led to the interesting finding that for compounds **3.1b**, **3.2b**, **3.3b**, **3.5** and **3.6** a trend exists in which  $k_{\text{inact}}$  increase as the corresponding LUMO energies decrease, suggesting that the chemical inactivation step of papain might be a function of the LUMO energy of the inhibitor. Even so, as  $k_{\text{inact}}$  values vary only 7-fold (**3.6** versus **3.1d**), whereas  $K_I$  values vary ~30-fold (**3.1b** versus **3.3b**), it would seem that the overall activity of the compounds toward papain is governed to a large extent by the molecular recognition of the inhibitor prior to the irreversible reaction step. Indeed, it was not possible to establish any correlation between the



apparent second-order rate constants,  $k_2$ , and LUMO energies, indicating that inhibitory activity does not parallel chemical reactivity.

**Papain-inhibitory activity of naphthoquinone, juglone and lawsone.** Naphthoquinone **3.8**, juglone **3.12** and lawsone **3.19** were shown to be time-dependent inhibitors but, unfortunately, plotting the enzyme residual activity against incubation time presented a scattering of points which were poorly fitted to a pseudo-first-order kinetics (Figure 3.17), so their inhibitory activity was evaluated at fixed time and concentration of the inhibitor.

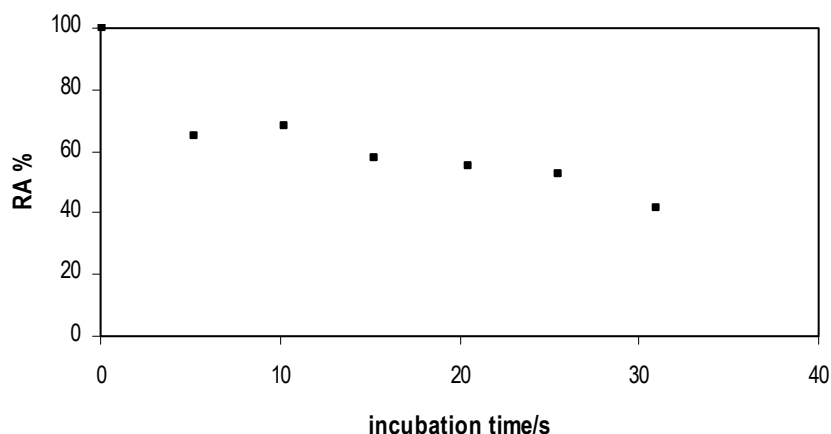


**Figure 3.17** Time course of papain inactivation by juglone **3.12**, at pH 7.0 at 25 °C. The inhibitor concentration was 65  $\mu\text{M}$ . The enzymatic activity is expressed as residual activity percentage (RA%). This inhibition pattern was observed for concentrations ranging from 50 to 130  $\mu\text{M}$ , up to 80-min incubation.

For compounds **3.8** and **3.12**, this departure from the usual behaviour was thought to be caused by the instability of the compounds in the reaction buffer with DTT. This hypothesis was formulated on the basis of two facts; first, that enzyme-inhibitor incubation mixture turned from pale yellow to brown, this colour change only occurring in the presence of DTT, and second, that these compounds have a high reactivity toward simple thiols, as reported by Öllinger *et al.*<sup>47</sup> and further observed in the present work (Section 3.2).

Thus, the possible interaction with DTT was further investigated by taking into account the contribution of the two properties used by quinones, redox *versus* electrophilicity.

As already mentioned, quinones may function as redox cyclers in the presence of DTT and oxygen, generating reactive oxygen species that inactivate cysteine proteases. When quinone is inhibiting the enzyme by this indirect mechanism, its action is prevented/reduced by performing the enzyme-inhibitor incubation in an antioxidant environment.<sup>138</sup> Having this in mind, compound **3.12** (65  $\mu$ M) was assayed keeping the incubation mixture under N<sub>2</sub> or, alternatively, by adding ascorbic acid to the incubation buffer. Inhibition was not prevented or reduced in both experiments, excluding the possible existence of significant redox mechanism.

On the other hand, when quinone is acting as an electrophile and is significantly reactive toward DTT, increasing the concentration of this agent should deplete the inhibitor, protecting the enzyme from inactivation.<sup>138</sup> The enzyme-inhibitor incubation was therefore carried out in the presence of an excess of DTT (13.1 mM *versus* the original 1.7 mM). As expected, compound **3.12** (65  $\mu$ M) failed to inhibit papain completely.

These results showed that the atypical inactivation pattern found for derivatives **3.8** and **3.12** may be ascribed to the presence of DTT that reacts with the compounds due to their excessively high electrophilicity. An accurate determination of inhibition kinetic parameters might be probably accomplished by performing the enzyme-inhibitor incubation in a medium free from DTT. However, this situation was not further investigated, as the efforts were focused on the detailed assessment of less chemical reactive compounds, such as glycine derivatives, more suitable for drug development.

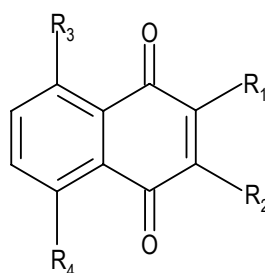
In the case of lawsone **3.19**, the unusual pattern of inhibition was related to the instability of the compound in phosphate buffer pH 7.0, because the enzyme-inhibitor incubation mixture developed an intense orange coloration, even in the absence of DTT. Although this observation could result from the natural colour of the compound, it was suspicious that the coloration presented by the incubation mixture could be as intense as the stock solution of the inhibitor (almost ten times more concentrated). Taking into account the knowledge that lawsone and derivatives are indicators in solution (red in alkaline media and light yellow in acidic media),<sup>125</sup> the colour enhancement was rationalised in terms of a change in the quinoid chromophore structure, due to the ionization of the hydroxyl function at C-2, whose pK<sub>a</sub> value is 4.10.<sup>140</sup>

### 3.3.2 Bovine spleen cathepsin B inhibition studies

The naphthoquinones with highest papain-inhibitory activity were also evaluated against bovine spleen cathepsin B ( $k_{\text{obs}}$  values are listed in Appendix VI). As shown in Table 3.4, compounds were found to be time-dependent inhibitors, with second-order rate constant  $k_2$  values 3-20 times smaller than those for papain. The most potent inhibitor for papain, the glycine derivative **3.1b**, was also the most active against cathepsin B. Its dissociation constant  $K_1$  is also the lowest in the series, with a similar value to that with papain. In contrast, 2-bromo-1,4-naphthoquinone **3.6** exhibited a linear dependence between  $k_{\text{obs}}$  and  $[I]$  instead of the hyperbolic relationship observed for papain, suggesting a drastic increase in the  $K_1$  value.

The Leu-*i*-Am derivative **3.1d** was also assayed. After 3-h incubation, it inhibited the enzyme by 50% at 156  $\mu\text{M}$  (the maximal concentration tested against papain). The compound was not further investigated, as the kinetic results might be compromised by the instability of cathepsin after 4-h incubation (see Appendix I, Section AI.2.2). However, it should be noted that the same concentration of inhibitor inactivated papain *ca.* 3-fold times faster than inhibited cathepsin B.

**Table 3.4** LUMO energies and kinetic data for inactivation of bovine spleen cathepsin B by naphthoquinones.



Compound	R <sup>1</sup>	R <sup>2</sup>	R <sup>3</sup>	R <sup>4</sup>	Bovine spleen cathepsin B		
					$k_2$ ( $\text{M}^{-1} \text{s}^{-1}$ )	$k_{\text{inact}}$ ( $10^{-4} \text{s}^{-1}$ )	$K_1$ ( $\mu\text{M}$ )
<b>3.1b</b>	GlyOEt	H	H	H	8.03	$1.12 \pm 0.06$	$14.0 \pm 3.07$
<b>3.2b</b>	GlyOEt	Br	H	H	4.37	$2.44 \pm 0.24$	$55.9 \pm 14.1$
<b>3.5</b>	OEt	H	H	H	0.54	$4.28 \pm 0.63$	$797 \pm 228$
<b>3.6</b>	Br	H	H	H	5.65	—	—

### 3.3.3 Falcipain-2 and *Plasmodium falciparum* inhibition studies

The indolequinone **3.22** and some of the naphthoquinones were evaluated against recombinant falcipain-2 and *Plasmodium falciparum* W2 (the tested compounds are indicated by an asterisk in Table 3.3). These studies were carried out by Dr. Philip J. Rosenthal's group (University of California), following a reported protocol.<sup>16</sup>

Derivative **3.3a** exhibited the best IC<sub>50</sub> value against *Plasmodium falciparum* (3.02 μM), but this effect was not associated with a favourable inactivation of falcipain-2 (IC<sub>50</sub> >10 μM). Therefore, antimalarial activity is probably due to a different mechanism than inhibition of this enzyme, but this subject is beyond the scope of this thesis and it was not further investigated.

For the remaining compounds, all IC<sub>50</sub> values were over 10 μM (the accurate value was not determined beyond this concentration limit). This situation was not totally unexpected due to the simplicity of the 1,4-naphthoquinone derivatives and the lack of a specific sequence to probe the interaction with the active site of falcipain.

It should be noted that Kapadia *et al.*<sup>141</sup> reported the activity against *Plasmodium falciparum* W2 of compounds **3.8**, **3.9**, **3.12**, **3.13** and **3.19**, with IC<sub>50</sub> values ranging from 8.18 μM (**3.8**) to 72.9 μM (**3.12**).

### 3.3.4 Porcine pancreatic elastase inhibition studies

The group of derivatives assayed for activity against cathepsin B (Section 3.3.2) was also evaluated against porcine pancreatic elastase, a serine protease. They revealed to be inactive when incubated for 2 h over the same range of concentrations used against papain and cathepsin B.

## **CHAPTER 4**

### **CONCLUSIONS AND FUTURE DIRECTIONS**



## 4. CONCLUSIONS AND FUTURE DIRECTIONS

This thesis aimed the achievement of novel irreversible inhibitors of papain-like cysteine proteases. The design of the inhibitors involved the attachment of vinyl sultam or 1,4-naphthoquinone cores to a peptide segment complementary to the target enzyme.

Five dipeptide vinyl sultams were synthesised, but they all demonstrated weak activity against falcipain-2 ( $IC_{50}$  between 13.7 and 48.4  $\mu\text{M}$ ) and *Plasmodium falciparum* W2 ( $IC_{50} > 7.8 \mu\text{M}$ ), although selectivity for falcipain-2 over papain was demonstrated (compounds lack papain-inhibitory activity). Docking studies suggested that the binding mode of vinyl sultams to cysteine proteases (cruzain and papain) does not favour the inhibition reaction, *i.e.* the conjugate addition of Cys25 to the vinyl sultam system.

Therefore, the vinyl sultam, *i.e.*  $\gamma$ - and  $\delta$ - vinyl sultams, is not a good scaffold from which to obtain inhibition of papain-like enzymes.

The 1,4-naphthoquinone derivatives have been evaluated against papain and bovine spleen cathepsin B, exhibiting an irreversible inhibitory action in both enzymes with second-order rate constants,  $k_2$ , ranging from 0.67 to 35.4  $\text{M}^{-1} \text{s}^{-1}$  for papain, and from 0.54 to 8.03  $\text{M}^{-1} \text{s}^{-1}$  for cathepsin B. Some compounds displayed a hyperbolic dependence of the first-order inactivation rate constant,  $k_{\text{obs}}$ , with the inhibitor concentration, indicative of a specific interaction process between enzyme and inhibitor, with  $K_I$  values between 9.57 and 266  $\mu\text{M}$  for papain, and between 14.0 and 797  $\mu\text{M}$  for cathepsin B. In addition, compounds failed the inhibition of porcine pancreatic elastase, a serine protease, suggesting selectivity for cysteine proteases.

As stated before (Section 1.3), the intrinsic chemical reactivity of quinones may be cited as a potential limitation to their clinical use. On the other hand, it is recognised that the quinone system can be structurally modified in such a way that selective targeting can be achieved. Atovaquone **1.18**, a drug approved and commercialised for human use, is a clear “proof of concept” within this context.

In connection, the present investigation found that enzyme inhibitory activity of the 1,4-naphthoquinone derivatives does not parallel chemical reactivity toward the model thiol cysteine. Instead, it appears to be mainly affected by how well these inhibitors fit into the enzyme active site. In fact, it must be stressed that glycine derivative **3.1b** (structure is conveniently repeated in Figure 4.1), though being one of the least reactive compounds toward the thiol cysteine, is one of the best papain inactivators ( $k_2 = 35.4 \text{M}^{-1} \text{s}^{-1}$ ). A  $10^3$ -fold

ratio between the enzymatic and non-enzymatic reactivity of naphthoquinones can be estimated by inferring the second-order rate constant,  $k_{\text{cat}}$  ( $0.033 \text{ M}^{-1} \text{ s}^{-1}$ ), for the reaction of **3.1b** with cysteine at pH 7.0 (the pH value of the papain inhibition studies). This selectivity points toward the fundamental role of enzyme binding in the inhibition process, as **3.1b** has the lowest  $K_1$  ( $9.57 \text{ }\mu\text{M}$ ) in the series, and it is quite important considering that, under biological conditions, thiol species are expected to occur at high concentrations, *e.g.*, GSH, promoting unspecific undesirable conjugations.

According to this preliminary information, the 1,4-naphthoquinone scaffold appears to be a promising lead structure in the design of papain-like cysteine protease inhibitors. However, the viability of this approach is dependent on the cytotoxicity of the compounds, which could not be investigated due to time limitations and that should be a primary subject in the following steps of the project.

The present study found a linear correlation between the chemical reactivity toward cysteine and LUMO energies, used as a parameter of electrophilicity. This finding strongly suggests that the LUMO values can be useful predictors of the chemical reactivity of another 1,4-naphthoquinone derivatives. It is imperative to investigate if a similar relationship exists in a cellular context. It would be very helpful if limiting LUMO energy values could be found as corresponding to a safe cytotoxic profile, because the energies could be calculated in the design of new derivatives, anticipating the cytotoxicity of future generations of compounds and deciding about their feasibility before synthetic work.

Another remaining subject is the unambiguously assess of the nature of the interaction between papain and the 1,4-naphthoquinone derivatives using mass spectrometry, namely MALDI-MS of tryptic digests. As discussed in Section 3.3.1, all evidences point out to a covalent bonding rather than oxidation, with Cys25 being the most likely site of modification. Nevertheless, this should be clarified.

Further efforts should focus on (i) the adjustment of the inherent chemical reactivity to biological tolerable values and (ii) on the exploitation of the specific binding requirements to the target enzyme. In this latter context, the design of novel inhibitors must be necessarily based on computer-aided structure-based techniques. As described in Section 3.3.1, docking of **3.1b** into papain revealed that the inhibitor is pointing toward the specificity site, *i.e.* P2, although not reaching it. Therefore, modelling studies may proceed from this compound, by manipulating the glycinylyl substituent in order to find extra binding interactions with the P2 pocket.



Another approach is suggested in Figure 4.2. The general structure **4.1** encompasses a recognition segment, which is also an electron-withdrawing and leaving group. This strategy was derived from the interesting inactivation of papain by 2-bromo-1,4-naphthoquinone **3.6**, ( $k_2 = 33.3 \text{ M}^{-1} \text{ s}^{-1}$ ), in which the chemical inactivation step, assessed by  $k_{\text{inact}}$ , plays an important role (it was the highest  $k_{\text{inact}}$  in the series). Thus, it is expected that derivatives **4.1** might lead to stronger inhibitors by increasing specificity and chemical reactivity. Whether this latter property will be tolerable is, at this point, unknown.

One of the best inhibitors for papain in this thesis was the indolequinone **3.21** (structure is conveniently repeated in Figure 4.1), with  $k_2 = 35.2 \text{ M}^{-1} \text{ s}^{-1}$ . This compound and its analogue **3.22** can be easily processed by derivatisation of the hydroxyl/aldehyde group.

As papain is a good model for its family of enzymes, it may be reasoned that **3.1b**, **3.21** and **4.1** might be also starting points for other papain-like proteases. Extending the 1,4-naphthoquinone/indolequinone “warhead” to cysteine proteases that are potential therapeutic targets will be the ultimate and most important goal of the research line initiated in this thesis.

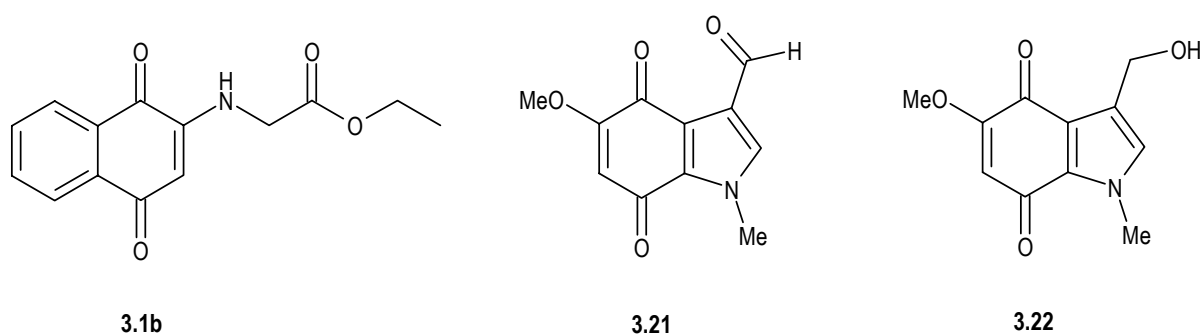


Figure 4.1 Inhibitors **3.1b**, **3.21** and **3.22**.

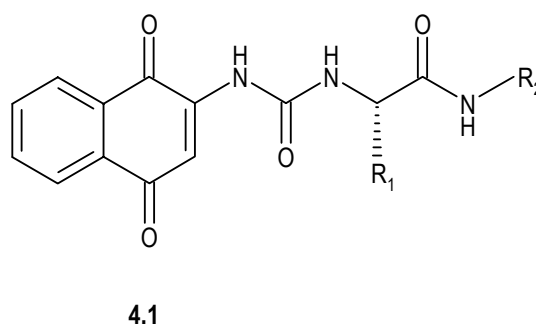


Figure 4.2 Proposed structure for inhibitor development.



## **CHAPTER 5**

### **EXPERIMENTAL SECTION**



---

## 5. EXPERIMENTAL SECTION

### 5.1 Synthesis

#### 5.1.1 Reagents and Solvents

Reagent grade chemicals were bought from Sigma-Aldrich and Merck (solvents). The amines were dried over potassium hydroxide and distilled under reduced pressure, with the exception of TEA and pyridine, which were distilled under atmospheric pressure. DMSO, DCM and MeOH were dried by distillation from calcium hydride. THF was dried by distillation from sodium-benzophenone. Isopropanol was dried by distillation from Mg/I<sub>2</sub>.<sup>108</sup> The remaining compounds were used without further purification.

#### 5.1.2 Chromatography

Column chromatography was performed with silica gel (Merck, 230-400 mesh ASTM). Preparative TLC was performed on silica gel GF<sub>254</sub> (Merck 1.07730). TLC was performed on pre-coated silica gel 60 F<sub>254</sub> (Merck) and visualized under UV light or by exposure to iodine vapour. All the reactions were monitored by TLC unless otherwise stated.

#### 5.1.3 Equipment

Melting points were determined using a Kofler camera Bock Monoscope M and are uncorrected. The IR spectra were determined using thin films on NaCl plates or preparing KBr pellets on a Nicolet Impact 400 FTIR spectrophotometer and only the most significant absorption bands are reported. Low-resolution mass spectra were recorded using a VG Quattro LCMS instruments. GC-MS spectra were performed on a Hewlett Packard 5890 Series II with a 5970 Series mass detector. Optical rotations were obtained using a Perkin Elmer 241 polarimeter, using a 1 dm length cuvette (concentration is expressed in g/100 mL). Elemental analyses were performed using an EA 1110 CE Instruments automatic analyser.

HR-ESI-MS were recorded on an ESI-TOF spectrometer (Biotof II Model, Bruker). NMR spectra were recorded on a Bruker Avance 400 NMR spectrometer ( $^1\text{H}$  400 MHz;  $^{13}\text{C}$  100.61 MHz), on a Jeol JNM-300 ( $^1\text{H}$  300 MHz;  $^{13}\text{C}$  75 MHz) or on a Jeol JNM-60 ( $^1\text{H}$  60 MHz).  $^1\text{H}$  and  $^{13}\text{C}$  chemical shifts,  $\delta$ , are expressed in ppm (parts *per* million) and are relative to the corresponding resonance of tetramethylsilane. Coupling constants ( $J$ ) are reported in hertz (Hz).

#### 5.1.4 Experimental procedures and product characterisation

##### 5.1.4.1 *N*-Phenyl- $\beta$ -sultam

###### ***N*-Phenylethanesulfonamide (2.46a) and 2-chloro-*N*-phenylethanesulfonamide (2.48)**

2-Chloroethanesulfonyl chloride **2.20a** (3.2 mL; 30.7 mmol) diluted with DCM (5 mL) was added slowly to a solution of aniline (2.8 mL; 30.7 mmol) in DCM (100 mL) with TEA (4.3 mL; 30.7 mmol), at  $-10\text{ }^\circ\text{C}$ . The reaction mixture was vigorously shaken between the additions of 2-chloroethanesulfonyl chloride. At this point, the formation of a white precipitate (TEA salt) was observed. Stirring at  $-10\text{ }^\circ\text{C}$  was continued for a further 20 min, after which the reaction medium was extracted with 2M-sodium hydroxide ( $2\times 100\text{ mL}$ ). The aqueous layer became turbid after acidification with conc. hydrochloric acid; it was then extracted with DCM ( $4\times 50\text{ mL}$ ). The organic layer was washed with water (100 mL) and dried with anhydrous magnesium sulfate. The solvent was removed to afford 3.6 g (65%) of **2.46a**.

Alternatively, a mixture of aniline (1.1 mL; 12.3 mmol) and 2-chloroethanesulfonyl chloride **2.20a** (0.64 mL; 6.1 mmol), in toluene (20 mL), was stirred for 24 h at rt. The reaction medium was washed with hydrochloric acid 5% (w/v) and water, then it was submitted to a column chromatography on silica gel (*n*-hexane/DCM 1:4 $\rightarrow$ 0:1) to afford compounds **2.46a** (412 mg; 37%) and **2.48** (46 mg; 3%).

**2.46a**; yellow oil; IR (film):  $\nu_{\text{max}} = 3265$  (NH), 1598, 1495, 1411, 1340 (S=O), 1150 (S=O), 925, 753, 695, 665  $\text{cm}^{-1}$ .  $\delta$   $^1\text{H}$  NMR (300 MHz,  $\text{CDCl}_3$ ): 5.94 (dd, 1H,  $J = 0.4, 9.7$ ,  $\text{H}_b$ ), 6.27 (dd, 1H,  $J = 0.4, 16.5$ ,  $\text{H}_a$ ), 6.54 (dd, 1H,  $J = 9.7, 16.5$ ,  $\text{H}_c$ ), 7.21–7.41 (m, 6H, Ph and NH).  $\delta$   $^{13}\text{C}$  NMR (75 MHz,  $\text{CDCl}_3$ ): 121.2 (CH), 125.6 (CH), 128.6 ( $\text{CH}_2=$ ), 129.6 (CH), 135.2

(=CH), 136.3 (C). Carbon signal assignments were made using HMQC and DEPT techniques. ESI-MS  $m/z$  (rel. int.) 201 ( $\text{MNH}_4^+$ ) (56).

**2.48**; yellow oil; IR (film):  $\nu_{\text{max}} = 3268$  (NH), 1599, 1494, 1412, 1344 (S=O), 1153 (S=O), 930, 753, 695, 663  $\text{cm}^{-1}$ .  $\delta$   $^1\text{H}$  NMR (300 MHz,  $\text{CDCl}_3$ ): 3.48 (t, 2H,  $J = 7.0$ ,  $\text{CH}_2\text{SO}_2$ ), 3.86 (t, 2H,  $J = 7.0$ ,  $\text{CH}_2\text{Cl}$ ), 7.20–7.37 (m, 6H, Ph and NH).  $\delta$   $^{13}\text{C}$  NMR (75 MHz,  $\text{CDCl}_3$ ): 36.7 ( $\text{CH}_2\text{SO}_2$ ), 52.7 ( $\text{CH}_2\text{Cl}$ ), 121.2 (CH), 125.9 (CH), 129.8 (CH), 135.9 (C). ESI-MS  $m/z$  (rel. int.) 242 ( $\text{MNa}^+$ ) (95).

### ***N*-Phenyl-2-hydroxyethanesulfonamide (2.25a)**

Compound **2.46a** (1.0 g; 5.4 mmol) was added to a solution of sodium hydroxide (1.3 g; 32.5 mmol) in water (25 mL). The resultant yellow suspension was refluxed for 3 days, during which time the mixture turned white milky. Then, it was acidified with conc. hydrochloric acid and extracted with DCM (3×40 mL). The organic layer was washed (100 mL) with water, dried with anhydrous magnesium sulfate and evaporated to yield a yellow oil (487 mg), which gave **2.25a** (422 mg) by column chromatography on silica gel (50 g) using a gradient of DCM/EtOAc (1:0→7:3).

**2.25a**; yellow oil (39%); IR (film):  $\nu_{\text{max}} = 3505$  (OH), 3263 (NH), 1598, 1493, 1416, 1334 (S=O), 1143 (S=O), 926, 755, 695  $\text{cm}^{-1}$ .  $\delta$   $^1\text{H}$  NMR (300 MHz,  $\text{CDCl}_3$ ): 2.05 (brs, 1H, OH), 3.26 (t, 2H,  $J = 5.2$ ,  $\text{CH}_2\text{SO}_2$ ), 4.07 (t, 2H,  $J = 5.2$ ,  $\text{CH}_2\text{OH}$ ), 6.82 (brs, 1H, NH), 7.14–7.34 (m, 6H, Ph e NH).  $\delta$   $^{13}\text{C}$  NMR (75 MHz,  $\text{CDCl}_3$ ): 52.4 ( $\text{CH}_2\text{SO}_2$ ), 57.4 ( $\text{CH}_2\text{OH}$ ), 121.7 (CH), 125.8 (CH), 129.7 (CH), 136.6 (C). The  $^1\text{H}$  NMR spectrum is consistent with the one published.<sup>67</sup> Carbon signal assignments were based on the chemical shift and on DEPT techniques. ESI-MS  $m/z$  (rel. int.) 219 ( $\text{MNH}_4^+$ ) (100).

### ***N*-Phenyl-2-hydroxyethanesulfonamide Mesylate (2.8a)**

The reaction was carried out under  $\text{N}_2$ . Mesyl chloride (0.58 mL; 7.5 mmol) was added to a solution of **2.25a** (1.0 g; 5.0 mmol) in dry DCM (25 mL) with TEA (1.0 mL; 7.5 mmol), at 0 °C. After 30 min of stirring, at 0 °C, the reaction mixture was washed with 20 mL of hydrochloric acid 5% (w/v), of saturated sodium chloride solution and of water. Then, it was dried with anhydrous magnesium sulfate and the solvent was evaporated to afford a yellowish solid (1.2 g). Compound **2.8a** (644 mg) was purified by washing crude product with cold chloroform.

**2.8a**; white crystals (46%); m.p. 101-103 °C, lit.<sup>67</sup> 94-95 °C; IR (film):  $\nu_{\text{max}} = 3274$  (NH), 1598, 1493, 1347 (S=O), 1173 and 1149 (S=O), 990, 964, 797, 756  $\text{cm}^{-1}$ .  $\delta$   $^1\text{H}$  NMR (300

MHz, CD<sub>3</sub>CN): 3.01 (s, 3H, CH<sub>3</sub>SO<sub>2</sub>O), 3.47 (t, 2H,  $J = 5.8$ , CH<sub>2</sub>SO<sub>2</sub>), 4.49 (t, 2H,  $J = 5.8$ , MsOCH<sub>2</sub>), 7.16–7.39 (m, 5H, Ph), 7.72 (brs, 1H, NH).  $\delta$  <sup>13</sup>C NMR (75 MHz, CD<sub>3</sub>CN): 37.9 (CH<sub>3</sub>SO<sub>2</sub>O), 51.1 (CH<sub>2</sub>SO<sub>2</sub>), 65.2 (MsOCH<sub>2</sub>), 122.1 (CH), 126.3 (CH), 130.8 (CH), 138.4 (C). The <sup>1</sup>H NMR spectrum is consistent with the one published.<sup>67</sup> Carbon signal assignments were based on the chemical shift and on DEPT techniques. ESI-MS  $m/z$  (rel. int.) 297 (MNH<sub>4</sub><sup>+</sup>) (100).

### 2-Phenyl-1,2-thiazetidine 1,1-dioxide (2.5a)

To a solution of **2.8a** (122 mg; 0.4 mmol) in dry DMSO (20 mL) was added ground sodium carbonate (140 mg; 1.3 mmol). The mixture was stirred at 60 °C for 1 h under N<sub>2</sub>, after which it was diluted with water and extracted with DCM (4×20 mL) and EtOAc (2×20 mL). The organic layers were washed with water (2×20 mL), combined, dried with anhydrous magnesium sulfate and evaporated to give an oil (30 mg), which crystallized in a mixture of EtOH/water to yield **2.5a** (7 mg).

**2.5a**; white crystals (9%); m.p. 133-135 °C, lit. 132 °C,<sup>65</sup> 128-129 °C;<sup>67</sup> IR (film):  $\nu_{\max} = 1590, 1498, 1317$  (S=O), 1205 and 1180 (d, S=O), 1151 (S=O), 760, 694 cm<sup>-1</sup>.  $\delta$  <sup>1</sup>H NMR (300 MHz, CDCl<sub>3</sub>): 3.65 (t, 2H,  $J = 6.6$ , CH<sub>2</sub>N), 4.21 (t, 2H,  $J = 6.6$ , CH<sub>2</sub>SO<sub>2</sub>), 6.84–7.30 (m, 5H, Ph).  $\delta$  <sup>13</sup>C NMR (75 MHz, CDCl<sub>3</sub>): 33.1 (CH<sub>2</sub>N), 57.3 (CH<sub>2</sub>SO<sub>2</sub>), 115.1 (CH), 123.4 (CH), 129.6 (CH), 138.3 (C). The <sup>1</sup>H NMR spectrum is consistent with the one published.<sup>67</sup> Carbon signal assignments were based on the chemical shift and on DEPT techniques. ESI-MS  $m/z$  (rel. int.) 201 (MNH<sub>4</sub><sup>+</sup>) (63).

### N-Phenylmethanesulfonamide (2.50)

According to Page *et al.*,<sup>67</sup> mesyl chloride (4.5 mL; 58.2 mmol) was added slowly to a solution of aniline (10.6 mL; 116.3 mmol) in toluene (50 mL), which led to the formation of a white precipitate. The mixture was refluxed for 2 h and the solvent was removed to give a brown solid (9.0 g), which was recrystallized from a mixture of EtOH/water to give **2.50** (5.7 g).

**2.50**; white crystals (57%); m.p. 102-104 °C, lit.<sup>67</sup> 101-102 °C; IR (film):  $\nu_{\max} = 3257$  (NH), 1595, 1498, 1473, 1322 (S=O), 1158 (S=O), 760, 694 cm<sup>-1</sup>.  $\delta$  <sup>1</sup>H NMR (60 MHz, CDCl<sub>3</sub>): 3.03 (s, 3H, CH<sub>3</sub>), 7.33 (m, 6H, Ph and NH).

This compound was initially synthesised with lower yields following two further procedures (Table 5.1).



**Table 5.1** Conditions for the synthesis of *N*-phenylmethanesulfonamide.

NH <sub>2</sub> Ph (mol eq)	NaOH (mol eq)	TEA (mol eq)	Procedure	Temperature/Reaction time	Yield%
1.5	1.1	—	A	rt/2 h	23
1.5	1.1	—	A	reflux/1 h	17
1.5	1.1	—	A	rt/12 h	13
1.5	—	1.1	B	rt/3 h	40

Procedure A was based on the literature<sup>108</sup> and consisted in the addition of aniline and mesyl chloride to an aqueous solution of sodium hydroxide. The mixture was vigorously stirred (except for the reflux conditions), then it was washed with ethyl ether and acidified with conc. hydrochloric acid to afford **2.50** as a white solid, which was collected by filtration *in vacuo*. The product was recrystallized from a mixture of EtOH/water.

In procedure B, mesyl chloride was added dropwise to a solution of aniline in DCM. After stirring, extraction of the reaction medium with 2M-sodium hydroxide, followed by acidification with conc. hydrochloric acid induced the precipitation of **2.50**. After being collected by filtration *in vacuo*, the product was recrystallized from a mixture of EtOH/water.

#### ***N*-(Chloromethyl)-*N*-phenylmethanesulfonamide (2.49a)**

A mixture of *N*-phenylmethanesulfonamide **2.50** (466 mg; 2.7 mmol), paraformaldehyde (150 mg) and chlorotrimethylsilane (10.5 mL; 83.0 mmol) in DCM (5 mL) was refluxed for 21 h, after which the solution was no longer cloudy. DCM and chlorotrimethylsilane were evaporated to afford compounds **2.49a** and **2.50** as a 4:1 mixture (584 mg). The reaction was monitored at 5 h and 21 h using aliquots (1 mL) from the reaction medium which were evaporated, analysed by <sup>1</sup>H NMR and put back into the reaction mixture.

**2.49a**; white amorphous solid (81%); δ <sup>1</sup>H NMR (60 MHz, CDCl<sub>3</sub>): 3.02 (s, CH<sub>3</sub> of **2.50**), 3.14 (s, 3H, CH<sub>3</sub>SO<sub>2</sub>), 5.74 (s, 2H, CH<sub>2</sub>Cl), 7.52–7.64 (m, 5H, Ph).

#### **Preparation of LDA** (employed in the reactions described in Table 2.1, Chapter 2)

Preparation of LDA was carried out under N<sub>2</sub> at 0 °C. In a typical experimental procedure, a 1.6 M solution of *n*-BuLi in *n*-hexane (1.6 mmol) was added to a solution of diisopropylamine (0.2 mL; 1.6 mmol) in dry THF (3 mL) and stirred for 15 min.<sup>67</sup>

#### 5.1.4.2 *N*-Benzyl- $\beta$ -sultam

##### *N*-Benzylethanesulfonamide (**2.46b**)

**2.46b** (1.4 g) was prepared from benzylamine (1.3 mL; 12.3 mmol) using the method described earlier for **2.46a**.

**2.46b**; pale oil (58%); IR (film):  $\nu_{\max}$  = 3287 (NH), 1496, 1454, 1425, 1327 (S=O), 1148 (S=O), 971, 841, 739, 699  $\text{cm}^{-1}$ .  $\delta$   $^1\text{H}$  NMR (300 MHz,  $\text{CDCl}_3$ ): 4.16 (brd, 2H,  $J$  = 1.9,  $\text{CH}_2\text{Ph}$ ), 4.54 (brs, 1H, NH), 5.86 (brd, 1H,  $J$  = 9.7,  $\text{H}_b$ ), 6.20 (dd, 1H,  $J$  = 0.9, 16.5,  $\text{H}_a$ ), 6.42 (dd, 1H,  $J$  = 9.7, 16.5,  $\text{H}_c$ ), 7.24–7.29 (m, 5H,  $\text{Ph}$ ).  $\delta$   $^{13}\text{C}$  NMR (75 MHz,  $\text{CDCl}_3$ ): 47.3 ( $\text{CH}_2\text{Ph}$ ), 126.8 ( $\text{CH}_2=$ ), 127.9 (CH), 128.1 (CH), 128.8 (CH), 136.0 (=CH), 136.4 (C). ESI-MS  $m/z$  (rel. int.) 215 ( $\text{MNH}_4^+$ ) (98).

##### *N*-Benzyl-2-hydroxyethanesulfonamide (**2.25b**)

**2.25b** (115 mg) was prepared from **2.46b** (293 mg; 1.5 mmol) using the method described earlier for **2.25a**. Reaction time: 3 h. Purification by column chromatography on silica gel using a gradient of DCM/EtOAc (1:0→3:2).

**2.25b**; white crystals (36%); m.p. 60–62  $^\circ\text{C}$ ; IR (film):  $\nu_{\max}$  = 3452–3305 (br, OH and NH), 1429, 1322 and 1298 (d, S=O), 1136 (S=O), 846, 736, 699  $\text{cm}^{-1}$ .  $\delta$   $^1\text{H}$  NMR (300 MHz,  $\text{CDCl}_3$ ): 2.37 (t, 1H,  $J$  = 5.7, OH), 3.11 (t, 2H,  $J$  = 5.3,  $\text{CH}_2\text{SO}_2$ ), 3.96 (q, 2H,  $J$  = 5.5,  $\text{CH}_2\text{OH}$ ), 4.26 (d, 2H,  $J$  = 6.1,  $\text{CH}_2\text{Ph}$ ), 4.69 (brs, 1H, NH), 7.27–7.30 (m, 5H,  $\text{Ph}$ ).  $\delta$   $^{13}\text{C}$  NMR (75 MHz,  $\text{CDCl}_3$ ): 47.4 ( $\text{CH}_2\text{SO}_2$ ), 54.7 ( $\text{CH}_2\text{OH}$ ), 57.4 ( $\text{CH}_2\text{Ph}$ ), 128.1 (CH), 128.3 (CH), 129.0 (CH), 136.6 (C). ESI-MS  $m/z$  (rel. int.) 233 ( $\text{MNH}_4^+$ ) (100).

##### *N*-Benzyl-2-hydroxyethanesulfonamide Mesylate (**2.8b**)

**2.8b** was prepared from **2.25b** (449 mg; 2.1 mmol) using the method described earlier for **2.8a**. Reaction time: 30 min. Crude product (548 mg) was washed with cold chloroform to give pure **2.8b** (127 mg).

**2.8b**; white crystals (21%); m.p. 88–89  $^\circ\text{C}$ ; IR (film):  $\nu_{\max}$  = 3240 (NH), 1453, 1433, 1345 and 1310 (d, S=O), 1170 and 1135 (d, S=O), 804, 732, 696  $\text{cm}^{-1}$ .  $\delta$   $^1\text{H}$  NMR (300 MHz,  $\text{CD}_3\text{CN}$ ): 3.06 (s, 3H,  $\text{CH}_3\text{SO}_2\text{O}$ ), 3.31 (t, 2H,  $J$  = 6.0,  $\text{CH}_2\text{SO}_2$ ), 4.25 (d, 2H,  $J$  = 6.2,  $\text{CH}_2\text{Ph}$ ), 4.48 (t, 2H,  $J$  = 6.0,  $\text{MsOCH}_2$ ), 5.83 (brs, 1H, NH), 7.37–7.38 (m, 5H,  $\text{Ph}$ ).  $\delta$   $^{13}\text{C}$  NMR (75 MHz,  $\text{CD}_3\text{CN}$ ): 37.8 ( $\text{CH}_3\text{SO}_2\text{O}$ ), 47.6 ( $\text{CH}_2\text{SO}_2$ ), 52.2 ( $\text{CH}_2\text{Ph}$ ), 65.4 ( $\text{MsOCH}_2$ ), 128.7 (CH), 129.0 (CH), 129.7 (CH), 138.9 (C). ESI-MS  $m/z$  (rel. int.) 311 ( $\text{MNH}_4^+$ ) (100).

**2-(Benzylamino)ethanesulfonic acid (2.15b)**

A mixture of finely ground sodium 2-chloroethanesulfonate **2.17a** (1.0 g; 5.3 mmol) and benzylamine (2.3 mL; 20.0 mmol) was stirred at 100 °C for 2 h. During this time, the sulfonate was gradually dissolved in benzylamine and a green color started to develop. The amine was removed under reduced pressure to afford a white solid (1.0 g), which was crystallized from a mixture of EtOH/water<sup>65</sup> to give **2.15b** (450 mg).

**2.15b**; white solid (39%); m.p. 220-222 °C, lit.<sup>65</sup> 225 °C; IR (KBr):  $\nu_{\max}$  = 3445 (NH), 1600, 1450, 1420, 1251, 1130, 935, 870, 790, 755, 740  $\text{cm}^{-1}$ . <sup>1</sup>H NMR (300 MHz, d<sub>6</sub>-DMSO): 2.81 (t, 2H,  $J$  = 7.0, CH<sub>2</sub>N), 3.12 (t, 2H,  $J$  = 7.0, CH<sub>2</sub>SO<sub>3</sub>), 4.14 (s, 2H, CH<sub>2</sub>Ph), 7.36–7.49 (m, 5H, Ph). The <sup>1</sup>H NMR spectrum is in agreement with that reported in the literature.<sup>65</sup>

**2-Chloroethanesulfonyl fluoride (2.20b)**

A solution of 2-chloroethanesulfonyl chloride **2.20a** (0.9 mL; 8.6 mmol) in dioxane (8 mL) was added dropwise to a solution of potassium fluoride (1.0 g; 17.2 mmol) in water (10 mL). After stirring for 2 h, at rt, the reaction medium was diluted with water (25 mL) and extracted with ethyl ether (2×25 mL). The organic layer was washed with water, dried with anhydrous magnesium sulfate, evaporated and distilled under reduced pressure (39 mm Hg) to give **2.20b** (0.6 g). *This product is eye irritant.*

**2.20b**; yellow liquid (48%); b.p. 100 °C (39 mmHg), lit.<sup>79</sup> 93 °C (52 mmHg), 72-73 °C (18.5 mmHg); IR (film):  $\nu_{\max}$  = 1411 (S=O), 1197 (S=O)  $\text{cm}^{-1}$ .  $\delta$  <sup>1</sup>H NMR (60 MHz, CDCl<sub>3</sub>): 3.62-3.88 (m). GC-MS  $m/z$  (rel. int.) 146 (M<sup>+</sup>) (40), 63 (ClCH<sub>2</sub>CH<sub>2</sub><sup>+</sup>) (70), 27 (CH<sub>2</sub>CH<sup>+</sup>) (100).

**5.1.4.3  $\gamma$ -Sultams core****2-Phenylisothiazolidine 1,1-dioxide (2.27a)**

A mixture of aniline (2.5 mL; 27.0 mmol), TEA (3.8 mL; 27.0 mmol) and 3-chloropropanesulfonyl chloride **2.41a** (3.4 mL; 27.0 mmol) in DCM (40 mL) was refluxed for 1 h. Then, it was washed with 30 mL of hydrochloric acid 5% (w/v) and of saturated sodium chloride solution, dried with anhydrous magnesium sulfate and evaporated to afford 3-chloro-*N*-phenylpropane-1-sulfonamide **2.39a** (5.2 g; 22.4 mmol). This product was subsequently refluxed for 90 min with a solution of sodium hydroxide (0.9 g; 22.4 mmol) and TEA (3.1 mL; 22.4 mmol) in MeOH (28 mL). The solvent was evaporated and the mixture was redissolved in DCM (150 mL), after which it was washed with 100 mL of hydrochloric acid

5% (w/v), of 2M-sodium hydroxide and of water. The organic solution was dried with anhydrous magnesium sulfate and evaporated to afford **2.27a** (2.6 g) as a white amorphous solid which was purified by column chromatography on silica gel using ethyl ether and a mixture of ethyl ether/EtOAc (1:1) as eluents. Alternatively, purification was achieved by recrystallization from a mixture of MeOH/water.<sup>83</sup>

**2.39a**; yellow oil; IR (film):  $\nu_{\max}$  = 3266 (NH), 1599, 1494, 1341 (br, S=O), 1151 (S=O), 925, 754, 695  $\text{cm}^{-1}$ .  $\delta$   $^1\text{H}$  NMR (300 MHz,  $\text{CDCl}_3$ ): 2.30 (tt, 2H,  $J$  = 6.1, 7.5,  $\text{CH}_2\text{CH}_2\text{CH}_2$ ), 3.29 (t, 2H,  $J$  = 7.5,  $\text{CH}_2\text{SO}_2$ ), 3.65 (t, 2H,  $J$  = 6.1,  $\text{CH}_2\text{Cl}$ ), 6.55 (brs, 1H, NH), 7.34–7.51 (m, 5H, Ph).  $\delta$   $^{13}\text{C}$  NMR (75 MHz,  $\text{CDCl}_3$ ): 26.8 ( $\text{CH}_2\text{CH}_2\text{CH}_2$ ), 42.6 ( $\text{CH}_2\text{SO}_2$ ), 49.1 ( $\text{CH}_2\text{Cl}$ ), 120.9 (CH), 125.6 (CH), 129.8 (CH), 136.4 (C). ESI-MS  $m/z$  (rel. int.) 251 ( $\text{MNH}_4^+$ ) (46), 253 ( $\text{MNH}_4^++2$ ) (18).

**2.27a**; white amorphous solid (49%, 2 steps) or white crystals (MeOH/water); m.p. 125-127 °C, lit. 119-120 °C<sup>83</sup> (MeOH/water), 120-121 °C<sup>85</sup> (acetone); IR (film):  $\nu_{\max}$  = 1597, 1498, 1452, 1310, 1291, 1138 (S=O), 908, 765, 736, 694  $\text{cm}^{-1}$ .  $\delta$   $^1\text{H}$  NMR (300 MHz,  $\text{CDCl}_3$ ): 2.52 (tt, 2H,  $J$  = 6.6, 7.5,  $\text{CH}_2\text{CH}_2\text{CH}_2$ ), 3.37 (t, 2H,  $J$  = 7.5,  $\text{CH}_2\text{N}$ ), 3.77 (t, 2H,  $J$  = 6.6,  $\text{CH}_2\text{SO}_2$ ), 7.12–7.40 (m, 5H, Ph).  $\delta$   $^{13}\text{C}$  NMR (75 MHz,  $\text{CDCl}_3$ ): 18.8 ( $\text{CH}_2\text{CH}_2\text{CH}_2$ ), 46.7 ( $\text{CH}_2\text{N}$ ), 48.3 ( $\text{CH}_2\text{SO}_2$ ), 119.4 (CH), 124.5 (CH), 129.3 (CH), 137.6 (C).  $^1\text{H}$  and  $^{13}\text{C}$  NMR signal assignments were based on the chemical shift and on the splitting pattern.  $^1\text{H}$  NMR spectrum of **2.27a** showed to be in agreement with the one reported.<sup>84</sup> ESI-MS  $m/z$  (rel. int.) 215 ( $\text{MNH}_4^+$ ) (100).

### 2-Benzylisothiazolidine 1,1-dioxide (**2.27b**)

Benzylamine (7.9 mL; 72.6 mmol) was added slowly to a solution of 3-chloropropanesulfonyl chloride **2.41a** (4.5 mL; 36.3 mmol) in DCM (150 mL), at  $-10$  °C. The reaction mixture was vigorously shaken between the additions of benzylamine. A white precipitate (benzylamine salt) was observed. The mixture was stirred for another 60 min, at  $-10$  °C, after which it was washed with 100 mL of hydrochloric acid 5% (w/v), of saturated sodium chloride solution and of water, dried with anhydrous magnesium sulfate and evaporated to give 3-chloro-*N*-benzylpropane-1-sulfonamide **2.39b** (8.1 g; 32.8 mmol). This product was subsequently treated as described for **2.39a** (reaction time: 30 min) and submitted to the same extractive work-up to afford **2.27b** (6.0 g).

**2.39b**; white amorphous solid; IR (film):  $\nu_{\max}$  = 3228 (NH), 1452, 1435, 1295 (br), 1131 (S=O), 767, 731, 695  $\text{cm}^{-1}$ .  $\delta$   $^1\text{H}$  NMR (300 MHz,  $\text{CDCl}_3$ ): 2.23 (tt, 2H,  $J$  = 6.2, 7.4,  $\text{CH}_2\text{CH}_2\text{CH}_2$ ), 3.10 (t, 2H,  $J$  = 7.4,  $\text{CH}_2\text{SO}_2$ ), 3.61 (t, 2H,  $J$  = 6.2,  $\text{CH}_2\text{Cl}$ ), 4.32 (d, 2H,  $J$  =

6.1,  $\text{CH}_2\text{Ph}$ ), 4.59 (brs, 1H, NH), 7.32–7.39 (m, 5H,  $\text{Ph}$ ).  $\delta^{13}\text{C}$  NMR (75 MHz,  $\text{CDCl}_3$ ): 27.0 ( $\text{CH}_2\text{CH}_2\text{CH}_2$ ), 42.9 ( $\text{CH}_2\text{SO}_2$ ), 47.4 ( $\text{CH}_2\text{Cl}$ ), 50.7 ( $\text{CH}_2\text{Ph}$ ), 128.1 (CH), 128.4 (CH), 129.1 (CH), 136.7 (C). ESI-MS  $m/z$  (rel. int.) 266 ( $\text{MNH}_4^+$ ) (46).

**2.27b**; yellow oil (79%, 2 steps); IR (film):  $\nu_{\text{max}} = 1604, 1496, 1453, 1361, 1303$  (br), 1139 (S=O), 959, 770, 737, 706  $\text{cm}^{-1}$ .  $\delta^1\text{H}$  NMR (300 MHz,  $\text{CDCl}_3$ ): 2.29 (tt, 2H,  $J = 6.8, 7.7$ ,  $\text{CH}_2\text{CH}_2\text{CH}_2$ ), 3.10 (t, 2H,  $J = 6.8$ ,  $\text{CH}_2\text{N}$ ), 3.19 (t, 2H,  $J = 7.7$ ,  $\text{CH}_2\text{SO}_2$ ), 4.16 (s, 2H,  $\text{CH}_2\text{Ph}$ ), 7.58–7.60 (m, 5H,  $\text{Ph}$ ).  $\delta^{13}\text{C}$  NMR (75 MHz,  $\text{CDCl}_3$ ): 18.5 ( $\text{CH}_2\text{CH}_2\text{CH}_2$ ), 45.9 ( $\text{CH}_2\text{N}$ ), 46.5 ( $\text{CH}_2\text{SO}_2$ ), 48.2 ( $\text{CH}_2\text{Ph}$ ), 128.1 (CH), 128.7 (CH), 128.8 (CH), 135.7 (C). Carbon signal assignments of **2.27b** were confirmed by HMQC techniques.  $^1\text{H}$  and  $^{13}\text{C}$  NMR spectra of **2.27b** showed to be in agreement with those reported.<sup>97</sup> The ESI-MS  $m/z$  (rel. int.) 229 ( $\text{MNH}_4^+$ ) (100).

#### 5.1.4.4 $\delta$ -Sultams core

##### 2-Phenyl-1,2-thiazinane 1,1-dioxide (**2.28b**)

1,4-Butane sultone **2.36** (3.0 mL; 29.4 mmol) and aniline (4.0 mL; 44.1 mmol) were heated at 100 °C, under agitation, until the formation of a glassy solid (approximately 30 min). This product was refluxed for 90 min with phosphorus oxychloride (74 mL; 793.8 mmol), whereupon it was gradually dissolved. The remaining phosphorus oxychloride was evaporated under reduced pressure to give a brown oil (12.9 g), which was suspended in EtOAc (300 mL). Sodium carbonate (11 g; 104 mmol) was added and the mixture was stirred at rt for 1 h, after which it was filtered and evaporated to afford **2.28b** as a brown solid (8.0 g). The compound (2.6 g) was purified by column chromatography on silica gel (80 g) using DCM (1 L) as eluent.

In a separate run, the reaction mixture was filtered, washed with hydrochloric acid 5% (w/v) and water, dried and evaporated. Purification was achieved by recrystallization from MeOH,<sup>83</sup> but the process required several charcoal treatments.

**2.28b**; white amorphous solid (43%, 3 steps) or white crystals (MeOH); m.p. 115–116 °C, lit.<sup>83</sup> 109–110 °C; IR (film):  $\nu_{\text{max}} = 1595, 1492, 1449, 1325, 1294, 1138$  (S=O), 884, 767, 743, 697  $\text{cm}^{-1}$ .  $\delta^1\text{H}$  NMR (400 MHz,  $\text{CDCl}_3$ ): 1.91 (tt, 2H,  $J = 5.4, 6.4$ ,  $\text{CH}_2\text{CH}_2\text{N}$ ), 2.33 (tt, 2H,  $J = 5.4, 5.6$ ,  $\text{CH}_2\text{CH}_2\text{SO}_2$ ), 3.21 (t, 2H,  $J = 6.4$ ,  $\text{CH}_2\text{N}$ ), 3.74 (t, 2H,  $J = 5.6$ ,  $\text{CH}_2\text{SO}_2$ ), 7.28–7.39 (m, 5H,  $\text{Ph}$ ).  $\delta^{13}\text{C}$  NMR (100.61 MHz,  $\text{CDCl}_3$ ): 24.5 ( $\text{CH}_2\text{CH}_2\text{N}$ ), 24.9

( $\underline{\text{C}}\text{H}_2\text{CH}_2\text{SO}_2$ ), 51.0 ( $\text{CH}_2\text{N}$ ), 53.8 ( $\text{CH}_2\text{SO}_2$ ), 127.3 (CH), 127.7 (CH), 129.4 (CH), 140.8 (C).  $^1\text{H}$  and  $^{13}\text{C}$  NMR signal assignments were based on the chemical shift and on the splitting pattern. ESI-MS  $m/z$  (rel. int.) 229 ( $\text{MNH}_4^+$ ) (100).

### 2-Benzyl-1,2-thiazinane 1,1-dioxide (2.28c)

- By cyclisation of 4-(benzylamino)butanesulfonyl chloride hydrochloride 2.30b:

**2.28c** (4.4 g) was prepared from benzylamine (7.2 mL; 66 mmol) using the method described earlier for **2.28b**. Purification was carried out by column chromatography on silica gel using DCM as eluent. Alternatively, the compound was purified by recrystallization from MeOH.

**2.28c**; yellow oil (44%, 3 steps) or white crystals (MeOH); m.p. 74-76 °C, lit.<sup>89</sup> 74 °C; IR (film):  $\nu_{\text{max}}$  = 1495, 1454, 1327, 1292, 1139 (S=O), 896, 767, 744, 704  $\text{cm}^{-1}$ .  $\delta$   $^1\text{H}$  NMR (400 MHz,  $\text{CDCl}_3$ ): 1.59–1.64 (m, 2H,  $\underline{\text{C}}\text{H}_2\text{CH}_2\text{N}$ ), 2.22 (tt, 2H,  $J$  = 5.6, 6.4,  $\underline{\text{C}}\text{H}_2\text{CH}_2\text{SO}_2$ ), 3.10 (t, 2H,  $J$  = 6.4,  $\text{CH}_2\text{N}$ ), 3.22 (t, 2H,  $J$  = 5.6,  $\text{CH}_2\text{SO}_2$ ), 4.31 (s, 2H,  $\underline{\text{C}}\text{H}_2\text{Ph}$ ), 7.35–7.36 (m, 5H, Ph).  $\delta$   $^{13}\text{C}$  NMR (100.61 MHz,  $\text{CDCl}_3$ ): 22.0 ( $\underline{\text{C}}\text{H}_2\text{CH}_2\text{N}$ ), 24.3 ( $\underline{\text{C}}\text{H}_2\text{CH}_2\text{SO}_2$ ), 48.6 ( $\text{CH}_2\text{N}$ ), 49.1 ( $\text{CH}_2\text{SO}_2$ ), 50.3 ( $\underline{\text{C}}\text{H}_2\text{Ph}$ ), 128.1 (CH), 128.8 (CH), 128.9 (CH), 136.3 (C).  $^1\text{H}$  and  $^{13}\text{C}$  NMR signal assignments were based on the chemical shift and on the splitting pattern.  $^1\text{H}$  NMR spectrum was in agreement with the one reported.<sup>90</sup> ESI-MS  $m/z$  (rel. int.) 226 ( $\text{MH}^+$ ) (85).

- By cyclisation of 4-bromo-*N*-benzylbutanesulfonamide 2.40a:

Step 1) To a solution of 1,4-butane sultone **2.36** (0.75 mL; 7.3 mmol) in MeOH (10 mL) was added potassium bromide (996 mg; 8.4 mmol). The resultant suspension was refluxed for 48 h, after which time a precipitate was still present. The solvent was evaporated and the residue, 4-bromobutane-1-sulfonate **2.38a** (1.7 g), was washed with *n*-hexane to remove the remaining 1,4-butane sultone **2.36**.

Step 2) 4-Bromobutane-1-sulfonate **2.38a** (1.7 g; 6.8 mmol) was triturated (3-4 min) with finely ground phosphorus pentachloride (1.6 g; 7.8 mmol). During this process, bubbling was observed and an orange coloration developed. The mixture was diluted with chloroform (25 mL) and it was triturated for a further 15 min. Ethyl ether (50 mL) was added to precipitate the remaining phosphorus pentachloride. The medium was filtrated and evaporated to give 4-bromobutane-1-sulfonyl chloride **2.42a** (1.0 g), which was immediately used in the following step.

Step 3) A solution of 4-bromobutane-1-sulfonyl chloride **2.42a** freshly prepared (1.0 g; 4.6 mmol) in DCM (5 mL) was slowly added to a solution of benzylamine (1.0 mL; 9.2 mmol) in DCM (40 mL), at  $-10\text{ }^{\circ}\text{C}$ . The reaction mixture was vigorously shaken between the additions of **2.42a**, with formation of a white precipitate (benzylamine salt). Stirring at  $-10\text{ }^{\circ}\text{C}$  was continued for a further 60 min, after which the medium was washed with 50 mL of hydrochloric acid 5% (w/v) and of water, dried over anhydrous magnesium sulfate and evaporated to yield 4-bromo-*N*-benzylbutanesulfonamide **2.40a** (609 mg).

Step 4) 4-Bromo-*N*-benzylbutanesulfonamide **2.40a** (609 mg; 2.0 mmol) was refluxed for 1 h with a solution of sodium hydroxide (80 mg; 2.0 mmol) and TEA (0.3 mL; 2.0 mmol) in MeOH (20 mL). The solvent was evaporated to give 2-benzyl-1,2-thiazinane 1,1-dioxide **2.28c** (288 mg). No further work-up was performed.

**2.38a**; white amorphous solid; IR (KBr):  $\nu_{\text{max}} = 1351, 1198, 1172, 1058\text{ cm}^{-1}$ .

**2.42a**; yellow liquid; IR (film):  $\nu_{\text{max}} = 1380, 1170\text{ cm}^{-1}$ .  $\delta\text{ }^1\text{H NMR}$  (60 MHz,  $\text{CDCl}_3$ )<sup>c</sup>: 1.73-2.10 (m), 2.13-2.50 (m), 3.17-3.63 (m).

**2.40a**; yellow oil; IR (film): 3303 (NH), 1452, 1350 (S=O), 1168 and 1148 (S=O), 910, 828, 782, 704  $\text{cm}^{-1}$ .  $\delta\text{ }^1\text{H NMR}$  (300 MHz,  $\text{CDCl}_3$ )<sup>c</sup>: 1.40-1.90 (m), 1.93-2.43 (m), 2.80-3.23 (m), 4.12 (d,  $J = 6.0$ ,  $\text{CH}_2\text{Ph}$ ), 7.00-7.10 (m, Ph). ESI-MS  $m/z$  (rel. int.) 307 ( $\text{MH}^+$ ) (82), 309 ( $\text{MH}^++2$ ) (100).

**2.28c**; yellow oil (18%, crude yield, 4 steps); IR (film):  $\nu_{\text{max}} = 1454, 1329, 1293, 1139\text{ (S=O)}$ , 896, 766, 710  $\text{cm}^{-1}$ .  $\delta\text{ }^1\text{H NMR}$  (300 MHz,  $\text{CDCl}_3$ )<sup>c</sup>: 1.63-1.97 (m), 2.07-2.50 (m), 3.10-3.33 (m), 4.33 (s,  $\text{CH}_2\text{Ph}$ ), 7.33-7.35 (m, Ph). ESI-MS  $m/z$  (rel. int.) 226 ( $\text{MH}^+$ ) (100).

#### 5.1.4.5 Aminoacid and dipeptide aldehydes

##### *N*-tert-Butoxycarbonyl-*S*-phenylalanyl-glycine ethyl ester (**2.62a**)

To a solution of *N*-Boc-*S*-phenylalanine-*N*-hydroxysuccinimide ester (1.0 g; 2.8 mmol) in dry THF (14 mL) was added glycine ethyl ester hydrochloride (390 mg; 2.8 mmol) and TEA (0.4 mL; 2.8 mmol). The resultant suspension was stirred at rt for 38 h, then it was filtered *in vacuo* and evaporated. The resultant residue (1.4 g) was submitted to column chromatography on silica gel (40 g), using EtOAc as eluent (0.15 mL), to afford **2.62a** (860 mg).

<sup>c</sup> Impure compound. Signal integral ratio was inconsistent.

**2.62a**; white crystals (89%); m.p. 90-92 °C; IR (film):  $\nu_{\max}$  = 3319 (NH), 1747 (C=O of COOEt), 1664 (C=O of Boc), 1530 (br), 1204 and 1172 (d, C-O), 702  $\text{cm}^{-1}$ .  $^1\text{H}$  NMR (400 MHz,  $\text{CDCl}_3$ ): 1.27 (t, 3H,  $J$  = 7.2,  $\text{OCH}_2\text{CH}_3$ ), 1.40 (s, 9H,  $\text{CH}_3$ -Boc), 3.05 (dd, 1H,  $J$  = 6.4, 13.8,  $\text{CHHPh}$ ), 3.12 (dd, 1H,  $J$  = 6.6, 13.8,  $\text{CHHPh}$ ), 3.92 (dd, 1H,  $J$  = 4.8, 18.4,  $\text{CHH}_{\text{gli}}$ ), 4.03 (dd, 1H,  $J$  = 5.6, 18.4,  $\text{CHH}_{\text{gli}}$ ), 4.19 (q, 2H,  $J$  = 7.2,  $\text{OCH}_2\text{CH}_3$ )<sup>d</sup>, 4.41–4.42 (m, 1H,  $\text{CHCH}_2\text{Ph}$ ), 5.02 (brs, 1H, Boc-NH), 6.45 (t, 1H,  $J$  = 4.4,  $\text{NH}_{\text{gli}}$ ), 7.20–7.32 (m, 5H,  $\text{Ph}$ ).  $\delta$   $^{13}\text{C}$  NMR (100.61 MHz,  $\text{CDCl}_3$ ): 14.3 ( $\text{OCH}_2\text{CH}_3$ ), 28.3 ( $\text{CH}_3$ -Boc), 38.4 ( $\text{CH}_2\text{Ph}$ ), 41.4 ( $\text{CH}_{2\text{gli}}$ ), 55.7 ( $\text{CHCH}_2\text{Ph}$ ), 61.6 ( $\text{OCH}_2\text{CH}_3$ ), 80.3 (C-Boc), 127.0 (CH), 128.7 (CH), 129.3 (CH), 136.6 (C), 155.5 ( $\text{CO}$ -Boc), 169.4 (CONH), 171.5 ( $\text{COOEt}$ ).  $^1\text{H}$  and  $^{13}\text{C}$  NMR signal assignments were made by comparison with those reported for the analogous *N*-tert-butoxycarbonyl-*R*-phenylalanyl-glycine ethyl ester.<sup>100</sup> ESI-MS  $m/z$  (rel. int.) 724 ( $\text{M}_2\text{Na}^+$ ) (100).

#### ***N*-tert-Butoxycarbonyl-*S*-phenylalanyl-*S*-phenylalanine ethyl ester (2.62b)**

**2.62b** (1.1 g) was prepared from *S*-phenylalanine ethyl ester hydrochloride (634 mg; 2.8 mmol) using the method described for **2.62a**.

**2.62b**; white crystals (91%); m.p. 95-97 °C; IR (film):  $\nu_{\max}$  = 3321 (NH), 1745 (C=O of COOEt), 1660 (C=O of Boc), 1500, 1485, 1241 (C-O), 1170 (C-O), 750, 701  $\text{cm}^{-1}$ .  $^1\text{H}$  NMR (400 MHz,  $\text{CDCl}_3$ ): 1.20 (t, 3H,  $J$  = 7.0,  $\text{OCH}_2\text{CH}_3$ ), 1.40 (s, 9H,  $\text{CH}_3$ -Boc), 3.00–3.09 (m, 4H,  $2 \times \text{CH}_2\text{Ph}$ ), 4.05–4.15 (m, 2H,  $\text{OCH}_2\text{CH}_3$ ), 4.33–4.34 (m, 1H,  $\text{CHCH}_2\text{Ph}$ ), 4.75 (dd, 1H,  $J$  = 6.0, 12.4,  $\text{CHCH}_2\text{Ph}$ ), 4.95 (brs, 1H, NH), 6.31 (d, 1H,  $J$  = 6.8, NH), 6.98–7.01 (m, 2H,  $\text{Ph}$ ), 7.18–7.31 (m, 8H,  $\text{Ph}$ ).  $\delta$   $^{13}\text{C}$  NMR (100.61 MHz,  $\text{CDCl}_3$ ): 14.1 ( $\text{OCH}_2\text{CH}_3$ ), 28.3 ( $\text{CH}_3$ -Boc), 38.0 ( $\text{CH}_2\text{Ph}$ ), 38.3 ( $\text{CH}_2\text{Ph}$ ), 53.3 ( $\text{CHCH}_2\text{Ph}$ ), 55.7 ( $\text{CHCH}_2\text{Ph}$ ), 61.5 ( $\text{OCH}_2\text{CH}_3$ ), 80.2 (C-Boc), 127.0 (CH), 127.1 (CH), 128.5 (CH), 128.7 (CH), 129.3 (CH), 129.4 (CH), 135.7 (C), 136.5 (C), 155.3 ( $\text{CO}$ -Boc), 170.7 (CONH), 170.9 ( $\text{COOEt}$ ).  $^1\text{H}$  NMR signal assignments were based on chemical shift, relative integration and on the splitting pattern. Carbon signals assignments were based on chemical shift. ESI-MS  $m/z$  (rel. int.) 903 ( $\text{M}_2\text{Na}^+$ ) (100).

#### ***N*-tert-Butoxycarbonyl-*S*-phenylalanyl-glycine (2.63a)**

A solution of **2.62a** (860 mg; 2.5 mmol) in distilled THF (12 mL) and 1M-sodium hydroxide (2.5 mmol) was refluxed for 25 min. Then, THF was evaporated and the aqueous residue was

<sup>d</sup> Co-incident peak.



submitted to chromatography using an HCl-activated Amberlite IR 120H ion-exchange column, using as eluent a mixture of EtOH/water 1:1, to yield **2.63a** (710 mg).

**2.63a**; white amorphous solid (90%); IR (KBr):  $\nu_{\max}$  = 3357 (NH), 3267 (NH), 1716 (C=O of acid), 1676 (C=O), 1635 (C=O), 1575, 1445, 1244 (C-O), 1168 (C-O), 740, 702  $\text{cm}^{-1}$ .  $^1\text{H}$  NMR (400 MHz,  $\text{CDCl}_3$  + MeOD): 1.24 (s, 9H,  $\text{CH}_3$ -Boc), 2.79 (m, 1H), 3.04 (m, 1H), 3.78 (brd, 1H,  $J$  = 18.0), 3.86 (brd, 1H,  $J$  = 18.0), 4.26 (m, 1H), 7.08–7.17 (m, 5H,  $\text{Ph}$ ).  $\delta$   $^{13}\text{C}$  NMR (100.61 MHz,  $\text{CDCl}_3$  + MeOD): 27.9 ( $\text{CH}_3$ -Boc), 38.3 ( $\text{CH}_2\text{Ph}$ ), 40.9 ( $\text{CH}_{2\text{gli}}$ ), 60.2 ( $\text{CHCH}_2\text{Ph}$ ), 126.6 (CH), 128.3 (CH), 129.1 (CH), 171.3 (CO). ESI-MS  $m/z$  (rel. int.) 668 ( $\text{M}_2\text{Na}^+$ ) (100).

### ***N*-tert-Butoxycarbonyl-*S*-phenylalanyl-*S*-phenylalanine (2.63b)**

**2.63b** (910 mg) was prepared from **2.62b** (1.1 g; 2.5 mmol) using the method described for **2.63a**.

**2.63b**; white amorphous solid (88%); IR (KBr):  $\nu_{\max}$  = 3396 (NH), 3353 (NH), 1734 (C=O of acid), 1695 (C=O), 1664 (C=O), 1539 and 1515 (d), 1448, 1249 (C-O), 1166 (C-O), 747, 698  $\text{cm}^{-1}$ .  $^1\text{H}$  NMR (400 MHz,  $\text{CDCl}_3$  + MeOD): 1.34 (s, 9H,  $\text{CH}_3$ -Boc), 2.83–2.89 (m, 1H), 2.99–3.04 (m, 2H), 3.12 (brdd, 1H,  $J$  = 5.0, 13.8), 4.27–4.34 (m, 1H), 4.67–4.72 (m, 1H), 7.06 (brd, 1H,  $J$  = 6.4,  $\text{Ph}$ ), 7.13 (brd, 1H,  $J$  = 6.8,  $\text{Ph}$ ), 7.19–7.25 (m, 6H,  $\text{Ph}$ ).  $^{13}\text{C}$  NMR (100.61 MHz,  $\text{CDCl}_3$  + MeOD): 28.1 ( $\text{CH}_3$ -Boc), 37.5 ( $\text{CH}_2\text{Ph}$ ), 60.4 ( $\text{CHCH}_2\text{Ph}$ ), 126.9 (2 $\times$ CH), 128.4 (CH), 128.5 (CH), 129.3 (CH), 129.4 (CH), 136.1 (C), 136.5 (C), 156.1 ( $\text{CO}$ -Boc), 172.9 (CO). ESI-MS  $m/z$  (rel. int.) 848 ( $\text{M}_2\text{Na}^+$ ) (100).

### **Synthesis of hydroxamates**

- Using isobutyl chloroformate as coupling reagent:

TEA (6.5 mL; 46.2 mmol) was added to a solution of *N*-Boc-*S*-phenylalanine (6.0 g; 22.6 mmol) in DCM (150 mL) and the mixture was cooled down to  $-10$  °C. Isobutyl chloroformate (3.0 mL; 22.4 mmol) was added dropwise, followed after 30 min by *O*, *N*-dimethylhydroxylamine hydrochloride (2.3 g; 23.4 mmol). The resultant suspension became clear after an overnight at rt. The medium was worked up with 100 mL of 3M-hydrochloric acid, of saturated sodium hydrogen carbonate solution and of saturated sodium chloride solution, and then it was dried with anhydrous magnesium sulfate and evaporated. The

resultant oil (6.0 g) was submitted to a column chromatography on silica gel (150 g), using as eluent a mixture of *n*-hexane/EtOAc 1:1 (0.8 L), to afford **2.54** (4.2 g).

- Using BOP as coupling reagent:

BOP (1.4 g; 3.0 mmol) was added to a solution of *N*-Boc-*S*-phenylalanine (800 mg; 3.0 mmol) in DCM (10 mL) with TEA (0.4 mL; 3.0 mmol). After 5 min of stirring at rt, *O*, *N*-dimethylhydroxylamine hydrochloride (324 mg; 3.3 mmol) and TEA (0.5 mL; 3.3 mmol) were added and the resultant suspension was stirred for a further 1.5 h, during which time the medium became clear. The reaction was diluted with DCM (50 mL), washed with 30 mL of 3M-hydrochloric acid, of saturated sodium hydrogen carbonate solution and of saturated sodium chloride solution, then it was dried with anhydrous magnesium sulfate. The solvent was evaporated to give an yellow oil (1.2 g), which was submitted to a column chromatography on silica gel (40 g), using as eluent a mixture of *n*-hexane/EtOAc 1:1 (0.2 L), to afford **2.54** (716 mg).

- Using TBTU as coupling reagent:

This technique followed the procedure described for BOP, with the exception that the addition of TBTU resulted in a suspension that was stirred until it became clear ( $\approx$  30 min). Only then, *O*, *N*-dimethylhydroxylamine hydrochloride was added.

***N*-Methoxy-*N*-methyl *N'*-*tert*-butoxycarbonyl-*S*-phenylalanyl amide (2.54)**; white oil 61% (isobutyl chloroformate), 77% (BOP), 83% (TBTU); IR (film):  $\nu_{\max}$  = 3295 (NH), 1702 (C=O), 1655 (C=O), 1498, 1389 and 1367 (d), 1170 (C-O), 856, 750, 698  $\text{cm}^{-1}$ .  $\delta$   $^1\text{H}$  NMR (400 MHz,  $\text{CDCl}_3$ ): 1.41 (s, 9H,  $\text{CH}_3$ -Boc), 2.89 (m, 1H,  $\text{CHHPH}$ ), 3.07 (dd, 1H,  $J$  = 6.0, 13.6,  $\text{CHHPH}$ ), 3.19 (s, 3H,  $\text{NCH}_3$ ), 3.67 (s, 3H,  $\text{OCH}_3$ ), 4.96–4.98 (m, 1H,  $\text{CHCH}_2\text{Ph}$ ), 5.19 (brd, 1H,  $J$  = 8.4, NH), 7.18–7.32 (m, 5H,  $\text{Ph}$ ).  $\delta$   $^{13}\text{C}$  NMR (100.61 MHz,  $\text{CDCl}_3$ ): 28.3 ( $\text{CH}_3$ -Boc), 32.1 ( $\text{NCH}_3$ ), 38.9 ( $\text{CH}_2\text{Ph}$ ), 51.5 ( $\text{CHCH}_2\text{Ph}$ ), 61.6 ( $\text{OCH}_3$ ), 79.6 (C-Boc), 126.8 (CH), 128.4 (CH), 129.5 (CH), 136.6 (C), 155.2 ( $\text{CO}$ -Boc), 172.3 ( $\text{CONCH}_3$ ).  $^1\text{H}$  NMR spectrum signals were assigned according to the literature.<sup>99</sup> Carbon signal assignments were made using HMQC and DEPT techniques. ESI-MS  $m/z$  (rel. int.) 347 ( $\text{MK}^+$ ) (100).

***N*-Methoxy-*N*-methyl (*N'*-*tert*-butoxycarbonyl-*S*-phenylalanylglyciny)amide (2.61a)**

**2.61a** (255 mg) was prepared from **2.63a** (400 mg; 1.2 mmol) using TBTU-mediated coupling. Reaction time: 13 h. Purification by column chromatography on silica gel using a gradient of *n*-hexane/EtOAc (1:1→1:3).

**2.61a**; white oil (56%); IR (film):  $\nu_{\max}$  = 3317 (br, NH), 1714–1661 (br, 3×C=O), 1519 (br), 1451, 1250 (C-O), 1171 (C-O), 740, 701  $\text{cm}^{-1}$ .  $^1\text{H}$  NMR (400 MHz,  $\text{CDCl}_3$ ): 1.36 (s, 9H,  $\text{CH}_3$ -Boc), 2.36 (m, 1H,  $\text{CHHPh}$ ), 2.97–3.03 (m, 1H,  $\text{CHHPh}$ ), 3.17 (NCH<sub>3</sub>), 3.69 (OCH<sub>3</sub>), 4.07 (brd, 1H,  $J$  = 18.0,  $\text{CHH}_{\text{gli}}$ )<sup>e</sup>, 4.21 (dd, 1H,  $J$  = 4.4, 18.4,  $\text{CHH}_{\text{gli}}$ ), 4.46–4.48 (m, 1H,  $\text{CHCH}_2\text{Ph}$ ), 5.24 (brs, 1H, Boc-NH), 6.90 (brs, 1H,  $\text{NH}_{\text{gli}}$ ), 7.18–7.27 (m, 5H,  $\text{Ph}$ ).  $^1\text{H}$  NMR signals were assigned by comparison with the ester **2.62a** and hydroxamate **2.54**. ESI-MS *m/z* (rel. int.) 753 ( $\text{M}_2\text{Na}^+$ ) (100).

***N*-Methoxy-*N*-methyl (*N'*-*tert*-butoxycarbonyl-*S*-phenylalanyl-*S*-phenylalanyl)amide (2.61b)**

**2.61b** (166 mg) was prepared from **2.63b** (200 mg; 0.5 mmol) using TBTU-mediated coupling. Reaction time: 13 h. Purification by column chromatography on silica gel using a mixture of *n*-hexane/EtOAc.

**2.61b**; pale oil (75%); IR (film):  $\nu_{\max}$  = 3306 (br, NH), 1715–1651 (br, 3×C=O), 1536–1498, 1249 (C-O), 1166 (C-O), 740, 698  $\text{cm}^{-1}$ .  $^1\text{H}$  NMR (400 MHz,  $\text{CDCl}_3$ ): 1.41 (s, 9H,  $\text{CH}_3$ -Boc), 2.91 (brdd, 2H,  $J$  = 6.8, 13.6,  $\text{CH}_2\text{Ph}$ )<sup>f</sup>, 3.06 (brdd, 2H,  $J$  = 6.4, 14.0,  $\text{CH}_2\text{Ph}$ )<sup>f</sup>, 3.15 (s, 3H, NCH<sub>3</sub>), 3.62 (s, 3H, OCH<sub>3</sub>), 4.36–4.38 (m, 1H,  $\text{CHCH}_2\text{Ph}$ ), 4.93–4.94 (m, 1H), 5.20–5.21 (m, 1H), 6.53 (d, 1H,  $J$  = 8.0, NH), 7.04–7.09 (m, 2H,  $\text{Ph}$ ), 7.19–7.31 (m, 8H,  $\text{Ph}$ ).  $\delta$   $^{13}\text{C}$  NMR (100.61 MHz,  $\text{CDCl}_3$ ): 28.2 ( $\text{CH}_3$ -Boc), 32.0 (NCH<sub>3</sub>), 38.4 ( $\text{CH}_2\text{Ph}$ ), 38.6 ( $\text{CH}_2\text{Ph}$ ), 50.2 ( $\text{CHCH}_2\text{Ph}$ ), 55.5 ( $\text{CHCH}_2\text{Ph}$ ), 61.5 (OCH<sub>3</sub>), 80.0 (C-Boc), 126.9 (CH), 128.4 (CH), 128.6 (CH), 129.4 (2×CH), 136.0 (C), 136.6 (C), 155.2 ( $\text{CO}$ -Boc), 170.6 (CONH), 171.0 ( $\text{CONCH}_3$ ).  $^1\text{H}$  and  $^{13}\text{C}$  NMR signals were assigned by comparison with the ester **2.62b** and hydroxamate **2.54**. ESI-MS *m/z* (rel. int.) 479 ( $\text{MNa}^+$ ) (84).

***N*-*tert*-Butoxycarbonyl-*S*-phenylalanal (2.53)**

Lithium aluminium hydride (41 mg; 1.0 mmol) was added to a solution of **2.54** (251 mg; 0.8 mmol) in dry THF (8 mL), at 0 °C. The reaction was stirred at 0 °C for 30 min, after which it was quenched using a solution of potassium hydrogen sulfate (194 mg; 1.4 mmol) in water (2

<sup>e</sup> Not well resolved signal.

<sup>f</sup> Co-incident peak.

mL). Then, it was diluted with water (40 mL) and extracted with ethyl ether (3×30 mL). The organic layer was washed with 30 mL of 3M-hydrochloric acid, of saturated sodium hydrogen carbonate solution and of saturated sodium chloride solution, dried with anhydrous magnesium sulfate and evaporated to afford **2.53** (168 mg), sufficiently pure for the next step.

**2.53**; white amorphous solid (83%); IR (film):  $\nu_{\max}$  = 3354 (NH), 2816 (H-CO), 2722 (H-CO), 1695 (br), 1506, 1451, 1251 (C-O), 1168 (C-O), 849, 743, 701  $\text{cm}^{-1}$ .  $\delta$   $^1\text{H}$  NMR (400 MHz,  $\text{CDCl}_3$ ): 1.45 (s, 9H,  $\text{CH}_3$ -Boc), 3.14 (brd, 2H,  $J$  = 6.8,  $\text{CH}_2\text{Ph}$ )<sup>g</sup>, 4.45 (brdd, 1H,  $J$  = 6.2, 13.0,  $\text{CHCH}_2\text{Ph}$ ), 5.07 (brs, 1H, NH), 7.19 (d, 2H,  $J$  = 7.2,  $\text{Ph}$ ), 7.28 (t, 1H,  $J$  = 3.6,  $\text{Ph}$ ), 7.34 (t, 2H,  $J$  = 7.2,  $\text{Ph}$ ), 9.65 (s, 1H, COH).  $\delta$   $^{13}\text{C}$  NMR (100.61 MHz,  $\text{CDCl}_3$ ): 28.3 ( $\text{CH}_3$ -Boc), 35.5 ( $\text{CH}_2\text{Ph}$ ), 60.8 ( $\text{CHCH}_2\text{Ph}$ ), 80.2 (C-Boc), 127.1 (CH), 128.8 (CH), 129.3 (CH), 135.8 (C), 155.2 ( $\text{CO}$ -Boc), 199.4 (COH).  $^1\text{H}$  NMR spectrum signals were assigned according to the literature.<sup>99</sup> Carbon signal assignments were made using HMQC and DEPT techniques. ESI-MS  $m/z$  (rel. int.) 499 ( $\text{M}_2\text{H}^+$ ) (100).

#### ***N*-tert-Butoxycarbonyl-*S*-phenylalanine ethyl ester (2.59)**

TEA (3.3 mL; 24.0 mmol) was added to a suspension of *S*-phenylalanine ethyl ester hydrochloride (500 mg; 2.2 mmol) in distilled THF (10 mL). The mixture was cooled to 0 °C and stirred for 20 min, after which Boc anhydride (0.5 mL; 2.4 mmol) was added dropwise. The reaction was stirred for a further 30 min at 0 °C and then for additional 2 h at rt, after which it was acidified with conc. hydrochloric acid and extracted with DCM (3×20 mL). The organic layer was washed with 2×40 mL of water, dried with anhydrous magnesium sulfate and evaporated to give **2.59** (418 mg).

**2.59**; yellow oil; (65%); IR (film):  $\nu_{\max}$  = 3370 (NH), 1715 (br, 2×C=O), 1500, 1251 (C-O), 1169 (C-O), 748, 701  $\text{cm}^{-1}$ .  $\delta$   $^1\text{H}$  NMR (400 MHz,  $\text{CDCl}_3$ ): 1.14 (brt, 3H,  $J$  = 7.2,  $\text{OCH}_2\text{CH}_3$ )<sup>h</sup>, 1.34 (s, 9H,  $\text{CH}_3$ -Boc), 2.95–3.05 (m, 2H,  $\text{CH}_2\text{Ph}$ ), 4.07 (brq, 2H,  $J$  = 7.2,  $\text{OCH}_2\text{CH}_3$ )<sup>g</sup>, 4.48 (m, 1H,  $\text{CHCH}_2\text{Ph}$ ), 4.96 (brd, 1H,  $J$  = 7.2, NH), 7.06 (d, 2H,  $J$  = 7.2,  $\text{Ph}$ ), 7.13–7.22 (m, 3H,  $\text{Ph}$ ).  $\delta$   $^{13}\text{C}$  NMR (100.61 MHz,  $\text{CDCl}_3$ ): 14.1 ( $\text{OCH}_2\text{CH}_3$ ), 28.3 ( $\text{CH}_3$ -Boc), 38.4 ( $\text{CH}_2\text{Ph}$ ), 54.5 ( $\text{CHCH}_2\text{Ph}$ ), 61.3 ( $\text{OCH}_2\text{CH}_3$ ), 80.3 (C-Boc), 127.0 (CH), 128.5 (CH), 129.4 (CH), 136.1 (C), 155.1 ( $\text{CO}$ -Boc), 172.0 ( $\text{COOEt}$ ).  $^1\text{H}$  NMR signal assignments were based on the relative integration and on the splitting pattern. Carbon signal assignments were made using HMQC technique. ESI-MS  $m/z$  (rel. int.) 332 ( $\text{MK}^+$ ) (100).

<sup>g</sup> Co-incident peak.

<sup>h</sup> Not well resolved signal.

***N*-tert-Butoxycarbonyl-*S*-phenylalaninol (2.58)**

The reaction was carried out under N<sub>2</sub>. A 1.0 M solution of DIBAL in heptane (1.0 mmol) was added dropwise to a solution of **2.59** (77 mg; 0.3 mmol) in dry THF (2 mL) at -78 °C. The mixture was stirred 1 h, after which MeOH (0.3 mL) was added slowly, followed by a solution of potassium sodium (+) tartrate (3.8 g; 13.4 mmol) in water (6 mL). After being vigorously stirred at rt for 1.5 h, it was extracted with EtOAc (3×20 mL). The organic layer was washed with 40 mL of saturated aqueous solution of sodium chloride, dried with anhydrous magnesium sulfate and evaporated to afford **2.58** (60 mg).

**2.58**; white amorphous solid (91%); IR (film):  $\nu_{\max}$  = 3355 (NH and OH), 1687 (C=O), 1527, 1444, 1269 (C-O), 1170 (C-O), 752, 738 and 699 cm<sup>-1</sup>.  $\delta$  <sup>1</sup>H NMR (400 MHz, CDCl<sub>3</sub>): 1.34 (s, 9H, CH<sub>3</sub>-Boc), 2.58 (brs, 1H, OH), 2.77 (d, 2H, *J* = 7.2, CH<sub>2</sub>Ph)<sup>i</sup>, 3.47 (dd, 1H, *J* = 5.0, 10.6, CHHOH), 3.57–3.59 (m, 1H, CHHOH), 3.80 (brs, 1H, CHCH<sub>2</sub>Ph), 4.75 (brs, 1H, NH), 7.13–7.25 (m, 5H, Ph).  $\delta$  <sup>13</sup>C NMR (100.61 MHz, CDCl<sub>3</sub>): 28.4 (CH<sub>3</sub>-Boc), 37.4 (CH<sub>2</sub>Ph), 53.7 (CHCH<sub>2</sub>Ph), 64.3 (CH<sub>2</sub>OH), 79.7 (C-Boc), 126.5 (CH), 128.6 (CH), 129.3 (CH), 137.8 (C), 156.2 (CO-Boc). <sup>1</sup>H and <sup>13</sup>C NMR signals were assigned by comparison with analogues **2.53**, **2.54** and **2.59**. ESI-MS *m/z* (rel. int.) 252 (MH<sup>+</sup>) (100).

**5.1.4.6 Sultam phosphonates**

- Typical experimental procedure:

The reaction was carried out under N<sub>2</sub>. A 1.6 M solution of *n*-BuLi in *n*-hexane (22.6 mmol) was added to a solution of diisopropylamine (3.0 mL; 21.6 mmol) in dry THF (38 mL) at 0 °C. After 15 min, the solution was cooled to -78 °C, followed by the addition of a solution of *N*-benzyl- $\delta$ -sultam **2.28c** (4.4 g; 19.4 mmol) in dry THF (40 mL). The mixture was stirred for 10 min, and then a solution of diethyl chlorophosphate (1.6 mL; 11.0 mmol) in dry THF (8 mL) was added dropwise. After 1 h, the reaction medium was quenched using a saturated aqueous solution of sodium chloride (100 mL) and extracted with DCM (3×30 mL) and EtOAc (30 mL). The organic layers were washed with water, combined and dried with anhydrous magnesium sulfate. The solvent was evaporated to yield a crude product (3.5 g), which was fractionated by column chromatography on silica gel (150 g) using a gradient of

---

<sup>i</sup> Co-incident peak.

DCM/EtOAc (1:0→0:1) to afford phosphonate **2.66b** (1.3 g; 34%). Compounds **2.65a**, **2.65b** and **2.66a** were prepared using the same method from **2.27a**, **2.27b** and **2.28b**, respectively.

**2-Phenyl-5-diethylphosphoryl-isothiazolidine 1,1-dioxide (2.65a)**; yellow oil (65%); IR (film):  $\nu_{\max}$  = 1596, 1496, 1323 (S=O), 1261 (P=O), 1148 (S=O), 1023 and 955 (d, P-O-C), 833, 757, 695  $\text{cm}^{-1}$ .  $\delta$   $^1\text{H}$  and  $^{13}\text{C}$  NMR see Table 2.5 in Chapter 2. ESI-MS  $m/z$  (rel. int.) 684 ( $\text{M}_2\text{NH}_4^+$ ) (100).

**2-Benzyl-5-diethylphosphoryl-isothiazolidine 1,1-dioxide (2.65b)**; yellow oil (43%); IR (film):  $\nu_{\max}$  = 1449, 1316 (S=O), 1260 (P=O), 1158 (S=O), 1025 and 970 (d, P-O-C), 774, 731, 700  $\text{cm}^{-1}$ .  $\delta$   $^1\text{H}$  NMR (400 MHz,  $\text{CDCl}_3$ ): 1.36–1.41 (m, 6H,  $2\times\text{OCH}_2\text{CH}_3$ ), 2.47–2.66 (m, 2H,  $\text{CHCH}_2$ ), 3.10 (ddd, 1H,  $J = 2.0, 7.5, 14.4$ ,  $\text{CHHN}$ ), 3.20 (ddd, 1H,  $J = 5.2, 7.5, 9.7$ ,  $\text{CHHN}$ ), 3.62 (ddd, 1H,  $J = 8.7, 8.8$  and  $J_{\text{HP}} = 15.7$ , CH), 4.22 (m,  $\text{CH}_2\text{Ph}$ )<sup>j</sup>, 4.25 (m,  $\text{OCH}_2\text{CH}_3$ )<sup>j</sup>, 4.32 (m,  $\text{OCH}_2\text{CH}_3$ )<sup>j</sup>, 7.34–7.36 (m, 5H, Ph).  $\delta$   $^{13}\text{C}$  NMR (100.61 MHz,  $\text{CDCl}_3$ ): 16.4–16.5 (m,  $2\times\text{OCH}_2\text{CH}_3$ ), 22.0 (d,  $J_{\text{CP}} = 3.0$ ,  $\text{CHCH}_2$ ), 44.8 (d,  $J_{\text{CP}} = 8.0$ ,  $\text{CH}_2\text{N}$ ), 49.2 ( $\text{CH}_2\text{Ph}$ ), 54.5 (d,  $J_{\text{CP}} = 149.9$ , CH), 63.4 (d,  $J_{\text{CP}} = 7.0$ ,  $\text{OCH}_2\text{CH}_3$ ), 64.3 (d,  $J_{\text{CP}} = 6.0$ ,  $\text{OCH}_2\text{CH}_3$ ), 128.0 (CH), 128.5 (CH), 128.7 (CH), 135.4 (C). ESI-MS  $m/z$  (rel. int.) 347 ( $\text{M}^+$ ) (59).

**2-Phenyl-5-diethylphosphoryl-1,2-thiazinane 1,1-dioxide (2.66a)**; yellow oil (45%); IR (film):  $\nu_{\max}$  = 1594, 1492, 1337 (S=O), 1257 (P=O), 1152 (S=O), 1026 and 972 (d, P-O-C), 848, 801, 763, 697  $\text{cm}^{-1}$ .  $\delta$   $^1\text{H}$  NMR (400 MHz,  $\text{CDCl}_3$ ): 1.34–1.38 (m, 6H,  $2\times\text{OCH}_2\text{CH}_3$ ), 1.92–2.05 (m, 2H,  $\text{CH}_2\text{CH}_2\text{N}$ ), 2.51–2.65 (m, 2H,  $\text{CHCH}_2$ ), 3.61–3.62 (m, 2H,  $\text{CHHN}$  and CH), 4.03 (ddd,  $J = 4.4, 10.4, 14.0$ ,  $\text{CHHN}$ ), 4.22 (m,  $\text{OCH}_2\text{CH}_3$ )<sup>k</sup>, 4.28 (m,  $\text{OCH}_2\text{CH}_3$ )<sup>k</sup>, 7.25–7.38 (m, 5H, Ph).  $\delta$   $^{13}\text{C}$  NMR (100.61 MHz,  $\text{CDCl}_3$ ): 16.3–16.4 (m,  $2\times\text{OCH}_2\text{CH}_3$ ), 24.2 (d,  $J_{\text{CP}} = 9.8$ ,  $\text{CH}_2\text{CH}_2\text{N}$ ), 27.1 (d,  $J_{\text{CP}} = 3.7$ ,  $\text{CHCH}_2$ ), 53.4 ( $\text{CH}_2\text{N}$ ), 58.6 (d,  $J_{\text{CP}} = 136.9$ , CH), 63.4 (d,  $J_{\text{CP}} = 6.6$ ,  $\text{OCH}_2\text{CH}_3$ ), 64.0 (d,  $J_{\text{CP}} = 6.9$ ,  $\text{OCH}_2\text{CH}_3$ ), 126.9 (CH), 127.4 (CH), 129.2 (CH), 140.7 (C). ESI-MS  $m/z$  (rel. int.) 712 ( $\text{M}_2\text{NH}_4^+$ ) (100).

**2-Benzyl-5-diethylphosphoryl-1,2-thiazinane 1,1-dioxide (2.66b)**; yellow oil (34%); IR (film):  $\nu_{\max}$  = 1447, 1356 (S=O), 1257 (P=O), 1156 (S=O), 1025 and 974 (d, P-O-C), 808, 772, 727, 702  $\text{cm}^{-1}$ .  $\delta$   $^1\text{H}$  NMR (400 MHz,  $\text{CDCl}_3$ ): 1.36–1.45 (m, 6H,  $2\times\text{OCH}_2\text{CH}_3$ ),

<sup>j</sup> Overlapped signals.  $\delta$  Values from HMQC spectrum.

<sup>k</sup> Overlapped signals.  $\delta$  Values from HMQC spectrum.

1.58–1.73 (m, 2H,  $\text{CH}_2\text{CH}_2\text{N}$ ), 2.37–2.51 (m, 2H,  $\text{CHCH}_2$ ), 3.16 (ddd, 1H,  $J = 4.0, 4.0, 14.4$ ,  $\text{CHHN}$ ), 3.47 (m, CH)<sup>1</sup>, 3.50 (m,  $\text{CHHN}$ )<sup>1</sup>, 4.22–4.32 (m, 5H,  $2 \times \text{OCH}_2\text{CH}_3$  and  $\text{CHHPh}$ ), 4.49 (d, 1H,  $J = 14.4$ ,  $\text{CHHPh}$ ), 7.28–7.35 (m, 5H,  $\text{Ph}$ ).  $\delta$   $^{13}\text{C}$  NMR (100.61 MHz,  $\text{CDCl}_3$ ): 16.3–16.4 (m,  $2 \times \text{OCH}_2\text{CH}_3$ ), 20.2 (d,  $J_{\text{CP}} = 8.0$ ,  $\text{CH}_2\text{CH}_2\text{N}$ ), 27.0 (d,  $J_{\text{CP}} = 3.0$ ,  $\text{CHCH}_2$ ), 47.9 ( $\text{CH}_2\text{N}$ ), 51.5 ( $\text{CH}_2\text{Ph}$ ), 56.5 (d,  $J_{\text{CP}} = 137.8$ , CH), 63.3 (d,  $J_{\text{CP}} = 6.0$ ,  $\text{OCH}_2\text{CH}_3$ ), 63.9 (d,  $J_{\text{CP}} = 7.0$ ,  $\text{OCH}_2\text{CH}_3$ ), 128.0 (CH), 128.4 (CH), 128.7 (CH), 136.0 (C). ESI-MS  $m/z$  (rel. int.) 740 ( $\text{M}_2\text{NH}_4^+$ ) (70).

#### 5.1.4.7 Horner-Wadsworth-Emmons reaction

- Typical experimental procedure:

All manipulations were made under  $\text{N}_2$ . A 1.6 M solution of *n*-BuLi in *n*-hexane (1.2 mmol) was added to a solution of phosphonate **2.66b** (428 mg; 1.2 mmol) in dry THF (23 mL) at  $-78$  °C. The mixture was stirred for 20 min, during which time the temperature was allowed to gradually warm up to rt. Then, *N*-Boc-*S*-phenylalaninal **2.53** (325 mg; 1.3 mmol) in dry THF (6 mL) was added dropwise. After 20 min, the solvent was evaporated to afford a mixture of isomers **2.70a,b** (863 mg), which were separated by column chromatography on silica gel (30 g) using as eluent a mixture of *n*-hexane/EtOAc 1:1 (0.15 L). Isomers **2.67a,b**, **2.68a,b** and **2.69a,b** were prepared using the same method from **2.65a**, **2.65b** and **2.66a**, respectively.  $^1\text{H}$  and  $^{13}\text{C}$  NMR signal assignments were possible using DEPT and 2D NMR techniques ( $^1\text{H}$ - $^1\text{H}$  COSY, HMQC and HMBC).

**(*E*)-2-Phenyl-5-[(2*S*)-*N*-tert-butoxycarbonyl-2-amino-3-phenyl-**

**propylidene]isothiazolidine 1,1-dioxide (**2.67a**); white crystals after crystallization with MeOH (60%); m.p. 166–169 °C; IR (KBr):  $\nu_{\text{max}} = 3379$  (NH), 1688 (C=O), 1597, 1499, 1366 (S=O), 1252 (C-O), 1156 (br), 827, 746, 694  $\text{cm}^{-1}$ .  $\delta$   $^1\text{H}$  NMR (400 MHz,  $\text{CDCl}_3$ ): 1.43 (s, 9H,  $\text{CH}_3$ -Boc), 2.33 (m, 1H, =CCHH), 2.83 (dd, 1H,  $J = 8.4, 13.2$ ,  $\text{CHHPh}$ ), 2.98 (m, 1H, =CCHH), 3.03 (dd, 1H,  $J = 5.6, 13.2$ ,  $\text{CHHPh}$ ), 3.45 (ddd, 1H,  $J = 5.6, 8.0, 9.0$ ,  $\text{CHHN}$ ), 3.59 (ddd, 1H,  $J = 5.6, 8.0, 8.8$ ,  $\text{CHHN}$ ), 4.53 (brs, 1H,  $\text{CHCH}_2\text{Ph}$ ), 4.71 (brs, 1H, NH), 6.31 (brd, 1H,  $J = 8.8$ , =CH), 7.18–7.39 (m, 10H,  $\text{Ph}$ ).  $\delta$   $^{13}\text{C}$  NMR (100.61 MHz,  $\text{CDCl}_3$ ): 21.7 (=CCH<sub>2</sub>), 28.4 ( $\text{CH}_3$ -Boc), 41.1 ( $\text{CH}_2\text{Ph}$ ), 44.1 ( $\text{CH}_2\text{N}$ ), 50.9 ( $\text{CHCH}_2\text{Ph}$ ), 80.2 (C-Boc),**

<sup>1</sup> Overlapped signals.  $\delta$  Values from HMQC spectrum.

121.0 (CH), 125.5 (CH), 127.1 (CH), 128.7 (CH), 129.4 (CH), 129.7 (CH), 131.3 (=CH), 136.1 (C), 137.5 (=C), 138.6 (C), 154.9 (C=O). HR-ESI-MS calcd. for C<sub>23</sub>H<sub>32</sub>N<sub>3</sub>O<sub>4</sub>S (MNH<sub>4</sub><sup>+</sup>) 446.5840, found 446.2105.

**(Z)-2-Phenyl-5-[(2S)-N-tert-butoxycarbonyl-2-amino-3-phenyl-**

**propylidene]isothiazolidine 1,1-dioxide (2.67b)**; white amorphous solid (16%); IR (film):  $\nu_{\max}$  = 3373 (NH), 1702 (C=O), 1596, 1498, 1366 (S=O), 1263 (C-O), 1165 (br), 753, 723, 697 cm<sup>-1</sup>.  $\delta$  <sup>1</sup>H NMR (400 MHz, CDCl<sub>3</sub>): 1.40 (s, 9H, CH<sub>3</sub>-Boc), 3.02–3.11 (m, 4H, CHHN, CHHPh and =CCH<sub>2</sub>), 3.76 (m, 2H, CHHN and CHHPh), 4.91 (m, 2H, NH and CHCH<sub>2</sub>Ph), 6.35 (brs, 1H, =CH), 7.20–7.42 (m, 10H, Ph).  $\delta$  <sup>13</sup>C NMR (100.61 MHz, CDCl<sub>3</sub>): 25.8 (=CCH<sub>2</sub>), 28.3 (CH<sub>3</sub>-Boc), 44.7 (CH<sub>2</sub>Ph and CH<sub>2</sub>N)<sup>m</sup>, 50.8 (CHCH<sub>2</sub>Ph), 79.8 (C-Boc), 121.3 (CH), 125.7 (CH), 126.8 (CH), 128.6 (CH), 129.5 (CH), 129.6 (CH), 134.8 (C), 135.4 (=C), 137.2 (C), 155.1 (C=O). HR-ESI-MS calcd. for C<sub>23</sub>H<sub>32</sub>N<sub>3</sub>O<sub>4</sub>S (MNH<sub>4</sub><sup>+</sup>) 446.5840, found 446.2103.

**(E)-2-Benzyl-5-[(2S)-N-tert-butoxycarbonyl-2-amino-3-phenyl-**

**propylidene]isothiazolidine 1,1-dioxide (2.68a)**; pale oil (58%); IR (film):  $\nu_{\max}$  = 3364 (NH), 1704 (C=O), 1505, 1451, 1366 (S=O), 1247 (C-O), 1159 (br), 780, 738, 702 cm<sup>-1</sup>.  $\delta$  <sup>1</sup>H NMR (400 MHz, CDCl<sub>3</sub>): 1.43 (s, 9H, CH<sub>3</sub>-Boc), 2.10-2.14 (m, 1H, =CCHH), 2.83 (m, =CCHH)<sup>n</sup>, 2.84 (m, CHCHHPh)<sup>n</sup>, 2.85 (m, CHHN)<sup>n</sup>, 2.97 (m, CHHN)<sup>o</sup>, 3.02 (m, CHCHHPh)<sup>o</sup>, 4.11 (brd, 1H, *J* = 14.0, NCHHPh), 4.17 (brd, 1H, *J* = 14.0, NCHHPh), 4.48 (m, 1H, CHCH<sub>2</sub>Ph), 4.78 (brs, 1H, NH), 6.29 (brd, 1H, *J* = 9.2, =CH), 7.21–7.36 (m, 10H, Ph).  $\delta$  <sup>13</sup>C NMR (100.61 MHz, CDCl<sub>3</sub>): 21.7 (=CCH<sub>2</sub>), 28.4 (CH<sub>3</sub>-Boc), 41.1 (CHCH<sub>2</sub>Ph), 43.2 (CH<sub>2</sub>N), 47.9 (NCH<sub>2</sub>Ph), 51.0 (CHCH<sub>2</sub>Ph), 80.1 (C-Boc), 127.0 (CH), 128.1 (CH), 128.7 (2×CH), 129.7 (CH), 130.9 (=CH), 134.9 (C), 136.1 (C), 138.3 (=C), 154.9 (C=O). HR-ESI-MS calcd. for C<sub>24</sub>H<sub>30</sub>N<sub>2</sub>NaO<sub>4</sub>S (MNa<sup>+</sup>) 465.5618, found 465.1818.

**(Z)-2-Benzyl-5-[(2S)-N-tert-butoxycarbonyl-2-amino-3-phenyl-**

**propylidene]isothiazolidine 1,1-dioxide (2.68b)**; white crystals (29%); m.p. 138–140 °C; IR (film):  $\nu_{\max}$  = 3365 (NH), 1707 (C=O), 1500, 1451, 1367 (S=O), 1250 (C-O), 1164 (br), 774,

<sup>m</sup> Signal assignment was effected using HMQC and HMBC techniques.

<sup>n</sup> Overlapped signals.  $\delta$  Values from HMQC spectrum.

<sup>o</sup> Overlapped signals.  $\delta$  Values from HMQC spectrum.



736, 701  $\text{cm}^{-1}$ .  $\delta$   $^1\text{H}$  NMR (400 MHz,  $\text{CDCl}_3$ ): 1.43 (s, 9H,  $\text{CH}_3$ -Boc), 2.83 (m, =C $\underline{\text{C}}\text{H}\text{H}$ )<sup>p</sup>, 2.84 (m,  $\text{CHC}\underline{\text{H}}\text{HPh}$ )<sup>p</sup>, 3.07 (m, =C $\underline{\text{C}}\text{H}\text{H}$ )<sup>q</sup>, 3.10 (m,  $\text{CHC}\underline{\text{H}}\text{HPh}$  and  $\text{CH}_2\text{N}$ )<sup>q</sup>, 4.21 (s, 2H,  $\text{NCH}_2\text{Ph}$ ), 4.96 (m, 2H,  $\text{CHCH}_2\text{Ph}$  and NH), 6.26 (brs, 1H, =CH), 7.18–7.39 (m, 10H,  $\text{Ph}$ ).  $\delta$   $^{13}\text{C}$  NMR (100.61 MHz,  $\text{CDCl}_3$ ): 25.7 (=C $\underline{\text{C}}\text{H}_2$ ), 28.3 ( $\underline{\text{C}}\text{H}_3$ -Boc), 43.7 ( $\text{CHC}\underline{\text{H}}_2\text{Ph}$  and  $\text{CH}_2\text{N}$ )<sup>r</sup>, 47.8 ( $\text{NCH}_2\text{Ph}$ ), 50.8 ( $\text{CHCH}_2\text{Ph}$ ), 79.6 (C-Boc), 126.8 (CH), 128.1 (CH), 128.6 (CH), 128.7 (CH), 128.8 (CH), 129.6 (CH), 134.7 (C), 135.0 (C), 155.1 (C=O). HR-ESI-MS calcd. for  $\text{C}_{24}\text{H}_{30}\text{N}_2\text{NaO}_4\text{S}$  ( $\text{MNa}^+$ ) 465.5618, found 465.1818.

**(E)-2-Phenyl-5-[(2S)-N-tert-butoxycarbonyl-2-amino-3-phenyl-propylidene]-1,2-**

**thiazinane 1,1-dioxide (2.69a)**; pale oil (65%); IR (film):  $\nu_{\text{max}}$  = 3368 (NH), 1701 (C=O), 1595, 1499, 1450, 1339 (S=O), 1247 (C-O), 1162 (br), 854, 738, 697  $\text{cm}^{-1}$ .  $\delta$   $^1\text{H}$  NMR (400 MHz,  $\text{CDCl}_3$ ): 1.47 (s, 9H,  $\text{CH}_3$ -Boc), 1.50 (m, 1H, =C $\text{CH}_2\text{C}\underline{\text{H}}\text{H}$ ), 1.92 (m, 1H, =C $\text{CH}_2\text{C}\underline{\text{H}}\text{H}$ ), 2.59–2.66 (m, 1H, =C $\underline{\text{C}}\text{H}\text{H}$ ), 2.77 (dd, 1H,  $J$  = 8.2, 13.4,  $\text{C}\underline{\text{H}}\text{HPh}$ ), 2.87–2.89 (m, 1H, =C $\underline{\text{C}}\text{H}\text{H}$ ), 3.04 (dd, 1H,  $J$  = 5.0, 13.4,  $\text{C}\underline{\text{H}}\text{HPh}$ ), 3.77–3.80 (m, 2H,  $\text{CH}_2\text{N}$ ), 4.71 (m, 2H,  $\text{CHCH}_2\text{Ph}$  and NH), 6.24 (brd, 1H,  $J$  = 8.8, =CH), 7.20–7.35 (m, 10H,  $\text{Ph}$ ).  $\delta$   $^{13}\text{C}$  NMR (100.61 MHz,  $\text{CDCl}_3$ ): 26.2 (=C $\text{CH}_2\text{C}\underline{\text{H}}_2$ ), 27.1 (=C $\underline{\text{C}}\text{H}_2$ ), 28.4 ( $\underline{\text{C}}\text{H}_3$ -Boc), 41.2 ( $\underline{\text{C}}\text{H}_2\text{Ph}$ ), 49.0 ( $\underline{\text{C}}\text{HCH}_2\text{Ph}$ ), 53.4 ( $\text{CH}_2\text{N}$ ), 80.0 (C-Boc), 126.9 (CH), 127.0 (CH), 127.2 (CH), 128.7 (CH), 129.1 (CH), 129.5 (CH), 131.3 (=CH), 136.2 (C), 140.0 (=C), 141.2 (C), 154.9 (C=O). HR-ESI-MS calcd. for  $\text{C}_{24}\text{H}_{30}\text{N}_2\text{NaO}_4\text{S}$  ( $\text{MNa}^+$ ) 465.5618, found 465.1818.

**(Z)-2-Phenyl-5-[(2S)-N-tert-butoxycarbonyl-2-amino-3-phenyl-propylidene]-1,2-**

**thiazinane 1,1-dioxide (2.69b)**; white amorphous solid (7%); IR (film):  $\nu_{\text{max}}$  = 3365 (NH), 1702 (C=O), 1498, 1453, 1337 (S=O), 1246 (C-O), 1162 (br), 855, 749, 693  $\text{cm}^{-1}$ .  $\delta$   $^1\text{H}$  NMR (400 MHz,  $\text{CDCl}_3$ ): 1.41 (s, 9H,  $\text{CH}_3$ -Boc), 1.95–2.07 (m, 2H, =C $\text{CH}_2\text{C}\underline{\text{H}}_2$ ), 2.90 (m, =C $\underline{\text{C}}\text{H}_2$ )<sup>s</sup>, 2.95 (m,  $\text{CH}_2\text{Ph}$ )<sup>s</sup>, 3.85–3.98 (m, 2H,  $\text{CH}_2\text{N}$ ), 4.71 (brs, 1H, NH), 5.10 (brs, 1H,  $\text{CHCH}_2\text{Ph}$ ), 6.12 (brs, 1H, =CH), 7.19–7.39 (m, 10H,  $\text{Ph}$ ).  $\delta$   $^{13}\text{C}$  NMR (100.61 MHz,  $\text{CDCl}_3$ ): 26.3 (=C $\text{CH}_2\text{C}\underline{\text{H}}_2$ ), 28.3 ( $\underline{\text{C}}\text{H}_3$ -Boc), 35.0 (=C $\underline{\text{C}}\text{H}_2$ ), 40.4 ( $\underline{\text{C}}\text{H}_2\text{Ph}$ ), 50.0 ( $\text{CHCH}_2\text{Ph}$ ), 53.8 ( $\text{CH}_2\text{N}$ ), 79.5 (C-Boc), 126.6 (CH), 127.3 (2 $\times$ CH), 128.5 (CH), 129.2 (CH), 129.5 (CH), 136.0 (=C), 136.5 (=CH), 137.3 (C), 141.3 (C), 155.2 (C=O). HR-ESI-MS calcd. for  $\text{C}_{24}\text{H}_{31}\text{N}_2\text{O}_4\text{S}$  ( $\text{MH}^+$ ) 443.5800, found 443.1999.

<sup>p</sup> Overlapped signals.  $\delta$  Values from HMQC spectrum.

<sup>q</sup> Overlapped signals.  $\delta$  Values from HMQC spectrum.

<sup>r</sup> Signal assignment was effected using HMQC,  $^1\text{H}$ - $^1\text{H}$  COSY and HMBC techniques.

<sup>s</sup> Overlapped signals.  $\delta$  Values from HMQC spectrum.

**(E)-2-Benzyl-5-[(2S)-N-tert-butoxycarbonyl-2-amino-3-phenyl-propylidene]-1,2-thiazinane 1,1-dioxide (2.70a)**; pale oil (54%); IR (film):  $\nu_{\max}$  = 3367 (NH), 1704 (C=O), 1502, 1452, 1334 (S=O), 1247 (C-O), 1163 (br), 855, 769, 739, 701  $\text{cm}^{-1}$ .  $\delta$   $^1\text{H}$  NMR (400 MHz,  $\text{CDCl}_3$ ): 1.48 (s, 9H,  $\text{CH}_3$ -Boc), 1.64 (m, 2H, =CCH $_2$ CH $_2$ ), 2.56-2.57 (m, 1H, =CCHH), 2.73 (m, =CCHH)<sup>†</sup>, 2.74 (m, CHCHHPh)<sup>†</sup>, 3.13 (dd, 1H,  $J$  = 5.0, 13.4, CHCHHPh), 3.19-3.27 (m, 2H, CH $_2$ N), 3.82 (brd, 1H,  $J$  = 14.2, NCHHPh), 4.07 (brd, 1H,  $J$  = 14.2, NCHHPh), 4.68-4.74 (m, 2H, CHCH $_2$ Ph and NH), 6.21 (d, 1H,  $J$  = 9.6, =CH), 7.24-7.39 (m, 10H, Ph).  $\delta$   $^{13}\text{C}$  NMR (100.61 MHz,  $\text{CDCl}_3$ ): 23.0 (=CCH $_2$ CH $_2$ ), 27.0 (=CCH $_2$ ), 28.4 ( $\text{CH}_3$ -Boc), 41.3 (CHCH $_2$ Ph), 47.4 (CH $_2$ N), 49.1 (CHCH $_2$ Ph), 50.2 (NCH $_2$ Ph), 80.1 (C-Boc), 127.1 (CH), 127.8 (CH), 128.4 (CH), 128.6 (CH), 128.8 (CH), 129.6 (CH), 132.4 (=CH), 136.0 (C), 136.5 (C), 138.4 (=C), 154.9 (C=O). HR-ESI-MS calcd. for  $\text{C}_{25}\text{H}_{32}\text{N}_2\text{NaO}_4\text{S}$  ( $\text{MNa}^+$ ) 479.5884, found 479.1975.

**(Z)-2-Benzyl-5-[(2S)-N-tert-butoxycarbonyl-2-amino-3-phenyl-propylidene]-1,2-thiazinane 1,1-dioxide (2.70b)**; white amorphous solid (9%); IR (film):  $\nu_{\max}$  = 3409 (NH), 1696 (C=O), 1512, 1335 (S=O), 1250 (C-O), 1156 (br), 856, 769, 732, 698  $\text{cm}^{-1}$ .  $\delta$   $^1\text{H}$  NMR (400 MHz,  $\text{CDCl}_3$ ): 1.34 (s, 9H,  $\text{CH}_3$ -Boc), 1.65 (m, 2H, =CCH $_2$ CH $_2$ ), 2.65-2.66 (m, 2H, =CCH $_2$ ), 2.94 (brs, 2H, CHCH $_2$ Ph), 3.26 (m, 2H, CH $_2$ N), 4.06 (d, 1H,  $J$  = 14.0, NCHHPh), 4.21 (brd, 1H, NCHHPh)<sup>u</sup>, 4.66 (brs, 1H, NH), 5.17 (brs, 1H, CHCH $_2$ Ph), 5.98 (brs, 1H, =CH), 7.13-7.30 (m, 10H, Ph).  $\delta$   $^{13}\text{C}$  NMR (100.61 MHz,  $\text{CDCl}_3$ ): 23.6 (=CCH $_2$ CH $_2$ ), 28.4 ( $\text{CH}_3$ -Boc), 34.8 (=CCH $_2$ ), 41.0 (CHCH $_2$ Ph), 47.6 (CH $_2$ N), 49.8 (CHCH $_2$ Ph), 50.4 (NCH $_2$ Ph), 77.8 (C-Boc), 126.8 (CH), 127.8 (CH), 128.4 (CH), 128.5 (CH), 128.7 (CH), 129.6 (CH), 135.3 (=C), 136.0 (C), 136.7 (C and =CH)<sup>v</sup>, 155.1 (C=O). HR-ESI-MS calcd. for  $\text{C}_{25}\text{H}_{32}\text{N}_2\text{NaO}_4\text{S}$  ( $\text{MNa}^+$ ) 479.5884, found 479.1975.

#### 5.1.4.8 Deprotection (removal of Boc protecting group)

Compound **2.69a** (232 mg; 0.5 mmol) was dissolved in a solution (2.4 mL) of TFA 50% (w/v DCM solution). The mixture was stirred at rt for 20 min and then excess TFA was neutralized by dropwise addition of aqueous potassium carbonate at 30% (w/v) until pH 10. After dilution

<sup>†</sup> Overlapped signals.  $\delta$  Values from HMQC spectrum.

<sup>u</sup> Not well resolved signal.

<sup>v</sup> Signal assignment was effected using HMQC and HMBC techniques.

with water (30 mL), the reaction medium was extracted with EtOAc (3×20 mL) and DCM (3×20 mL). The organic layers were washed with water, combined, dried with anhydrous magnesium sulfate and evaporated to give **2.73a** (143 mg). Compounds **2.72a**, **2.72b**, **2.73b**, **2.74a** and **2.74b** were prepared using the same method from **2.68a**, **2.68b**, **2.69b**, **2.70a** and **2.70b**, respectively.

**(E)-2-Benzyl-5-[(2S)-2-amino-3-phenyl-propylidene]isothiazolidine 1,1-dioxide (2.72a)**; yellow oil (78%); IR (film):  $\nu_{\max}$  = 3364 (NH), 3305 (NH), 1600, 1497, 1449, 1298, 1156 (S=O), 784, 748, 696  $\text{cm}^{-1}$ .  $\delta$   $^1\text{H}$  NMR (400 MHz,  $\text{CDCl}_3$ ): 2.06–2.14 (m, 1H), 2.56–2.64 (m, 1H), 2.75–2.89 (m, 3H), 2.92–2.97 (m, 1H), 3.67–3.72 (m, 1H), 4.09 (d, 1H,  $J$  = 14.0,  $\text{NCHHPh}$ ), 4.16 (d, 1H,  $J$  = 14.0,  $\text{NCHHPh}$ ), 6.36 (td, 1H,  $J$  = 2.8, 8.9, =CH), 7.18–7.37 (m, 10H, Ph). ESI-MS  $m/z$  (rel. int.) 685 ( $\text{M}_2\text{H}^+$ ) (100).

**(Z)-2-Benzyl-5-[(2S)-2-amino-3-phenyl-propylidene]isothiazolidine 1,1-dioxide (2.72b)**; yellow oil (73%); IR (film):  $\nu_{\max}$  = 3364 (NH), 3296 (NH), 1600, 1498, 1459, 1288, 1151 (S=O), 775, 733, 701  $\text{cm}^{-1}$ .  $\delta$   $^1\text{H}$  NMR (400 MHz,  $\text{CDCl}_3$ ): 2.61–2.67 (m, 1H), 2.78–2.81 (m, 2H), 2.99–3.08 (m, 3H), 4.18 (brd, 2H,  $J$  = 2.4,  $\text{NCH}_2\text{Ph}$ )<sup>w</sup>, 4.63 (brddd, 1H,  $J$  = 4.4, 9.0, 9.8,  $\text{CHCH}_2\text{Ph}$ )<sup>x</sup>, 5.93 (td, 1H,  $J$  = 2.0, 9.8, =CH), 7.28–7.37 (m, 10H, Ph). ESI-MS  $m/z$  (rel. int.) 685 ( $\text{M}_2\text{H}^+$ ) (100).

**(E)-2-Phenyl-6-[(2S)-2-amino-3-phenyl-propylidene]-1,2-thiazinane 1,1-dioxide (2.73a)**; yellow oil (80%); IR (film):  $\nu_{\max}$  = 3364 (NH), 3296 (NH), 1595, 1488, 1337 (S=O), 1156 (S=O), 856, 831, 756, 699  $\text{cm}^{-1}$ .  $\delta$   $^1\text{H}$  NMR (400 MHz,  $\text{CDCl}_3$ ): 1.31–1.41 (m, 1H), 1.69–1.78 (m, 1H), 2.57–2.64 (m, 1H), 2.68–2.77 (m, 2H), 2.95 (dd, 1H,  $J$  = 6.0, 13.2,  $\text{CHHPh}$ ), 3.60–3.65 (m, 1H), 3.80–3.93 (m, 2H), 6.35 (d, 1H,  $J$  = 9.6, =CH), 7.18–7.36 (m, 10H, Ph). ESI-MS  $m/z$  (rel. int.) 685 ( $\text{M}_2\text{H}^+$ ) (100).

**(Z)-2-Phenyl-6-[(2S)-2-amino-3-phenyl-propylidene]-1,2-thiazinane 1,1-dioxide (2.73b)**; yellow oil (83%); IR (film):  $\nu_{\max}$  = 3374 (NH), 3286 (NH), 1595, 1488, 1342 (S=O), 1151 (S=O), 836, 721, 699  $\text{cm}^{-1}$ .  $^1\text{H}$  NMR (400 MHz,  $\text{CDCl}_3$ ): 1.91–2.07 (m, 2H), 2.55 (dd, 1H,  $J$  = 9.0, 13.4,  $\text{CHHPh}$ ), 2.83–2.96 (m, 3H), 3.79–3.85 (m, 1H), 3.89–3.95 (m, 1H), 4.67–4.73

<sup>w</sup> Co-incident peak.

<sup>x</sup> Not well resolved signal.

(m, 1H), 5.80 (d, 1H,  $J = 8.8$ , =CH), 7.18–7.37 (m, 10H, Ph). ESI-MS  $m/z$  (rel. int.) 343 ( $MH^+$ ) (100).

**(E)-2-Benzyl-6-[(2S)-2-amino-3-phenyl-propylidene]-1,2-thiazinane 1,1-dioxide (2.74a)**; yellowish amorphous solid (84%); IR (film):  $\nu_{\max} = 3364$  (NH), 3296 (NH), 1493, 1454, 1327 (S=O), 1161 (S=O), 851, 768, 740, 701  $\text{cm}^{-1}$ .  $\delta$   $^1\text{H}$  NMR (400 MHz,  $\text{CDCl}_3$ ): 0.97–1.08 (m, 1H), 1.34–1.44 (m, 1H), 2.45–2.51 (m, 1H), 2.55–2.62 (m, 1H), 2.66 (dd, 1H,  $J = 10.4$ , 13.2, CHCH $\underline{\text{H}}$ Ph), 2.98 (dddd, 1H,  $J = 1.2$ , 4.2, 4.6, 14.5, =CCH $\underline{\text{H}}$ ), 3.06 (dd, 1H,  $J = 5.8$ , 13.2, CHCH $\underline{\text{H}}$ Ph), 3.37 (ddd, 1H,  $J = 3.0$ , 10.7, 14.4), 3.69 (d, 1H,  $J = 14.4$ , NCH $\underline{\text{H}}$ Ph), 3.89–3.97 (m, 1H), 4.16 (d, 1H,  $J = 14.4$ , NCH $\underline{\text{H}}$ Ph), 6.32 (d, 1H,  $J = 9.6$ , =CH), 7.22–7.36 (m, 10H, Ph). ESI-MS  $m/z$  (rel. int.) 713 ( $M_2H^+$ ) (100).

**(Z)-2-Benzyl-6-[(2S)-2-amino-3-phenyl-propylidene]-1,2-thiazinane 1,1-dioxide (2.74b)**; yellow oil (79%); IR (film):  $\nu_{\max} = 3364$  (NH), 3296 (NH), 1498, 1454, 1332 (S=O), 1151 (S=O), 848, 765, 731, 699  $\text{cm}^{-1}$ .  $\delta$   $^1\text{H}$  NMR (400 MHz,  $\text{CDCl}_3$ ): 1.68–1.74 (m, 2H), 2.66–2.79 (m, 3H), 2.87 (dd, 1H,  $J = 5.6$ , 13.2, CHCH $\underline{\text{H}}$ Ph), 3.23–3.29 (m, 1H), 3.34–3.41 (m, 1H), 3.92 (d, 1H,  $J = 14.0$ , NCH $\underline{\text{H}}$ Ph), 4.12 (d, 1H,  $J = 14.0$ , NCH $\underline{\text{H}}$ Ph), 4.79–4.85 (m, 1H), 5.81 (d, 1H,  $J = 9.2$ , =CH), 7.20–7.36 (m, Ph). ESI-MS  $m/z$  (rel. int.) 713 ( $M_2H^+$ ) (100).

**(E)-2-Phenyl-5-[(2S)-2-amino-3-phenyl-propylidene]isothiazolidine 1,1-dioxide hydrochloride (2.75)**

Compound **2.67a** (150 mg; 0.4 mmol) was dissolved in a solution (1.6 mL) of TFA 50% (w/v DCM solution). The mixture was stirred at rt for 20 min, then DCM was evaporated and the residue was washed with small portions of ethyl ether to afford **2.75** (100 mg).

**2.75**; white amorphous solid (76%); IR (KBr):  $\nu_{\max} = 3290$  (br, NH), 2000 (br), 1585, 1496, 1420 (br), 1317 (S=O), 1150 (S=O), 920, 753, 698  $\text{cm}^{-1}$ .  $\delta$   $^1\text{H}$  NMR (400 MHz, MeOD): 1.85–2.00 (m, 1H), 2.72–2.79 (m, 1H), 2.85 (dd, 1H,  $J = 7.8$ , 13.0, CH $\underline{\text{H}}$ Ph), 3.02 (dd, 1H,  $J = 7.6$ , 13.0, CH $\underline{\text{H}}$ Ph), 3.04–3.06 (m, 1H), 3.55–3.60 (m, 1H), 4.02–4.05 (m, 1H), 6.24 (td, 1H,  $J = 2.5$ , 9.6, =CH), 7.20–7.25 (m, 5H, Ph). ESI-MS  $m/z$  (rel. int.) 329 ( $M^+$ ) (100).

#### 5.1.4.9 Coupling with aminoacids and endcapping of the dipeptide moiety

##### **(*E*)-2-Phenyl-6-[(2*S*)-*N*-(*N*'-acetyl-*S*-phenylalanyl)-2-amino-3-phenyl-propylidene]-1,2-thiazinane 1,1-dioxide (2.1)**

TEA (212 mg; 2.1 mmol) was added to a solution of **2.73a** (169 mg; 0.5 mmol) in DCM (9 mL), at 0 °C. Then, *N*-Ac-*S*-phenylalanine (102 mg; 0.5 mmol) was added, followed by HOBt (81 mg; 0.6 mmol) and DCC (125 mg; 0.6 mmol). The reaction was stirred at rt for 3 days. The precipitate formed was removed by filtration and the filtrate was diluted with DCM (20 mL), washed with 20 mL of hydrochloric acid 5% (w/v) and of water, and dried with anhydrous magnesium sulfate. The solvent was evaporated to afford a mixture (144 mg), which was subject to column chromatography on silica gel (14 g) using a gradient of DCM/EtOAc (1:0→0:1) to yield **2.1** (35 mg).

**2.1**; white amorphous solid (13%);  $[\alpha]_D^{21} = +33^\circ$  (CHCl<sub>3</sub>, *c* 0.82). IR (film):  $\nu_{\max} = 3281$  (br, NH), 1644 (br, C=O), 1498, 1339 (S=O), 1158 (S=O), 737, 698 cm<sup>-1</sup>. HR-ESI-MS calcd. for C<sub>30</sub>H<sub>34</sub>N<sub>3</sub>O<sub>4</sub>S (MH<sup>+</sup>) 532.6748, found 532.2265. <sup>1</sup>H and <sup>13</sup>C NMR see Table 2.9 in Chapter 2.

##### **Condensation with *N*-Boc-*S*-leucine-*N*-hydroxysuccinimide ester – synthesis of compounds 2.76a,b, 2.77 and 2.78a,b**

*N*-Boc-*S*-leucine-*N*-hydroxysuccinimide ester (127 mg; 0.4 mmol) was added to a solution of **2.73a** (132 mg; 0.4 mmol) in dry THF (2 mL) with TEA (39 mg; 0.4 mmol). The reaction mixture was stirred at rt for 14 h, then it was evaporated to leave a product, which was dissolved in DCM (40 mL) and washed with 40 mL of hydrochloric acid 5% (w/v) and of water. After being dried with anhydrous magnesium sulfate, the solvent was evaporated to yield **2.77** (173 mg), which was purified by column chromatography on silica gel (17 g) using EtOAc as eluent (50 mL). <sup>1</sup>H and <sup>13</sup>C NMR signal assignments were possible using DEPT and 2D NMR techniques (<sup>1</sup>H-<sup>1</sup>H COSY and HMQC).

##### **(*E*)-2-Benzyl-5-[(2*S*)-*N*-(*N*'-tert-butoxycarbonyl-*S*-leucinyloxy)-2-amino-3-phenyl-propylidene]isothiazolidine 1,1-dioxide (2.76a)**

**2.76a** was prepared from **2.72a** (reaction time: 48 h); yellow oil (54%); IR (film):  $\nu_{\max} = 3331$  (NH), 3280 (NH), 1689 (C=O), 1651 (C=O), 1523, 1453, 1306, 1166, 779, 704 cm<sup>-1</sup>.  $\delta$  <sup>1</sup>H NMR (400 MHz, CDCl<sub>3</sub>): 0.87–0.93 [m, 6H, 2×CH<sub>3</sub> (Leu)], 1.44 (s, 9H, CH<sub>3</sub>-Boc), 1.55–1.63 [m, 3H, CH<sub>2</sub> and CH(CH<sub>3</sub>)<sub>2</sub> (Leu)], 2.17 (m, 1H, =CCHH), 2.82–2.89 [m, 3H,

=CCHH, CHHPh (Phe) and CHHN], 2.91–3.01 [m, 2H, CHHPhe (Phe) and CHHN], 4.03 [m, 1H, CHCO (Leu)], 4.08 (d, 1H,  $J = 14.2$ , NCHHPh), 4.14 (d, 1H,  $J = 14.2$ , NCHHPh), 4.66–4.78 [m, 2H, CHCH<sub>2</sub>Ph (Phe) and NH (Leu)], 6.26 (brd, 1H,  $J = 9.2$ , =CH), 6.51 [brs, 1H, NH (Phe)], 7.18–7.34 (m, 10H, Ph).  $\delta$  <sup>13</sup>C NMR (100.61 MHz, CDCl<sub>3</sub>): 21.8 [CH<sub>3</sub> (Leu) and =CCH<sub>2</sub>], 23.0 [CH<sub>3</sub> (Leu)], 24.7 [CH(CH<sub>3</sub>)<sub>2</sub> (Leu)], 28.3 (CH<sub>3</sub>-Boc), 40.6 [CH<sub>2</sub>Ph (Phe)]<sup>y</sup>, 40.7 [CH<sub>2</sub> (Leu)]<sup>y</sup>, 43.2 (CH<sub>2</sub>N), 47.9 (NCH<sub>2</sub>Ph), 49.4 [CHCH<sub>2</sub>Ph (Phe)], 53.1 [CHCO (Leu)], 127.1 (CH), 128.0 (CH), 128.7 (3×CH), 129.6 (CH)<sup>z</sup>, 129.8 (=CH)<sup>z</sup>, 134.9 (C), 136.0 (C)<sup>aa</sup>, 139.2 (=C)<sup>aa</sup>, 155.9 (CO-Boc), 172.1 [CO (Leu)]. ESI-MS  $m/z$  (rel. int.) 579 (MNa<sup>+</sup>) (100).

**(Z)-2-Benzyl-5-[(2S)-N-(N'-tert-butoxycarbonyl-S-leuciny)-2-amino-3-phenyl-propylidene]isothiazolidine 1,1-dioxide (2.76b)**

**2.76b** was prepared from **2.72b** (reaction time: 18 h); white amorphous solid (62%); IR (film):  $\nu_{\max} = 3344$  (NH), 3280 (NH), 1683 (C=O), 1659 (C=O), 1517, 1453, 1294, 1160, 772, 734, 702 cm<sup>-1</sup>.  $\delta$  <sup>1</sup>H NMR (400 MHz, CDCl<sub>3</sub>): 0.89 [brd, 6H,  $J = 5.6$ , 2×CH<sub>3</sub> (Leu)], 1.42 (s, 9H, CH<sub>3</sub>-Boc), 1.55–1.62 (m, 2H), 2.78–2.81 (m, 2H), 3.05–3.23 (m, 4H), 4.05 (m, 1H), 4.18 (brd, 2H,  $J = 2.0$ ), 4.76 (brd, 1H,  $J = 7.2$ ), 5.02–5.10 (m, 1H), 6.23 (brd, 1H,  $J = 8.0$ ), 6.50 (brd, 1H,  $J = 6.8$ ), 7.23–7.37 (m, 10H, Ph).  $\delta$  <sup>13</sup>C NMR (100.61 MHz, CDCl<sub>3</sub>): 21.8 [CH<sub>3</sub> (Leu)], 23.0 [CH<sub>3</sub> (Leu)], 24.7 [CH(CH<sub>3</sub>)<sub>2</sub> (Leu)], 25.7 (=CCH<sub>2</sub>), 28.3 (CH<sub>3</sub>-Boc), 39.4 [CH<sub>2</sub>Ph (Phe)], 41.2 [CH<sub>2</sub> (Leu)], 43.6 (CH<sub>2</sub>N), 47.9 (NCH<sub>2</sub>Ph), 50.2 [CHCH<sub>2</sub>Ph (Phe)], 53.0 [CHCO (Leu)], 126.8 (CH), 128.1 (CH), 128.6 (CH), 128.7 (CH), 128.8 (CH), 129.5 (CH), 133.7, 134.9, 137.1, 172.5 [CO (Leu)]. ESI-MS  $m/z$  (rel. int.) 579 (MNa<sup>+</sup>) (100).

**(E)-2-Phenyl-6-[(2S)-N-(N'-tert-butoxycarbonyl-S-leuciny)-2-amino-3-phenyl-propylidene]-1,2-thiazinane 1,1-dioxide (2.77)**

**2.77**; yellowish amorphous solid (70%); IR (film):  $\nu_{\max} = 3342$  (NH), 3282 (NH), 1687 (C=O), 1651 (C=O), 1520, 1295, 1165, 777, 735, 702 cm<sup>-1</sup>.  $\delta$  <sup>1</sup>H NMR (400 MHz, CDCl<sub>3</sub>): 0.89–0.94 [m, 6H, 2×CH<sub>3</sub> (Leu)], 1.44 (s, 9H, CH<sub>3</sub>-Boc), 1.56–1.65 (m, 2H), 1.83–2.00 (m, 1H), 2.61 (m, 1H), 2.75–2.88 (m, 2H), 2.96–3.04 (m, 1H), 3.68–3.84 (m, 2H), 4.05 (m, 1H), 4.73–4.78 (m, 1H), 4.94 (ddd, 1H,  $J = 5.6, 8.8, 17.6$ ),

<sup>y</sup>  $\delta$  Values are interchangeable.

<sup>z</sup>  $\delta$  Values are interchangeable.

<sup>aa</sup>  $\delta$  Values are interchangeable.

6.23 (d, 1H,  $J = 9.6$ , =CH), 6.50 [brs, 1H, NH (Phe)], 7.18–7.34 (m, 10H, Ph). ESI-MS  $m/z$  (rel. int.) 579 ( $MNa^+$ ) (100).

**(*E*)-2-Benzyl-6-[(2*S*)-*N*-(*N'*-*tert*-butoxycarbonyl-*S*-leuciny)]-2-amino-3-phenyl-propylidene]-1,2-thiazinane 1,1-dioxide (2.78a)**

**2.78a** was prepared from **2.74a** (reaction time: 19h); yellowish amorphous solid (67%); IR (film):  $\nu_{\max} = 3293$  (br, NH), 1683 (C=O), 1651 (C=O), 1529, 1453, 1338 (S=O), 1166, 772, 740, 701  $\text{cm}^{-1}$ .  $\delta$   $^1\text{H}$  NMR (400 MHz,  $\text{CDCl}_3$ ): 0.91–0.94 [m, 6H,  $2 \times \text{CH}_3$  (Leu)], 1.10–1.20 (m, 1H), 1.45 (s, 9H,  $\text{CH}_3$ -Boc), 1.58–1.68 (m, 3H), 2.57 (m, 1H), 2.65–2.81 (m, 2H), 3.10 [dd, 1H,  $J = 5.2, 13.2$ ,  $\text{CHHPh}$  (Phe)]<sup>bb</sup>, 3.07–3.15 (m, 1H)<sup>bb</sup>, 3.24–3.29 (m 1H), 3.76–3.81 (m, 1H), 4.02 (brs, 1H,  $\text{NCHHPh}$ ), 4.06 (brs, 1H,  $\text{NCHHPh}$ ), 4.78–4.85 (m, 1H), 4.95 (ddd, 1H,  $J = 5.2, 9.4, 17.8$ ), 6.21 (d, 1H,  $J = 9.6$ , =CH), 6.59 [brs, 1H, NH (Phe)], 7.22–7.34 (m, 10H, Ph).  $\delta$   $^{13}\text{C}$  NMR (100.61 MHz,  $\text{CDCl}_3$ ): 22.0 [ $\text{CH}_3$  (Leu)], 23.0 [ $\text{CH}_3$  (Leu)]<sup>cc</sup>, 23.1 (=C $\text{CH}_2\text{CH}_2$ )<sup>cc</sup>, 24.8 [ $\text{CH}(\text{CH}_3)_2$  (Leu)], 27.0 (=C $\text{CH}_2$ ), 28.3 ( $\text{CH}_3$ -Boc), 40.9 [ $\text{CH}_2\text{Ph}$  (Phe)], 41.0 [ $\text{CH}_2$  (Leu)], 47.4 ( $\text{CH}_2\text{N}$ ), 47.7 [ $\text{CHCH}_2\text{Ph}$  (Phe)], 50.2 ( $\text{NCH}_2\text{Ph}$ ), 127.1 (CH), 127.8 (CH), 128.5 (CH), 128.6 (CH), 128.8 (CH), 129.5 (CH), 131.4 (=CH), 135.9 (C), 136.4 (C), 139.2 (=C), 155.0 ( $\text{CO}$ -Boc), 172.0 [ $\text{CO}$  (Leu)]. ESI-MS  $m/z$  (rel. int.) 593 ( $MNa^+$ ) (100).

**(*Z*)-2-Benzyl-6-[(2*S*)-*N*-(*N'*-*tert*-butoxycarbonyl-*S*-leuciny)]-2-amino-3-phenyl-propylidene]-1,2-thiazinane 1,1-dioxide (2.78b)**

**2.78b** was prepared from **2.74b** (reaction time: 19h); yellowish amorphous solid (64%); IR (film):  $\nu_{\max} = 3293$  (br, NH), 1689 (C=O), 1651 (C=O), 1523, 1447, 1338 (S=O), 1160, 766, 730, 695  $\text{cm}^{-1}$ .  $\delta$   $^1\text{H}$  NMR (400 MHz,  $\text{CDCl}_3$ ): 0.87–0.89 [m, 6H,  $2 \times \text{CH}_3$  (Leu)], 1.43 (s, 9H,  $\text{CH}_3$ -Boc), 1.56–1.59 (m, 2H), 1.76–1.86 (m, 2H), 2.63–2.69 (m, 1H), 2.76–2.82 (m, 1H), 3.26–3.30 (m, 1H), 3.33 (brd, 2H,  $J = 7.2$ ), 3.40–3.46 (m, 1H), 4.01 (m, 1H), 4.10 (d, 1H,  $J = 14.4$ ,  $\text{NCHHPh}$ ), 4.25 (d, 1H,  $J = 14.4$ ,  $\text{NCHHPh}$ ), 4.69 (m, 1H), 5.43–5.50 (m, 1H), 5.98 (d, 1H,  $J = 8.4$ , =CH), 6.36 [brd, 1H,  $J = 6.0$ , NH (Phe)], 7.22–7.34 (m, 10H, Ph).  $\delta$   $^{13}\text{C}$  NMR (100.61 MHz,  $\text{CDCl}_3$ ): 21.8 [ $\text{CH}_3$  (Leu)], 23.0 [ $\text{CH}_3$  (Leu)], 23.5 (=C $\text{CH}_2\text{CH}_2$ ), 24.7 [ $\text{CH}(\text{CH}_3)_2$  (Leu)], 28.3 ( $\text{CH}_3$ -Boc), 34.8 (=C $\text{CH}_2$ ), 40.7 [ $\text{CH}_2\text{Ph}$  (Phe)], 41.0 [ $\text{CH}_2$  (Leu)], 47.6 ( $\text{CH}_2\text{N}$ ), 49.1 [ $\text{CHCH}_2\text{Ph}$  (Phe)], 50.5 ( $\text{NCH}_2\text{Ph}$ ), 80.1 (C-Boc), 126.9 (CH), 127.8 (CH),

<sup>bb</sup> Overlapped signals.

<sup>cc</sup>  $\delta$  Values are interchangeable.

128.5 (2×CH), 128.6 (CH), 129.4 (CH), 129.5 (CH), 136.1, 137.0, 172.3 [CO (Leu)]. ESI-MS  $m/z$  (rel. int.) 593 (MNa<sup>+</sup>) (81).

***N*-Boc group deprotection of dipeptide vinyl sultams – synthesis of compounds 2.79a,b, 2.80 and 2.81a,b**

**2.79a,b, 2.80 and 2.81a,b** were respectively prepared from **2.76a,b, 2.77 and 2.78a,b** using the method described earlier for **2.72-2.74**.

**(*E*)-2-Benzyl-5-[(2*S*)-*N*-*S*-leuciny-2-amino-3-phenyl-propylidene]isothiazolidine 1,1-dioxide (2.79a)**; yellow oil (73%); IR (film):  $\nu_{\max}$  = 3315 (br, NH), 1654 (C=O), 1498, 1366, 1293, 1166 (S=O), 782, 699 cm<sup>-1</sup>.  $\delta$  <sup>1</sup>H NMR (400 MHz, CDCl<sub>3</sub>): 0.88–0.93 [m, 6H, 2×CH<sub>3</sub> (Leu)], 1.15–1.25 (m, 2H), 1.58–1.67 (m)<sup>dd</sup>, 2.18–2.35 (m, 1H), 2.79–3.02 (m, 5H), 3.32–3.35 (m, 1H), 4.10 (d, 1H,  $J$  = 14.0, NCHHPh), 4.16 (d, 1H,  $J$  = 14.0, NCHHPh), 4.71–4.79 (m, 1H), 6.28 (td, 1H,  $J$  = 2.4, 9.6, =CH), 7.19–7.36 (m, 10H, Ph), 7.69 (d, 1H,  $J$  = 8.4, NH). ESI-MS  $m/z$  (rel. int.) 456 (MH<sup>+</sup>) (100).

**(*Z*)-2-Benzyl-5-[(2*S*)-*N*-*S*-leuciny-2-amino-3-phenyl-propylidene]isothiazolidine 1,1-dioxide (2.79b)**; yellow oil (56%); IR (film):  $\nu_{\max}$  = 3315 (br, NH), 1654 (C=O), 1454, 1293, 1156 (S=O), 777, 736, 701 cm<sup>-1</sup>.  $\delta$  <sup>1</sup>H NMR (400 MHz, CDCl<sub>3</sub>): 0.88 [d, 3H,  $J$  = 6.4, CH<sub>3</sub> (Leu)], 0.90 [d, 3H,  $J$  = 6.4, CH<sub>3</sub> (Leu)], 1.17–1.28 (m, 3H), 2.78–2.81 (m, 2H), 3.04–3.20 (m, 4H), 3.36 (dd, 1H,  $J$  = 4.0, 9.6), 4.14 (d, 1H,  $J$  = 14.0, NCHHPh), 4.21 (d, 1H,  $J$  = 14.0, NCHHPh), 4.99–5.07 (m, 1H), 6.24 (td, 1H,  $J$  = 2.0, 7.7, =CH), 7.23–7.37 (m, 10H, Ph), 7.72 (d, 1H,  $J$  = 7.2, NH). ESI-MS  $m/z$  (rel. int.) 911 (M<sub>2</sub><sup>+</sup>) (100).

**(*E*)-2-Phenyl-6-[(2*S*)-*N*-*S*-leuciny-2-amino-3-phenyl-propylidene]-1,2-thiazinane 1,1-dioxide (2.80)**; yellow oil (88%); IR (film):  $\nu_{\max}$  = 3325 (br, NH), 1654 (C=O), 1595, 1488, 1341 (S=O), 1161 (S=O), 856, 833, 736, 699 cm<sup>-1</sup>.  $\delta$  <sup>1</sup>H NMR (400 MHz, CDCl<sub>3</sub>): 0.91–0.97 [m, 6H, 2×CH<sub>3</sub> (Leu)], 1.60–1.72 (m)<sup>dd</sup>, 1.89–1.97 (m, 1H), 2.67–2.73 (m, 1H), 2.82 [dd, 1H,  $J$  = 8.4, 13.2, CHHPh (Phe)], 2.88–2.95 (m, 1H), 2.99 [dd, 1H,  $J$  = 6.2, 13.2, CHHPh (Phe)], 3.33–3.37 (m, 1H), 3.69–3.85 (m, 2H), 4.92–5.00 (m, 1H), 6.25 (d, 1H,  $J$  = 9.6, =CH), 7.19–7.33 (m, 10H, Ph), 7.66 (brd, 1H,  $J$  = 8.4, NH). ESI-MS  $m/z$  (rel. int.) 911 (M<sub>2</sub><sup>+</sup>) (100).

<sup>dd</sup> Obscured under water resonance.



**(E)-2-Benzyl-6-[(2S)-N-S-leucinyl-2-amino-3-phenyl-propylidene]-1,2-thiazinane 1,1-dioxide (2.81a)**; yellow oil (73%); IR (film):  $\nu_{\max}$  = 3315 (br, NH), 1654 (C=O), 1498, 1337 (S=O), 1161 (S=O), 770, 735, 701  $\text{cm}^{-1}$ .  $\delta$   $^1\text{H}$  NMR (400 MHz,  $\text{CDCl}_3$ ): 0.93 [d, 3H,  $J$  = 6.2,  $\text{CH}_3$  (Leu)], 0.96 [d, 3H,  $J$  = 6.2,  $\text{CH}_3$  (Leu)], 1.14–1.32 (m, 3H), 1.60–1.71 (m, 2H), 2.59–2.81 (m, 3H), 3.07–3.13 (m, 2H), 3.26–3.33 (m, 1H), 3.38 [dd, 1H,  $J$  = 3.2, 13.2,  $\text{CHHPh}$  (Phe)], 3.75 (d, 1H,  $J$  = 14.2,  $\text{NCHHPh}$ ), 4.06 (d, 1H,  $J$  = 14.2,  $\text{NCHHPh}$ ), 4.96 (ddd, 1H,  $J$  = 5.6, 9.2, 18.4), 6.24 (d, 1H,  $J$  = 10.0, =CH), 7.24–7.36 (m, 10H,  $\text{Ph}$ ), 7.70 (m, 1H, NH). ESI-MS  $m/z$  (rel. int.) 471 ( $\text{MH}^+$ ) (100).

**(Z)-2-Benzyl-6-[(2S)-N-S-leucinyl-2-amino-3-phenyl-propylidene]-1,2-thiazinane 1,1-dioxide (2.81b)**; yellowish amorphous solid (86%);  $\delta$   $^1\text{H}$  NMR (400 MHz,  $\text{CDCl}_3$ ): 0.86–0.90 [m, 6H,  $2 \times \text{CH}_3$  (Leu)], 1.24–1.28 (m), 1.43 (s,  $\text{CH}_3$ -Boc of **2.78b**), 1.77–1.86 (m), 2.63–2.70 (m), 2.77–2.84 (m), 3.02–3.12 (m), 3.25–3.33 (m), 3.41–3.49 (m), 4.09–4.17 (m), 4.20–4.31 (m), 5.35–5.49 (m), 6.04 (d,  $J$  = 8.4, =CH), 6.34–6.35 (m), 7.21–7.34 (m,  $\text{Ph}$ ), 7.52–7.54 (m). ESI-MS  $m/z$  (rel. int.) 471 ( $\text{MH}^+$ ) (100).

### Condensation with 4-morpholinecarbonyl chloride – synthesis of compounds **2.2**, **2.3** and **2.4a,b**

4-Morpholinecarbonyl chloride (44 mg; 0.2 mmol) diluted with dry THF (0.5 mL) was added to a solution of **2.80** (93 mg; 0.2 mmol) in dry THF (1.5 mL) with TEA (21 mg; 0.2 mmol). The reaction was stirred at rt for 16 h, during which the formation of a precipitate was observed. The solvent was evaporated, then the residue was dissolved in DCM (40 mL) and washed with 40 mL of hydrochloric acid 5% (w/v) and of water. After being dried with anhydrous magnesium sulfate, the solvent was evaporated to give a mixture (96 mg), which was subject to column chromatography on silica gel (15 g) using EtOAc as eluent (0.1 L) to give **2.3** (18 mg).

### **(E)-2-Benzyl-5-[(2S)-N-(N'-4-morpholinylcarbonyl-S-leucinyl)-2-amino-3-phenyl-propylidene]isothiazolidine 1,1-dioxide (2.2)**

**2.2** (44 mg) was prepared from **2.79a** (reaction time: 14 h); white amorphous solid (50%);  $[\alpha]_{\text{D}}^{21} = -14^\circ$  ( $\text{CHCl}_3$ ,  $c$  0.17). IR (film):  $\nu_{\max}$  = 3269 (br, NH), 1623 (br, C=O), 1456, 1300, 1155 (S=O), 738, 701  $\text{cm}^{-1}$ . HR-ESI-MS calcd. for  $\text{C}_{30}\text{H}_{41}\text{N}_4\text{O}_5\text{S}$  ( $\text{MH}^+$ ) 569.7365, found 569.2792.  $^1\text{H}$  and  $^{13}\text{C}$  NMR see Table 2.10 in Chapter 2.

**(E)-2-Phenyl-6-[(2S)-N-(N'-4-morpholinylcarbonyl-S-leuciny)]-2-amino-3-phenyl-propylidene]-1,2-thiazinane 1,1-dioxide (2.3)**; white amorphous solid (15%);  $[\alpha]_D^{21} = -26^\circ$  (CHCl<sub>3</sub>, *c* 0.67). IR (film):  $\nu_{\max} = 3264$  (br, NH), 1622 (br, C=O), 1455, 1342 (S=O), 1158 (S=O), 736, 695 cm<sup>-1</sup>. HR-ESI-MS calcd. for C<sub>30</sub>H<sub>41</sub>N<sub>4</sub>O<sub>5</sub>S (MH<sup>+</sup>) 569.7365, found 569.2792. <sup>1</sup>H and <sup>13</sup>C NMR see Table 2.11 in Chapter 2.

**(E)-2-Benzyl-6-[(2S)-N-(N'-4-morpholinylcarbonyl-S-leuciny)]-2-amino-3-phenyl-propylidene]-1,2-thiazinane 1,1-dioxide (2.4a)**

**2.4a** (68 mg) was prepared from **2.81a** (reaction time: 15 h); white amorphous solid (39%);  $[\alpha]_D^{21} = -20^\circ$  (CHCl<sub>3</sub>, *c* 0.13). IR (film):  $\nu_{\max} = 3318$  (br, NH), 1621 (br, C=O), 1457, 1336 (S=O), 1157 (S=O), 737, 699 cm<sup>-1</sup>. HR-ESI-MS calcd. for C<sub>31</sub>H<sub>42</sub>N<sub>4</sub>NaO<sub>5</sub>S (MNa<sup>+</sup>) 605.7449, found 605.2768. <sup>1</sup>H and <sup>13</sup>C NMR see Table 2.12 in Chapter 2.

**(Z)-2-Benzyl-6-[(2S)-N-(N'-4-morpholinylcarbonyl-S-leuciny)]-2-amino-3-phenyl-propylidene]-1,2-thiazinane 1,1-dioxide (2.4b)**

**2.4b** (14 mg) was prepared from **2.81b** (reaction time: 15 h); white amorphous solid (28%);  $[\alpha]_D^{21} = -14^\circ$  (CHCl<sub>3</sub>, *c* 0.16). IR (film):  $\nu_{\max} = 3368$  (NH), 1621 (br, C=O), 1455, 1331 (S=O), 1155 (S=O), 756, 699 cm<sup>-1</sup>. HR-ESI-MS calcd. for C<sub>31</sub>H<sub>42</sub>N<sub>4</sub>NaO<sub>5</sub>S (MNa<sup>+</sup>) 605.7449, found 605.2768. <sup>1</sup>H and <sup>13</sup>C NMR see Table 2.13 in Chapter 2.

**N-(4-Morpholinylcarbonyl)-S-phenylalanine (2.82)**

TEA (1.0 mL; 6.9 mmol) and 4-morpholinecarbonyl chloride (0.8 mL; 6.9 mmol) were added to a suspension of *S*-phenylalanine (1.0 g; 6.0 mmol) in THF (20 mL). The mixture was refluxed for 4 h. Then, it was acidified with conc. hydrochloric acid, diluted with water (80 mL) and extracted with DCM (2×20 mL) and EtOAc (2×20 mL). The organic layers were washed with water, combined and dried with magnesium sulfate. The solvent was evaporated to yield **2.82** (0.9 g).

**2.82**; yellow oil (54%); IR (film):  $\nu_{\max} = 3331$  (br, NH and OH), 1721 (C=O of acid), 1632 (C=O of amide), 1530 (br), 1460, 1268 (br, C-O), 1115 (br, C-O), 878, 737, 702 cm<sup>-1</sup>.  $\delta$  <sup>1</sup>H NMR (400 MHz, CDCl<sub>3</sub>): 3.13 (dd, 1H, *J* = 7.2, 13.8, CHHP<sub>h</sub>), 3.23 (dd, 1H, *J* = 5.6, 13.8, CHHP<sub>h</sub>), 3.27–3.33 (m, 4H, CH<sub>2</sub>N), 3.57–3.73 (m, 4H, CH<sub>2</sub>O), 4.62–4.71 (m, 1H, CHCH<sub>2</sub>Ph), 4.96 (d, 1H, *J* = 7.2, NH), 7.17–7.32 (m, 5H, Ph).  $\delta$  <sup>13</sup>C NMR (100.61 MHz, CDCl<sub>3</sub>): 43.9 (CH<sub>2</sub>Ph), 47.2 (CH<sub>2</sub>N), 54.8 (CHCH<sub>2</sub>Ph), 66.3 (CH<sub>2</sub>O), 127.2 (CH), 128.7

(CH), 129.3 (CH), 136.2 (C), 174.2 (COOH).  $^1\text{H}$  NMR signal assignments were based on chemical shift, on relative integration and on the splitting pattern. Carbon signals assignments were made using HMQC and DEPT techniques. ESI-MS  $m/z$  (rel. int.) 279 ( $\text{MH}^+$ ) (100).

This compound was initially synthesised with lower yields following an adapted procedure.<sup>142</sup> 4-Morpholinecarbonyl chloride (0.8 mL; 6.9 mmol) was added to a solution of *S*-phenylalanine (1.0 g; 6.0 mmol) in 6M-sodium hydroxide (1.3 mL; 7.8 mmol). When the mixture was shaken, it became warm and a precipitate was observed. Initially, the solid was collected by filtration *in vacuo* and washed with cold water, but according to the  $^1\text{H}$  NMR spectrum (400 MHz,  $\text{D}_2\text{O}$ ) it revealed to be *S*-phenylalanine. In the following attempts, an excess of 1M-sodium hydroxide was added until the medium became clear and alkaline. Then, the solution was acidified with conc. hydrochloric acid and extracted with EtOAc (2×40 mL). The organic layer was washed with water, dried with magnesium sulfate and evaporated to give **2.82** (134 mg, 8%).

#### 5.1.4.10 Synthesis of vinyl sulfonamides

##### *N*-Methyl-*N*-phenylmethanesulfonamide (**2.85**)

Mesyl chloride (3.6 mL; 45.5 mmol) was added slowly to a solution of *N*-methylaniline (10.0 mL; 91.0 mmol) in DCM (40 mL). The mixture was stirred at rt for 2 h. Then, it was washed with 40 mL of hydrochloric acid 5% (w/v) and of water, it was dried with anhydrous magnesium sulfate and the solvent was evaporated to afford **2.85** (6.8 g).

**2.85**; white crystals (81%); mp 75-77 °C; IR (KBr):  $\nu_{\text{max}}$  = 1590, 1493, 1332 (S=O), 1146 (S=O), 767, 634  $\text{cm}^{-1}$ .  $\delta$   $^1\text{H}$  NMR (400 MHz,  $\text{CDCl}_3$ ): 2.86 (s, 3H,  $\text{CH}_3\text{SO}_2$ ), 3.35 (s, 3H,  $\text{CH}_3\text{N}$ ), 7.30–7.34 (m, 1H, Ph), 7.39–7.44 (m, 4H, Ph). ESI-MS  $m/z$  (rel. int.) 208 ( $\text{MNa}^+$ ) (100).

Alternatively, **2.85** was obtained from *N*-phenylmethanesulfonamide **2.50** by the following procedure: to a solution of **2.50** (1.0 g; 5.8 mmol) in DCM (10 mL) was added tetrabutylammonium hydroxide 30-hydrate (47 mg; 58.5  $\mu\text{mol}$ ), followed by a solution of sodium hydroxide (610 mg; 15.0 mmol) in water (1.5 mL). The formation of a white precipitate was observed. Then, iodomethane (1.0 g; 5.8 mmol) was added dropwise. After stirring at rt for 30 min, the precipitate still remained. The reaction was refluxed for 45 min, during which time the medium became clear. The mixture was diluted with 30 mL of DCM and saturated aqueous solution of sodium chloride. The organic layer was washed with water

(30 mL), dried with anhydrous magnesium sulfate and evaporated to yield **2.85** (448 mg; 41%).

#### ***N*-Methyl-*N*-phenyl diethylphosphorylmethanesulfonamide (2.86)**

The reaction was carried out under N<sub>2</sub> at rt. A 1.6 M solution of *n*-BuLi in *n*-hexane (18.0 mmol) was added to **2.85** (3.0 g; 16.2 mmol) in dry THF (50 mL), which turned the solution yellow. TMEDA (2.7 mL; 18.0 mmol) was added, followed after 10 min by a solution of diethyl chlorophosphate (1.3 mL; 9.0 mmol) in dry THF (6 mL). The mixture was stirred for 1 h (development of an orange coloration), after which it was quenched using a saturated aqueous solution of sodium chloride (100 mL) and extracted with DCM (3×100 mL) and EtOAc (100 mL). The organic layers were washed with water, combined and dried with anhydrous magnesium sulfate. The solvent was evaporated to yield a crude product (3.4 g), which was subjected twice to column chromatography on silica gel using ethyl ether as eluent to afford **2.86** (324 mg). The process also gave 81 mg of impure **2.86**, which was no further purified.

**2.86**; yellow oil (11%); IR (film):  $\nu_{\max}$  = 1595, 1493, 1354 (S=O), 1261 (P=O), 1153 (S=O), 1026 and 973 (d, P-O-C), 879, 796, 699 cm<sup>-1</sup>. ESI-MS *m/z* (rel. int.) 344 (MNa<sup>+</sup>) (100). <sup>1</sup>H and <sup>13</sup>C NMR see Table 2.14 in Chapter 2.

#### **(*E*) *N*-Methyl-*N*-phenyl (3*S*)-*N*-*tert*-butoxycarbonyl-3-amino-4-phenyl-but-1-enyl sulfonamide (2.84a) and its (*Z*) Isomer (2.84b)**

Compounds **2.84a** (61 mg) and **2.84b** (14 mg) were prepared from **2.86** (296 mg; 0.9 mmol) and *N*-Boc-*S*-phenylalaninal (**2.53**) according to the typical experimental procedure for the Horner-Wadsworth-Emmons reaction (Section 5.1.4.7).

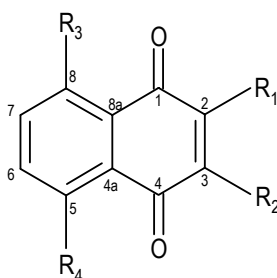
**2.84a**; white amorphous solid (16%); IR (film):  $\nu_{\max}$  = 3369 (NH), 1707 (C=O), 1497, 1349 (S=O), 1251 (C-O), 1167 (br), 870, 765, 742, 699 cm<sup>-1</sup>.  $\delta$  <sup>1</sup>H NMR (400 MHz, CDCl<sub>3</sub>): 1.44 (s, 9H, CH<sub>3</sub>-Boc), 2.86–2.98 (m, 2H, CH<sub>2</sub>Ph), 3.15 (s, 3H, NCH<sub>3</sub>), 4.59 (m, 2H, NH and CHCH<sub>2</sub>Ph), 6.17 (d, 1H, *J* = 14.8, CHSO<sub>2</sub>), 6.62 (dd, 1H, *J* = 5.2, 14.8, CH=CHSO<sub>2</sub>), 7.16–7.20 (m, 2H, Ph), 7.24–7.36 (m, 8H, Ph).  $\delta$  <sup>13</sup>C NMR (100.61 MHz, CDCl<sub>3</sub>): 28.3 (CH<sub>3</sub>-Boc), 38.1 (NCH<sub>3</sub>), 40.3 (CH<sub>2</sub>Ph), 52.2 (CHCH<sub>2</sub>Ph), 80.2 (C-Boc), 124.7 (CHSO<sub>2</sub>), 127.0 (CH), 127.2 (CH), 127.5 (CH), 128.8 (CH), 129.1 (CH), 129.3 (CH), 135.8 (C), 141.3 (C), 145.7 (CH=CHSO<sub>2</sub>), 154.8 (CO-Boc). <sup>1</sup>H NMR signal assignments were based on the chemical shift and on the splitting pattern. Carbon signal assignments were made using HMQC and DEPT techniques. ESI-MS *m/z* (rel. int.) 439 (MNa<sup>+</sup>) (100). Anal. Calcd

(C<sub>22</sub>H<sub>28</sub>N<sub>2</sub>O<sub>4</sub>S): C, 63.44; H, 6.78; N, 6.73; S, 7.70. Found: C, 63.96; H, 7.12; N, 6.64; S, 7.61.

**2.84b**; white amorphous solid;  $\delta$  <sup>1</sup>H NMR (400 MHz, CDCl<sub>3</sub>): 1.40 (s, 9H, CH<sub>3</sub>-Boc), 2.88–2.95 (m, 2H, CH<sub>2</sub>Ph), 3.34 (s, 3H, NCH<sub>3</sub>), 4.55 (brs, 1H), 5.02 (brs, 1H), 6.09 (d, 1H, *J* = 10.8), 6.41 (brs, 1H), 7.16–7.18 (m, 2H, Ph), 7.23–7.40 (m, 8H, Ph). ESI-MS *m/z* (rel. int.) 439 (MNa<sup>+</sup>) (100). This compound was obtained with the presence of small amounts of the *E* isomer.

#### 5.1.4.11 1,4-Naphthoquinone derivatives

For nomenclature and NMR assignment purposes, carbon atoms and protons were numbered as follows:<sup>143,144</sup>



#### Reaction of 1,4-naphthoquinones with amino acid ethyl esters

*S*-Phenylalanine ethyl ester hydrochloride (97 mg; 0.4 mmol) and TEA (85 mg; 0.8 mmol) were added to a solution of 2-bromo-1,4-naphthoquinone **3.6** (102 mg; 0.4 mmol) in abs EtOH (15 mL). After stirring at rt for 1 h, the solvent was evaporated to yield crude product (300 mg). Compounds **3.1a** (61 mg) and **3.2a** (16 mg) were separated by column chromatography on silica gel (30 g) using DCM as eluent (0.5 L). Compounds **3.1b**, **3.2b** and **3.3a,b** were prepared using the same method from the appropriate naphthoquinone and amino acid ethyl ester.

*N*-(1,4-Naphthoquinon-2-yl)-*S*-phenylalanine ethyl ester (**3.1a**); light orange gummy solid (42%); IR (film):  $\nu_{\max}$  = 3374 (NH), 1737 (C=O of COOEt), 1673 and 1571 (C=O of quinone) cm<sup>-1</sup>.  $\delta$  <sup>1</sup>H NMR (400 MHz, CDCl<sub>3</sub>): 1.24–1.27 (m, 3H, CH<sub>2</sub>CH<sub>3</sub>), 3.19 (dd, 1H, *J* = 6.6, 14.0, CHHPh), 3.28 (dd, 1H, *J* = 5.6, 14.0, CHHPh), 4.19–4.24 (m, 2H, CH<sub>2</sub>CH<sub>3</sub>), 4.32

(brddd, 1H,  $J = 5.6, 6.6, 7.6$ , CH)<sup>ee</sup>, 5.71 (s, 1H, H-3), 6.33 (d, 1H,  $J = 7.6$ , NH), 7.16–7.18 (m, 2H, Ph), 7.25–7.34 (m, 3H, Ph), 7.64 (dt, 1H,  $J = 1.2, 7.6$ , H-7), 7.74 (dt, 1H,  $J = 1.2, 7.6$ , H-6), 8.06 (brdd, 1H,  $J = 0.8; 7.6$ , H-8)<sup>ee</sup>, 8.09 (brdd, 1H,  $J = 0.4, 7.6$ , H-5)<sup>ee</sup>.  $\delta$  <sup>13</sup>C NMR (100.61 MHz, CDCl<sub>3</sub>): 14.1 (CH<sub>2</sub>CH<sub>3</sub>), 37.5 (CH<sub>2</sub>Ph), 56.1 (CHCH<sub>2</sub>Ph), 62.0 (CH<sub>2</sub>CH<sub>3</sub>), 102.1 (C-3), 126.2 (C-8), 126.4 (C-5), 127.5 (CH), 128.8 (CH), 129.2 (CH), 130.5 (C-8a), 132.2 (C-7), 133.2 (C-4a), 134.8 (C-6), 135.1 (C), 146.6 (C-2), 170.3 (CO), 181.2 (C-1), 183.2 (C-4). <sup>1</sup>H and <sup>13</sup>C NMR signal assignments were possible using DEPT and 2D NMR techniques (HMQC and HMBC). ESI-MS  $m/z$  (rel. int.) 350 (MH<sup>+</sup>) (100). Anal. Calcd (C<sub>21</sub>H<sub>19</sub>NO<sub>4</sub>): C, 72.19; H, 5.48; N, 4.01. Found: C, 72.45; H, 5.61; N, 4.13.

***N*-(3-Bromo-1,4-naphthoquinon-2-yl)-*S*-phenylalanine ethyl ester (3.2a)**; orange oil (9%); IR (film):  $\nu_{\max} = 3317$  (NH), 1737 (C=O of COOEt), 1673 and 1571 (C=O of quinone) cm<sup>-1</sup>.  $\delta$  <sup>1</sup>H NMR (400 MHz, CDCl<sub>3</sub>): 1.26–1.30 (m, 3H, CH<sub>2</sub>CH<sub>3</sub>), 3.20–3.31 (m, 2H, CH<sub>2</sub>Ph), 4.21–4.27 (m, 2H, CH<sub>2</sub>CH<sub>3</sub>), 5.58 (m, 1H, CH), 6.28 (brs, 1H, NH), 7.20–7.22 (m, 2H, Ph), 7.24–7.34 (m, 3H, Ph), 7.65 (dt, 1H,  $J = 1.2, 7.6$ , H-7), 7.72 (dt, 1H,  $J = 1.2, 7.6$ , H-6), 8.00 (brd, 1H,  $J = 7.6$ , H-8)<sup>ee</sup>, 8.14 (brd, 1H,  $J = 6.8$ , H-5)<sup>ee</sup>.  $\delta$  <sup>13</sup>C NMR (100.61 MHz, CDCl<sub>3</sub>): 14.1 (CH<sub>2</sub>CH<sub>3</sub>), 40.0 (CH<sub>2</sub>Ph), 57.6 (CHCH<sub>2</sub>Ph), 61.9 (CH<sub>2</sub>CH<sub>3</sub>), 126.9 (C-5 and C-8), 127.5 (CH), 128.8 (CH), 129.4 (CH), 131.9 (C-4a), 132.6 (C-7), 134.7 (C-6), 135.0 (C), 171.2 (CO), 176.4 (C-4), 179.8 (C-1); the following <sup>1</sup>H and <sup>13</sup>C signal assignments are interchangeable: C-1 with C-4, C-4a with C-8a, H-5 with H-8 and H-6/C-6 with H-7/C-7. Proton-carbon correlations were assigned from the HMQC spectrum. ESI-MS  $m/z$  (rel. int.) 428 (MH<sup>+</sup>) (83), 430 (MH<sup>+</sup>+2) (100). Anal. Calcd (C<sub>21</sub>H<sub>18</sub>BrNO<sub>4</sub>): C, 58.89; H, 4.24; N, 3.27. Found: C, 58.77; H, 4.44; N, 3.42.

***N*-(3-Chloro-1,4-naphthoquinon-2-yl)-*S*-phenylalanine ethyl ester (3.3a)**

Compound **3.3a** (18 mg) was prepared from 2,3-dichloro-1,4-naphthoquinone **3.9** (102 mg; 0.4 mmol) and *S*-phenylalanine ethyl ester hydrochloride (101 mg; 0.4 mmol).

**3.3a**; orange oil (11%); IR (film):  $\nu_{\max} = 3315$  (NH), 1737 (C=O of COOEt), 1673 and 1571 (C=O of quinone) cm<sup>-1</sup>.  $\delta$  <sup>1</sup>H NMR (400 MHz, CDCl<sub>3</sub>): 1.27 (t, 3H,  $J = 7.2$ , CH<sub>2</sub>CH<sub>3</sub>), 3.24–3.27 (m, 2H, CH<sub>2</sub>Ph), 4.20–4.28 (m, 2H, CH<sub>2</sub>CH<sub>3</sub>), 5.51 (ddd, 1H,  $J = 2.0, 6.0; 12.2$ , CH), 6.34 (brs, 1H, NH), 7.19–7.21 (m, 2H, Ph), 7.27–7.34 (m, 3H, Ph), 7.66 (dt, 1H,  $J = 1.2$ ,

<sup>ee</sup> Not well resolved signal.

7.6, H-7), 7.74 (dt, 1H,  $J = 1.2$ , 7.6, H-6), 8.03 (brd, 1H,  $J = 7.6$ , H-8)<sup>ff</sup>, 8.15 (brd, 1H,  $J = 7.6$ , H-5)<sup>ff</sup>.  $\delta$   $^{13}\text{C}$  NMR (100.61 MHz,  $\text{CDCl}_3$ ): 14.2 ( $\text{CH}_2\text{CH}_3$ ), 40.2 ( $\text{CH}_2\text{Ph}$ ), 57.3 ( $\text{CHCH}_2\text{Ph}$ ), 61.9 ( $\text{CH}_2\text{CH}_3$ ), 126.8 (C-8), 126.9 (C-5), 127.6 (CH), 128.9 (CH), 129.4 (CH), 130.0 (C-8a), 132.3 (C-4a), 132.7 (C-7), 134.9 (C-6), 135.1 (C), 171.3 (CO), 176.8 (C-4), 180.1 (C-1); the following  $^1\text{H}$  and  $^{13}\text{C}$  signal assignments are interchangeable: C-1 with C-4, C-4a with C-8a, H-5/C-5 with H-8/C-8, and H-6/C-6 with H-7/C-7. Proton-carbon correlations were assigned from the HMQC spectrum. ESI-MS  $m/z$  (rel. int.) 384 ( $\text{MH}^+$ ) (100), 386 ( $\text{MH}^++2$ ) (30). Anal. Calcd ( $\text{C}_{21}\text{H}_{18}\text{ClNO}_4$ ): C, 65.71; H, 4.73; N, 3.65. Found: C, 65.73; H, 4.45; N, 3.66.

### ***N*-(1,4-Naphthoquinon-2-yl)glycine ethyl ester (3.1b)**

Compound **3.1b** (19 mg) was prepared from 2-bromo-1,4-naphthoquinone **3.6** (201 mg; 0.8 mmol) and glycine ethyl ester hydrochloride (116 mg; 0.8 mmol). The process also gave 65 mg of impure **3.1b** which was no further purified.

**3.1b**; orange amorphous solid (9%); IR (film):  $\nu_{\text{max}} = 3373$  (NH), 1743 (C=O of COOEt), 1677 and 1573 (C=O of quinone)  $\text{cm}^{-1}$ .  $\delta$   $^1\text{H}$  NMR (400 MHz,  $\text{CDCl}_3$ ): 1.34 (t, 3H,  $J = 7.2$ ,  $\text{CH}_2\text{CH}_3$ ), 3.94 (d, 2H,  $J = 5.2$ , NCH<sub>2</sub>), 4.31 (q, 2H,  $J = 7.2$ ,  $\text{CH}_2\text{CH}_3$ ), 5.66 (s, 1H, H-3), 6.41 (brs, 1H, NH), 7.64 (brt, 1H,  $J = 7.6$ , H-7)<sup>ff</sup>, 7.73 (brt, 1H,  $J = 7.6$ , H-6)<sup>ff</sup>, 8.05–8.10 (m, 2H, H-5 and H-8).  $\delta$   $^{13}\text{C}$  NMR (100.61 MHz,  $\text{CDCl}_3$ ): 14.2 ( $\text{CH}_2\text{CH}_3$ ), 43.9 (NCH<sub>2</sub>), 62.1 ( $\text{CH}_2\text{CH}_3$ ), 102.1 (C-3), 126.2 (C-8), 126.4 (C-5), 130.5 (C-8a), 132.3 (C-7), 133.3 (C-4a), 134.8 (C-6), 147.2 (C-2), 168.3 (CO), 181.2 (C-1), 183.2 (C-4). NMR signals for aromatic protons and quaternary carbons were assigned by comparison with analogue **3.1a**. The remaining carbon signal assignments were made using HMQC and DEPT techniques. ESI-MS  $m/z$  (rel. int.) 260 ( $\text{MH}^+$ ) (50). Anal. Calcd ( $\text{C}_{14}\text{H}_{13}\text{NO}_4$ ): C, 64.86; H, 5.05; N, 5.40. Found: C, 64.59; H, 5.01; N, 5.60.

### ***N*-(3-Bromo-1,4-naphthoquinon-2-yl)glycine ethyl ester (3.2b)**

Compound **3.2b** (18 mg) was obtained together with compound **3.1b**.

**3.2b**; orange amorphous solid (6%); IR (film):  $\nu_{\text{max}} = 3317$  (NH), 1741 (C=O of COOEt), 1677 and 1569 (C=O of quinone)  $\text{cm}^{-1}$ .  $\delta$   $^1\text{H}$  NMR (400 MHz,  $\text{CDCl}_3$ ): 1.34 (t, 3H,  $J = 7.2$ ,  $\text{CH}_2\text{CH}_3$ ), 4.31 (q, 2H,  $J = 7.2$ ,  $\text{CH}_2\text{CH}_3$ ), 4.62 (d, 2H,  $J = 5.6$ , NCH<sub>2</sub>), 6.54 (brs, 1H, NH), 7.66 (dt, 1H,  $J = 1.0$ ; 7.6, H-7), 7.73 (dt, 1H,  $J = 1.2$ ; 7.6, H-6), 8.05 (brd, 1H,  $J = 7.6$ , H-8)<sup>ff</sup>, 8.15 (brd, 1H,  $J = 7.6$ , H-5)<sup>ff</sup>.  $\delta$   $^{13}\text{C}$  NMR (100.61 MHz,  $\text{CDCl}_3$ ): 14.2 ( $\text{CH}_2\text{CH}_3$ ), 46.7 (NCH<sub>2</sub>), 62.1 ( $\text{CH}_2\text{CH}_3$ ), 127.0 (C-5 and C-8), 129.9 (C-8a), 132.0 (C-4a), 132.6 (C-7), 134.8

<sup>ff</sup> Not well resolved signal.

(C-6), 146.2 (C-2), 169.5 (CO), 176.5 (C-4), 179.8 (C-1); the following  $^1\text{H}$  and  $^{13}\text{C}$  signal assignments are interchangeable: C-1 with C-4, C-4a with C-8a, H-5 with H-8 and H-6/C-6 with H-7/C-7. Proton-carbon correlations were assigned from the HMQC spectrum. Carbon at C-2 was assigned on the basis of a HMBC experiment. ESI-MS  $m/z$  (rel. int.) 338 ( $\text{MH}^+$ ) (78), 340 ( $\text{MH}^++2$ ) (100). Anal. Calcd ( $\text{C}_{14}\text{H}_{12}\text{BrNO}_4$ ): C, 49.73; H, 3.58; N, 4.14. Found: C, 50.30; H, 3.60; N, 4.15.

### ***N*-(3-Chloro-1,4-naphthoquinon-2-yl)glycine ethyl ester (3.3b)**

Compound **3.3b** (11 mg) was prepared from 2,3-dichloro-1,4-naphthoquinone **3.9** (121 mg; 0.5 mmol) and glycine ethyl ester hydrochloride (73 mg; 0.5 mmol).

**3.3b**; orange amorphous solid (7%); IR (film):  $\nu_{\text{max}}$  = 3315 (NH), 1737 (C=O of COOEt), 1673 and 1571 (C=O of quinone)  $\text{cm}^{-1}$ .  $\delta$   $^1\text{H}$  NMR (400 MHz,  $\text{CDCl}_3$ ): 1.34 (t, 3H,  $J = 7.2$ ,  $\text{CH}_2\text{CH}_3$ ), 4.31 (q, 2H,  $J = 7.2$ ,  $\text{CH}_2\text{CH}_3$ ), 4.61 (d, 2H,  $J = 6.0$ , NCH<sub>2</sub>), 6.53 (brs, 1H, NH), 7.66 (dt, 1H,  $J = 0.8$ ; 7.6, H-7), 7.75 (dt, 1H,  $J = 0.8$ ; 7.6, H-6), 8.06 (brd, 1H,  $J = 7.6$ , H-8)<sup>eg</sup>, 8.16 (brd, 1H,  $J = 7.6$ , H-5)<sup>eg</sup>.  $\delta$   $^{13}\text{C}$  NMR (100.61 MHz,  $\text{CDCl}_3$ ): 14.2 ( $\text{CH}_2\text{CH}_3$ ), 46.3 (NCH<sub>2</sub>), 62.1 ( $\text{CH}_2\text{CH}_3$ ), 126.8 (C-8), 126.9 (C-5), 129.9 (C-8a), 132.3 (C-4a), 132.7 (C-7), 134.9 (C-6), 143.9 (C-2), 169.5 (CO), 176.9 (C-4), 180.1 (C-1); the following  $^1\text{H}$  and  $^{13}\text{C}$  signal assignments are interchangeable: C-1 with C-4, C-4a with C-8a, H-5/C-5 with H-8/C-8 and H-6/C-6 with H-7/C-7. Proton-carbon correlations were assigned from the HMQC spectrum. Carbon at C-2 was assigned on the basis of a HMBC experiment. The  $^1\text{H}$  NMR spectrum is in agreement with that reported in the literature.<sup>114</sup> ESI-MS  $m/z$  (rel. int.) 294 ( $\text{MH}^+$ ) (100), 296 ( $\text{MH}^++2$ ) (37). Anal. Calcd ( $\text{C}_{14}\text{H}_{12}\text{ClNO}_4$ ): C, 57.25; H, 4.12; N, 4.77. Found: C, 57.30; H, 4.30; N, 4.60.

### **2-(Methylamino)-1,4-naphthoquinone (3.1c) and 2-(methylamino)-3-bromo-1,4-naphthoquinone (3.2c)**

To a solution of 2-bromo-1,4-naphthoquinone **3.6** (283 mg; 1.2 mmol) in abs EtOH (40 mL) was added an excess of 40% aqueous methylamine solution (182 mg; 2.3 mmol). The mixture instantly turned orange. After vigorous stirring at rt for 40 min, the solvent was evaporated to yield crude product (330 mg). Compounds **3.1c** (170 mg) and **3.2c** (19 mg) were separated by column chromatography on silica gel (40 g) using as eluents DCM (0.2 L) and a mixture of DCM:EtOAc 3:1 (0.2 L).

<sup>eg</sup> Not well resolved signal.



**3.1c**; red amorphous solid (78%); IR (film):  $\nu_{\max}$  = 3335 (NH), 1678 and 1566 (C=O of quinone)  $\text{cm}^{-1}$ .  $\delta$   $^1\text{H}$  NMR (400 MHz,  $\text{CDCl}_3$ ): 2.96 (d, 3H,  $J$  = 5.6,  $\text{CH}_3$ ), 5.74 (s, 1H, H-3), 5.97 (brs, 1H, NH), 7.64 (dt, 1H,  $J$  = 1.2, 7.6, H-7), 7.75 (dt, 1H,  $J$  = 1.2, 7.6, H-6), 8.06 (brdd, 1H,  $J$  = 0.8; 7.6, H-8)<sup>hh</sup>, 8.12 (brdd, 1H,  $J$  = 0.8, 7.6, H-5)<sup>hh</sup>.  $\delta$   $^{13}\text{C}$  NMR (100.61 MHz,  $\text{CDCl}_3$ ): 29.2 ( $\text{CH}_3$ ), 100.7 (C-3), 126.3 (C-5 and C-8), 130.5 (C-8a), 132.0 (C-7), 133.7 (C-4a), 134.8 (C-6), 149.0 (C-2), 181.9 (C-1), 182.9 (C-4). NMR signals for aromatic protons were assigned by comparison with analogue **3.1a**. Carbon signal assignments were made using DEPT and 2D NMR techniques (HMQC and HMBC). ESI-MS  $m/z$  (rel. int.) 188 ( $\text{MH}^+$ ) (100). Anal. Calcd ( $\text{C}_{11}\text{H}_9\text{NO}_2$ ): C, 70.58; H, 4.85; N, 7.48. Found: C, 70.96; H, 4.88; N, 7.43.

**3.2c**; red amorphous solid (6%); IR (film):  $\nu_{\max}$  = 3315 (NH), 1678 and 1571 (C=O of quinone)  $\text{cm}^{-1}$ .  $\delta$   $^1\text{H}$  NMR (400 MHz,  $\text{CDCl}_3$ ): 3.47 (d, 3H,  $J$  = 5.6,  $\text{CH}_3$ ), 6.17 (brs, 1H, NH), 7.64 (dt, 1H,  $J$  = 1.2, 7.6, H-7), 7.73 (dt, 1H,  $J$  = 1.2, 7.6, H-6), 8.04 (brdd, 1H,  $J$  = 0.8; 7.6, H-8)<sup>hh</sup>, 8.17 (brdd, 1H,  $J$  = 0.8, 7.6, H-5)<sup>hh</sup>.  $\delta$   $^{13}\text{C}$  NMR (100.61 MHz,  $\text{CDCl}_3$ ): 33.1 ( $\text{CH}_3$ ), 126.9 (C-8), 127.1 (C-5), 129.8 (C-8a), 132.4 (C-4a), 132.5 (C-7), 134.9 (C-6), 147.0 (C-2), 176.5 (C-4), 180.2 (C-1); the following  $^1\text{H}$  and  $^{13}\text{C}$  signal assignments are interchangeable: C-1 with C-4, C-4a with C-8a, H-5/C-5 with H-8/C-8 and H-6/C-6 with H-7/C-7. Proton-carbon correlations were assigned from the HMQC spectrum. Carbon at C-2 was assigned on the basis of a HMBC experiment. ESI-MS  $m/z$  (rel. int.) 266 ( $\text{MH}^+$ ) (86), 268 ( $\text{MH}^++2$ ) (100). Anal. Calcd ( $\text{C}_{11}\text{H}_8\text{BrNO}_2$ ): C, 49.65; H, 3.03; N, 5.26. Found: C, 49.87; H, 2.98; N, 5.21.

### 1-[(1,4-Naphthoquinon-2-yl)-*S*-leucylamido]-3-methylbutane (**3.1d**)

The process began with the synthesis of *N*-Boc-*S*-leucyl-isopentylamine **3.23** (180 mg) from *N*-Boc-*S*-leucine-*N*-hydroxysuccinimide ester (60 mg; 0.7 mmol) and *iso*-amylamine (60 mg; 0.7 mmol) using the method described for **2.77** (Section 5.1.4.9), but with no need of chromatographic purification. The *N*-Boc group of **3.23** (173 mg; 0.6 mmol) was easily cleaved (see experimental for **2.73a**, Section 5.1.4.8) to afford *S*-leucyl-isopentylamine **3.24** (135 mg). This compound (131 mg; 0.7 mmol) was added to a solution of 1,4-naphthoquinone **3.8** (110 mg; 0.7 mmol) in abs EtOH (10 mL) with TEA (66 mg; 0.7 mmol). The reaction mixture was vigorously stirred at rt for 1 h and then the solvent was evaporated. Compound **3.1d** (42 mg) was purified by column chromatography on silica gel (40 g) using as eluents DCM (0.2 L) and a mixture of DCM:EtOAc 19:1 (0.5 L).

<sup>hh</sup> Not well resolved signal.

**3.23**; white amorphous solid (88%); IR (film):  $\nu_{\max}$  = 3305 (br, NH), 1683 and 1649 (d,  $2\times\text{C}=\text{O}$ ), 1244 (C-O)  $\text{cm}^{-1}$ .  $\delta$   $^1\text{H}$  NMR (400 MHz,  $\text{CDCl}_3$ ): 0.91–0.96 (m, 12H), 1.40–1.45 (m, 4H), 1.45 (s, 9H,  $\text{CH}_3$ -Boc), 1.57–1.69 (m, 2H), 3.25–3.30 (m, 2H), 4.06 (m, 1H), 4.96 (brd, 1H,  $J = 7.6$ ), 6.21 (m, 1H). ESI-MS  $m/z$  (rel. int.) 601 ( $\text{M}_2^+$ ) (86).

**3.24**; yellow oil (93%); IR (film):  $\nu_{\max}$  = 3295 (br, NH), 1654 (C=O)  $\text{cm}^{-1}$ .  $\delta$   $^1\text{H}$  NMR (400 MHz,  $\text{CDCl}_3$ ): 0.81–0.97 (m, 9H), 1.28–1.45 (m, 3H), 1.54–1.70 (m, 3H), 3.15–3.20 (m, 1H), 3.28–3.37 (m, 2H), 5.15 (brs, 1H), 7.35–7.45 (m, 1H), 8.12 (m, 1H). ESI-MS  $m/z$  (rel. int.) 401 ( $\text{M}_2^+$ ) (100).

**3.1d**; brown oil (18%); IR (film):  $\nu_{\max}$  = 3335 (NH), 1675 and 1572 (C=O of quinone), 1640 (C=O of amide)  $\text{cm}^{-1}$ .  $\delta$   $^1\text{H}$  NMR (400 MHz,  $\text{CDCl}_3$ ): 0.90 [d, 6H,  $J = 6.8$ ,  $2\times\text{CH}_3$  (*i*-Am)]<sup>ii</sup>, 0.95 [d, 3H,  $J = 6.4$ ,  $\text{CH}_3$  (Leu)], 1.02 [d, 3H,  $J = 6.0$ ,  $\text{CH}_3$  (Leu)], 1.37–1.42 [m, 2H,  $\text{CH}_2\text{CH}$  (*i*-Am)], 1.55–1.63 [m, 1H, CH (*i*-Am)], 1.70–1.79 [m, 2H,  $\text{CHH}$  and  $\text{CH}(\text{CH}_3)_2$  (Leu)], 1.88–1.92 [m, 1H,  $\text{CHH}$  (Leu)], 3.28–3.33 [m, 2H,  $\text{NHCH}_2$  (*i*-Am)], 3.89–3.92 [m, 1H,  $\text{CHNH}$  (Leu)], 5.82 (s, 1H, H-3), 6.13 [d, 1H,  $J = 6.8$ , NH (Leu)], 6.28 [m, 1H, NH (*i*-Am)], 7.66 (dt, 1H,  $J = 1.2$ , 7.6, H-7), 7.76 (dt, 1H,  $J = 1.2$ , 7.6, H-6), 8.07–8.10 (m, 2H, H-5 and H-8).  $\delta$   $^{13}\text{C}$  NMR (100.61 MHz,  $\text{CDCl}_3$ ): 21.9 [ $\text{CH}_3$  (Leu)], 22.4 [ $2\times\text{CH}_3$  (*i*-Am)]<sup>ii</sup>, 22.9 [ $\text{CH}_3$  (Leu)], 25.1 [ $\text{CH}(\text{CH}_3)_2$  (Leu)], 25.9 [CH (*i*-Am)], 38.0 [ $\text{NHCH}_2$  (*i*-Am)], 38.3 [ $\text{CH}_2\text{CH}$  (*i*-Am)], 41.8 [ $\text{CH}_2$  (Leu)], 55.9 [CHNH (Leu)], 102.4 (C-3), 126.3 (C-8), 126.5 (C-5), 130.4 (C-8a), 132.4 (C-7), 133.2 (C-4a), 135.0 (C-6), 147.4 (C-2), 170.3 [CO (Leu)], 181.2 (C-1), 183.2 (C-4).  $^1\text{H}$  and  $^{13}\text{C}$  NMR signal assignments were possible using DEPT and 2D NMR techniques (HMQC and HMBC). ESI-MS  $m/z$  (rel. int.) 357 ( $\text{MH}^+$ ) (100). Anal. Calcd ( $\text{C}_{21}\text{H}_{28}\text{N}_2\text{O}_3$ ): C, 70.76; H, 7.92; N, 7.86. Found: C, 70.95; H, 7.45; N, 7.53.

### 2-Ethoxy-1,4-naphthoquinone (3.5)

A solution of 1,4-naphthoquinone **3.8** (311 mg; 1.9 mmol) in abs EtOH (40 mL) with TEA (192 mg; 1.9 mmol) was vigorously stirred at rt for 1 h, during which time a red color was found to develop. After stirring for another 12 h, the solvent was evaporated to yield crude product (529 mg), which was fractionated by column chromatography on silica gel (40 g) using DCM (0.45 L) as eluent to afford 110 mg of **3.5**.

**3.5**; yellow amorphous solid (29%); IR (film):  $\nu_{\max}$  = 1682, 1656, 1610  $\text{cm}^{-1}$ .  $\delta$   $^1\text{H}$  NMR (400 MHz,  $\text{CDCl}_3$ ): 1.55 (t, 3H,  $J = 6.8$ ,  $\text{CH}_2\text{CH}_3$ ), 4.12 (q, 2H,  $J = 6.8$ ,  $\text{CH}_2\text{CH}_3$ ), 6.17 (s, 1H, H-3), 7.73 (dt, 1H,  $J = 1.6$ , 7.6, H-7), 7.77 (dt, 1H,  $J = 1.6$ , 7.6, H-6), 8.10 (brdd, 1H,  $J = 1.6$ ;

<sup>ii</sup> Co-incident peak.

7.4, H-8)<sup>jj</sup>, 8.15 (brdd, 1H,  $J = 1.6, 6.8$ , H-5)<sup>jj</sup>.  $\delta$   $^{13}\text{C}$  NMR (100.61 MHz,  $\text{CDCl}_3$ ): 13.9 ( $\text{CH}_2\text{CH}_3$ ), 65.4 ( $\text{CH}_2\text{CH}_3$ ), 110.2 (C-3), 126.1 (C-8), 126.7 (C-5), 131.2 (C-8a), 132.0 (C-7), 133.3 (C-4a), 134.3 (C-6), 159.7 (C-2), 180.2 (C-1), 185.1 (C-4). NMR signals for aromatic protons and quaternary carbons were assigned by comparison with analogue **3.1a**. The remaining carbon signal assignments were made using HMQC and DEPT techniques. ESI-MS  $m/z$  (rel. int.) 422 ( $\text{M}_2\text{NH}_4^+$ ) (82). Anal. Calcd ( $\text{C}_{12}\text{H}_{10}\text{O}_3$ ): C, 71.28; H, 4.98. Found: C, 71.30; H, 4.58.

### 2-(Bromomethyl)-1,4-naphthoquinone (3.10b)

*N*-Bromo-succinimide (431 mg; 2.4 mmol) was added to a solution of 2-methyl-1,4-naphthoquinone **3.11** (405 mg; 2.3 mmol) in  $\text{CCl}_4$  (20 mL). To this suspension, benzoyl peroxide (56 mg; 0.2 mmol) was added and the mixture was refluxed for 17 h. A second addition of *N*-bromo-succinimide (431 mg) was made and the reaction was refluxed for a further 7 h. The solvent was evaporated to give a product (1.3 g) which was subjected twice to column chromatography on silica gel using DCM as eluent to afford **3.10b** (208 mg).

**3.10b**; yellow amorphous solid (36%).  $^1\text{H}$  NMR (400 MHz,  $\text{CDCl}_3$ ): 4.42 (brs, 2H,  $\text{CH}_2\text{Br}$ ), 7.12 (brs, 1H, =CH), 7.78–7.81 (m, 2H, Ph), 8.09–8.12 (m, 1H, Ph), 8.15–8.17 (m, 1H, Ph).  $\delta$   $^{13}\text{C}$  NMR (100.61 MHz,  $\text{CDCl}_3$ ): 25.4 ( $\text{CH}_2\text{Br}$ ), 126.4 (CH), 126.9 (CH), 131.8 (C), 132.2 (C), 134.1 (CH), 134.2 (CH), 136.8 (=CH), 146.1 (C), 183.2 (C=O), 184.7 (C=O). Carbon signal assignments were made using HMQC techniques.

## 5.2 Kinetic study of the reaction with cysteine

### 5.2.1 Reagents and Solvents

DMSO and buffer materials for kinetic measurements were of analytical grade and were purchased from Merck (Germany). Ellman's reagent was from Sigma-Aldrich. Freshly deionised water was used throughout.

<sup>jj</sup> Not well resolved peak.

### 5.2.2 Equipment

Measurement of pH values was carried out at  $25.0 \pm 0.1$  °C, using a digital microprocessor pH meter (model micro pH 2002, Crisson Instruments S.A.), calibrated with standard buffers (Merck). Kinetic measurements were carried out using either Shimadzu UV-2100 or Shimadzu UV-1603 spectrophotometers, equipped with a temperature controller (CPS).

### 5.2.3 Buffers and substrate solutions

The stock solutions of vinyl sultams, vinyl sulfonamide and naphthoquinones were prepared in DMSO.

For vinyl sultams/vinyl sulfonamide, thiol solutions were prepared by dissolution of cysteine in 50 mM  $K_2HPO_4/KH_2PO_4$  buffer, pH 6.9, containing KCl to maintain ionic strength at 0.5 M and 30% (v/v) acetonitrile (due to vinyl sultams solubility problems). For naphthoquinones, thiol solutions were prepared by dissolution of cysteine in 50 mM  $K_2HPO_4/KH_2PO_4$  buffer, pH 7.1, containing KCl to maintain ionic strength at 0.5 M. In the case of 2-methyl-1,4-naphthoquinone, **3.11**, the rates were measured at three additional pH values using thiol solutions prepared in sodium borate/HCl buffer (pH 7.9, 8.0 and 8.8).<sup>145</sup> In all cases, thiol solutions with a change in the final pH value greater than 0.05 comparatively to the one of the employed buffer were rejected.

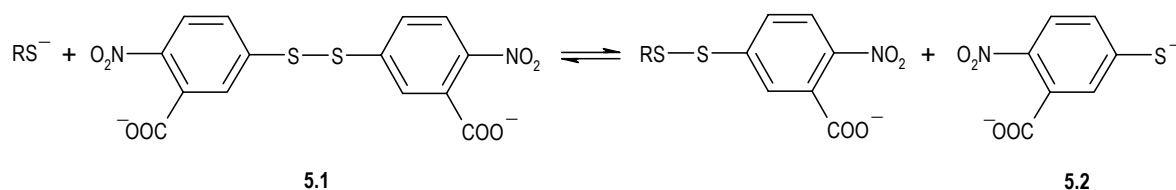
Cysteine concentration ranged between *ca.* 1 and 4 mM for vinyl sultams/vinyl sulfonamide and between *ca.* 0.5 and 5 mM for naphthoquinones, except in the kinetics of naphthoquinone **3.8**, in which the range was 0.06–5 mM.

Because thiols are prone to oxidation, cysteine solutions were prepared immediately before use and the concentration of thiol in solution was measured just before use by Ellman's method (Section 5.2.4).<sup>146</sup>

### 5.2.4 Determination of free thiol content

The free thiol content was assayed using Ellman's reagent **5.1**, *i.e.* DTNB = 5,5'-dithiobis(2-nitrobenzoic acid).<sup>146</sup> The reaction of a thiol with DTNB gives a mole equivalent

of the yellow 5-thio-2-nitrobenzoic acid anion **5.2** (Scheme 5.1), which can be measured by UV spectrophotometry (molar extinction coefficient of  $14.15 \times 10^3 \text{ M}^{-1} \text{ cm}^{-1}$ ).<sup>146</sup>



**Scheme 5.1** Reaction of Ellman's reagent with thiols.<sup>147</sup>

In general, aliquots of the cysteine solutions ( $\leq 50 \mu\text{L}$ ) were added to a preincubated quartz cuvette at  $25.0 \pm 0.1 \text{ }^\circ\text{C}$ , containing a  $0.1 \text{ mM}$  solution of DTNB<sup>kk</sup> in  $0.1 \text{ M}$   $\text{K}_2\text{HPO}_4/\text{KH}_2\text{PO}_4$  buffer, pH 7.4, to give a total volume of  $1 \text{ mL}$ . Under these conditions, thiol concentrations in the cuvette ranged between  $20$  and  $120 \mu\text{M}$  (absorbance values between  $0.3$  and  $1.7$ ), where Lambert-Beer's law is valid (see Figure 5.1).

The absorbance at  $412 \text{ nm}$  was read after  $5 \text{ min}$ ,<sup>ll</sup> against a blank solution lacking thiol. A new blank was prepared for every sample containing cysteine (this is recommended by the literature<sup>146</sup> due to the possible degradation of DTNB during the time of the experiment).

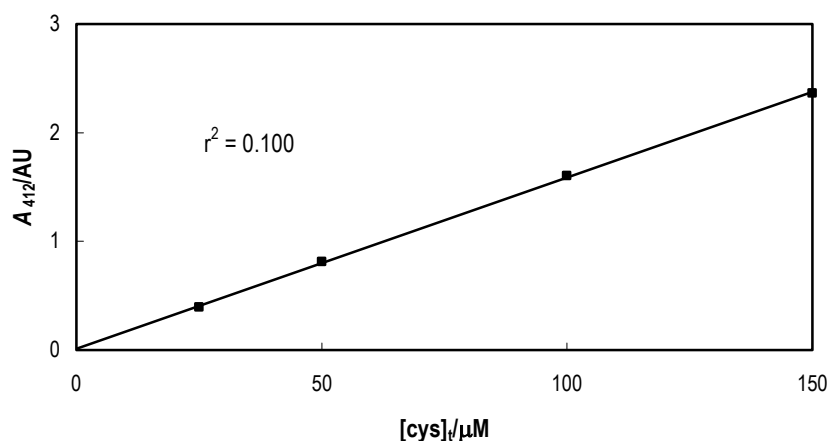


**Figure 5.1** Thiol titration curve for a cysteine solution using Ellman's reagent. The assay was performed by adding  $5, 10, 20$  and  $30 \mu\text{L}$  of a cysteine solution ( $5 \text{ mM}$  in  $4 \text{ mM}$   $\text{K}_2\text{HPO}_4/\text{KH}_2\text{PO}_4$  buffer, pH 7.5) into a quartz cuvette with Ellman's reagent ( $0.1 \text{ mM}$  solution in  $0.1 \text{ M}$   $\text{K}_2\text{HPO}_4/\text{KH}_2\text{PO}_4$  buffer, pH 7.4), to complete a total volume of  $1 \text{ mL}$ . Points are experimental and line is from linear regression analysis of the data.

<sup>kk</sup>Caution: DTNB and its solutions must be protected from light during storage to prevent formation of yellow photodegradation products.<sup>146</sup>

<sup>ll</sup> It was observed that absorbance values became reproducible after this period of time. Albeck *et al.*<sup>148</sup> also indicate a  $5 \text{ min}$  incubation period before the determination of absorbance.

### 5.2.5 UV Spectrophotometry

The kinetic measurements were carried out at  $25.0 \pm 0.1$  °C.

Reactions were initiated by addition of an aliquot of vinyl sultam/vinyl sulfonamide/naphthoquinone stock solution (50, 100 or 150  $\mu\text{L}$ ) to a quartz cuvette containing DMSO (100, 50 and 0  $\mu\text{L}$ , respectively) and 2.85 mL of a cysteine solution (Section 5.2.3). The absorbance was recorded against a blank of cysteine solution (2.85 mL) and DMSO (150  $\mu\text{L}$ ).

The initial concentration of the vinyl sultam/vinyl sulfonamide/naphthoquinone in the cuvette and the wavelengths used to monitor the kinetic reactions were as follows: **2.67a** (50  $\mu\text{M}$ ; decrease at 260 nm), **2.67b** (50  $\mu\text{M}$ ; decrease at 260 nm), **2.68a** (75  $\mu\text{M}$ , decrease at 260 nm), **2.69b** (25  $\mu\text{M}$ ; decrease at 260 nm), **2.84a** (75  $\mu\text{M}$ , decrease at 255 nm), **3.1a** (32  $\mu\text{M}$ ; decrease at 265 nm), **3.1b** (50  $\mu\text{M}$ ; increase at 277.3 nm), **3.1c** (50  $\mu\text{M}$ ; increase at 300 nm), **3.5** (50  $\mu\text{M}$ ; decrease at 282 nm), **3.8** (50  $\mu\text{M}$ ; increase at 360 nm), **3.11** (50  $\mu\text{M}$ ; increase at 279.8 nm), **3.13** (10  $\mu\text{M}$ ; decrease at 500 nm). The absorbance was recorded until a plateau region had been reached (see Figure 5.2 for a typical example).

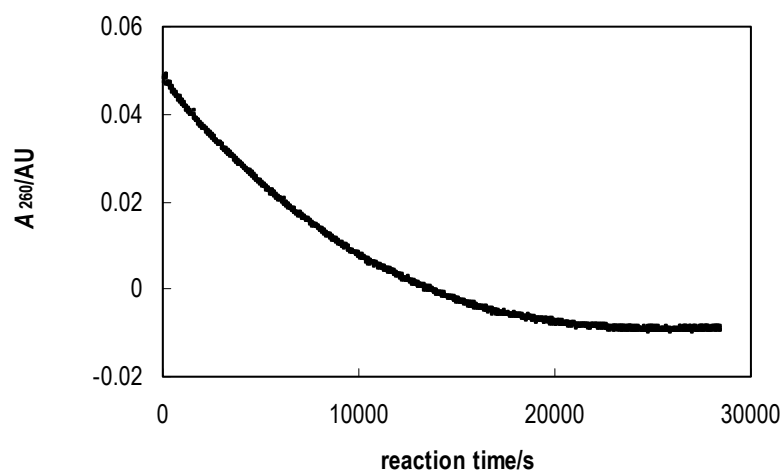


**Figure 5.2** Progress curve for the reaction of vinyl sultam **2.68a** with cysteine (895  $\mu\text{M}$ ), at pH 6.93 at 25 °C and ionic strength 0.5 M.

### 5.2.6 Determination of $k_{\text{obs}}$

The pseudo first-order rate constants,  $k_{\text{obs}}$ , were obtained from the slopes of the plots of  $\ln(\delta A)$  versus time, where  $\delta A$  represents the difference in absorbance between each time  $t$  and time infinity (plateau region).

## 5.3 Molecular modelling

Molecular docking enzyme–inhibitor studies were performed with the flexible GOLD 3.0 (Genetic Optimisation for Ligand Docking) package.<sup>149</sup> GOLD program uses a genetic algorithm (which mimics the process of evolution by applying genetic operators) to explore the full range of ligand conformational and rotational flexibility, and has been fully validated against 305 diverse and extensively checked protein-ligand complexes from the PDB database. The docking results were ranked based on the goldscore scoring function (fitness function).<sup>150</sup> Goldscore function is defined as the sum of four components (protein-ligand hydrogen bond energy, protein-ligand Van der Waals, energy ligand internal Van der Waals energy, and ligand torsional strain energy) and is specially featured to predict ligand-binding positions. Each run of Gold generated a file with the atomic coordinates in the conformation that best fitted the enzyme active site and computed a fitness score.

The papain structure used in the calculations (PDB code 1PPN) was obtained by deletion of one oxygen and the methanol present in the crystal structure. The structure was energy-minimized.

The cruzain structure used in the calculations (PDB code 1F2A) was obtained by deletion from the active site of the ligand **1.2d** present in the crystal structure. To confirm the reliability of the final cruzain structure we have performed some docking calculations with the known covalent complex and confirmed that the final enzyme-complex structures are very close to the corresponding x-ray structures obtained from the literature.

For each ligand (previously energy-minimized with density functional theory) 50 docking runs were performed (100,000 genetic algorithm operations, 5 islands).

## 5.4 Molecular orbital calculations

LUMO energies were calculated using density functional theory (DFT). DFT<sup>151</sup> calculations were carried out with the Gaussian 03 suite of programs.<sup>152</sup> 1,4-Naphthoquinone structures were optimised without symmetry constraints using the hybrid B3LYP functional, which is a combination of the Becke's three-parameter (B3) exchange functional<sup>153</sup> with the Lee, Yang, and Parr (LYP) correlation functional,<sup>154</sup> in conjunction with 6-311G(d,p)<sup>155</sup> basis set. All geometries were found to be minima on the respective potential energy surfaces. LUMO energies were calculated at this level of theory.



## **APPENDICES**



---

## APPENDIX I. Protocols for enzymatic assays

This appendix concerns itself with the development of procedures to evaluate the activity of potential inhibitors against papain and bovine spleen cathepsin B. In addition, it describes the inhibition assay for porcine pancreatic elastase.

### AI.1 Papain

This section is divided in three parts; firstly, the establishment of the inhibition assay; secondly, a gel-filtration chromatography procedure for the purification of the activated enzyme, and finally, a dialysis experiment.

#### AI.1.1 Development of papain inhibition assay

##### AI.1.1.1 Introductory remarks

Papain has been extensively investigated since the earlier twentieth century. Thus, several methods exist for the measurement of its activity.<sup>156</sup> Nevertheless, not all are simple enough to be used in inhibition studies. For example, the *Sigma quality control test procedure*<sup>157</sup> for papain (Sigma P4762) consists in a titrimetric determination of the acid produced during the hydrolysis of the benzoyl-*S*-arginine ethyl ester (BAEE). On the other hand, a search for papers describing new inhibitors revealed more convenient methods, *i.e.* spectrophotometric, although some have been reported lacking important experimental details, such as the enzyme or the substrate concentration.<sup>158-160</sup>

In general, papain requires an optimum pH conditions, a reducing environment and a good substrate.

The pH optima of papain vary from 6.0 to 7.0,<sup>157</sup> what is related to the existence of a thiolate/imidazolium ion pair, crucial for the catalytic activity. Thereby, at neutral pH, the percentage of papain presents as its ion-pair form has been determined and is in the range of at least 50% to almost 100% of the total enzyme.<sup>23</sup>

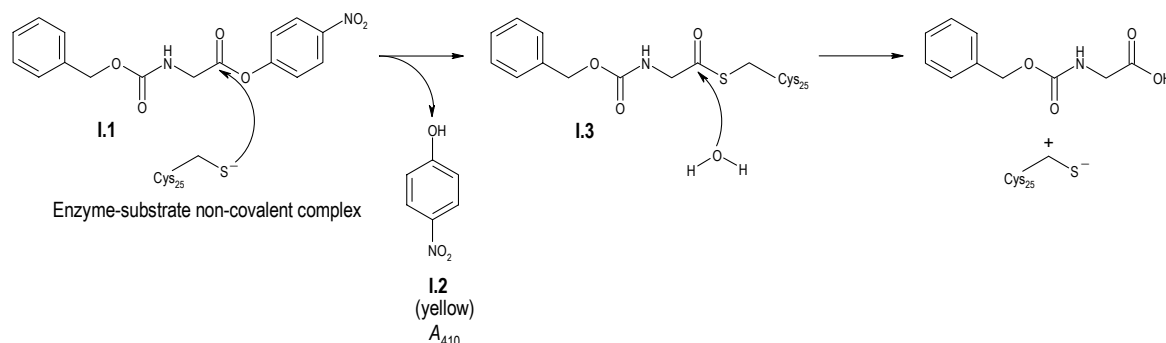
A reducing agent, such as a thiol reagent or sodium borohydride, is required for the maximum hydrolytic activity of papain.<sup>156</sup> This situation is due to the fact that the enzyme is isolated from *Carica papaya* as an inactive form, in which Cys25 is blocked by a disulfide bond. Thus, the reducing reagent is used to deblock it (activation of papain). In connection, the free Cys25 thiol group must be protected from oxidation in the reaction medium. The presence of a chelating agent, such as EDTA, is therefore required to remove traces of metal ions impurities, which are known oxidants.<sup>156</sup>

Concerning substrates, papain is a fairly good catalyst in the hydrolysis of *N*-benzoyl and *N*-carbobenzoxy derivatives of single amino acids. This situation is ascribed to the binding of the *N*-acyl aromatic groups to the S2 subsite, which is the most important element of substrate specificity, as mentioned in Section 1.1.3). Among amino acids, papain hydrolyses the derivatives of Gln, His, Gly, Tyr, Arg and Lys. The two latter are considered the most susceptible.<sup>161</sup>

In order to develop the papain inhibition assay, the present work focused on two reported procedures with different substrates, one involving Cbz-Gly-ONp and another involving BAPA.

#### AI.1.1.2 Determination of the papain activity in the presence of Cbz-Gly-ONp

The compound Cbz-Gly-ONp **I.1** (Scheme AI.1) is considered to be a convenient substrate for papain due to its  $K_m$  ( $9.3 \mu\text{M}$ )<sup>mm</sup> and fair solubility. In addition, the reaction is spectrophotometric because it generates the yellow product *p*-nitrophenol **I.2**.<sup>162</sup>



**Scheme AI.1** Determination of the papain activity using Cbz-Gly-ONp as substrate.

<sup>mm</sup> At pH 6.8 at 25 °C.

Briefly, the present work used papain freshly activated by sodium cyanoborohydride and carried out the reaction in  $K_2HPO_4/KH_2PO_4$  buffer, pH 7.0, containing EDTA. The employed buffer and reducing agent were reported by Guo *et al.*<sup>158</sup>

Papain activation followed the commonly reported incubation conditions of 1 h at 25 °C.

Substrate stock solutions were prepared in DMSO and 100  $\mu$ L aliquots were transferred to the 1 mL cuvette, such that the organic solvent did not exceed 10% of the total volume.<sup>160</sup>

Initially, the enzyme concentration was arbitrarily established in 100  $\mu$ g/mL and the substrate was employed in a saturating amount (300  $\mu$ M).

These conditions resulted in a clear *burst* (Figure AI.1a). Such behaviour has already been reported for the papain-catalysed hydrolysis of similar Cbz-amino acid esters,<sup>163</sup> and it is a quite general phenomenon, as it has been observed for other enzymes and substrates.<sup>139</sup> This type of situation occurs in a two-step mechanism, in which the substrate rapidly reacts with the enzyme to form a covalent enzyme-bound intermediate, but then the turnover into the products is slow (although not negligible).<sup>139</sup> In Cbz-Gly-ONp hydrolysis, deacylation of the enzyme is the slow step. Thus, there is an initial accumulation of the acyl-enzyme intermediate **I.3** (Scheme AI.1) associated with a rapid release of *p*-nitrophenol, which causes the *burst*, but then the reaction proceeds slowly because it depends on the slow breakdown of **I.3** to restore free papain.<sup>139</sup>

It is known that *burst* may be overcome by decreasing the substrate concentration.<sup>139</sup> The papain activity was therefore measured in the presence of two lower concentrations of Cbz-Gly-ONp (30  $\mu$ M and 3  $\mu$ M), that led to a better linear region, particularly the 3  $\mu$ M concentration (Figures AI.1b and AI.1c). However, this situation resulted in smaller absorbance values with higher associated error. In addition, the enzyme activity was reasonably low (*ca.*  $6 \times 10^{-5}$  AU/s for Figure AI.1c). As this assay was planned to be used in inhibition studies, a high reaction rate (good slope) was required in order to assess its decay in the presence of the inhibitor. Thus, the conditions remained unsuitable and an alternative spectrophotometric assay was exploited (following section).

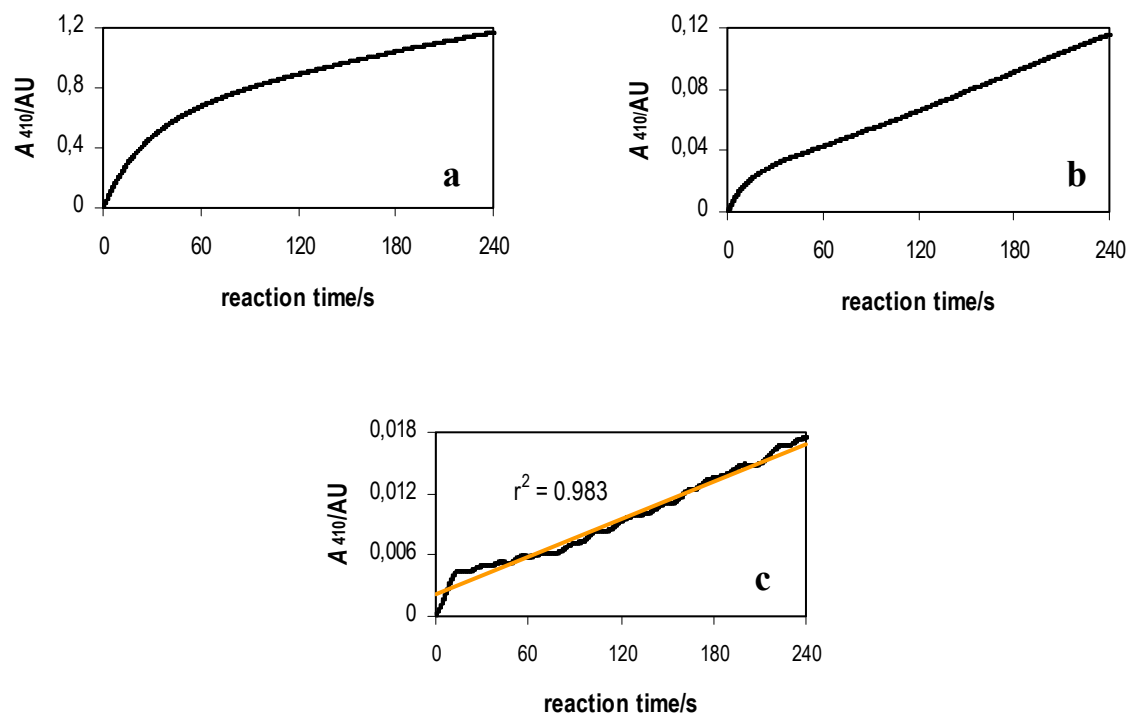


**Figure AI.1 Progression curves for the papain-catalysed hydrolysis of Cbz-Gly-ONp.** The experiment was carried out at pH 7.0 at 25 °C, using Cbz-Gly-ONp in the following concentrations: (a) 300  $\mu\text{M}$ , (b) 30  $\mu\text{M}$  and (c) 3  $\mu\text{M}$ . For experiment (c), points are experimental and line is from linear regression analysis of the data.

### AI.1.1.3 Determination of the papain activity in the presence of BAPA

In order to use BAPA I.4 as substrate (Figure AI.2), the present study focused on the method used by Zhao *et al.*<sup>164</sup> Thus, papain activity was determined under the following conditions.

Papain (1 mg/mL) was activated by incubation at 25 °C, for 1 h, in 50 mM  $\text{K}_2\text{HPO}_4/\text{KH}_2\text{PO}_4$  buffer, pH 7.0, containing 2.5 mM EDTA and 15 mM DTT. The reaction was started by the addition of papain (30  $\mu\text{L}$  of the stock solution 1 mg/mL) into a cuvette containing 100  $\mu\text{L}$  of BAPA stock solution (10 mM in DMSO) and 870  $\mu\text{L}$  of 50 mM  $\text{K}_2\text{HPO}_4/\text{KH}_2\text{PO}_4$  buffer, pH 7.0, containing 2.5 mM EDTA and 15 mM DTT. Enzymatic activity was determined by following the release of *p*-nitroaniline from BAPA at  $25.0 \pm 0.1$  °C at 410 nm during 4 min, against a blank of 50 mM  $\text{K}_2\text{HPO}_4/\text{KH}_2\text{PO}_4$  buffer, pH 7.0, containing 2.5 mM EDTA and 15 mM DTT. According to Zhao *et al.*, under these conditions, the papain concentration in the reaction medium is *ca.* 30  $\mu\text{g}/\text{mL}$ .

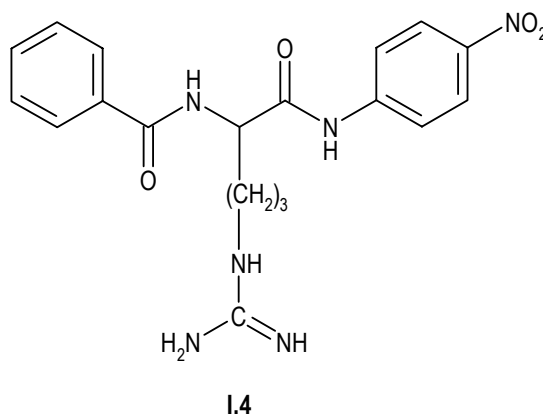


**Figure AI.2 Benzoyl-S-arginine-4-nitroanilide (BAPA).**

It should be noted that the buffer composition was reported, but no pH value was given. Thus, it was established to work under optimum conditions for papain, *i.e.* at neutral pH.

The report also lacked information on the solvent of BAPA stock solution. The substrate was therefore dissolved in DMSO, which did not exceed the already mentioned (Section AI.1.1.2) maximum of 10% in the reaction medium.

Another important issue concerns papain concentration. In the published procedure,<sup>164</sup> it was determined from the protein absorption at *ca.* 280 nm.<sup>mn</sup> However, it is known that activation does not lead to an enzyme containing 1.0 free thiol group *per* molecule of papain, what is tentatively ascribed to the further oxidation of thiol function to sulfinic and sulfonic acids.<sup>156</sup> Thus, the accurate amount of active papain can only be determined by sulfhydryl titration with the inactivator E-64 (Section 1.2.2) or using Ellman's reagent (Section 5.2.4).

The present investigation did not assess the concentration of active enzyme in the several employed papain solutions. Instead, it was assumed that the assays were being performed under similar conditions because equivalent enzyme activities were obtained, *ca.*  $2.5 \times 10^{-4}$  AU/s, corresponding to a fairly good slope of the plot of absorbance *versus* BAPA hydrolysis reaction time.

<sup>mn</sup> Proteins absorb at 280 nm due to the presence of Trp, Tyr, Phe and cystine bonds.<sup>165</sup>

**Investigation on reducing agent.** As mentioned earlier (Section AI.1.1.1), papain must be activated in the presence of a reducing agent. The present investigation found that this reagent must also be present in the cuvette buffer, because performing the reaction between activated papain and BAPA in buffer lacking DTT led to a reasonable decrease in the initial velocity  $v$  (70% of the original enzymatic activity). This situation is consistent with the one reported by Sanner *et al.*,<sup>166</sup> who observed that papain activity in the absence of cysteine varied from 30% to 60% of that determined in its presence. The fact was associated with the evidence that thiols increase  $k_{\text{cat}}$  value, suggesting that these agents not only activate papain by reducing disulfide bonds, but they also contribute to papain activity by another mechanism, which could not be disclosed by Sanner *et al.*<sup>166</sup>

The need for DTT in the assay buffer led to a concern with the stability of BAPA. Because this substrate reacts with a cysteine protease, it was considered that it might be also susceptible to DTT. Thus, two cuvettes with BAPA (100  $\mu\text{L}$ ) were prepared, one containing buffer with DTT (900  $\mu\text{L}$ ) and another with buffer lacking this agent. The absorbance was monitored during the established 4 min at 410 nm, against a blank of 50 mM  $\text{K}_2\text{HPO}_4/\text{KH}_2\text{PO}_4$  buffer, pH 7.0, containing 2.5 mM EDTA and 2.0 mM DTT (the thiol was included in the blank only when BAPA was assayed in its presence). There was no absorbance increase, independently of the presence or absence of DTT, and BAPA was therefore considered stable under the assay conditions.

By searching the literature it was found that most of the assays reported for cysteine protease inhibitors perform the enzyme-inhibitor incubation in the presence of the reducing agent. This is clearly a tricky situation, because the search for a suitable inhibitor involves several compounds and some of them may be sufficiently chemical reactive to form adducts with irrelevant nucleophiles, namely thiols. Thus, the presence of such agent in the assay buffer may result in the inhibitor depletion leading to loss of a significant part of its activity. Considering that *in vivo* other thiol species are expected to occur at high concentrations, the *in vitro* results may therefore provide an insight into the behaviour under biological conditions. On the other hand, this situation may underestimate the inhibitor efficiency and should always be kept in mind when performing structure-activity studies and planning future compounds.

In this context and as a reasonable compromise, it was decided to bring DTT in the buffer into the minimal effective concentration. Table AI.1 lists the papain activity for different DTT concentrations. The 1.7 mM solution was the lowest concentration whose activity was comparable to the one presented by the original 13.1 mM solution, and it was therefore employed in the following assays.



**Table AI.1 Papain activity in the presence of different DTT concentrations.**

[DTT] stock solution (mM)	[DTT] reaction medium (mM)	Papain activity ( $10^{-4}$ AU/s) <sup>a</sup>
15	13.1	$2.66 \pm 0.07$
10	8.7	$2.64 \pm 0.32$
5	4.4	$2.57 \pm 0.21$
2	1.7	$2.65 \pm 0.24$
1	0.87	$2.25 \pm 0.24$
0.5	0.44	$1.78 \pm 0.25$

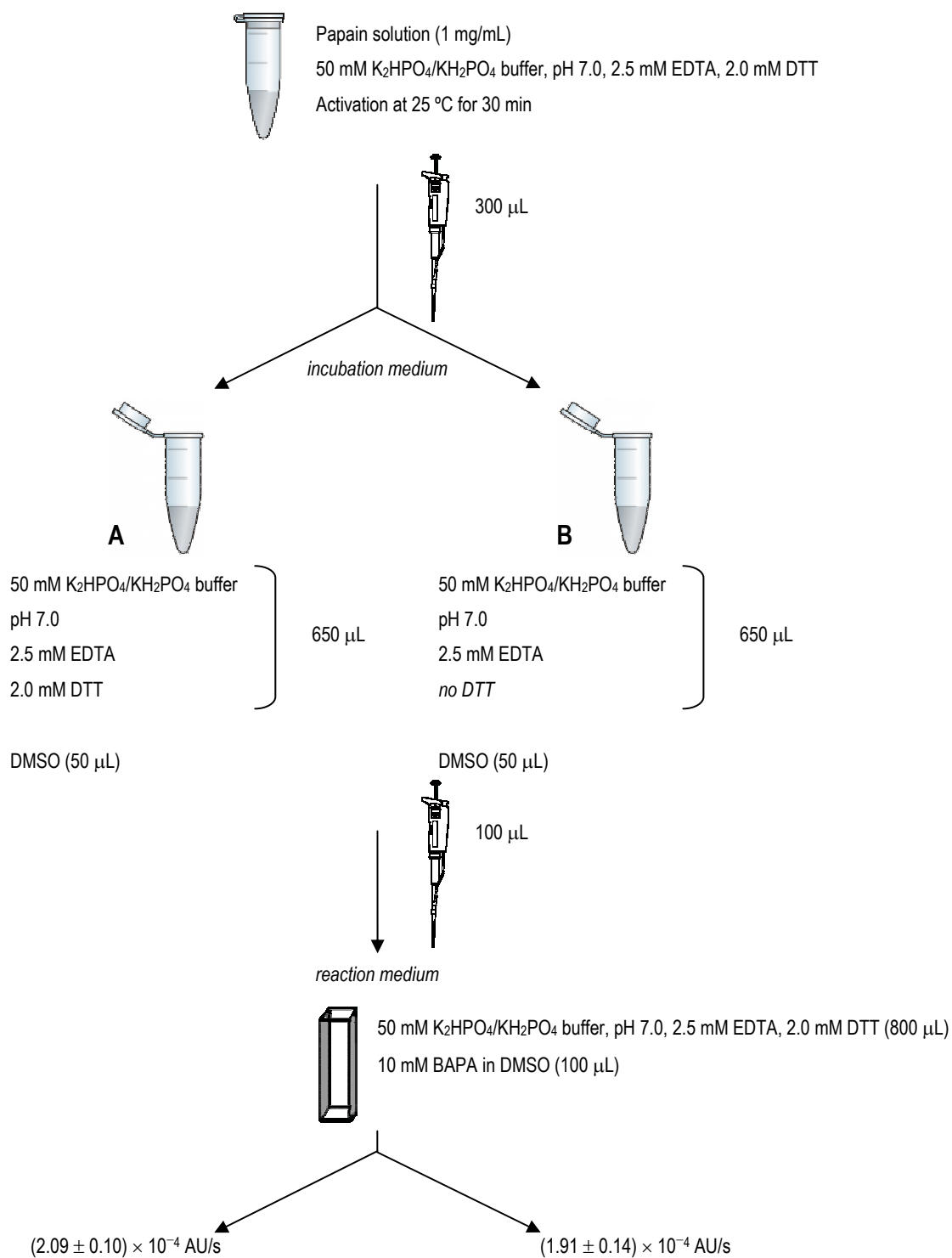
<sup>a</sup> Values are the mean of three determinations.

The DTT efficiency was compared to the one of sodium cyanoborohydride by carrying out parallel experiments with each of these reducing agents in the same concentration (2 mM stock solution). No activity was observed with sodium cyanoborohydride.

Finally, the inhibition assay was planned by adding an incubation phase, in such a way that the employed concentration of enzyme and substrate in the reaction medium were the originally reported. To investigate if papain required the presence of DTT in the incubation buffer, two experiments were made (see Experiments A and B in Scheme AI.2). As shown, the enzyme reaction rates were similar, indicating that the DTT from the activation buffer is sufficient to maintain the active form of papain in the incubation mixture.

The conditions of Experiment B appeared as more suitable for the inhibition studies, on the basis that a lower DTT concentration in the incubation medium leads to a smaller depletion of highly chemical reactive inhibitors. In addition, it was found that, under conditions B, the enzyme retains *ca.* 90% of its activity after 5 h in the incubation medium. Thus, the assay could be employed in inhibition studies, bearing in mind that beyond this period of time the kinetic results could be compromised.

A positive control inhibition assay was carried out by employing the successful papain inhibitor, E-64 (Section 1.2.2), in a 50  $\mu$ M concentration. As expected, it led to an enzyme residual activity of *ca.* 10%, after 1 min of incubation.



**Scheme AI.2 Possible procedures to be used for the inhibition assay.** In order to achieve an enzyme inactivation curve with nine experimental points, the volume of the samples, from the 1 mL incubation medium, was established in 100 µL. It was also decided to use the papain concentration (reaction medium) reported by Zhao *et al.*, *i.e.*, *ca.* 30 µg/mL.<sup>164</sup> Taking together, these conditions resulted in a 300 µg/mL concentration for papain in the incubation medium.

**Investigation on activation time.** The original procedure activated papain for 1 h. This period of time was investigated (Table AI.2) and it was found that, under the adapted conditions, the maximum enzymatic activity is reached after 30 min of incubation. The activation time was therefore established in 30 min.

**Table AI.2 Papain activity for several activation time periods.<sup>a</sup>**

Activation times (min)	Relative papain activity (%) <sup>b</sup>
1	63
15	95
30	100
60	100

<sup>a</sup> These experiments were performed by Luisa Martins (from the Faculty of Pharmacy, University of Lisbon). <sup>b</sup> The results are expressed comparatively to the activity detected after 60 min activation. The assays were performed using the 2 mM DTT stock solution.

Papain was immediately used after activation or kept at  $-20\text{ }^{\circ}\text{C}$  between assays. In general, no significant loss of enzymatic activity was detected after 24 h storage (conserved *ca.* 90% of its original value).

**Determination of  $K_m$ .** It is known that any change in enzymatic assay conditions may compromise the obedience to Michaelis-Menten equation.<sup>167</sup> As the present work established a modified procedure for the assessment of papain activity, it was necessary to check the equation's validity under the new conditions.

Thus, the enzyme reaction rate,  $v$ , was measured in the presence of different BAPA amounts to reveal the expected hyperbolic dependence of velocity on substrate concentration (Figure AI.3). The range of BAPA concentrations included the one employed in the enzymatic assay, *i.e.* 1 mM. It was therefore demonstrated that, under the established conditions, the enzymatic reaction obeys Michaelis-Menten kinetics.

The data were computer-fitted (Sigma Plot<sup>®</sup> software) to Michaelis-Menten equation, allowing the determination of  $K_m$   $(4.63 \pm 0.94) \times 10^{-3}$  M and  $V_{\max}$   $(1.35 \pm 0.15) \times 10^{-3}$  AU/s.

The value found for  $K_m$  is consistent with the ones revealed by the literature, *i.e.*  $4.4 \times 10^{-3}$  M (in presence of 30 mM cysteine at 35 °C and pH 7.2),<sup>168</sup> and  $(3.00 \pm 0.35) \times 10^{-3}$  M (in presence of 5.0 mM  $\beta$ -mercaptoethanol at 25 °C and pH 7.01).<sup>169</sup>

An interesting result obtained with a BAPA analogue, benzoyl-*S*-arginine amide, is that  $K_m$  for the hydrolysis of this substrate by papain is dependent on the reducing agent used as well as on its concentration, with an appreciable enhancement in  $K_m$  value with increasing

cysteine concentration.<sup>166</sup> It was reasoned that this effect might occur for other thiol-activating enzymes.<sup>166</sup>

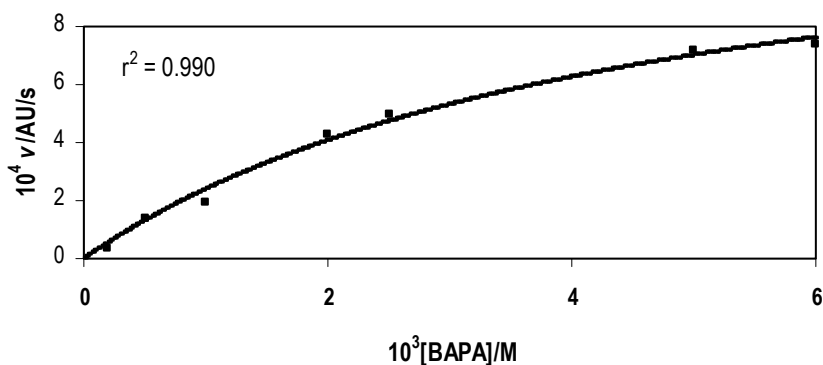


**Figure AI.3** Reaction rate,  $v$ , plotted against the BAPA concentration,  $[BAPA]$ , for the papain-catalysed hydrolysis of this compound, at pH 7.0 at 25 °C. Points are experimental and line is theoretical for  $K_m$  ( $4.63 \pm 0.94$ )  $\times 10^{-3}$  M and  $V_{max}$  ( $1.35 \pm 0.15$ )  $\times 10^{-3}$  AU/s.

### AI.1.2 Purification of papain by gel-filtration chromatography

As described in the previous sections, this work established a papain inhibition assay involving an enzyme-inhibitor incubation mixture, whose buffer contains DTT (provided by the enzyme stock solution). The thiol presence may, however, become a limitation when testing inhibitors with sufficiently chemical reactivity to be depleted by DTT, a situation that leads to a decrease or abolition of the inhibitory activity of the compounds. To overcome this problem it would be necessary to employ papain free from DTT.

Activated papain is easily purified from the reducing agent by gel-filtration chromatography on Sephadex columns.<sup>148,158,170</sup> The present investigation used a PD-10 desalting column, which efficiently separates molecules of high ( $M_r > 5000$ )<sup>oo</sup> from low molecular weight substances ( $M_r < 1000$ ).<sup>171</sup>

After gel-chromatography, the eluted fractions were assayed for papain content by measuring their  $A_{280}$ . This yielded a chromatogram, exemplified by the one in Figure AI.4, which reveals a bell-shape elution profile for papain (in blue). The absorbance, however, did

<sup>oo</sup> Papain is a 23406-molecular weight ( $M_r$ ) protein.<sup>157</sup>

not return to the baseline level, what was thought to be caused by the later elution of DTT, as this thiol also absorbs at 280 nm, although weakly than papain.<sup>157</sup> This situation was confirmed by recording the  $A_{412}$  of the latter fractions, after reaction with Ellman's reagent (Section 5.2.4). As no significant amounts of papain are expected to occur at this stage, the increase in the  $A_{412}$ , *i.e.* the increase in free thiol content, could be essentially ascribed to DTT.

The slight increase in the absorbance, seen around fraction 11, was also detected in other experiments and may be due to the remaining elution of the protein along with the starting elution of DTT. Thus, to ensure the complete separation of papain from the thiol agent, only fractions 2 to 8 were combined.

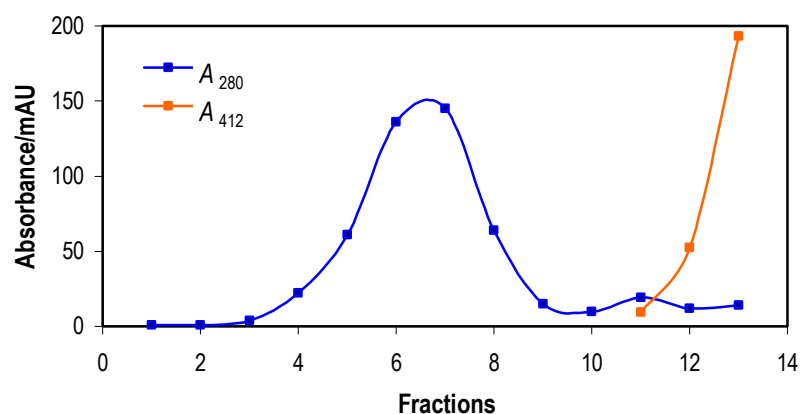


**Figure AI.4** Elution profile (absorbance *versus* collected fractions) for papain purification by gel-filtration chromatography using a PD-10 desalting column. The buffer used was 50 mM  $K_2HPO_4/KH_2PO_4$  buffer, pH 7.0, 2.5 mM EDTA.

The resultant papain stock solution could be easily assayed for effective active enzyme concentration using Ellman's reagent, without interference from DTT. Nevertheless, this parameter was not assessed in the procedure lacking gel-filtration chromatography, in which the concentration of papain was calculated by weighing an accurate amount of enzyme. Thus, in order to equal the concentration employed in both protocols, it was decided to assay the purified enzyme solution for total protein concentration by measuring the  $A_{280}$ . Calculations were done by using an extinction coefficient of  $57.6 \text{ mM}^{-1} \text{ cm}^{-1}$  and a 23406-molecular weight.<sup>157</sup> When required, the purified papain was diluted with 50 mM  $K_2HPO_4/KH_2PO_4$

buffer, pH 7.0, 2.5 mM EDTA. By working in this way, comparable enzyme activities were obtained (purified *versus* non-purified).

It is known that the linear relationship between enzyme amount and enzyme reaction rate,  $v$ , is a reliable test for the validity of the Michaelis-Menten equation.<sup>167</sup> For purified papain, investigation on such dependence resulted in the expected correlation (Figure AI.5), which means that no departure from Michaelis-Menten kinetics exists when the enzyme is employed up to 60  $\mu\text{g/mL}$  in the reaction medium (the established assay uses a concentration of *ca.* 30  $\mu\text{g/mL}$ ).

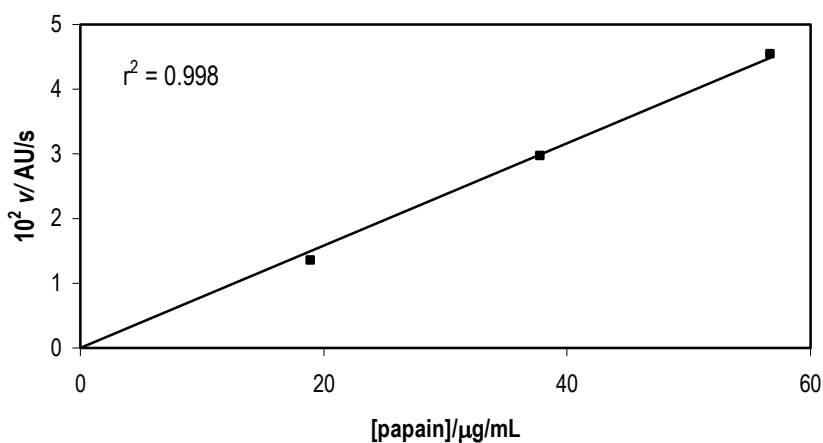


**Figure AI.5** Reaction rate,  $v$ , plotted against the papain concentration, [papain], for the papain-catalysed hydrolysis of BAPA, at pH 7.0 at 25 °C. Points are experimental and line is from linear regression analysis of the data.

A positive control inhibition assay was performed with the 2-bromo-1,4-naphthoquinone derivative **3.6**, which was found to be one of the most potent papain inhibitors in this work (Section 3.3.1). Interestingly, the enzyme was inactivated to an extent similar to the one observed when employing non-purified papain (Figure AI.6). This situation suggests that this inhibitor is not significantly affected by the thiol presence.

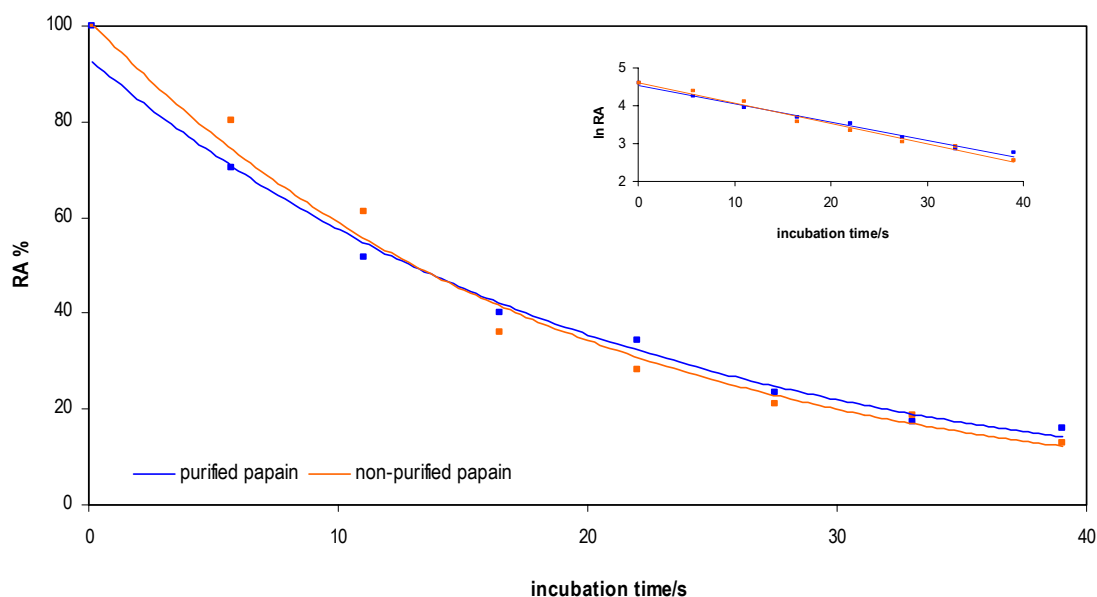


**Figure AI.6** Time course of papain inactivation by 2-bromo-1,4-naphthoquinone derivative 3.6, at pH 7.0 at 25 °C. The inhibitor concentration was 50  $\mu\text{M}$ . The enzymatic activity is expressed as residual activity percentage (RA%). The inset presents a semi-logarithmic plot of RA *versus* time. Points are experimental and line is theoretical for  $k_{\text{obs}}$   $(8.05 \pm 0.52) \times 10^{-4} \text{ s}^{-1}$  (purified papain) and  $(8.54 \pm 0.67) \times 10^{-4} \text{ s}^{-1}$  (non-purified papain).

Overall, it was demonstrated that purified papain, provided by gel-filtration chromatography (PD-10 desalting column), can be applied to the inhibition assay adapted in the present thesis. This alternative procedure may be carried out for the accurate evaluation of highly chemical reactive compounds.

Although not investigated, a probability exists that purification leads to a less stable enzyme due to the absence of a reducing environment. Therefore, careful attention should be taken with the durability of the inhibition study. As usual, the reliability of the results would be assessed by a blank control, which must be assayed throughout the experiment.

### AI.1.3 Dialysis experiment

A dialysis experiment was performed to check the irreversibility of papain inactivation by the naphthoquinone derivatives presented in Section 3.3.1. The enzyme-inhibitor complex was dialysed against phosphate buffer, containing DTT. This thiol is required to maintain the reducing conditions essential for papain activity. In fact, when the experiment was carried out

in buffer without DTT, the control enzyme lost *ca.* 40% of its activity after 2 h of dialysis, *ca.* 60% after 10 h and *ca.* 80% after 24 h.

The change in the enzymatic activity, during dialysis, was evaluated by taking periodical aliquots from the papain solution. However, differences in protease activity may be caused by the dilution of papain solution throughout dialysis, as the water from the buffer tends to cross the membrane (osmosis). Thus, for comparison purposes between assays, the enzymatic activity was expressed as AU/s/ $\mu\text{g}$  papain, where AU/s represents the increase in  $A_{410}$  during 4 min, due to the cleavage of BAPA into *p*-nitroaniline. Finally, the enzymatic activity was converted to a percentage of the value found immediately before the dialysis.

Concerning papain concentration, it was stated before (Section AI.1.1.3) that the concentration of a protein may be determined from its UV absorption (280 nm), using Lambert-Beer's law. However, the method could not be used due to the interference from the inhibitor, which also absorbs at this wavelength (see the spectrum in Appendix III). The Bradford assay provided, therefore, a suitable alternative. It is also a spectrophometric method, whose absorbance results were converted to the approximate protein concentration according to the equation

$$A_{595} = 32.4 \times 10^{-3} \times [\text{protein concentration}] + 4.4 \times 10^{-3} \quad (\text{AI.1})$$

where the protein concentration is given in  $\mu\text{g}/\text{mL}$ . This equation showed to be valid up to 15  $\mu\text{g}/\text{mL}$  ( $r^2 = 0.983$ ).<sup>pp</sup>

## AI.2 Bovine spleen cathepsin B

### AI.2.1 Introductory remarks

Cathepsin B is one of the best characterised mammalian cysteine proteases, whose role in human pathological processes was mentioned in Section 1.1.2.

---

<sup>pp</sup> This equation was previously obtained by Luisa Martins (from the Faculty of Pharmacy, University of Lisbon), by assaying six solutions of bovine serum albumin of different concentrations, using a procedure similar to the one employed in this work (the Bradford assay is described in Section AI.4.5).



Bovine spleen cathepsin B shares about 80% amino acid sequence homology with the human liver variety.<sup>172</sup> Thus, it provided a suitable model for the human protease, at a lower price.

The search for a convenient enzymatic assay was a straightforward task as the *Sigma quality control test procedure*<sup>157</sup> for cathepsin B (Sigma C6286) consists in a convenient spectrophotometric method, which was first described by Bajkowski *et al.*<sup>173</sup> Similarly to papain, cathepsin B requires a reducing environment and the presence of a chelating agent for full hydrolytic activity. However, while papain has a neutral pH optimum, cathepsin B is most active in an acidic medium (pH values from 4.0 to 6.5), which is in accordance with its activity within lysosomes.<sup>11,161</sup>

### AI.2.2 Development of cathepsin B inhibition assay

According to *Sigma*, the bovine spleen cathepsin B stock solution is prepared in 20 mM sodium acetate buffer, pH 5.0, containing 1.0 mM EDTA and 5.0 mM cysteine. Proteolytic activity is measured in the same buffer by following the release of *p*-nitrophenol from Cbz-*S*-Lys-ONp at 326 nm for approximately 3 min at 25 °C. In the reaction mixture, the substrate concentration is 80 μM and the enzyme concentration is between  $8.2 \times 10^{-3}$  and  $16.3 \times 10^{-3}$  units/mL.

In the present work, the enzyme concentration was arbitrarily established in  $10.0 \times 10^{-3}$  units/mL for the reaction with the substrate, which was employed in the concentration reported by *Sigma*, *i.e.* 80 μM.

The main concern in adapting this procedure was the type of reducing agent used as well as its concentration because the potential inhibitors may react more or less significantly with the thiol present in the buffer. Thus, it was thought that comparative studies on the compounds efficiency against several cysteine proteases would give more reliable results if the inhibitor was exposed to the same thiol (type and concentration), independently of the target enzyme. It was therefore decided to employ the conditions previously established for papain, *i.e.*, 0.6 mM DTT in the incubation medium and *ca.* 2 mM in the reaction cuvette. Interestingly, this latter concentration was used by Bajkowski *et al.*<sup>173</sup> to carry out the cathepsin B-catalysed hydrolysis of the substrate used in this thesis.

It is known that cathepsin B requires thiol activation.<sup>161</sup> The *Sigma* protocol does not indicate an activation time period before the reaction with the substrate, but Bajkowski *et*

*al.*<sup>173</sup> described a 15-min incubation phase at 25 °C, which was adapted in the present investigation.<sup>99</sup> Because the enzyme is supplied in sealed ampoules, it was dissolved in the activation buffer, then it was activated and kept within the sealed ampoule, at –20 °C, between assays. No loss of enzymatic activity was detected during approximately two weeks.

Under these conditions, plotting the Cbz-*S*-Lys-ONp hydrolysis reaction time against the increase in the absorbance resulted in a slope sufficiently high (*ca.*  $1 \times 10^{-3}$  AU/s) to assess its decay in the presence of the inhibitor.

Another important subject was the stability of Cbz-*S*-Lys-ONp in the assay buffer. This was investigated by preparing a cuvette with substrate (100  $\mu$ L of the stock solution 0.8 mM) and 900  $\mu$ L of 20 mM sodium acetate buffer, pH 5.0, containing 1.0 mM EDTA and 2.0 mM DTT. The absorbance was recorded during the reported 3 min at 326 nm, against a blank of 20 mM sodium acetate buffer, pH 5.0, containing 1.0 mM EDTA and 2.0 mM DTT. There was an absorbance increase of *ca.*  $0.1 \times 10^{-3}$  AU/s, corresponding to *ca.* 10% of the one above-mentioned, in the presence of the enzyme. These data indicated a slight degree of spontaneous chemical hydrolysis of the substrate, but this interference could be easily removed by adding substrate to the blank cuvette. Later, it was found that the kinetic results were not compromised by the substrate stability, because comparable results for  $K_m$  value ( $39.4 \pm 7.11 \mu\text{M}$  versus  $47.4 \pm 9.00 \mu\text{M}$ ) were obtained in two independent experiments, one with substrate in the blank cuvette and another lacking this component. The presence of the substrate in the blank was therefore excluded in the inhibition studies.

Figure AI.7 shows the hyperbolic dependence of reaction rate on substrate concentration. The value found for  $K_m$  is slightly different from the one reported by Bajkowski *et al.*,<sup>173</sup> which is  $2.7 \pm 0.30 \mu\text{M}$ . This inconsistency is not easy to explain as both investigations assayed the enzyme in equal conditions, *i.e.* sodium acetate buffer (20 mM in this thesis and 25 mM in the Bajkowski's work), pH 5, containing 1 mM EDTA and DTT *ca.* 2 mM.

On the other hand, the calculation of  $K_m$  value followed a different approach from the one described by Bajkowski *et al.*<sup>173</sup> These authors followed the reactions to completion and converted the absorbance data to rate data using the molar extinction coefficient of Cbz-*S*-Lys-ONp, whereas the present work measured the initial rates,  $v$ . The calculation method was therefore considered as the most probable reason for discrepancy.

The most important, however, is the evidence that the hydrolysis of Cbz-*S*-Lys-ONp by cathepsin B obeys Michaelis-Menten kinetics, under the established conditions.

---

<sup>99</sup> The present work and Bajkowski *et al.* activated the enzyme under equal conditions, *i.e.* in the presence of 30 mM DTT.

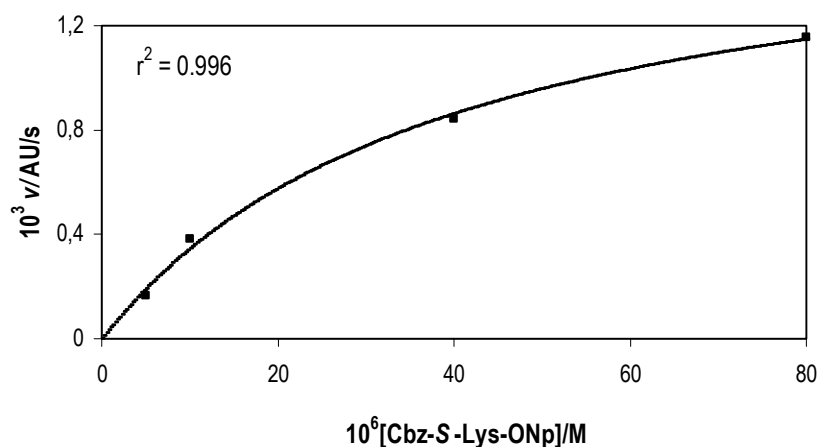


**Figure AI.7** Reaction rate,  $v$ , plotted against the Cbz-S-Lys-ONp concentration, [Cbz-S-Lys-ONp], for the bovine spleen cathepsin B-catalysed hydrolysis of this compound, at pH 5.0 at 25 °C. Points are experimental and line is theoretical for  $K_m$   $(39.4 \pm 7.11) \times 10^{-6}$  M and  $V_{\max}$   $(1.71 \pm 0.14) \times 10^{-3}$  AU/s.

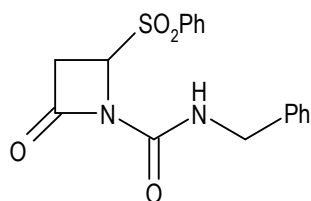
A positive control inhibition assay was carried out by employing the successful papain inhibitor, E-64 (Section 1.2.2), in a 50  $\mu\text{M}$  concentration. As expected, it led to an enzyme residual activity of *ca.* 10%, after 1 min of incubation.

Concerning the enzyme stability in the incubation mixture, it was found that cathepsin B retains *ca.* 80% of its activity after 4 h and *ca.* 60% after 7 h. This should be kept in mind when evaluating the reliability of the kinetic results, provided by the inhibition studies.

### AI.3 Inhibition assay for porcine pancreatic elastase

The protocol for porcine pancreatic elastase was already established in the host laboratory, and it was adapted from a procedure described by Hinchliffe *et al.*<sup>174</sup>

A positive control inhibition assay was carried out by employing an in-house inhibitor, **I.5**<sup>175</sup> (Figure AI.8), which totally inactivated the enzyme.



I.5

**Figure AI.8 Structure of I.5, an inhibitor of porcine pancreatic elastase.**

## AI.4 Experimental Section

### AI.4.1 Reagents and Solvents

Papain (Sigma P4762), bovine spleen cathepsin B (Sigma C6286, 10 U), porcine pancreatic elastase (Sigma E0258), BAPA, Cbz-*S*-Lys-ONp, Suc-Ala-Ala-Ala-4-nitroanilide, DTT and 0.1 M HEPES buffer (H9897) were obtained from Sigma-Aldrich. Cbz-Gly-ONp was from Bachem. Bradford Reagent was from Bio-Rad (500-0006 Bio-Rad Protein Assay Dye Reagent Concentrate). DMSO and buffer materials for kinetic measurements were of analytical grade and were purchased from Merck (Germany). Freshly deionised water was used throughout.

### AI.4.2 Gel-filtration chromatography

PD-10 Desalting columns were from GE Healthcare (Amersham Biosciences) and were kindly provided by Prof. K. Douglas, at the University of Manchester.

### AI.4.3 Dialysis experiments

Dialysis experiments were carried out with Spectra/Por 4 dialysis membranes, 12000-14000 MW (Spectrum Laboratories Inc. 132697).

#### AI.4.4 Equipment

Measurement of pH values was carried out at  $25.0 \pm 0.1$  °C, using a digital microprocessor pH meter (model micro pH 2002, Crisson Instruments S.A.), calibrated with standard buffers (Merck).

Activation of papain/cathepsin B was carried out at  $25.0 \pm 0.1$  °C using a thermostatic bath.

Incubation of potential inhibitors with papain/cathepsin B/porcine pancreatic elastase was carried out at  $25.0 \pm 0.1$  °C using a thermostatic bath.

Kinetic measurements were carried out at  $25.0 \pm 0.1$  °C using a Shimadzu UV-2100 spectrophotometer, equipped with a temperature controller (CPS).

#### AI.4.5 Procedures for papain

**Determination of the papain activity in the presence of Cbz-Gly-ONp.** Papain (1 mg/mL) was activated for 1 h in 50 mM  $K_2HPO_4/KH_2PO_4$  buffer, pH 7.0, containing 1.0 mM EDTA and 10 mM sodium cyanoborohydride. The reaction was started by the addition of papain (100  $\mu$ L of the stock solution 1 mg/mL) into a cuvette containing 100  $\mu$ L of Cbz-Gly-ONp stock solution (3 mM in DMSO) and 800  $\mu$ L of 50 mM  $K_2HPO_4/KH_2PO_4$  buffer, pH 7.0, containing 1.0 mM EDTA. Enzymatic activity was determined at 410 nm during 4 min, against a blank of 900  $\mu$ L of 50 mM  $K_2HPO_4/KH_2PO_4$  buffer, pH 7.0, containing 1.0 mM EDTA and 100  $\mu$ L of Cbz-Gly-ONp stock solution. Under these conditions, the initial concentration of Cbz-Gly-ONp was 300  $\mu$ M.

The experiment was also performed using two different concentrations of Cbz-Gly-ONp, 30  $\mu$ M (100  $\mu$ L of a stock solution 0.3 mM in DMSO) and 3  $\mu$ M (100  $\mu$ L of a stock solution 0.03 mM in DMSO).

**Papain inhibition assay.** Papain (1 mg/mL) was activated for 30 min by incubation in 50 mM  $K_2HPO_4/KH_2PO_4$  buffer, pH 7.0, containing 2.5 mM EDTA and 2.0 mM DTT. Reactions were started by the addition of the inhibitor stock solution in DMSO (50  $\mu$ L) to the incubation solution containing papain (300  $\mu$ L of the stock solution 1 mg/mL) and 650  $\mu$ L of 50 mM

K<sub>2</sub>HPO<sub>4</sub>/KH<sub>2</sub>PO<sub>4</sub> buffer, pH 7.0, containing only 2.5 mM EDTA. At different times, aliquots (100 µL) from the incubation mixture were withdrawn and transferred to a quartz cuvette containing 100 µL of BAPA stock solution (10 mM in DMSO) and 800 µL of 50 mM K<sub>2</sub>HPO<sub>4</sub>/KH<sub>2</sub>PO<sub>4</sub> buffer, pH 7.0, containing 2.5 mM EDTA and 2.0 mM DTT.

Enzymatic activity was determined at 410 nm during 4 min, against a blank of 50 mM K<sub>2</sub>HPO<sub>4</sub>/KH<sub>2</sub>PO<sub>4</sub> buffer, pH 7.0, containing 2.5 mM EDTA and 2.0 mM DTT.

A blank incubation mixture, replacing the inhibitor solution by DMSO, was run and assayed in parallel.

The assays in the presence of ascorbic acid were carried out as described above, except that the incubation buffer included ascorbic acid (2 and 30 mM).

For assays with an excess of DTT, the concentration of this agent in the incubation buffer was increased to 15 mM.

**Determination of  $K_m$  for the hydrolysis of BAPA by papain.** Experiments for determination of  $K_m$  were carried out as described above, except that the inhibitor solution in the incubation mixture was replaced by DMSO (50 µL). Substrate final concentrations in the cuvette ranged from 0.2 to 6.0 mM. Each concentration was assayed at least two times.

**Gel-filtration chromatography.** Gel-filtration chromatography was carried out on PD-10 desalting pre-packed columns (bed volume 8.3 mL and bed height 5 cm). These columns are composed of Sephadex G-25, with a particle size range from 85 to 260 µm. The columns are supplied in distilled water containing 0.15% Kathon™ CG/ICP biocide and must be equilibrated with *ca.* 25 mL elution buffer.<sup>171</sup> In this case, degassed 50 mM K<sub>2</sub>HPO<sub>4</sub>/KH<sub>2</sub>PO<sub>4</sub> buffer, pH 7.0, 2.5 mM EDTA.

Papain (3 mg/1 mL) was activated as described above. The purification proceeded according to the supplier instructions,<sup>171</sup> *i.e.* the 1 mL papain solution was diluted with elution buffer until a total volume of 2.5 mL, and then it was applied to the column, which was subsequently eluted with 3.5 mL buffer. It was decided to collect fractions of 10 drops each.

The gel-filtration chromatography was carried out under N<sub>2</sub> and the fractions were kept sealed to prevent oxidation of the free Cys25 thiol group.

To assess the papain content, aliquots (50  $\mu\text{L}$ ) from each fraction or from the final stock solution were withdrawn and transferred to a quartz cuvette containing 950  $\mu\text{L}$  of 50 mM  $\text{K}_2\text{HPO}_4/\text{KH}_2\text{PO}_4$  buffer, pH 7.0, 2.5 mM EDTA. The  $A_{280}$  of these solutions was recorded against a blank of 50 mM  $\text{K}_2\text{HPO}_4/\text{KH}_2\text{PO}_4$  buffer, pH 7.0, 2.5 mM EDTA.

The free thiol content was determined by Ellman's method (Section 5.2.4), using 50  $\mu\text{L}$  aliquots from each fraction.

### Dialysis experiments

- Dialysis membrane preparation

The membrane was cut into the desired length and soaked in distilled water. Then, it was boiled for 15 min in 10 mM sodium hydrogen carbonate solution, and another 15 min in 10 mM EDTA (this latter treatment was repeated with a fresh solution). Finally, the membrane was rinsed with deionised water and was stored, at 4  $^{\circ}\text{C}$ , in 20 mM Tris-HCl, pH 7.5. Before use, it was rinsed with deionised water and then with 50 mM  $\text{K}_2\text{HPO}_4/\text{KH}_2\text{PO}_4$  buffer, pH 7.0, containing 2.5 mM EDTA.

- Inactivation of papain and dialysis

Papain was inactivated by the compound **3.1b**. The inhibitor (100  $\mu\text{L}$  of a stock solution 580  $\mu\text{M}$ ) was added to a medium containing activated papain (600  $\mu\text{L}$  of a stock solution 1 mg/mL) and 1.3 mL of 50 mM  $\text{K}_2\text{HPO}_4/\text{KH}_2\text{PO}_4$  buffer, pH 7.0, containing 2.5 mM EDTA. When the enzymatic activity was assessed in the presence of BAPA, an inactivation degree of *ca.* 80% was found, after 2 h of incubation. The sample was also assayed for papain concentration using the Bradford Reagent (see below), allowing the expression of enzymatic activity as AU/s/ $\mu\text{g}$  papain. This value was used for comparison purposes with the dialysed sample.

The enzyme-inhibitor mixture was then dialysed at 4  $^{\circ}\text{C}$  over a period of 24 h, against 0.8 L of 50 mM  $\text{K}_2\text{HPO}_4/\text{KH}_2\text{PO}_4$  buffer, pH 7.0, containing 2.5 mM EDTA and 2 mM DTT. Aliquots of 200  $\mu\text{L}$  were removed at 5, 19 and 24 h of dialysis and assayed for enzymatic activity in the presence of BAPA, and for papain concentration using the Bradford Reagent.

A blank mixture, replacing the inhibitor solution by DMSO, was dialysed and assayed in parallel.

Both experiments (with and without the inhibitor) were run in duplicate.

- Determination of papain concentration

The papain concentration was assessed using the Bradford Reagent (Bio-Rad).<sup>176</sup> This product contains the dye Coomassie Brilliant Blue G-250, phosphoric acid and MeOH. The method is based on the observation that the absorbance maximum for an acidic solution of Coomassie Brilliant Blue G-250 shifts from 465 to 595 nm when it binds to protein. The dye-protein complex is relatively stable (absorbance may be recorded from 5 min to 1 h after complex formation).<sup>177</sup>

The supplier of Bradford Reagent indicates a microassay procedure (for protein concentrations  $\leq 25 \mu\text{g/mL}$ ), which was used as follows: 200  $\mu\text{L}$  of Bradford Reagent were added to a quartz cuvette with 50  $\mu\text{L}$  of the papain solution and 750  $\mu\text{L}$  of 50 mM  $\text{K}_2\text{HPO}_4/\text{KH}_2\text{PO}_4$  buffer, pH 7.0, containing 2.5 mM EDTA. Mixing was performed by inverting the cuvette several times. The  $A_{595}$  was read after 5 min against a blank solution with 200  $\mu\text{L}$  of Bradford Reagent and 800  $\mu\text{L}$  of 50 mM  $\text{K}_2\text{HPO}_4/\text{KH}_2\text{PO}_4$  buffer, pH 7.0, containing 2.5 mM EDTA.

By working in this way, dialysed-papain concentration in the cuvette is estimated in *ca.* 15  $\mu\text{g/mL}$ . Because this protein concentration is within the range indicated by the supplier, obedience to Lambert-Beer's law should be expected. Nevertheless, it was thought that departure might occur due to the presence of the bound inhibitor. The law's validity was therefore investigated by performing the experiment in Figure AI.9. In addition, Figure AI.10 also shows equal spectra for the dye-papain complex in the presence and absence of compound **3.1b**, excluding any interference from the inhibitor at 595 nm.

The protein content in the aliquots from incubation medium, during dialysis, was always superior to 80%. This percentage was calculated comparatively to the protein content determined before the dialysis.



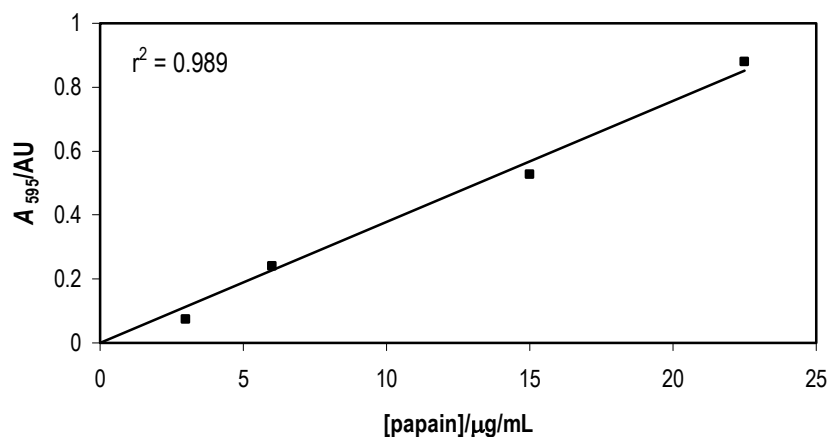


**Figure AI.9** Dependence of the absorption at 595 nm on the amount of papain inactivated by 3.1b. The assay was performed by adding 10, 20, 50 and 75  $\mu\text{L}$  of a papain-inhibitor incubation mixture (after inactivation) into a quartz cuvette with 50 mM  $\text{K}_2\text{HPO}_4/\text{KH}_2\text{PO}_4$  buffer, pH 7.0, containing 2.5 mM EDTA (790, 780, 750 and 725  $\mu\text{L}$ , respectively) and 200  $\mu\text{L}$  of Bradford Reagent. Points are experimental and line is from linear regression analysis of the data.

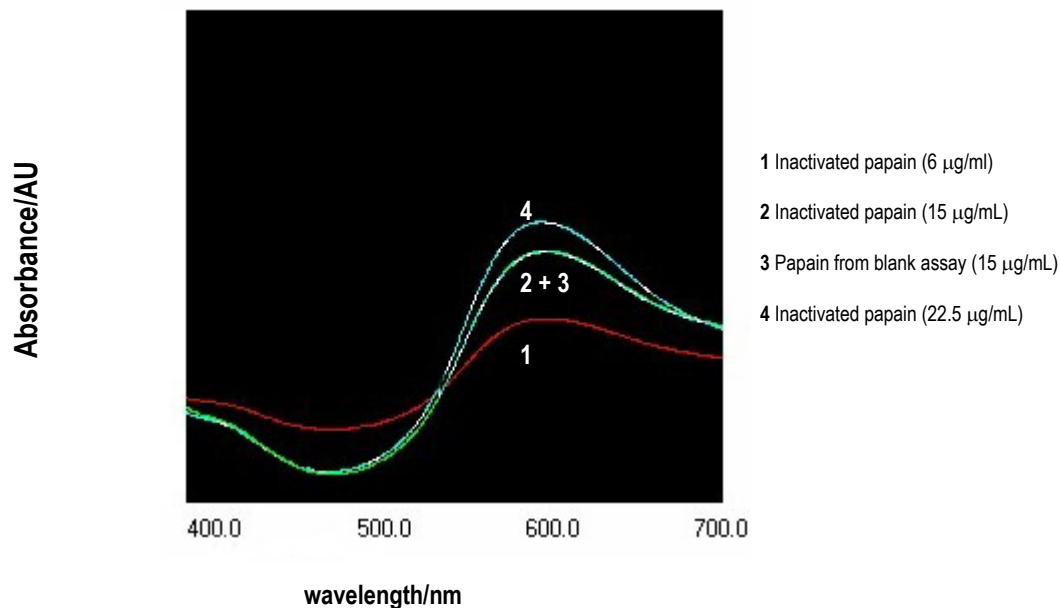


**Figure AI.10** Visible spectra depicting the dye-papain complex in the presence and absence of the inhibitor 3.1b.

#### **AI.4.6 Procedures for bovine spleen cathepsin B**

**Cathepsin B inhibition assay.** Cathepsin B (10 units/2 mL) was activated during 15 min in 20 mM sodium acetate buffer, pH 5.0, containing 1.0 mM EDTA and 30 mM DTT. Reactions were started by addition of the inhibitor stock solution in DMSO (50  $\mu$ L) to the incubation solution containing cathepsin B (20  $\mu$ L of the stock solution 10 units/2 mL) and 930  $\mu$ L of 20 mM sodium acetate buffer, pH 5.0, containing only 1.0 mM EDTA. At various time intervals, cathepsin B activity was assayed by taking a 100  $\mu$ L aliquot of the incubation solution and adding it to a quartz cuvette containing 100  $\mu$ L of the Cbz-S-Lys-ONp stock solution (0.8 mM in DMSO) and 800  $\mu$ L of 20 mM sodium acetate buffer, pH 5.0, containing 1.0 mM EDTA and 2.0 mM DTT. Enzymatic activity was monitored at 326 nm, over a period of 3 min, against a blank of 20 mM sodium acetate buffer, pH 5.0, containing 1.0 mM EDTA and 2.0 mM DTT.

A blank incubation mixture, replacing the inhibitor solution by DMSO, was run and assayed in parallel.

**Determination of  $K_m$ .** Experiments for determination of  $K_m$  were carried out as described above, except that the inhibitor solution in the incubation mixture was replaced by DMSO (50  $\mu$ L). Substrate final concentrations in the cuvette ranged from 5.0 to 80  $\mu$ M. When the concentrations were 5 and 10  $\mu$ M, the hydrolysis was complete after approximately 1 min and the rate,  $v$ , was calculated from the data obtained in the initial 30 s of the reaction.

Each concentration was assayed at least two times.

#### **AI.4.7 Inhibition assay for porcine pancreatic elastase**

The inhibitor (50  $\mu$ L of a stock solution in DMSO) was mixed with 750  $\mu$ L of 0.1 M Hepes buffer, previously adjusted to pH 7.2, and 200  $\mu$ L of a stock solution of enzyme (50  $\mu$ M in 0.1 M Hepes buffer, pH 7.2). Aliquots (100  $\mu$ L) were withdrawn at different time intervals and transferred to a quartz cuvette containing 5  $\mu$ L of the Suc-Ala-Ala-Ala-4-nitroanilide stock solution (12.5 mM in DMSO) and 895  $\mu$ L of 0.1 M Hepes buffer.

Proteolytic activity was measured by following the release of *p*-nitroaniline for 50 s at 390 nm against a blank of 0.1 M HEPES buffer.

#### AI.4.8 Determination of $k_{\text{obs}}$ , $k_2$ , $K_I$ and $k_{\text{inact}}$

The enzymatic activity,  $v$ , expressed as AU/s, was determined from the slopes of the plots of absorbance *versus* reaction time (see Figure AI.11 for a typical example).

When performing an inhibitor assay, the activity  $v$  found immediately after the addition of the inhibitor was referred to as  $v_0$  and it was usually similar to the one showed by the blank assay. The ratio  $v/v_0$  was referred to as RA (residual activity).

Pseudo first-order inactivation rate constants,  $k_{\text{obs}}$ , were determined from plots of  $\ln \text{RA}$  *versus* incubation time.

In the case of hyperbolic dependences,  $K_I$  and  $k_{\text{inact}}$  values were determined by computer-fit (Sigma Plot<sup>®</sup> software) using least squares nonlinear regression analysis to Equation 3.3 (Section 3.3.1).

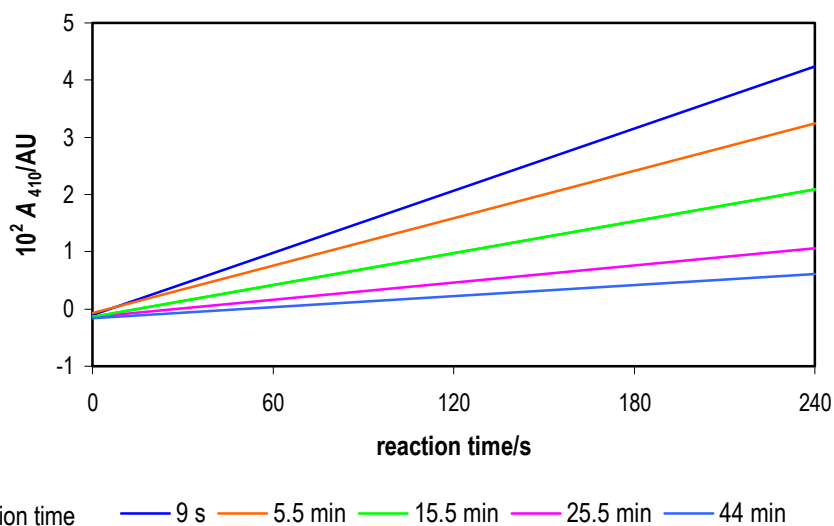


**Figure AI.11** Series of progression curves for the papain-catalysed hydrolysis of BAPA, at different times of the enzyme-inhibitor incubation. The experiment was carried out at pH 7.0 at 25 °C, using as inhibitor the naphthoquinone derivative **3.6** in a 50  $\mu\text{M}$  concentration.



## APPENDIX II. Pseudo first-order rate constants for the cysteine-catalysed decomposition of vinyl sultams, vinyl sulfonamide and naphthoquinones

Table AII.1 Pseudo first-order rate constants,  $k_{\text{obs}}$ , for the reaction of vinyl sultams 2.67a, 2.67b, 2.68a and 2.69b with cysteine at pH 6.9, at 25 °C and ionic strength 0.5 M.

### 2.67a

[cys] (mM)	$k_{\text{obs}}$ ( $10^{-4} \text{ s}^{-1}$ )
1.31	$1.86 \pm 0.01$
1.97	$2.11 \pm 0.15$
2.32	$2.37 \pm 0.06$
3.02	$3.50 \pm 0.03$

$$k_{\text{cat}} 0.11 \text{ M}^{-1} \text{ s}^{-1}$$

### 2.67b

[cys] (mM)	$k_{\text{obs}}$ ( $10^{-4} \text{ s}^{-1}$ )
1.48	$1.89 \pm 0.09$
1.94	$2.57 \pm 0.02$
2.36	$2.77 \pm 0.13$

$$k_{\text{cat}} 0.12 \text{ M}^{-1} \text{ s}^{-1}$$

### 2.68a

[cys] (mM)	$k_{\text{obs}}$ ( $10^{-4} \text{ s}^{-1}$ )
0.85	$1.70 \pm 0.23$
1.60	$2.34 \pm 0.18$
2.46	$3.76 \pm 0.12$
3.88	$5.21 \pm 0.11$

$$k_{\text{cat}} 0.13 \text{ M}^{-1} \text{ s}^{-1}$$

### 2.69b

[cys] (mM)	$k_{\text{obs}}$ ( $10^{-4} \text{ s}^{-1}$ )
0.85	$1.57 \pm 0.25$
1.60	$2.40 \pm 0.27$
2.46	$3.63 \pm 0.30$
3.88	$5.75 \pm 0.13$

$$k_{\text{cat}} 0.14 \text{ M}^{-1} \text{ s}^{-1}$$

Table AII.2 Pseudo first-order rate constants,  $k_{\text{obs}}$ , for the reaction of vinyl sulfonamide 2.84a with cysteine at pH 6.9, at 25 °C and ionic strength 0.5 M.

[cys] (mM)	$k_{\text{obs}}$ ( $10^{-4} \text{ s}^{-1}$ )
1.79	$2.24 \pm 0.08$
2.30	$2.57 \pm 0.08$
3.08	$3.24 \pm 0.06$
3.62	$5.02 \pm 0.05$

$$k_{\text{cat}} 0.13 \text{ M}^{-1} \text{ s}^{-1}$$

**Table AII.3 Pseudo first-order rate constants,  $k_{\text{obs}}$ , for the reaction of naphthoquinones 3.1a, 3.1b, 3.1c, 3.5, 3.8, 3.13 and 3.11 with cysteine at pH 7.1, at 25 °C and ionic strength 0.5 M. For 3.11, the rates were measured at three additional pH values: 7.9, 8.0 and 8.8.**

**3.1a**

[cys] (mM)	$k_{\text{obs}}$ ( $10^{-3} \text{ s}^{-1}$ )
0.44	$0.58 \pm 0.06$
0.90	$1.72 \pm 0.16$
1.93	$2.82 \pm 0.01$
3.19	$5.83 \pm 0.30$

$$k_{\text{cat}} 1.78 \text{ M}^{-1} \text{ s}^{-1}$$

**3.1b**

[cys] (mM)	$k_{\text{obs}}$ ( $10^{-4} \text{ s}^{-1}$ )
0.97	$0.48 \pm 0.07$
1.95	$0.58 \pm 0.01$
2.84	$0.86 \pm 0.06$
4.89	$2.20 \pm 0.10$

$$k_{\text{cat}} 0.04 \text{ M}^{-1} \text{ s}^{-1}$$

**3.1c**

[cys] (mM)	$k_{\text{obs}}$ ( $10^{-5} \text{ s}^{-1}$ )
1.86	$3.68 \pm 0.08$
3.34	$5.10 \pm 0.01$
3.75	$7.32 \pm 0.09$
4.84	$8.25 \pm 0.48$

$$k_{\text{cat}} 0.02 \text{ M}^{-1} \text{ s}^{-1}$$

**3.5**

[cys] (mM)	$k_{\text{obs}}$ ( $10^{-3} \text{ s}^{-1}$ )
0.71	$0.55 \pm 0.03$
1.13	$1.05 \pm 0.04$
1.93	$1.47 \pm 0.04$
2.58	$2.33 \pm 0.01$

$$k_{\text{cat}} 0.87 \text{ M}^{-1} \text{ s}^{-1}$$

**3.8**

[cys] (mM)	$k_{\text{obs}}$ ( $10^{-2} \text{ s}^{-1}$ )
0.06	$0.94 \pm 0.02$
0.17	$1.37 \pm 0.08$
2.01	$2.17 \pm 0.34$
3.33	$2.60 \pm 0.21$
5.41	$2.82 \pm 0.16$

**3.13**

[cys] (mM)	$k_{\text{obs}}$ ( $10^{-2} \text{ s}^{-1}$ )
0.44	$0.37 \pm 0.01$
1.90	$1.37 \pm 0.01$
3.42	$2.62 \pm 0.01$
4.37	$3.56 \pm 0.07$

$$k_{\text{cat}} 7.98 \text{ M}^{-1} \text{ s}^{-1}$$

**3.11 (pH 7.1)**

[cys] (mM)	$k_{\text{obs}}$ ( $10^{-2} \text{ s}^{-1}$ )
0.44	$0.36 \pm 0.04$
1.92	$1.38 \pm 0.00$
2.92	$2.19 \pm 0.07$
4.78	$3.24 \pm 0.13$

$$k_{\text{cat}} 6.84 \text{ M}^{-1} \text{ s}^{-1}$$

**3.11 (pH 7.9)**

[cys] (mM)	$k_{\text{obs}}$ ( $10^{-1} \text{ s}^{-1}$ )
2.77	$0.82 \pm 0.06$
3.92	$1.05 \pm 0.06$

$$k_{\text{cat}} 27.2 \text{ M}^{-1} \text{ s}^{-1}$$

**3.11 (pH 8.0)**

<b>[cys] (mM)</b>	<b><math>k_{\text{obs}}</math> (<math>10^{-2} \text{ s}^{-1}</math>)</b>
0.37	$1.46 \pm 0.02$
1.13	$3.96 \pm 0.12$
1.64	$5.57 \pm 0.10$

$$k_{\text{cat}} 33.6 \text{ M}^{-1} \text{ s}^{-1}$$

**3.11 (pH 8.8)**

<b>[cys] (mM)</b>	<b><math>k_{\text{obs}}</math> (<math>10^{-1} \text{ s}^{-1}</math>)</b>
0.37	$0.37 \pm 0.04$
1.80	$1.78 \pm 0.01$

$$k_{\text{cat}} 98.7 \text{ M}^{-1} \text{ s}^{-1}$$





## APPENDIX III. Spectral scanning for the reaction of a naphthoquinone with cysteine

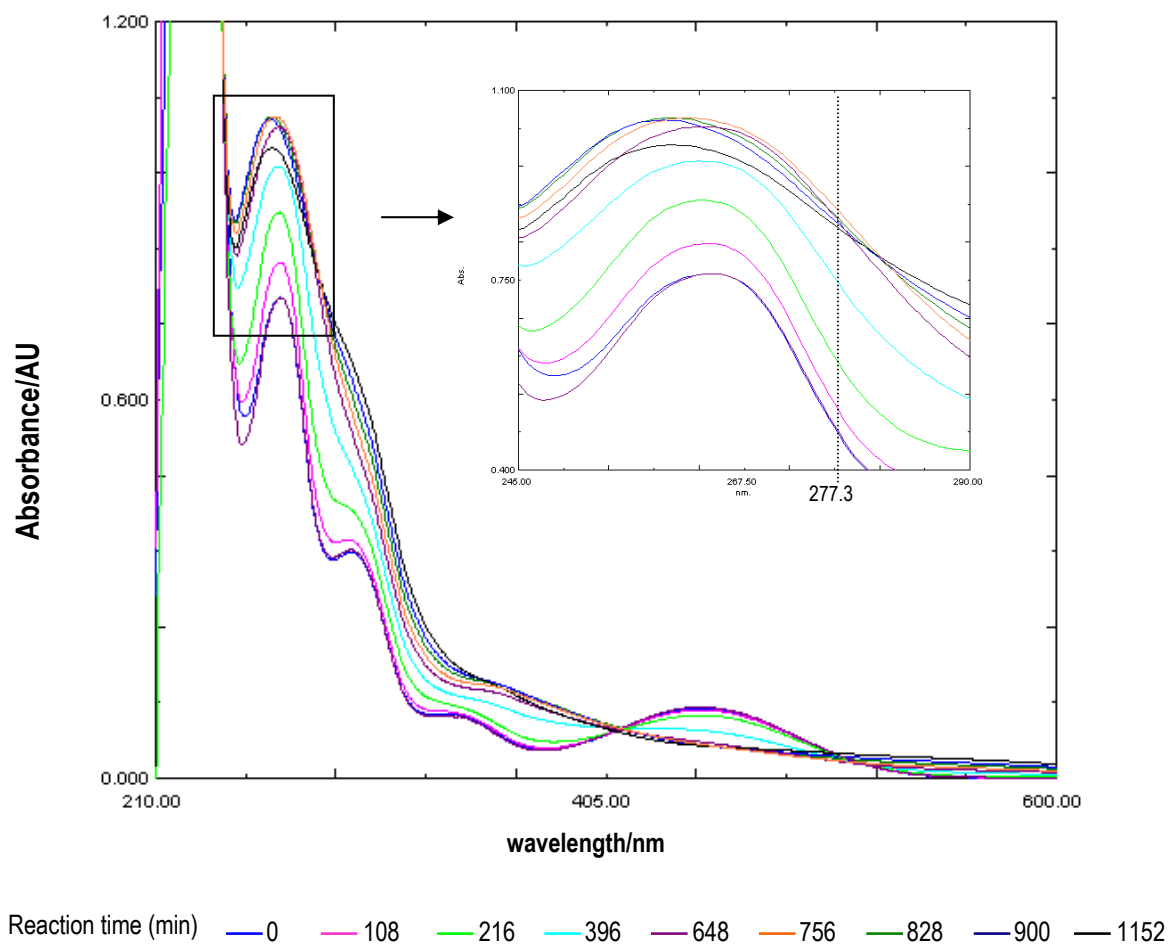


**Figure AIII.1** UV-visible spectra depicting the reaction, at 25 °C, of **3.1b** (50  $\mu\text{M}$ ) with cysteine *ca.* 5 mM in 50 mM  $\text{K}_2\text{HPO}_4/\text{KH}_2\text{PO}_4$  buffer, pH 7.14, containing KCl to maintain ionic strength at 0.5 M. Spectrum of **3.1b** in buffer lacking cysteine is in magenta and is overlapped with the first spectrum of the reaction. No isosbestic point could be detected. At 277.3 nm (wavelength used to monitor the kinetic reaction), the absorbance increased until a plateau region had been reached (*ca.* 756 min). Subsequently, there was a decrease in the absorption at this wavelength (reaction time  $\geq$  828 min).

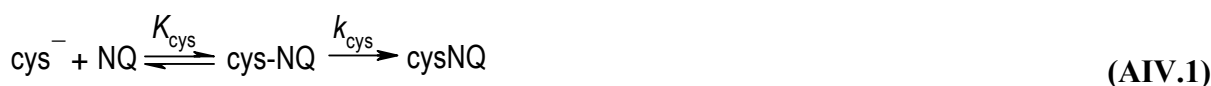


## APPENDIX IV. Kinetic equation for the reaction of 1,4-naphthoquinone with cysteine

In Section 3.2.2, the kinetic data for the reaction of naphthoquinone **3.8** with cysteine were computer-fitted to Equation 3.1.

$$k_{\text{obs}} = \frac{k_{\text{cys}} [\text{cys}]_t}{\left\{ \left( \frac{1}{K_{\text{cys}}} \right) \left( K_a + [\text{H}^+] \right) / K_a \right\} + [\text{cys}]_t} \quad (3.1)$$

As mentioned, in deriving this kinetic expression, it was assumed that reaction of **3.8**, *NQ*, with cysteine thiolate, *cys*<sup>-</sup>, involves initial and reversible formation of an adduct, *cys-NQ*, which decomposes into the final product, *cysNQ*. This situation can be described by the following equation,



Equation 3.1 was solved in the following manner. From Equation AIV.1,

$$K_{\text{cys}} = \frac{[\text{cys-NQ}]}{[\text{cys}^-][\text{NQ}]} \quad (\text{AIV.2})$$

and considering that the total naphthoquinone concentration,  $[\text{NQ}]_t$ , and that of the unreacted naphthoquinone,  $[\text{NQ}]$ , are related by

$$[\text{NQ}] = [\text{NQ}]_t - [\text{cys-NQ}] \quad (\text{AIV.3})$$

then,  $[\text{NQ}]$  from Equation AIV.2 may be substituted to give

$$[\text{cys-NQ}] = \frac{K_{\text{cys}} [\text{cys}^-][\text{NQ}]_t}{1 + K_{\text{cys}} [\text{cys}^-]} \quad (\text{AIV.4})$$

On the other hand, the rate,  $v$ , of formation of the product,  $cysNQ$ , is given by

$$v = k_{cys}[cys-NQ] \quad (\text{AIV.5})$$

where  $k_{cys}$  is a first-order rate constant. Thus,  $[cys-NQ]$  from Equation AIV.4 may be substituted to give

$$v = \frac{k_{cys} K_{cys} [cys^-][NQ]_t}{1 + K_{cys} [cys^-]} \quad (\text{AIV.6})$$

Taking into account that

$$v = k_{obs}[NQ]_t \quad (\text{AIV.7})$$

then, substitution of  $v$  from Equation AIV.6 gives Equation AIV.8, after division of the nominator and denominator by  $K_{cys}$

$$k_{obs} = \frac{k_{cys} [cys^-]}{1/K_{cys} + [cys^-]} \quad (\text{AIV.8})$$

Considering that



From Equation AIV.9,

$$K_a = \frac{[cys^-][H^+]}{[cys]} \quad (\text{AIV.10})$$

and considering that the total cysteine concentration,  $[\text{cys}]_t$ , and that of the undissociated cysteine,  $[\text{cys}]$ , are related by

$$[\text{cys}] = [\text{cys}]_t - [\text{cys}^-] \quad (\text{AIV.11})$$

Then,  $[\text{cys}]$  from Equation AIV.10 may be substituted to give

$$[\text{cys}^-] = \frac{K_a [\text{cys}]_t}{K_a + [\text{H}^+]} \quad (\text{AIV.12})$$

Substitution of  $[\text{cys}^-]$  from Equation AIV.8 gives Equation 3.1, after division of the nominator and denominator by  $K_a K_{\text{cys}}$

$$k_{\text{obs}} = \frac{k_{\text{cys}} [\text{cys}]_t}{\frac{K_a + [\text{H}^+]}{K_{\text{cys}} K_a} + [\text{cys}]_t} \quad (\text{3.1})$$

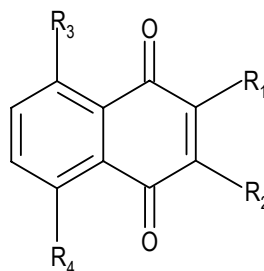
with

$$\frac{K_a + [\text{H}^+]}{K_a} = \frac{1}{\alpha} \quad (\text{AIV.13})$$



## APPENDIX V. Data for the graphical representation in Figure 3.11

Table AV.1 LUMO energies and Hammett  $\sigma_p$  constants for naphthoquinones.



Compound	R <sup>1</sup>	R <sup>2</sup>	R <sup>3</sup>	R <sup>4</sup>	E <sub>LUMO</sub> /Hartree	$\sigma_p^a$
3.1b	GlyOEt	H	H	H	-0.1097	-0.68
3.1c	NHMe	H	H	H	-0.1070	-0.84
3.5	OEt	H	H	H	-0.1114	-0.24
3.6	Br	H	H	H	-0.1320	0.22
3.8	H	H	H	H	-0.1245	0
3.9	Cl	Cl	H	H	-0.1370	0.46
3.11	Me	H	H	H	-0.1193	-0.17

<sup>a</sup> The  $\sigma_p$  values were obtained from Perrin *et al.*<sup>178</sup>





## APPENDIX VI. Pseudo first-order rate constants for papain- and cathepsin B-catalysed decomposition of quinones

Table AVI.1 Pseudo first-order rate constants,  $k_{\text{obs}}$ , for inactivation of the papain by quinones 3.1b-d, 3.2a-c, 3.3a,b, 3.5, 3.6, 3.9, 3.11, 3.13, 3.20, 3.21 and 3.22, at pH 7.0 at 25 °C.

### 3.1b

[3.1b] ( $\mu\text{M}$ )	$k_{\text{obs}}$ ( $10^{-4} \text{ s}^{-1}$ )
2.90	$0.52 \pm 0.01$
5.80	$1.13 \pm 0.10$
15.0	$2.41 \pm 0.48$
29.0	$2.73 \pm 0.45$
58.0	$2.63 \pm 0.13$

### 3.1c

[3.1c] (mM)	$k_{\text{obs}}$ ( $10^{-4} \text{ s}^{-1}$ )
0.15	1.00
0.30	$2.04 \pm 0.20$
0.45	$3.32 \pm 0.02$
0.62	$4.63 \pm 0.52$

### 3.1d

[3.1d] ( $\mu\text{M}$ )	$k_{\text{obs}}$ ( $10^{-4} \text{ s}^{-1}$ )
26.0	0.30
40.0	$0.43 \pm 0.05$
52.0	0.55
75.0	0.80
104.0	0.98
156.0	1.22

### 3.2a

[3.2a] ( $\mu\text{M}$ )	$k_{\text{obs}}$ ( $10^{-5} \text{ s}^{-1}$ )
9.30	1.83
23.3	$6.06 \pm 1.34$
34.9	$6.92 \pm 1.30$
46.5	$8.83 \pm 0.47$

### 3.2b

[3.2b] ( $\mu\text{M}$ )	$k_{\text{obs}}$ ( $10^{-3} \text{ s}^{-1}$ )
26.0	$0.29 \pm 0.03$
53.0	$0.52 \pm 0.04$
160.0	$0.82 \pm 0.02$
340.0	$1.06 \pm 0.02$
530.0	$1.14 \pm 0.03$

### 3.2c

[3.2c] ( $\mu\text{M}$ )	$k_{\text{obs}}$ ( $10^{-4} \text{ s}^{-1}$ )
60.0	$0.69 \pm 0.08$
120.0	$1.19 \pm 0.22$
180.0	$2.02 \pm 0.45$
270.0	$2.76 \pm 0.18$

### 3.3a

[3.3a] ( $\mu\text{M}$ )	$k_{\text{obs}}$ ( $10^{-5} \text{ s}^{-1}$ )
61.0	$4.09 \pm 0.58$

### 3.3b

[3.3b] ( $\mu\text{M}$ )	$k_{\text{obs}}$ ( $10^{-4} \text{ s}^{-1}$ )
50	$2.00 \pm 0.24$
150	4.97
300	$7.93 \pm 1.17$
400	8.83
500	$8.81 \pm 0.84$

**3.5**

[3.5] ( $\mu\text{M}$ )	$k_{\text{obs}}$ ( $10^{-3} \text{ s}^{-1}$ )
23.3	0.16
58.2	$0.37 \pm 0.02$
117.0	$0.80 \pm 0.05$
300.0	$0.98 \pm 0.02$
450	$1.03 \pm 0.07$

**3.9**

[3.9] ( $\mu\text{M}$ )	$k_{\text{obs}}$ ( $10^{-3} \text{ s}^{-1}$ )
75.0	$0.28 \pm 0.03$
150.0	0.86
175.0	$1.15 \pm 0.09$
200.0	1.18

**3.13**

[3.13] ( $\mu\text{M}$ )	$k_{\text{obs}}$ ( $10^{-3} \text{ s}^{-1}$ )
75.0	$0.69 \pm 0.10$
100.0	$0.63 \pm 0.08$
125.0	$1.02 \pm 0.08$
150.0	$1.12 \pm 0.11$
200.0	$1.98 \pm 0.40$

**3.21**

[3.21] ( $\mu\text{M}$ )	$k_{\text{obs}}$ ( $10^{-3} \text{ s}^{-1}$ )
24.0	$0.50 \pm 0.04$
48.0	0.91
72.0	1.04
96.0	$1.08 \pm 0.04$

**3.6**

[3.6] ( $\mu\text{M}$ )	$k_{\text{obs}}$ ( $10^{-3} \text{ s}^{-1}$ )
25.0	$0.71 \pm 0.13$
33.0	$0.66 \pm 0.04$
50.0	$0.85 \pm 0.07$
75.0	$1.26 \pm 0.11$
100.0	$1.30 \pm 0.12$
125.0	$1.44 \pm 0.18$

**3.11**

[3.11] ( $\mu\text{M}$ )	$k_{\text{obs}}$ ( $10^{-3} \text{ s}^{-1}$ )
100.0	$0.63 \pm 0.08$
150.0	$0.92 \pm 0.17$
200.0	$1.06 \pm 0.01$
250.0	$1.17 \pm 0.11$
300.0	$1.58 \pm 0.08$

**3.20**

[3.20] ( $\mu\text{M}$ )	$k_{\text{obs}}$ ( $10^{-3} \text{ s}^{-1}$ )
30.1	$0.59 \pm 0.02$
60.2	$0.87 \pm 0.13$
75.0	0.92
90.0	1.44
120.0	1.81

**3.22**

[3.22] (mM)	$k_{\text{obs}}$ ( $10^{-3} \text{ s}^{-1}$ )
0.52	$0.21 \pm 0.01$
0.98	$0.43 \pm 0.33$

Table AVI.2 Pseudo first-order rate constants,  $k_{\text{obs}}$ , for inactivation of bovine spleen cathepsin B by quinones 3.1b, 3.2b, 3.5 and 3.6 at pH 5.0 at 25 °C.

**3.1b**

[3.1b] ( $\mu\text{M}$ )	$k_{\text{obs}}$ ( $10^{-4} \text{ s}^{-1}$ )
5.80	0.35
15.0	$0.49 \pm 0.08$
29.0	0.83
58.0	0.90
116.0	$1.05 \pm 0.05$
290.0	$1.02 \pm 0.09$

**3.2b**

[3.2b] ( $\mu\text{M}$ )	$k_{\text{obs}}$ ( $10^{-4} \text{ s}^{-1}$ )
26.5	0.75
53.0	$1.18 \pm 0.15$
106.0	1.70
160.0	$1.74 \pm 0.20$

**3.5**

[3.5] (mM)	$k_{\text{obs}}$ ( $10^{-4} \text{ s}^{-1}$ )
0.06	0.45
0.30	$1.09 \pm 0.13$
0.45	1.62
0.80	$2.05 \pm 0.16$
1.20	$2.63 \pm 0.19$

**3.6**

[3.6] ( $\mu\text{M}$ )	$k_{\text{obs}}$ ( $10^{-4} \text{ s}^{-1}$ )
25.0	0.58
50.0	$2.98 \pm 1.10$
75.0	$4.34 \pm 0.62$
125.0	$6.68 \pm 0.12$



---

**BIBLIOGRAPHY**

1. Otto, H.-H.; Schirmeister, T. Cysteine proteases and their inhibitors. *Chem. Rev.* **1997**, *97*, 133-171.
2. Leung-Toung, R.; Zhao, Y.; Li, W.; Tam, T. F.; Karimian, K.; Spino, M. Thiol proteases: inhibitors and potential therapeutic targets. *Curr. Med. Chem.* **2006**, *13*, 547-581.
3. Lecaille, F.; Kaleta, J.; Brömme, D. Human and Parasitic papain-like cysteine proteases: their role in physiology and pathology and recent developments in inhibitor design. *Chem. Rev.* **2002**, *102*, 4459-4488.
4. Leung, D.; Abbenante, G.; Fairlie, D. P. Protease inhibitors: current status and future prospects. *J. Med. Chem.* **2000**, *43*, 305-341.
5. Vicik, R.; Busemann, M.; Baumann, K.; Schirmeister, T. Inhibitors of cysteine proteases. *Curr. Top. Med. Chem.* **2006**, *6*, 331-353.
6. Steverding, D.; Caffrey, C. R.; Sajid, M. Cysteine proteinase inhibitors as therapy for parasitic diseases: advances in inhibitor design. *Mini-Rev. Med. Chem.* **2006**, *6*, 1025-1032.
7. Powers, J. C.; Asgian, J. L.; Özlem, D. E.; James, K. E. Irreversible inhibitors of serine, cysteine, and threonine proteases. *Chem. Rev.* **2002**, *102*, 4639-4750.
8. Veber, D. F.; Thompson, S. K. The therapeutic potential of advances in cysteine protease inhibitor design. *Curr. Opin. in Drug Discovery & Development* **2000**, *3*, 362-369.
9. Rawlings, N. D.; Morton, F. R.; Barrett, A. J. MEROPS: the peptidase database. *Nucleic Acids Res.* **2006**, *34*, D270-D272.
10. GB Esp@cenet. <http://gb.espacenet.com>.
11. Frlan, R.; Gobec, S. Inhibitors of cathepsin B. *Curr. Med. Chem.* **2006**, *13*, 2309-2327.
12. Liñares, G. E. G.; Rodriguez, J. B. Current status and progresses made in malaria chemotherapy. *Curr. Med. Chem.* **2007**, *14*, 289-314.
13. Wang, S. X.; Pandey, K. C.; Somoza, J. R.; Sijwali, P. S.; Kortemme, T.; Brinen, L. S.; Fletterick, R. J.; Rosenthal, P. J.; McKerrow, J. H. Structural basis for unique mechanisms of folding and hemoglobin binding by a malarial protease. *Proc. Natl. Acad. Sci. U.S.A.* **2006**, *103*, 11503-11508.
14. Sijwali, P. S.; Kato, K.; Seydel, K. B.; Gut, J.; Lehman, J.; Klemba, M.; Goldberg, D. E.; Miller, L. H.; Rosenthal, P. J. *Plasmodium falciparum* cysteine protease falcipain-1 is not essential in erythrocytic stage malaria parasites. *Proc. Natl. Acad. Sci. U.S.A.* **2004**, *101*, 8721-8726.
15. Singh, N.; Sijwali, P. S.; Pandey, K. C.; Rosenthal, P. J. *Plasmodium falciparum*: biochemical characterization of the cysteine protease falcipain-2'. *Exp. Parasitol.* **2006**, *112*, 187-192.
16. Shenai, B. R.; Lee, B. J.; Alvarez-Hernandez, A.; Chong, P. Y.; Emal, C. D.; Neitz, R. J.; Roush, W. R.; Rosenthal, P. J. Structure-activity relationships for inhibition of cysteine protease activity and development of *Plasmodium falciparum* by peptidyl vinyl sulfones. *Antimicrob. Agents Chemother.* **2003**, *47*, 154-160.
17. World Health Organization. <http://www.who.int>.
18. SARS. [http://www.wpro.who.int/health\\_topics/sars](http://www.wpro.who.int/health_topics/sars).
19. Hogg, T.; Nagarajan, K.; Herzberg, S.; Chen, L.; Shen, X.; Jiang, H.; Wecke, M.; Blohmke, C.; Hilgenfed, R.; Schmidt, C. L. Structural and functional characterization of falcipain-2, a hemoglobinase from the malarial parasite *Plasmodium falciparum*. *J. Biol. Chem.* **2006**, *281*, 25425-25437.

20. RCSB Protein Data Bank. <http://www.rcsb.org>.
21. Gillmor, S. A.; Craik, C. S.; Fletterick, R. J. Structural determinants of specificity in the cysteine protease cruzain. *Protein Sci.* **1997**, *6*, 1603-1611.
22. Chibale, K.; Musonda, C. C. The synthesis of parasitic cysteine protease and trypanothione reductase inhibitors. *Curr. Med. Chem.* **2003**, *10*, 1863-1889.
23. Storer, A. C.; Ménard, R. Catalytic mechanism in papain family of cysteine peptidases. *Methods Enzymol.* **1994**, *244*, 486-500.
24. Brinen, L. S.; Hansell, E.; Cheng, J.; Roush, W. R.; McKerrow, J. H.; Fletterick, R. J. A target within the target: probing cruzain's P1' site to define structural determinants for the Chagas' disease protease. *Struct. Fold. Design* **2000**, *8*, 831-840.
25. Theodorou, L. G.; Bieth, J. G.; Papamichael, E. M. The catalytic mode of cysteine proteinases of papain (C1) family. *Bioresour. Technol.* **2007**, *98*, 1931-1939.
26. DeLano, W. L. *The PyMOL Molecular Graphics System*, DeLano Scientific: San Carlos, CA, USA, 2002. <http://www.pymol.org>.
27. McKerrow, J. H.; Engel, J. C.; Caffrey, C. R. Cysteine protease inhibitors as chemotherapy for parasitic infections. *Bioorg. Med. Chem.* **1999**, *7*, 639-644.
28. Hanzlik, R. P.; Thompson, S. A. Vinylogous amino acid esters: a new class of inactivators for thiol proteases. *J. Med. Chem.* **1984**, *27*, 711-712.
29. Thompson, S. A.; Andrews, P. R.; Hanzlik, R. P. Carboxyl-modified amino acids and peptides as protease inhibitors. *J. Med. Chem.* **1986**, *29*, 104-111.
30. Liu, S.; Hanzlik, R. P. Structure-activity relationships for inhibition of papain by peptide Michael acceptors. *J. Med. Chem.* **1992**, *35*, 1067-1075.
31. Palmer, J. T.; Rasnick, D.; Klaus, J. L.; Brömme, D. Vinyl sulfones as mechanism-based cysteine proteases inhibitors. *J. Med. Chem.* **1995**, *38*, 3193-3196.
32. Babine, R. E.; Bender, S. L. Molecular recognition of protein-ligand complexes: applications to drug design. *Chem. Rev.* **1997**, *97*, 1359-1472.
33. Roush, W. R.; Gwaltney II, S. L.; Cheng, J.; Scheidt, K. A.; McKerrow, J. H.; Hansell, E. Vinyl sulfonate esters and vinyl sulfonamides: potent, irreversible inhibitors of cysteine proteases. *J. Am. Chem. Soc.* **1998**, *120*, 10994-10995.
34. Roush, W. R.; Cheng, J.; Knapp-Reed, B.; Alvarez-Hernandez, A.; McKerrow, J. H.; Hansell, E.; Engel, J. C. Potent second generation vinyl sulfonamide inhibitors of the trypanosomal cysteine protease cruzain. *Bioorg. Med. Chem. Lett.* **2001**, *11*, 2759-2762.
35. Rosenthal, P. J.; Olson, J. E.; Lee, G. K.; Palmer, J. T.; Klaus, J. L.; Rasnick, D. Antimalarial effects of vinyl sulfone cysteine proteinase inhibitors. *Antimicrob. Agents Chemother.* **1996**, *40*, 1600-1603.
36. Olson, J. E.; Lee, G. K.; Semenov, A.; Rosenthal, P. J. Antimalarial effects in mice of orally administered peptidyl cysteine protease inhibitors. *Bioorg. Med. Chem.* **1999**, *7*, 633-638.
37. Engel, J. C.; Doyle, P. S.; Hsieh, I.; McKerrow, J. H. Cysteine protease inhibitors cure an experimental *Trypanosoma cruzi* infection. *J. Exp. Med.* **1998**, *188*, 725-734.
38. Carretero, J. C.; Demillequand, M.; Ghosez, L. Synthesis of  $\alpha,\beta$ -unsaturated sulphonates via the Wittig-Horner reaction. *Tetrahedron* **1987**, *43*, 5125-5134.

39. Götz, M. G.; Caffrey, C. R.; Hansell, E.; McKerrow, J. H.; Powers, J. C. Peptidyl allyl sulfones: a new class of inhibitors for clan CA cysteine proteases. *Bioorg. Med. Chem.* **2004**, *12*, 5203-5211
40. da Silva, M. N.; Ferreira, V. F.; de Souza, M. C. B. V. Um panorama atual da química e da farmacologia de naftoquinonas, com ênfase na  $\beta$ -lapachona e derivados. *Quim. Nova* **2003**, *26*, 407-416.
41. Brunmark, A.; Cadenas, E. Redox and addition chemistry of quinoid compounds and its biological implications. *Free Radical Biol. Med.* **1989**, *7*, 435-477.
42. O'Brien, P. J. Molecular mechanisms of quinone cytotoxicity. *Chem. Biol. Interact.* **1991**, *80*, 1-41.
43. Munday, R.; Smith, B. L.; Munday, C. M. Effect of inducers of DT-diaphorase on the haemolytic activity and nephrotoxicity of 2-amino-1,4-naphthoquinone in rats. *Chem. Biol. Interact.* **2005**, *155*, 140-147.
44. dos Santos, E. V. M.; Carneiro, J. W. M.; Ferreira, V. F. Quantitative structure-activity relationship in aziridiny-1,4-naphthoquinone antimalarials: study of theoretical correlations by the PM3 method. *Bioorg. Med. Chem.* **2004**, *12*, 87-93.
45. Baggish, A. L.; Hill, D. R. Antiparasitic agent atovaquone. *Antimicrob. Agents Chemother.* **2002**, *46*, 1163-1173.
46. Rozeboom, M. D.; Tegmo-Larsson, I.-M.; Houck, K. N. Frontier molecular orbital theory of substituent effects on regioselectivities of nucleophilic additions and cycloadditions to benzoquinones and naphthoquinones. *J. Org. Chem.* **1981**, *46*, 2338-2345.
47. Öllinger, K.; Brunmark, A. Effect of hydroxyl substituent position on 1,4-naphthoquinone toxicity to rat hepatocytes. *J. Biol. Chem.* **1991**, *266*, 21496-21503.
48. Ham, S. W.; Choe, J.-I.; Wang, M. F.; Peyregne, V.; Carr, B. I. Fluorinated quinoid inhibitor: possible 'pure' arylator predicted by the simple theoretical calculation. *Bioorg. Med. Chem.* **2004**, *14*, 4103-4105.
49. Nishikawa, Y.; Carr, B. I.; Wang, M.; Kar, S.; Finn, F.; Dowd, P.; Zheng, Z. B.; Kerns, J.; Naganathan, S. Growth inhibition of hepatoma cells induced by vitamin K and its analogs. *J. Biol. Chem.* **1995**, *270*, 28304-28310.
50. Ni, R.; Nishikawa, Y.; Carr, B. I. Cell growth inhibition by a novel vitamin K is associated with induction of protein tyrosine phosphorylation. *J. Biol. Chem.* **1998**, *273*, 9906-9911.
51. Wissner, A.; Floyd, M. B.; Johnson, B. D.; Frase, H.; Ingalls, C.; Nittoli, T.; Dushin, R. G.; Discafani, C.; Nilakantan, R.; Marini, J.; Ravi, M.; Cheung, K.; Tan, X.; Musto, S.; Annable, T.; Siegel, M. M.; Loganzo, F. 2-(Quinazolin-4-ylamino)-[1,4]benzoquinones as covalent-binding, irreversible inhibitors of the kinase domain of vascular endothelial growth factor receptor-2. *J. Med. Chem.* **2005**, *48*, 7560-7581.
52. Brun, M.-P.; Braud, E.; Angotti, D.; Mondésert, O.; Quaranta, M.; Montes, M.; Miteva, M.; Gresh, N.; Ducommun, B.; Garbay, C. Design, synthesis, and biological evaluation of novel naphthoquinone derivatives with CDC25 phosphatase inhibitory activity. *Bioorg. Med. Chem.* **2005**, *13*, 4871-4879.
53. Ertl, P.; Cooper, D.; Allen, G.; Slater, M. J. 2-Chloro-3-substituted-1,4-naphthoquinone inactivators of human cytomegalovirus protease. *Bioorg. Med. Chem. Lett.* **1999**, *9*, 2863-2866.
54. Hudson, A. T. Atovaquone - a novel broad-spectrum anti-infective drug. *Parasitol. Today* **1993**, *9*, 66-68.

55. Munday, R.; Smith, B. L.; Munday, C. M. Comparative toxicity of 2-hydroxy-3-alkyl-1,4-naphthoquinones in rats. *Chem. Biol. Interact.* **1995**, *98*, 185-192.
56. Schmidt, T. J. Helenanolide-type sesquiterpene lactones—III. Rates and stereochemistry in the reaction of helenalin and related helenanolides with sulfhydryl containing biomolecules. *Bioorg. Med. Chem.* **1997**, *5*, 645-653.
57. Steurer, S.; Podlech, J. Synthesis of highly functionalized amino acid and hydroxy acid derivatives from  $\gamma$ -aminoalkyl-substituted  $\alpha$ -methylene- $\gamma$ -butyrolactones. *Eur. J. Org. Chem.* **2002**, 899-916.
58. Rigoreau, L. J. M. Ph.D. thesis, The Department of Chemical and Biological Sciences, The University of Huddersfield, United Kingdom, 1999.
59. Hinchliffe, P. S. Ph.D. thesis, The Department of Chemical and Biological Sciences, The University of Huddersfield, United Kingdom, 2001.
60. Inagaki, M.; Tsuru, T.; Jyoyama, H.; Ono, T.; Yamada, K.; Kobayashi, M.; Hori, Y.; Arimura, A.; Yasui, K.; Ohno, K.; Kakudo, S.; Koizumi, K.; Suzuki, R.; Kato, M.; Kawai, S.; Matsumoto, S. Novel antiarthritic agents with 1,2-isothiazolidine-1,1-dioxide ( $\gamma$ -sultam) skeleton: cytokine suppressive dual inhibitors of cyclooxygenase-2 and 5-lipoxygenase. *J. Med. Chem.* **2000**, *43*, 2040-2048.
61. Merten, S.; Fröhlich, R.; Kataeva, O.; Metz, P. Synthesis of sultams by intramolecular Heck reaction. *Adv. Synth. Catal.* **2005**, *347*, 754-758.
62. Bliss, A. D.; Cline, W. K.; Sweeting, O. J. Synthesis of 1-butene-2,4-sultam. *J. Org. Chem.* **1964**, *29*, 2412-2416.
63. Inagaki, M.; Haga, N.; Kobayashi, M.; Ohta, N.; Kamata, S.; Tsuru, T. Highly *E*-selective and effective synthesis of antiarthritic drug candidate S-2474 using quinone methide derivatives. *J. Org. Chem.* **2002**, *67*, 125-128.
64. Kaiser, E. M.; Knutson, P. L. A. Preparation and reactions of  $\alpha$ -lithiobutanesultams. *J. Org. Chem.* **1975**, *40*, 1342-1346.
65. Champseix, A.; Chanet, J.; Étienne, A.; Le Berre, A.; Masson, J. C.; Napierala, C.; Vessière, R. Synthèses de  $\beta$ -sultames (thiazétidines-1,2 dioxyde-1,1). *Bull. Soc. Chim. Fr.* **1985**, 463-472.
66. Le Berre, A.; Petit, J. Sur la dioxo-1,1 thiazétidine-1,2 (éthanesultame). *Tetrahedron Lett.* **1972**, *13*, 213-216.
67. Baxter, N. J.; Rigoreau, L. J. M.; Laws, A. P.; Page, M. I. Reactivity and mechanism in the hydrolysis of  $\beta$ -sultams. *J. Am. Chem. Soc.* **2000**, *122*, 3375-3385.
68. Baganz, H.; Dransch, G. Reaktionen mit L-cystinderivaten, II. Oxydierend-chlorierende spaltung und darstellung von sultam-onen. *Chem. Ber.* **1960**, *93*, 784-791.
69. Meyle, E.; Otto, H-H. Eine einfache methode zur synthese substituierter 1,2-thiazetidin-1,1-dioxide. *Arch. Pharm. (Weinheim)* **1983**, *316*, 281-283.
70. Marvel, C. S.; Bailey, C. F.; Sparberg, M. S. A synthesis of taurine. *J. Am. Chem. Soc.* **1927**, *49*, 1833-1837.
71. Schick, J. W.; Degering, E. F. Synthesis of taurine and *N*-methyltaurine. *Ind. Eng. Chem.* **1947**, *39*, 906-909.
72. Le Berre, A.; Étienne, A.; Dumaitre, B. Sulfoéthylation. I. – Taurines et taurobétaines à partir d'amines primaires et secondaires. *Bull. Soc. Chim. Fr.* **1970**, 946-953.



73. Whitmore, W. F.; Landau, E. F. Preparation of ethylenesulfonic acid – salts and esters. *J. Am. Chem. Soc.* **1946**, *68*, 1797-1798.
74. Rumpf, P. Préparation d'acides aminoalcoylsulfoniques en vue d'une étude physicochimique comparative. *Bull. Soc. Chim. Paris, Mém.* **1938**, 877-888.
75. Ward Jr., K. The chlorinated ethylamines – a new type of vesicant. *J. Am. Chem. Soc.* **1935**, *57*, 914-916.
76. Cortese, F. On the synthesis of taurine. *J. Am. Chem. Soc.* **1936**, *58*, 191-192.
77. Goldberg, A. A. Taurine. *J. Chem. Soc.* **1943**, 4-5.
78. Le Berre, A.; Étienne, A.; Dumaitre, B. Sulfoéthylation. II. – Sulfoéthylbétaines à partir d'amines tertiaires. *Bull. Soc. Chim. Fr.* **1970**, 954-958.
79. Krutak, J. J.; Burpitt, R. D.; Moore, W. H.; Hyatt, J. A. Chemistry of ethenesulfonyl fluoride. Fluorosulfonylethylation of organic compounds. *J. Org. Chem.* **1979**, *44*, 3847-3858.
80. Thompson, M. E.  $\alpha$ ,*N*-Alkanesulfonamide dianions: formation and chemoselective C-alkylation. *J. Org. Chem.* **1984**, *49*, 1700-1703.
81. Dirscherl, W.; Weingarten, F. W.; Otto, K. Synthese von 1,4-butansultam. *Justus Liebigs Ann. Chem.* **1954**, *588*, 200-204.
82. Dirscherl, W.; Otto, K. Zur kenntnis des 1,4-butansultams und einiger aliphatischer aminosulfohalogenide. *Chem. Ber.* **1956**, *89*, 393-395.
83. Farbenfabriken Bayer Akt.-Ges. G.B. 810,356, 1959.
84. Shionogi & Co. US 6,525,081, 2003.
85. Erman, W. F.; Kretschmar, H. C. Syntheses and facile cleavage of five-membered ring sultams. *J. Org. Chem.* **1961**, *26*, 4841-4850.
86. Helberger, J. H.; Manecke, G.; Fischer, H. M. Zur kenntnis organischer sulfonsäuren. II. Die sulfochlorierung des 1-chlorbutans und anderer halogenalkyle; Synthese von sultonen und eines sultams. *Justus Liebigs Ann. Chem.* **1949**, *562*, 23-35.
87. Helferich, B.; Kleb, K. G. *N*-Aryl-Sultame. *Justus Liebigs Ann. Chem.* **1960**, *635*, 91-96.
88. *The chemistry of sulphonic acids, esters and their derivatives*; Patai, S.; Rappoport, Z., The Chemistry of Functional Groups Series; John Wiley & Sons: Chichester, 1991; Vol. XVI, pp 253, 854 and 857.
89. Helferich, B.; Geist, K.; Plümpe, H. Über sultame, V. *Justus Liebigs Ann. Chem.* **1962**, *651*, 17-29.
90. Merck & CO Inc. PCT Int. Appl. WO03/016294, 2003.
91. Hinchliffe, P. S.; Wood, J. M.; Davis, A. M.; Austin, R. P.; Beckett, R. P.; Page, M. I. Structure-reactivity relationships in the inactivation of elastase by  $\beta$ -sultams. *Org. Biomol. Chem.* **2003**, *1*, 67-80.
92. Mielniczak, G.; Łopusiński, A. Synthesis of 2-phosphoro-1,2-thiazetidino-1,1-dioxide. *Heteroat. Chem.* **1999**, *10*, 61-67.
93. Goldberg, A. A. Synthesis of derivatives of taurinimide. *J. Chem. Soc.* **1945**, 464-467.
94. Smith, M. B.; March, J. *March's advanced organic chemistry: reactions, mechanisms, and structure*; John Wiley & Sons: New York, 2001; pp 474, 575 and 1308.
95. Calheiros e Menezes, T. M. B. M. Ph.D. thesis, Faculdade de Ciências da Universidade de Lisboa, Portugal, 1997.
96. Moreira, R. F. A. Ph.D. thesis, Faculty of Pharmacy, University of Lisbon, Portugal, 1991.

97. Cooper, G. F. Synthesis of substituted 1,3-propanesultams from *N*-substituted 2-amino alcohols. *Synthesis (Stuttgart)* **1991**, *10*, 859-860.
98. Helberger, J. H.; Manecke, G.; Heyden, R. Zur kenntnis organischer sulfonsäuren III. Mitteilung: die alkylierungsreaktionen der sultone. *Justus Liebigs Ann. Chem.* **1949**, *565*, 22-35.
99. Fehrentz, J. A.; Castro, B. An efficient synthesis of optically active  $\alpha$ -(*t*-butoxycarbonylamino)-aldehydes from  $\alpha$ -amino acids. *Synthesis (Stuttgart)* **1983**, *8*, 676-678.
100. Valente, E. Master thesis, Faculty of Pharmacy, University of Lisbon, Portugal, 1999.
101. Portela, M. J.; Moreira, R. F. A.; Valente, E.; Constantino, L.; Iley, J.; Pinto, J.; Rosa, R.; Cravo, P.; do Rosário, V. E. Dipeptide derivatives of primaquine as transmission-blocking antimalarials: effect of aliphatic side-chain acylation on the gametocytocidal activity and on the formation of carboxyprimaquine in rat liver homogenates. *Pharm. Res.* **1999**, *16*, 949-955.
102. Friebolin, H. *Basic one- and two-dimensional NMR spectroscopy*; Wiley-VCH: Weinheim, 1998; pp 76 and 77.
103. Kalinowski, H-O.; Berger, S.; Braun, S. *Carbon-13 NMR spectroscopy*; John Wiley & Sons: Chichester, 1984; pp 586-593.
104. Reddick, J. J.; Cheng, J.; Roush, W. R. Relative rates of Michael reactions of 2'-(phenethyl)thiol with vinyl sulfones, vinyl sulfonate esters, and vinyl sulfonamides relevant to vinyl sulfonyl cysteine protease inhibitors. *Org. Lett.* **2003**, *5*, 1967-1970.
105. Motoyoshiya, J.; Kusaura, T.; Kokin, K.; Yokoya, Sei-ichi; Takaguchi, Y.; Narita, S.; Aoyama, H. The Horner-Wadsworth-Emmons reaction of mixed phosphonoacetates and aromatic aldehydes: geometrical selectivity and computational investigation. *Tetrahedron* **2001**, *57*, 1715-1721.
106. Gomes, P.; Araújo, M. J.; Rodrigues, M.; Vale, N.; Azevedo, Z.; Iley, J.; Chambel, P.; Morais, J.; Moreira, R. Synthesis of imidazolidin-4-one and 1*H*-imidazo[2,1- $\alpha$ ]isoindole-2,5(3*H*,9*bH*)-dione derivatives of primaquine: scope and limitations. *Tetrahedron* **2004**, *60*, 5551-5562.
107. Silverstein, R. M.; Webster, F. X. *Spectrometric identification of organic compounds*; John Wiley & Sons, Inc.: New York, 1998; pp 169, 212 and 213.
108. Furniss, B. S.; Hannaford, A. J.; Smith, P. W. G.; Tatchell, A. R. *Vogel's textbook of practical organic chemistry*; Longman Scientific & Technical: Harlow, 1989; pp 401, 584 and 1284.
109. Patani, G.A.; LaVoie, E. J. Bioisosterism: a rational approach in drug design. *Chem. Rev.* **1996**, *96*, 3147-3176.
110. Scheidt, K. A.; Roush, W. R.; McKerrow, J. H.; Selzer, P. M.; Hansell, E.; Rosenthal, P. J. Structure-based design, synthesis and evaluation of conformationally constrained cysteine protease inhibitors. *Bioorg. Med. Chem.* **1998**, *6*, 2477-2494.
111. Sajid, M.; McKerrow, J. H. Cysteine proteases of parasitic organisms. *Mol. Biochem. Parasitol.* **2002**, *120*, 1-21.
112. Desai, P. V.; Patny, A.; Sabnis, Y.; Tekwani, B.; Gut, J.; Rosenthal, P.; Srivastava, A.; Avery, M. Identification of novel parasitic cysteine protease inhibitors using virtual screening. 1. The ChemBridge database. *J. Med. Chem.* **2004**, *47*, 6609-6615.
113. Pickersgill, R. W.; Harris, G. W.; Garman, E. Structure of monoclinic papain at 1.60 Å resolution. *Acta Crystallogr., Sect. B* **1992**, *48*, 59-67.

114. Tandon, V. K.; Yadav, D. B.; Maurya, H. K.; Chatuverdi, A. K.; Shukla, P. K. Design, synthesis, and biological evaluation of 1,2,3-trisubstituted-1,4-dihydrobenzo[g]quinoxaline-5,10-diones and related compounds as antifungal and antibacterial agents. *Bioorg. Med. Chem.* **2006**, *14*, 6120-6126.
115. Prescott, B. Derivatives of 2-chloro-1,4-naphthoquinone. *J. Med. Chem.* **1969**, *12*, 181-182.
116. Rahimpour, S.; Weiner, L.; Fridkin, M.; Shrestha-Dawadi, P. B.; Bittner, S. Novel naphthoquinoyl derivatives: potential structural components for the synthesis of cytotoxic peptides. *Lett. Pept. Sci.* **1996**, *3*, 263-274.
117. Tandon, V. K.; Yadav, D. B.; Singh, R. V.; Chaturvedi, A. K.; Shukla, P. K. Synthesis and biological evaluation of novel (L)- $\alpha$ -amino acid methyl ester, heteroalkyl, and aryl substituted 1,4-naphthoquinone derivatives as antifungal and antibacterial agents. *Bioorg. Med. Chem. Lett.* **2005**, *15*, 5324-5328.
118. Shrestha-Dawadi, P. B.; Bittner, S.; Fridkin, M.; Rahimpour, S. On the synthesis of naphthoquinonyl heterocyclic amino acids. *Synthesis (Stuttgart)* **1996**, *12*, 1468-1472.
119. Lin, T.-S.; Zhu, L.-Y.; Xu, S.-P.; Divo, A. A.; Sartorelli, A. C. Synthesis and antimalarial activity of 2-aziridinyl- and 2,3-bis(aziridinyl)-1,4-naphthoquinoyl sulfonate and acylate derivatives. *J. Med. Chem.* **1991**, *34*, 1634-1639.
120. Nakazumi, H.; Kondo, K.; Kitao, T. Synthesis of 7,10-disubstituted benzo[b]phenazine-6,11-quinones. *Synthesis (Stuttgart)* **1982**, *10*, 878-879.
121. Couladouros, E. A.; Plyta, Z. F.; Papageorgiou, V. P. A general procedure for the efficient synthesis of (alkylamino)naphthoquinones. *J. Org. Chem.* **1996**, *61*, 3031-3033.
122. Kutyrev, A. A. Nucleophilic reactions of quinones. *Tetrahedron* **1991**, *47*, 8043-8065.
123. Choi, H. Y.; Chi, D. Y. Simple preparation of 7-alkylamino-2-methylquinoline-5,8-diones: regiochemistry in nucleophilic substitution reactions of the 6- or 7-bromo-2-methylquinoline-5,8-dione with amines. *Tetrahedron* **2004**, *60*, 4945-4951.
124. Dalglish, C. E. Naphthoquinone antimalarials. Mannich bases derived from lawsone. *J. Am. Chem. Soc.* **1949**, *71*, 1697-1702.
125. Leffler, M. T.; Hathaway, R. J. Naphthoquinone antimalarials. XIII. 2-Hydroxy-3-substituted-aminomethyl derivatives by the Mannich reaction. *J. Am. Chem. Soc.* **1948**, *70*, 3222-3223.
126. Prezhdo, V. V.; Ovsiankina, E. V.; Prezhdo, O. V. Conformational analysis of chloroalkyl derivatives of 1,4-naphthoquinone. *J. Mol. Struct.* **2000**, *522*, 71-77.
127. Prezhdo, V.; Prezhdo, O.; Ovsiankina, E. Synthesis of 2-chloroalkyl-1,4-naphthoquinones and their reactivity in the formation of autocomplexes. *Spectrochim. Acta, Part A* **1995**, *51*, 2465-2472.
128. Fieser, L. F.; Berliner, E.; Bondhus, F. J.; Chang, F. C.; Dauben, W. G.; Ettliger, M. G.; Fawaz, G.; Fields, M.; Heidelberger, C.; Heymann, H.; Vaughan, W. R.; Wilson, A. G.; Wilson, E.; Wu, M.-I.; Leffler, M. T.; Hamlin, K. E.; Matson, E. J.; Moore, E. E.; Moore, M. B.; Zaugg, H. E. Naphthoquinone antimalarials. IV-XI. Synthesis. *J. Am. Chem. Soc.* **1948**, *70*, 3174-3215.
129. Kawasaki Kasei Chemicals Ltd. US 5,225,578, 1993.
130. Kesteleyn, B.; De Kimpe, N. Synthesis of two naphthoquinone antibiotics, dehydroherbarin and 6-deoxybostrycoidin. *J. Org. Chem.* **2000**, *65*, 640-644.
131. Wilson, I.; Wardman, P.; Lin, T. S.; Sartorelli, A. C. Reactivity of thiols towards derivatives of 2- and 6-methyl-1,4-naphthoquinone bioreductive alkylating agents. *Chem. Biol. Interact.* **1987**, *61*, 229-240.

132. Hasinoff, B. B.; Wu, X.; Begleiter, A.; Guzic, L. J.; Guzic Jr, F.; Giorgianni, A.; Shaohua, Y.; Jiang, Y.; Yalowich, J. C. Structure-activity study of the interaction of bioreductive benzoquinone alkylating agents with DNA topoisomerase II. *Cancer Chemother. Pharmacol.* **2006**, *57*, 221-223.
133. Jameson, G. N. L.; Zhang, J.; Jameson, R. F.; Linert, W. Kinetic evidence that cysteine reacts with dopaminoquinone via reversible adduct formation to yield 5-cysteinyldopamine: an important precursor of neuromelanin. *Org. Biomol. Chem.* **2004**, *2*, 777-782.
134. Chan, A. W. E.; Golec, J. M. C. Prediction of relative potency of ketone protease inhibitors using molecular orbital theory. *Bioorg. Med. Chem.* **1996**, *4*, 1673-1677.
135. Rietjens, I. M. C. M.; Soffers, A. E. M. F.; Hooiveld, G. J. E. J.; Veeger, C.; Vervoort, J. Quantitative structure-activity relationships based on computer calculated parameters for the overall rate of glutathione S-transferase catalysed conjugation of a series of fluoronitrobenzenes. *Chem. Res. Toxicol.* **1995**, *8*, 481-488.
136. Aguilar-Martínez, M.; Macías-Ruvalcaba, N. A.; Bautista-Martínez, J. A.; Gómez, M.; González, F. J.; González, I. Hydrogen bond and protonation as modifying factors of the quinone reactivity. *Curr. Org. Chem.* **2004**, *8*, 1721-1738.
137. Kitz, R.; Wilson, I. B. Esters of methanesulfonic acid as irreversible inhibitors of acetylcholinesterase. *J. Biol. Chem.* **1962**, *237*, 3245-3249.
138. Rodriguez, C. E.; Fukuto, J. M.; Taguchi, K.; Froines, J.; Cho, A. K. The interactions of 9,10-phenanthrenequinone with glyceraldehyde-3-phosphate dehydrogenase (GAPDH), a potential site for toxic actions. *Chem. Biol. Interact.* **2005**, *155*, 97-110.
139. Fersht, A. *Structure and mechanism in protein science*; W. H. Freeman and Company: New York, 1998; pp 103-111 and 155-158.
140. Jewess, P. J.; Higgins, J.; Berry, K. J.; Moss, S. R.; Boogaard, A. B.; Khambay, B. P. S. Herbicidal action of 2-hydroxyl-3-alkyl-1,4-naphthoquinones. *Pest. Manag. Sci.* **2002**, *58*, 234-242.
141. Kapadia, G. J.; Azuine, M. A.; Balasubramanian, V.; Sridhar, R. Aminonaphthoquinones – a novel class of compounds with potent antimalarial activity against *Plasmodium falciparum*. *Pharm. Res.* **2001**, *43*, 363-367.
142. Mohrig, J. R.; Hammond, C. N.; Morrill, T. C.; Neckers, D. C. *Experimental organic chemistry. A balanced approach: macroscale and microscale*; W. H. Freeman and Company: New York, 1998; pp 306-312.
143. *A guide to IUPAC nomenclature of organic compounds: recommendations 1993*; Panico, R.; Powell, W.H.; Richer, J.-C., Blackwell Science: Oxford, 1993; pp 174.
144. Acheson, R. M. *An introduction to the chemistry of heterocyclic compounds*; John Wiley & Sons: New York, 1976.
145. Perrin, D. D.; Dempsey, B. *Buffers for pH and Metal ion Control*; Chapman and Hall Laboratory Manuals: London, 1974; pp 8, 20 and 148.
146. Eyer, P.; Worek, F.; Kiderlen, D.; Sinko, G.; Stuglin, A.; Simeon-Rudolf, V.; Reiner, E. Molar absorption coefficients for the reduced Ellman reagent: reassessment. *Anal. Biochem.* **2003**, *312*, 224-227.
147. Proteinchemist.com. <http://www.proteinchemist.com>.

148. Albeck, A.; Kliper, S. Mechanism of cysteine protease inactivation by peptidyl epoxides. *Biochem. J.* **1997**, *322*, 879-884.
149. CCDC Software Ltd.: Cambridge, U. K.,
150. Jones, G.; Willett, P.; Glen, R. C.; Leach, A. R.; Taylor, R. Development and validation of a genetic algorithm for flexible docking. *J. Mol. Biol.* **1997**, *267*, 727-748.
151. Parr, R. G.; Yang, W. *Density Functional Theory of Atoms and Molecules*; Oxford University Press: Oxford, U. K., 1989.
152. Frisch, M. J.; Trucks, G. W.; Schlegel, H. B.; Scuseria, G. E.; Robb, M. A.; Cheeseman, J. R.; Montgomery Jr., J. A.; Vreven, T.; Kudin, K. N.; Burant, J. C.; Millam, J. M.; Iyengar, S. S.; Tomasi, J.; Barone, V.; Mennucci, B.; Cossi, M.; Scalmani, G.; Rega, N.; Petersson, G. A.; Nakatsuji, H.; Hada, M.; Ehara, M.; Toyota, K.; Fukuda, R.; Hasegawa, J.; Ishida, M.; Nakajima, T.; Honda, Y.; Kitao, O.; Nakai, H.; Klene, M.; Li, X.; Knox, J. E.; Hratchian, H. P.; Cross, J. B.; Bakken, V.; Adamo, C.; Jaramillo, J.; Gomperts, R.; Stratmann, R. E.; Yazyev, O.; Austin, A. J.; Cammi, R.; Pomelli, C.; Ochterski, J. W.; Ayala, P. Y.; Morokuma, K.; Voth, G. A.; Salvador, P.; Dannenberg, J. J.; Zakrzewski, V. G.; Dapprich, S.; Daniels, A. D.; Strain, M. C.; Farkas, O.; Malick, D. K.; Rabuck, A. D.; Raghavachari, K.; Foresman, J. B.; Ortiz, J. V.; Cui, Q.; Baboul, A. G.; Clifford, S.; Cioslowski, J.; Stefanov, B. B.; Liu, G.; Liashenko, A.; Piskorz, P.; Komaromi, I.; Martin, R. L.; Fox, D. J.; Keith, T.; Al-Laham, M. A.; Peng, C. Y.; Nanayakkara, A.; Challacombe, M.; Gill, P. M. W.; Johnson, B.; Chen, W.; Wong, M. W.; Gonzalez, C.; Pople, J. A. *Gaussian 03*, Revision C.02; Gaussian, Inc.: Wallingford CT, 2004.
153. Becke, A. D. Density-functional thermochemistry. III. The role of exact exchange. *J. Chem. Phys.* **1993**, *98*, 5648-5652.
154. Lee, C. T.; Yang, W.; Parr, R. G. Development of the Colle-Salvetti correlation-energy formula into a functional of the electron-density. *Phys. Rev. B* **1988**, *37*, 785-789.
155. Krishnan, R.; Binkley, J. S.; Seeger, R.; Pople, J. A. Self-consistent molecular-orbital methods. XX. Basis set for correlated wave-functions. *J. Chem. Phys.* **1980**, *72*, 650-654.
156. *Hydrolysis: Peptide bonds*; Boyer, P. D., The enzymes; Academic Press: New York, 1971; Vol. III, pp 511-514 and 518-519.
157. Sigma-Aldrich. <http://www.sigmaaldrich.com/>.
158. Guo, Z.; Ramirez, J.; Li, J.; Wang, P. G. Peptidyl *N*-nitrosoanilines: a novel class of cysteine protease inactivators. *J. Am. Chem. Soc.* **1998**, *120*, 3726-3734.
159. Albeck, A.; Fluss, S.; Persky, R. Peptidyl epoxides: novel selective inactivators of cysteine proteases. *J. Am. Chem. Soc.* **1996**, *118*, 3591-3596.
160. Schirmeister, T. New peptidic cysteine protease inhibitors derived from the electrophilic  $\alpha$ -amino acid aziridine-2,3-dicarboxylic acid. *J. Med. Chem.* **1999**, *42*, 560-572.
161. Polgár, L. *Mechanisms of protease action*; Boca Raton: Florida, 1989; pp 123-125.
162. Kirsch, J. K.; Igelström, M. The kinetics of the papain-catalysed hydrolysis of esters of carbobenzyglycine. Evidence for an acyl-enzyme intermediate. *Biochemistry* **1966**, *5*, 783-791.
163. Bender, M. L.; Brubacher, L. J. The kinetics and mechanism of papain-catalyzed hydrolyses. *J. Am. Chem. Soc.* **1966**, *88*, 5880-5889.

164. Zhao, G.; Zhou, Z. S. Vinyl sulfonium as novel proteolytic enzyme inhibitor. *Bioorg. Med. Chem. Lett.* **2001**, *11*, 2331-2335.
165. Edelhofer, H. Spectroscopic determination of tryptophan and tyrosine in proteins. *Biochemistry* **1967**, *6*, 1948-1954.
166. Sanner, T.; Pihl, A. Studies on the active -SH group of papain and on the mechanism of papain activation by thiols. *J. Biol. Chem.* **1963**, *238*, 165-171.
167. Bisswanger, H. *Practical enzymology*; WILEY-VCH Verlag GmbH & Co. KGaA: Weinheim, 2004; pp 10-22.
168. Tokura, S.; Nishi, N.; Noguchi, J. A new substrate for papain, benzoyl-L-arginine-*p*-nitroanilide (L-BAPA). *J. Biochem.* **1971**, *69*, 599-600.
169. Mole, J. E.; Horton, H. R. Kinetics of papain-catalyzed hydrolysis of  $\alpha$ -*N*-benzoyl-L-arginine-*p*-nitroanilide. *Biochemistry* **1973**, *12*, 816-822.
170. Mackenzie, N. E.; Malthouse, J. P. G.; Scott, A. I. Chemical synthesis and papain-catalysed hydrolysis of *N*- $\alpha$ -benzyloxycarbonyl-L-lysine *p*-nitroanilide. *Biochem. J.* **1985**, *226*, 601-606.
171. PD-10 Desalting Column Instructions Manual. Available online in <http://www5.gelifesciences.com>
172. Meloun, B.; Baudyš, M.; Pohl, J.; Pavlik, M.; Kostka, V. Amino acid sequence of bovine spleen cathepsin B. *J. Biol. Chem.* **1988**, *263*, 9087-9093.
173. Bajkowski, A. S.; Frankfater, A. Specific spectrophotometric assays for cathepsin B1. *Anal. Biochem.* **1975**, *68*, 119-127.
174. Hinchliffe, P. S.; Wood, J. M.; Davis, A. M.; Austin, R. P.; Beckett, R. P.; Page, M. I. Structure-reactivity relationships in the inactivation of elastase by  $\beta$ -sultams. *Org. Biomol. Chem.* **2003**, *1*, 67-80.
175. Mulchande, J.; Martins, L.; Moreira, R.; Archer, M.; Oliveira, T. F.; Iley, J. The efficiency of C-4 substituents in activating the  $\beta$ -lactam scaffold towards serine proteases and hydroxide ion. *Org. Biomol. Chem.* **2007**, *5*, 2617-2626.
176. Bradford, M. M. A rapid and sensitive method for the quantification of microgram quantities of protein utilizing the principle of protein-dye binding. *Anal. Biochem.* **1976**, *72*, 248-254.
177. Bio-Rad Protein Assay Instructions Manual. Available online in <http://www.bio-rad.com/>
178. Perrin, D. D.; Dempsey, B.; Serjeant, E. P. *pK<sub>a</sub> Prediction for organic acids and bases*; Chapman and Hall: London, 1981.

### **Publications resulting from this thesis**

Valente, C.; Guedes, R. C.; Moreira, R.; Iley, J.; Gut, J.; Rosenthal, P. J. Dipeptide vinyl sultams: synthesis *via* the Wittig-Horner reaction and activity against papain, falcipain-2 and *Plasmodium falciparum*. *Bioorg. Med. Chem. Lett.* **2006**, *16*, 4115-4119

Valente, C.; Moreira, R.; Guedes, R. C.; Iley, J.; Jaffar, M.; Douglas, K. T. The 1,4-naphthoquinone scaffold in the design of cysteine protease inhibitors. *Bioorg. Med. Chem.* **2007**, *15*, 5340-5350